Institute of Physiology
Academy of Sciences
of the Czech Republic

Application of biophysical methods in functional studies of defects of mitochondrial energy transformation

PhD Thesis

Alena Vojtíšková, MSc.

Prague 2005

Acknowledgements

I would like to express my thanks to my supervisors Josef Houštěk and Jaromír Plášek for providing me with scientific freedom, financial and intellectual support and for their patience. Special thanks belong to the lab in Lyon, Catherine Godinot, Eric Hervouet and Audrey Dubot, for generous sharing of the virtuosities of French science and cuisine. I want to thank to Zdeněk Drahota for his endless willingness to advise and Jiří Zeman for an excellent cooperation with the Pediatric Clinic.

Many thanks belong to Věra Fialová for her sincerity, Vlaďka Brožková for excellent work with cell cultures, Tomáš Mráček for the help with almost everything and for a lot of coffees. I would like to thank all my colleagues from the Department of Bioenergetics Petr Pecina, Ondřej Šebesta, Pavel Ješina, Vilma Kaplanová, Andrea Pícková, Alena Čížková, Kristýna Dudová, Jan Paul and Subir Chowdhury for moral support. Special thanks belong to my mother and sister.

This work was supported by grants from Grant Agency of the Ministry of Health of the Czech Republic (NR7790-3, NE6533-3), the Grant Agency of the Czech Republic (303/03/0794), the Grant Agency of the Charles University (166/2002, 8/2000/C, 14/2004), the institutional projects (VZ111100003, AV0Z501192, VZ113200001). It was also supported by the "Fondation Jerome Lejeune", the "Centre National de la Recherche Scientifique", the "Rhône-Alpes Région", the "Ligue Régionale Contre le Cancer" and the "Institut National de la Santé et de la Recherche Medical"(VIE0208)

Contents

Abbreviations

$\Delta\mu_{H^+}$	electrochemical proton gradient
Δp	protonmotive force
ΔpH	gradient of protons
$\Delta\Psi_m$	mitochondrial membrane potential
$\Delta\Psi_p$	plasma membrane potential
AA	antimycin A
ADP	adenosine diphosphate
ANT	adenine nucleotide translocator
Apaf1	apoptotic protease activating factor 1
Asp	aspartate
ATP	adenosine triphosphate
Atpaf1p, Atpaf2p	ATPase assembly proteins
BAT	brown adipose tissue
car	carnitine
CCRC	clear cell renal carcinoma
COX	cytochrome *c* oxidase
CPEO	chronic progressive external ophtalmopelia
CuZnSOD	copper and zinc superoxide dismutase
CyP D	cyclophilin D
cyt	cytochrome
DHAP	dihydroxyacetone phosphate
$DiOC_6(3)$	3,3′-dihexyloxacarbocyanine iodide
Dnm1	dynamin 1
Drp1	dynamin-related protein 1
ETF	electron-transferring flavoprotein
$FADH_2$	flavin adenine dinucleotide, reduced form
FCCP	carbonyl cyanide 4-(trifluoromethoxy)phenylhydrazone
FRET	fluorescence resonance energy transfer
Fzo1	fuzzy onion protein
G3P	glycerol-3-phosphate
Glu	glutamate
GTP	guanosine triphosphate
HIF	hypoxia-inducible transcription factor
JC-1	5,5′,6,6′-tetrachloro-1,1′,3,3′-tetraethylbenzimidazolylcarbocyanineiodide
KGDHC	α-ketoglutarate dehydrogenase complex
KSS	Kearns-Sayre syndrome
LHON	Leber hereditary optic neuropathy
MELAS	mitochondrial myopathy, encephalopathy, lactic acidosis and stroke-like episodes
MERRF	myoclonical epilepsy and ragged red fibers
Mfn1, Mfn2	mitofusins 1, 2

Mgm1	yeast dynamin-related GTPase, mediator of mitochondrial fusion
mGPDH	mitochondrial glycerophosphate dehydrogenase
MnSOD	manganese superoxide dismutase
mtDNA	mitochondrial deoxyribonucleic acid
Mxt	myxothiazol
NADH	nicotinamide adenine dinucleotide, reduced form
NAO	nonyl acridine orange
NARP	neurogenic muscle weakness, ataxia and retinitis pigmentosa
nDNA	nuclear deoxyribonucleic acid
NRF-1, NRF-2	nuclear respiratory factor 1, 2
OG	oxoglutarate
OPA1	human dynamin-related GTPase, mediator of mitochondrial fusion
OXA1	oxidase assembly protein 1
OxAc	oxalacetate
OXPHOS	oxidative phosphorylation
PDH	pyruvate dehydrogenase
PGC1α	peroxisome proliferator activated receptor γ coactivator 1α
PTP	permeability transition pore
pyr	pyruvate
ROS	reactive oxygen species
Rot	rotenone
RRF	ragged red fibers
rRNA	ribosomal ribonucleic acid
TCA	tricarboxylic acid cycle
Tfam	mitochondrial transcription factor A
TIM	translocases in the inner mitochondrial membrane
TMPD	N,N,N′,N′-tetramethyl-p-phenylenediamine dihydrochloride
TMRE	tetramethylrhodamine ethyl ester
TMRM	tetramethylrhodamine methyl ester
TNF	tumor necrosis factor
TOM	translocases in the outer mitochondrial membrane
TPP^+	tetraphenyl phosphonium
tRNA	transfer ribonucleic acid
UCP	uncoupling protein
VDAC	voltage-dependent anion channel
VHL	von Hippel-Lindau tumor suppressor protein

1 Introduction

1.1 Membrane – the essence of life

The cell is a highly organized biological system with many organelles such as nucleus, endoplasmic reticulum, Golgi aparatus or mitochondria. The cell and all its organelles are surrounded by one or more membranes that control fluxes of various substances inside or outside and thus regulate their content in the cell or organelle. Moreover, many fundamental processes are located on or in the membranes owing to specialized membrane proteins.

One of the most important functions of biological membranes is energy transduction. Cells require energy for various processes, including e.g. synthesis of biological molecules, active transport of molecules across cell membranes or the generation of force and movement. The energy transduction is associated with membrane-bound enzyme complexes that are found in a particular class of membranes. These energy-transducing membranes are plasma membranes of bacteria, thylakoid membranes of chloroplasts and the inner membranes of mitochondria (figure 1). The intensity of energy conversion taking place in energy-transducing membranes is much higher than in other membranes or in soluble systems.

The energy-transducing membranes are able to transport ions (protons in the case of mitochondria) and thus to create their concentration gradients, i.e. chemical potentials. Simultaneously, the charge separation by the membranes establishes the electric potential. Both the concentration gradient and the electrical potential are used for the synthesis of high-energy molecule adenosine triphosphate (ATP). The energy released by hydrolyzing the high-energy phosphoanhydride bond of ATP can power many energetically demanding processes (e.g. transport of molecules against a concentration gradient).

The energy-transducing membranes are not the only site of ATP generation but by far the most efficient. Eukaryotic cells are able to produce 32 molecules of ATP at the expense of energy obtained from one molecule of glucose via aerobic metabolism, taking advantage of mitochondrial energy-transducing membrane. Only two molecules of ATP are generated when glucose is utilized only by anaerobic glycolysis taking place in cytosol.

Eukaryotic cells contain many mitochondria, which occupy up to 25% of the volume of the cytoplasm. The mitochondria are surrounded by two functionally different

membranes which sometimes come together and form contact sites. The outer membrane surrounds the whole organelle and is assumed to be permeant to small molecules and ions. The inner membrane is largely impermeant and forms the major barrier between the cytosol and the mitochondrial matrix. Its surface area is greatly increased by a large number of infoldings, or cristae, enhancing its ability to generate ATP.

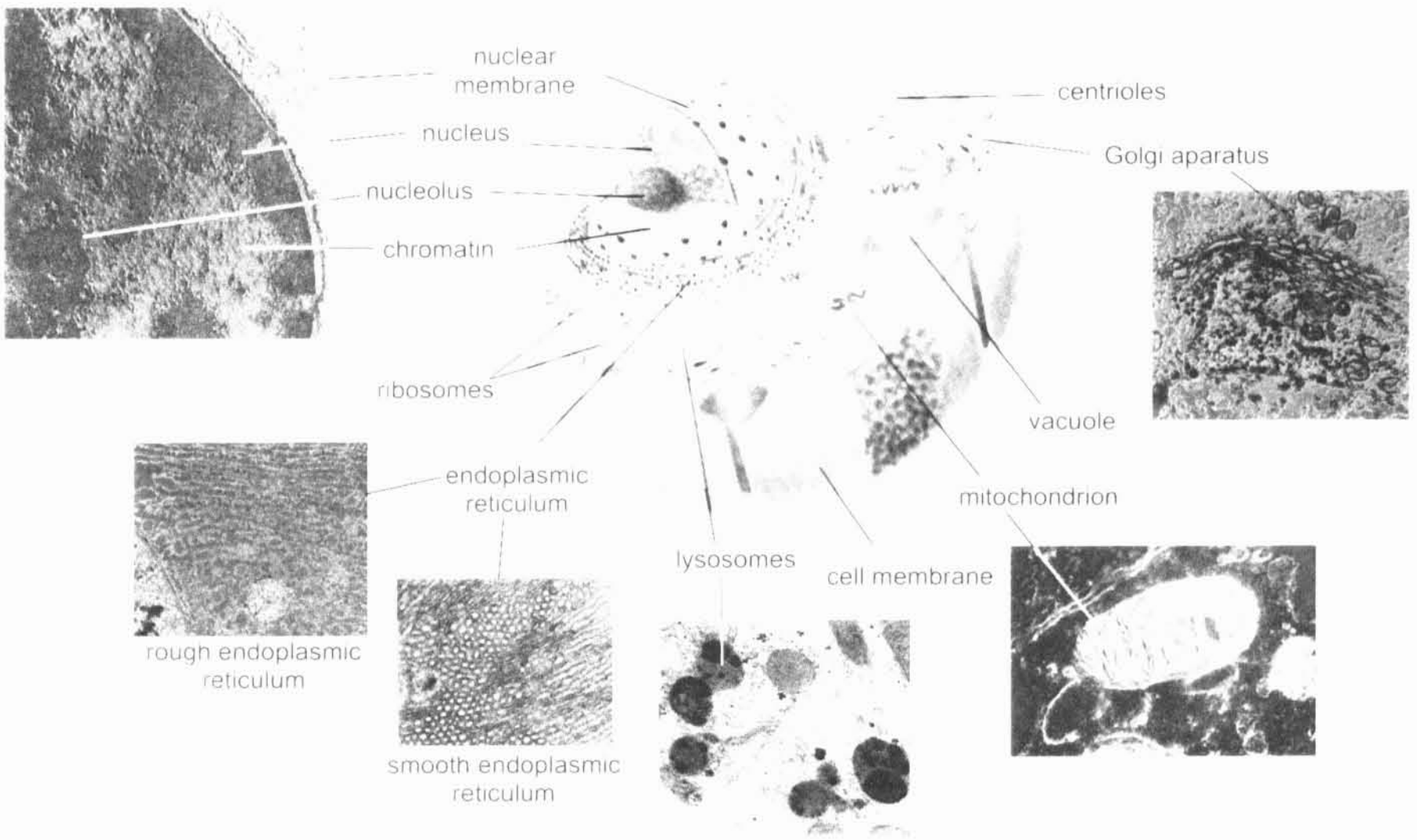

Figure 1
Schematic diagram of animal cell with electron micrographs of its organelles.

1.2 The mitochondria – cellular power plant

Mitochondria can be regarded as the "power plant" of the eukaryotic cell as they provide ATP for the majority of cellular processes. Apart from the ATP generation, some energy released in mitochondrial oxidation can be dissipated as heat or directly used for transport of molecules across the inner mitochondrial membrane. Moreover, mitochondria house a range of enzymes that are involved in ion and protein transport, Ca^{2+} sequestration and generation of reactive oxygen species (ROS) (Nicholls and Ward, 2000). In general, mitochondrial function is indispensable for cell survival. Hence, dysfunction of mitochondria caused by mitochondrial poisons such as cyanide or atractylate or by genetic defects of oxidative phosphorylation system may be critical for a number of cell functions and may result in a disease or even death.

1.2.1 The chemiosmotic theory

The key metabolic pathway in mitochondria is the tricarboxylic acid cycle (TCA) that breaks down carbon substrate - acetyl coenzyme A (which is derived either from pyruvate, fatty acid or amino acid breakdown) to generate carbon dioxide. During this process NAD^+ and FAD^{2+} are reduced to NADH and $FADH_2$ and these intermediates are utilized by the enzymes of the respiratory chain, complex I (NADH dehydrogenase) and complex II (succinate dehydrogenase). While the majority of electrons enter the respiratory chain in this way, other enzymes are also constituents of the respiratory chain although their capacity is smaller and their content is highly tissue specific. The examples of these enzymes are the electron-transferring flavoprotein (ETF)-ubiquinone oxidoreductase and mitochondrial glycerophosphate dehydrogenase (mGPDH) (figure 2). The first one transfers electrons via ETF from the flavin-linked oxidation step in the catabolism of fatty acids by β-oxidation (Nicholls and Ferguson, 2002), the latter is located at the outer surface of the inner mitochondrial membrane and is involved in oxidation of cytosolic NADH via glycerophosphate shuttle (Estabrook and Sacktor, 1958; Klingenberg, 1970).

The electrons are then transferred via single-electron carrier ubiquinone to complex III (ubiquinone cytochrome *c* reductase); cytochrome *c*, encountered in the intermembrane space, then shuttles electrons to complex IV (cytochrome *c* oxidase) that catalyzes the reduction of oxygen to water (figure 2).

Complexes I, III and IV consist of many protein subunits of mitochondrial or nucleic origin, while complex II, mGPDH and ETF-ubiquinone oxidoreductase are entirely encoded by nuclear DNA. The reactions of complexes I, III and IV are also associated with proton transfer across the mitochondrial inner membrane from matrix into the intermembrane space (figure 2), creating an electrochemical proton gradient ($\Delta\mu_{H^+}$). The proton gradient is utilized by ATPase (F_1F_o-ATP synthase or complex V) in mitochondria, which synthesizes the ATP from ADP and phosphate and regulates the respiratory rate. In this way, the respiratory rate and the rate of ATP synthesis are coupled through the gradient of protons (Mitchell, 1961). The Mitchell's theory refuted various hypotheses of a high-energy intermediate, which was proposed by many researchers who devoted years to the search for the intermediate. For this theory, Peter Mitchell was awarded the Nobel price in 1978.

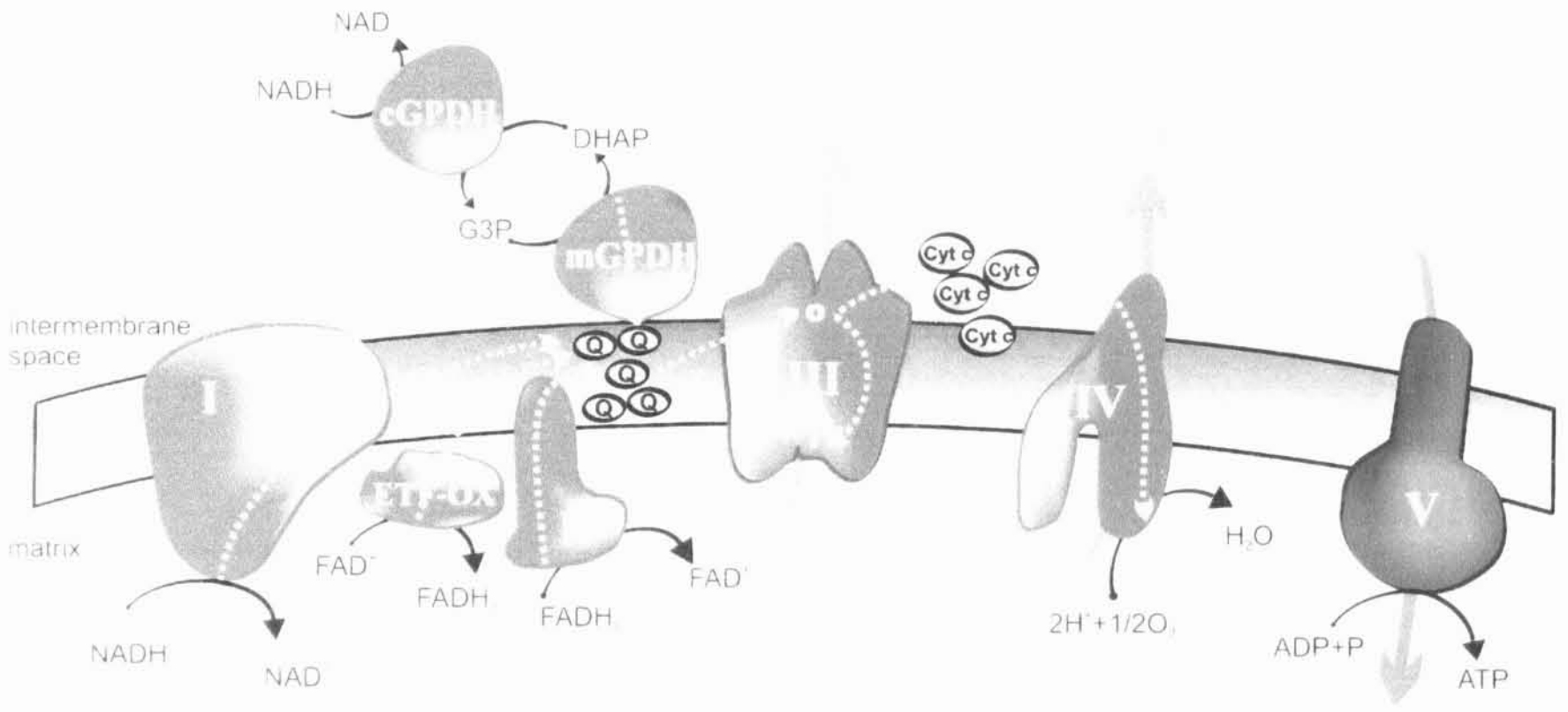

Figure 2
An overview of the mitochondrial respiratory chain.
cGPDH/mGPDH - cytosolic/mitochondrial glycerophosphate dehydrogenase; ETF-OX - electron-transferring flavoprotein ubiquinone oxidoreductase; Q - ubiquinone; cyt c - cytochrome c; G3P - glycerol-3-phosphate; DHAP - dihydroxyacetone phosphate; I, II, III, IV and V - complexes of respiratory chain. Red, yellow and black arrows represent proton transport pathways, electron transport pathways and reactions catalyzed by the enzyme complex, respectively.

1.2.2 Protonmotive force

Electrochemical gradient of protons across the inner mitochondrial membrane, $\Delta\mu_{H^+}$, is a thermodynamic measure of the extent to which a proton gradient is out of equilibrium. It has two components, ΔpH represents the concentration difference of H^+ across the membrane and the membrane potential, $\Delta\Psi_m$, the difference in electrical potential between aqueous phases separated by the membrane. The electrochemical gradient can be expressed as:

$$\Delta\mu_{H^+} = -F\Delta\Psi_m + 2.3RT\Delta pH \qquad (1)$$

It is conventional to convert $\Delta\mu_{H^+}$ into units of electrical potential (millivolts) as follows:

$$\Delta p\ (mV) = -\ \Delta\mu_{H^+}/F \qquad (2)$$

where Δp is the protonmotive force defined by Peter Mitchell (Mitchell, 1961), F, R, T are Faraday constant, gas constant and absolute temperature, respectively.

Substituting values for R and T at 25°C, the final equation is:

$$\Delta p\ (mV) = \Delta\Psi_m - 59\Delta pH \qquad (3)$$

To understand the energetic processes in mitochondria it is important to have tools for studying mitochondrial function by monitoring important bioenergetic parameters, in particular the protonmotive force. The typical Δp value of energized mitochondria is about 180 mV. The $\Delta\Psi_m$ component accounts for about 150 mV, the remaining 30 mV are derived from a small pH gradient of -0.5 units. It should be noted that the electrical capacity of the membrane is so low that the transfer of one nmol of H^+ per mg of protein across the membrane will establish a $\Delta\Psi_m$ of about 200 mV. In addition, the pH buffering capacity of mitochondrial matrix is about 20 nmol of H^+ per mg of protein per one pH unit; this means that the loss of 1 nmol of H^+ will increase the matrix pH by only 0.05 units (equivalent to 3 mV) (Nicholls and Ward, 2000; Nicholls and Ferguson, 2002). The ΔpH component can be minimized by increasing P_i concentration up to 5 mM (Lambert and Brand, 2004b) or adding nigericin (H^+-K^+ exchanger). Under such conditions, the $\Delta\Psi_m$ component accounts for the entire Δp and is therefore generally used as the bioenergetic marker of mitochondrial function (Nicholls and Ferguson, 2002; Duchen, 2004).

1.3 Mitochondrial physiology in health and disease

The bioenergetic behavior of intact cells is controlled by the supply of substrates from the cytoplasm, the turnover of ATP by energy-consuming processes and the ionic environment of the cytoplasm, particularly in relation to Ca^{2+}. Alterations of all these parameters occur in response to changes in energy demand, which is reflected by changes in mitochondrial membrane potential.

1.3.1 Mitochondrial biogenesis

It is generally accepted that mitochondria originate from pre-existing mitochondria and that mitochondrial biogenesis consists of the genetic and membrane continuity (Nisoli et al., 2004). Mitochondria have their own DNA (mtDNA) that is small and of prokaryotic character. Human mtDNA contains only 37 genes (2 genes encode ribosomal RNAs, 22 encode transfer RNAs, and 13 encode polypeptides of oxidative phosphorylation complexes). The majority of mitochondrial proteins of which the mitochondria are built, as well as those forming the machinery for assembling them are encoded by nuclear DNA (nDNA) and synthesized in the cytoplasm. Mitochondria can divide, fuse and create a reticular network associated with cytoskeleton. The degradation of mitochondria is performed by the lysosomes, which contain a range of hydrolases.

1.3.1.1 Coordination of mitochondrial biogenesis

The division and replication of mitochondria depend on the coordinated interplay between the genetic systems of the organelle and the nucleus. Recently identified transcription factors appear to play a key role in synchronization of the synthesis of proteins encoded by mtDNA or nDNA but relatively little is known about the pathways by which the proteins are regulated.

The most essential factor seems to be the transcription coactivator, PGC1α (peroxisome proliferator activated receptor γ coactivator 1α). PGC1α seems to activate the synthesis of nuclear encoded mitochondrial proteins via upregulation of transcription factors NRF-1 and 2 (nuclear respiratory factors). The transcription of Tfam protein, which promotes the increased production of the proteins encoded by mtDNA and replication of

mtDNA, is also increased. This system thus appears to coordinate the rate of synthesis of proteins from both genomes (Duchen, 2004). In addition, other regulatory factors are to be expected that may facilitate pro-mitochondrial effects of thyroxin or other hormones.

1.3.1.2 Mitochondrial protein transport

The majority of the mitochondrial proteins are synthesized in cytosol. These proteins are then transported and directed to the matrix, the intermembrane space or to the outer or inner mitochondrial membrane. The imported proteins usually comprise a targeting sequence, which allows them to reach their proper destination. In general, this sequence is located at the N-terminus of the protein, it is positively charged and is absent in mature protein.

The import of mitochondrial matrix proteins is mediated by translocases located in the outer (TOM) and inner (TIM) membrane (figure 3A). TOM complex involves three receptors for targeting motifs and a transport channel. To keep the precursor in the unfolded state, it is bound to the cytosolic chaperons, which requires ATP. Afterwards, the precursor is delivered to the appropriate TOM receptors (Tom20) and transported through the pore. TOM complex interacts with the inner membrane TIM complexes and this interaction is located at "contact sites", where the outer and the inner membranes are in physical contact. The driving force for the initial transport of positively charged precursors across the inner membrane is the $\Delta\Psi_m$. A complete transport of the protein is facilitated in ATP dependent manner by the heat-shock protein HSP 70. The translocated proteins are usually bound by the mitochondrial chaperon HSP 60 that prevents protein aggregation and premature folding. Then their targeting sequence is cleaved in one or several steps by mitochondrial proteases.

Some of the proteins directly inserted into the inner mitochondrial membrane, such as adenine nucleotide transporter or uncoupling protein, have internal cryptic targeting sequences. The sequences are recognized by a component of TOM complex (Tom70). The precursor is partially translocated, but remains attached to the TOM complex at its C-terminus. Together with intermembrane space proteins (Tim9 and Tim10), TOM complex assists in the folding of tertiary structure of the protein and the TIM22 complex inserts the folded protein into the inner mitochondrial membrane (figure 3B). The latter process is dependent on $\Delta\Psi_m$.

The nuclear encoded proteins of respiratory chain complexes (complex I, III, IV and V) are imported initially into the matrix and then inserted into the inner mitochondrial membrane together with mitochondrially encoded subunits via the translocase complex OXA1 (figure 3C) and numerous complex-specific assembly factors. For example, in case of cytochrome *c* oxidase, about 20 different essential "helper proteins" have been described in yeast and many of them are also known in mammalian mitochondria (e.g. SURF1, SCO1, SCO2 etc.)

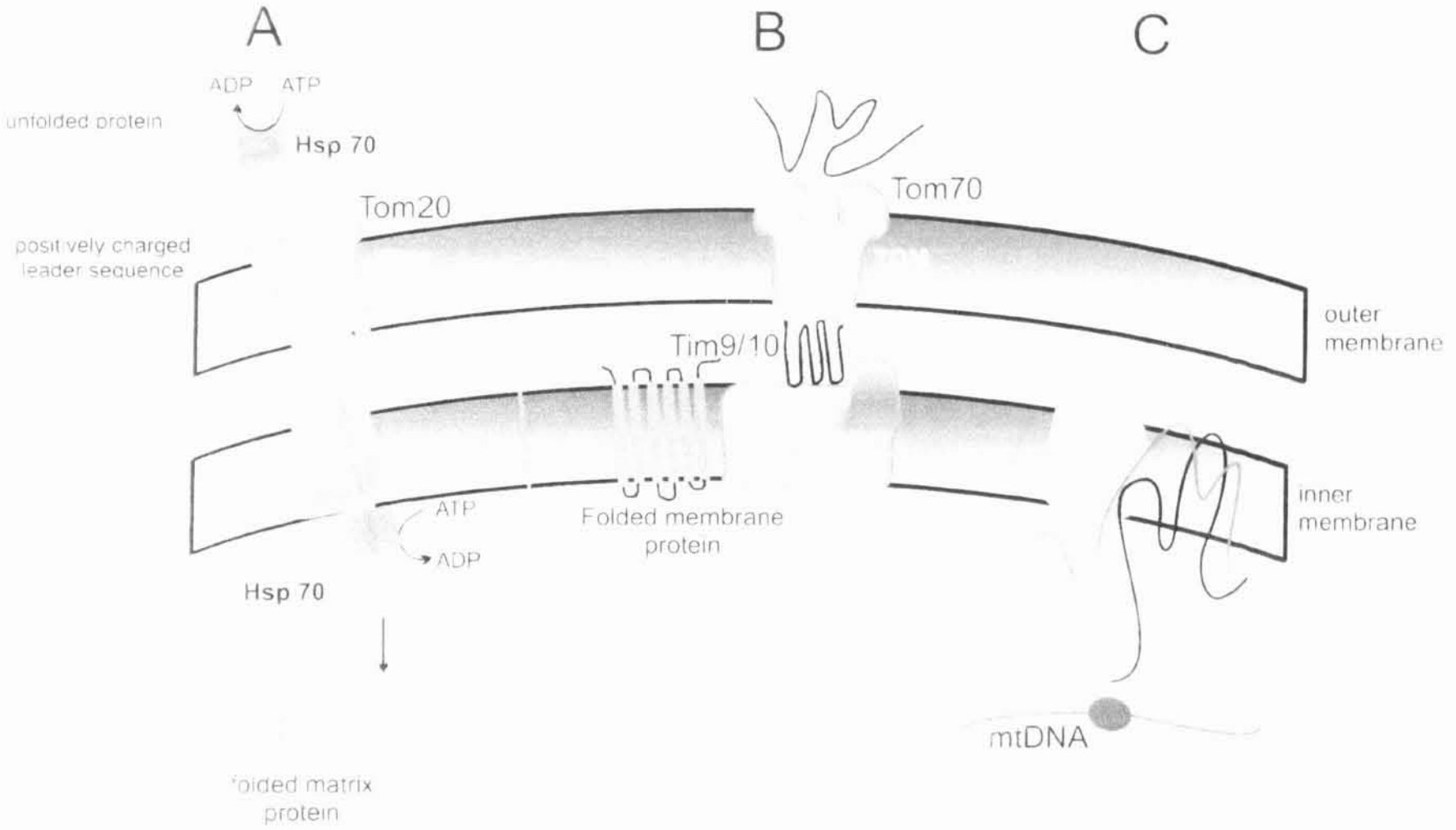

Figure 3

Mitochondrial protein import.

(A) transport of matrix proteins across the TOM and TIM complex; Hsp 70 - chaperon; (B) transport of integral inner membrane proteins; (C) insertion of co-assembled mitochondrial and nuclear peptides of respiratory chain complexes into the inner mitochondrial membrane by OXA1.

1.3.1.3 Mitochondrial fusion and fission

The mitochondrial reticulum is a dynamic structure that is maintained by an equilibrium between fusion and fission. It has become more evident that these processes are crucial for many cellular functions (e.g. fusion of mitochondria is required for the inheritance of mtDNA (Rapaport et al., 1998)). Both fusion and fission require distinct GTP-binding proteins that act at the mitochondrial surface. The yeast protein Dnm1 (dynamin 1) and its human homologue Drp1 (dynamin-related protein 1) seem to play a

key role in regulation of mitochondrial fission (Imoto et al., 1998; Bleazard et al., 1999). Dnm1 and Drp1 are localized on the outer mitochondrial membrane and colocalize with mitochondrial scission sites, but their molecular function is still unclear (Karbowski and Youle, 2003).

The first mediator of mitochondrial fusion, the fuzzy onion protein (Fzo1), was identified in *Drosophila melanogaster*. Mutations in *Fzo1* or knockout of the mammalian homologues of Fzo1, mitofusins 1 & 2 (Mfn1&2), result in the formation of fragmented mitochondria indicating its participation in mitochondrial fusion (Hermann et al., 1998; Chen et al., 2003). Another mediator of mitochondrial fusion, Mgm1 in yeast and OPA1 in humans, may participate in the fusion of the inner membrane, but its specific role is not clear (Wong et al., 2000; Olichon et al., 2002). The mutations in OPA1 were detected in patients with dominant optic atrophy (Alexander et al., 2000; Delettre et al., 2000).

1.3.2 Mitochondrial proton transport

The enzymatic complexes capable of proton transport in mitochondria play a central role in mitochondrial function as they establish a dynamic equilibrium between Δp formation and its utilization for the synthesis of ATP. Δp is formed at the level of respiratory chain enzyme complexes I, III and IV. Perhaps the most complicated, but very interesting mechanism of proton transport from matrix to the intermembrane space is found in complex IV – cytochrome *c* oxidase (COX). The utilization of Δp is performed by the enzyme possessing a unique mechanism of ATP synthesis driven by proton translocation – the complex V or F_1F_0-ATP synthase (ATPase). Alternatively, Δp can be dissipated by uncoupling proteins. In this case, the energy is transformed into heat but other physiological roles for these proteins have been proposed.

1.3.2.1 Cytochrome *c* oxidase

Mammalian COX is composed of 13 subunits. Mitochondrially encoded subunits I-III are evolutionarily conserved and contain the catalytic core of the enzyme. Ten smaller subunits are nuclear encoded and they do not participate directly in electron transport or proton translocation, but numerous studies show that they are involved in the assembly and

regulation of the enzyme activity (Poyton and McEwen, 1996; Kadenbach et al., 2000; Ludwig et al., 2001). The structure is summarized in figure 4.

The electron donated from cytochrome *c* enters the COX via Cu_A center and is subsequently transferred to heme *a* in subunit I. It is then transferred to the binuclear center (heme a_3 and electronically coupled Cu_B ion). When the first two electrons enter the center, oxygen is able to bind and the dioxygen bond is cleaved. Two further electrons reduce the oxygen to water. The binuclear center requires free access of its substrates (oxygen and protons) and probably is the key player in energy transduction (Ludwig et al., 2001).

Proton translocation by COX

Since the discovery of the vectorial proton translocation in COX by Wikstrom (Wikstrom and Saari, 1977) the mechanism of coupling between electron transport and proton pumping in COX is still debatable. During a complete oxygen cycle, four protons are taken up from the matrix side for the formation of water and four additional protons are assumed to be translocated from the matrix across the inner mitochondrial membrane to the cytosolic side. Two proton pathways, the D- and the K-channel (named after key aspartate and lysine residues) were suggested theoretically and according to mutational studies and were later confirmed by crystallographic studies (Abramson et al., 2001).

It was generally accepted that the H^+/e^- stoichiometry in COX of mitochondria and bacteria is 1.0, but several recent observations indicate that the H^+/e^- ratio in COX may be variable. Decreased H^+/e^- ratios in mammalian COX were obtained after removal of subunit III (Ludwig et al., 2001). Murphy and Brand (Murphy and Brand, 1987; Murphy and Brand, 1988) found a decrease in H^+/e^- ratio from 1 at low $\Delta\Psi_m$ to 0 at high $\Delta\Psi_m$.

Regulation of COX

The COX represents the perhaps most tightly regulated enzyme of the respiratory chain Recently, the regulatory role of nuclear encoded subunits of COX was confirmed for subunits IV, Va, Vb, VIaH (heart and skeletal muscle isoform) and VIaL (liver and kidney isoform). Consequently, a theory of COX regulation was postulated featuring the allosteric binding of adenine nucleotides to subunit VIa and phosphorylation of subunit IV (Ludwig et al., 2001).

A decrease of H^+/e^- ratio with increasing intraliposomal ATP/ADP ratio was observed with reconstituted COX from bovine heart and the nucleotide-binding site was identified in subunit VIaH (Frank and Kadenbach, 1996; Tsukihara et al., 1996; Huttemann

et al., 1999). Under the same conditions with reconstituted COX from bovine liver containing different isoform of subunit VIa no changes in H^+/e^- ratio with increasing intraliposomal ATP/ADP ratio were observed (Huttemann et al., 1999). These observations suggest a key role of subunit VIa in determining the efficiency of energy transduction by COX.

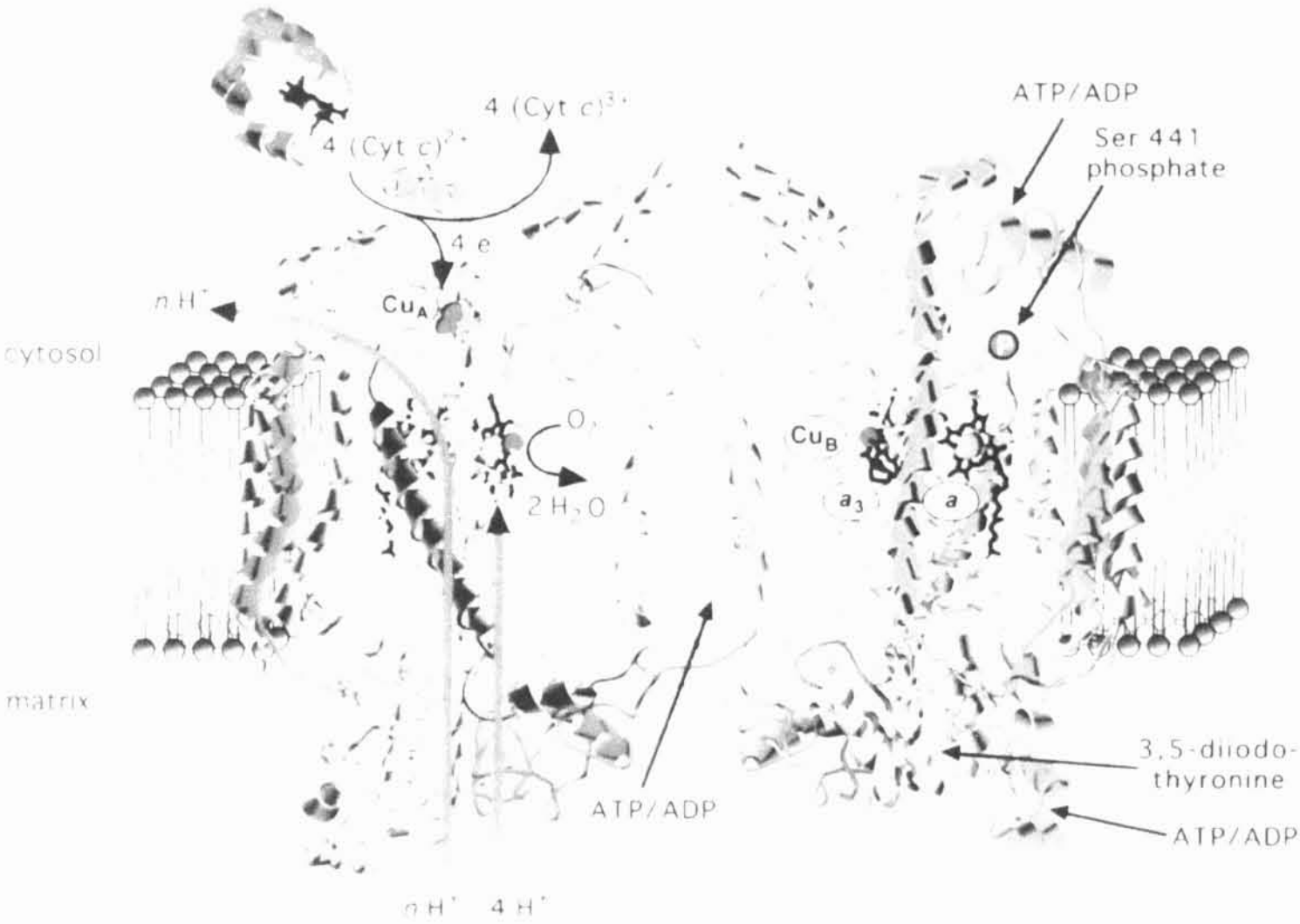

Figure 4
Structure of COX dimer from bovine heart mitochondria.
Binding sites for substrates (cyt c and O_2), allosteric regulatory factors (ATP/ADP, diiodothyronine) and phosphorylation epitope in subunit I (Ser 441) are indicated. Adapted from (Ludwig et al., 2001).

1.3.2.2 F_1F_o-ATP synthase

ATPase has two major domains known as F_1 (factor 1) and F_o (factor oligomycin). The globular F_1 catalytic domain in the mitochondrial enzyme is an assembly of five subunits with the stoichiometry $\alpha_3\beta_3\gamma_1\delta_1\varepsilon_1$. The $(\alpha\beta)_3$ subcomplex is oriented to the matrix and is linked to the membrane domain F_o by a central stalk formed by subunits γ, δ and ε (figure 5A) and also by a peripheral stalk that contains OSCP (oligomycin sensitivity conferring protein) subunit, subunits b, d and F_6 (Walker, 1998). The membrane F_o domain contains subunit a and 10 c subunits, which are in contact and form a proton channel

(Stock et al., 2000), and a number of small subunits that appear to have no direct role in catalysis (Collinson et al., 1994).

Three α and three β subunits are arranged alternatively around a central γ subunit. This arrangement suggested that the enzyme works by a mechanism involving the cyclic modulation of affinity of nucleotide binding sites in 3 catalytic β subunits by rotation of the asymmetrical γ subunit. During ATP synthesis, the rotation is generated in F_o by H^+ translocation (figure 5B). During ATP hydrolysis in F_1F_o or in F_1 alone, the energy released by hydrolysis would drive rotation in the opposite direction and reverse the direction of proton translocation (Stock et al., 2000).

Figure 5
Structure of F_1F_o-ATP synthase.
(A) Structure of the holoenzyme. The individual subunits are indicated. See text for details; (B) model of the generation of rotation by movement of the protons through the F_o domain. Adapted from (Stock et al., 2000).

1.3.2.3 Uncoupling proteins

Uncoupling proteins (UCP) are inner mitochondrial membrane complexes of about 36 kDa capable of transporting protons. They are sensitive to purine nucleotides and may include protonated and deprotonated forms of free fatty acids. The first uncoupling protein (UCP1) was discovered in the 1970's in brown adipose tissue (BAT) where it has a thermogenic role. BAT is found in small mammals at early stages of postnatal development and in hibernators. UCP1 allows the respiration to proceed in the absence of ATP synthesis by uncoupling the BAT mitochondria and during this process the heat is

generated (Heaton et al., 1978; Nicholls and Ferguson, 2002; Duchen, 2004). Recently, other uncoupling proteins (UCP2 and 3) were identified in different tissues and species, but their physiological role is debated.

1.3.3 Mitochondrial ion and metabolite transport

Mitochondria continuously exchange metabolites, end products and ions with the cell cytoplasm. Since most of those are charged and/or weak acids, their distribution will be affected by $\Delta\Psi_m$ or pH gradient. In practice, transport mechanisms may exploit these gradients to drive the accumulation of substrates or expulsion of products across the membrane. Some of the more common strategies are (Nicholls and Ferguson, 2002):

1. electroneutral proton symport or hydroxyl antiport leading to an accumulation driven by ΔpH (P_i^-/H^+ exchanger)
2. electrical uniport of a cation driven by $\Delta\Psi_m$ (Ca^{2+} accumulation)
3. electroneutral or electrogenic exchange of two metabolites (ATP^{4-}/ADP^{3-} antiporter)
4. electroneutral antiport of an ion or metabolite with protons (Na^+/H^+ antiporter)

1.3.3.1 Mitochondrial cation transport

Mitochondrial monovalent cation transport

The influx of Na^+ and K^+ salts and water that occurs at high $\Delta\Psi_m$ values can lead to excessive osmotic swelling and disruption of mitochondria. Hence, mitochondria possess the electroneutral Na^+/H^+ and K^+/H^+ antiporters which release K^+ and Na^+ out of the matrix. The K^+ for H^+ (from the oxidative phosphorylation) exchange will alkalinize the matrix causing phosphate to enter via the electroneutral P_i^-/H^+ symporter. When mitochondria synthesize ATP, $\Delta\Psi_m$ decreases and consequently the Na^+ and K^+ influx decreases. The imbalance between influx and efflux causes contraction of matrix volume. To prevent it the mitochondria possess the ATP-sensitive K^+ channel (Mironova et al., 1981; Diwan et al., 1988), which is opened in response to endogenous signals to restore matrix volume by the K^+ influx (Garlid and Paucek, 2003).

Mitochondrial Ca^{2+} transport

It seems that the majority of physiological calcium signals in most cells are associated with calcium accumulation in mitochondria (Rizzuto et al., 2004). Mitochondria accumulate Ca^{2+} by uniport (Kirichok et al., 2004) when exposed to increased Ca^{2+} concentrations and Ca^{2+} transport is primarily driven by $\Delta\Psi_m$ (Brookes et al., 2004; Duchen, 2004). At equilibrium, the Ca^{2+} uniporter would develop a concentration gradient across the inner mitochondrial membrane, but in practice, it does not occur. The reason is a Ca^{2+} efflux by xNa^+ /Ca^{2+} antiport but the stoichiometry of the exchanger is still contentious. It is suggested that it is either electroneutral $2Na^+$ /Ca^{2+} (Brand, 1985) or electrogenic $3Na^+$ /Ca^{2+} exchanger (Jung et al., 1995).

It was shown that Ca^{2+} upregulates three major rate limiting enzymes of the citric acid cycle (TCA) (McCormack et al., 1990) and that the magnitude of mitochondrial Ca^{2+} uptake during cytosolic calcium signaling is sufficient for TCA cycle regulation (Duchen, 1992; Pralong et al., 1992). Recently, Jouaville's group showed that mitochondrial calcium uptake increases ATP production (Jouaville et al., 1999). In general, it seems that any perturbation in Ca^{2+} homeostasis, for instance due to depolarization, could have profound implications for cell function, e.g. at the level of ATP synthesis.

1.3.3.2 Mitochondrial metabolite transport

To date, at least 25 distinct inner mitochondrial membrane transporters have been identified and their expression varies among tissues. Representative transporters of the inner mitochondrial membrane are listed in table 1. All mitochondria possess adenine nucleotide transporter (ANT) and phosphate transporter, which are responsible for ADP and P_i uptake and the release of ATP. Depending on the tissue, mitochondria have the transporters for the proper metabolic pathways present in the cell. For example, liver has transport pathways for most of the TCA cycle intermediates.

Transporter	Mechanism
phosphate	P_i^-/H^+
pyruvate	Pyr^-/OH^-
dicarboxylate	$malate^{2-}/P_i^{2-}$
tricarboxylate	$citrate^{3-}+H^+/malate^{2-}$
carnitine/acylcarnitin	$Carn^+/Acylcarn^+$
adenine nucleotide	ADP^{3-}/ATP^{4-}
2-oxoglutarate	$2OG^{2-}/Mal^{2-}$
glutamate	Glu^-/OH^-

Table 1
Representative mitochondrial inner membrane transporters.

One of the most important mitochondrial transport systems is responsible for transport of electrons from NADH to the respiratory chain. NADH is produced in glycolysis and cannot permeate the inner mitochondrial membrane. There are two strategies to transport the electrons to the respiratory chain. Firstly, cooperation of 2-oxoglutarate and glutamate-aspartate carriers allows the oxidation of cytoplasmic NADH creating the malate-aspartate shuttle (figure 6A). Cytoplasmic NADH is oxidized by malate dehydrogenase, malate enters matrix in exchange for 2-oxoglutarate and is reoxidized by the matrix malate dehydrogenase generating matrix NADH. Oxaloacetate transaminates with glutamate to form aspartate and 2-oxoglutarate. 2-oxoglutarate transaminates in the cytoplasm with transported aspartate to regenerate cytoplasmic oxaloacetate (Nicholls and Ferguson, 2002). The glycerophosphate shuttle provides an alternative way for the oxidation of cytoplasmic NADH (figure 6B). Cytoplasmic glycerophosphate dehydrogenase simultaneously oxidizes NADH and reduces dihydroxyacetone phosphate to glycerophosphate. Mitochondrial glycerophosphate dehydrogenase reoxidizes glycerophosphate and transports electrons directly to the coenzyme Q (Nicholls and Ferguson, 2002).

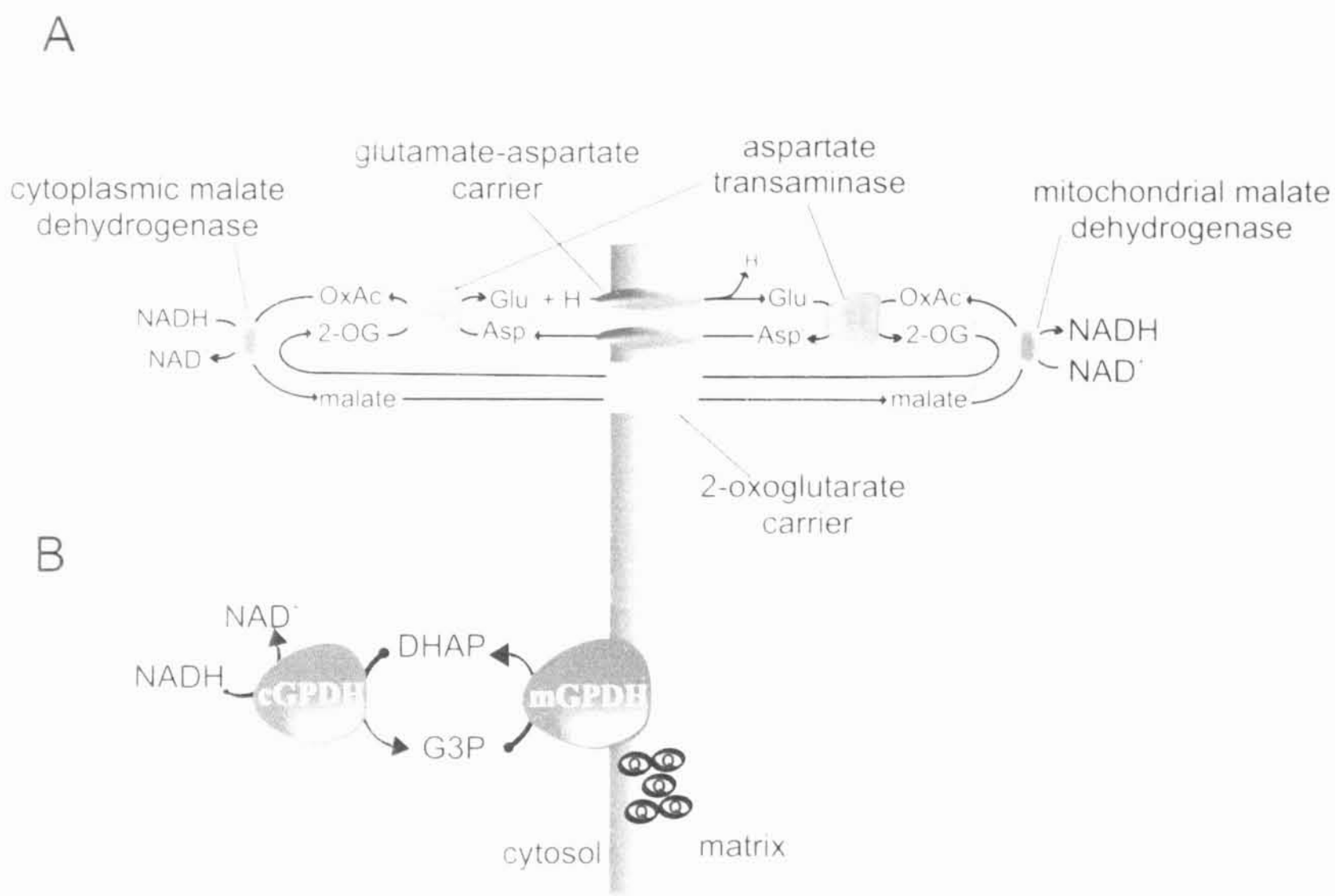

Figure 6
The oxidation of cytoplasmic NADH by mitochondria.
(A) the malate-aspartate shuttle, OxAc - oxaloacetate, 2-OG - 2-oxoglutarate, Glu - glutamate, Asp - aspartate, DHAP - dihydroxyacetone phosphate, G3P - glycerophosphate.

1.3.4 Free radical generation

Mitochondria appear to be the major source of free radicals or reactive oxygen species (ROS) in many types of cells. The main sites of ROS production were localized to the electron transport chain, the various one-electron carriers, including flavoproteins, iron-sulfur clusters and ubisemiquinone which are suited for an electron transfer to oxygen and give rise to superoxide (O_2^-) (Boveris and Cadenas, 1975; Boveris, 1984; Turrens et al., 1985; Turrens, 1997). The superoxide and free radicals in general seem to play a role in various pathological disorders (Halliwell and Gutteridge, 1999) and also in aging (Cadenas and Davies, 2000). In spite of antioxidant mechanisms, which neutralize ROS, the oxidative damage to macromolecules (enzymes, DNA, lipids etc.) is considered to be cumulative and can lead to cell dysfunction. Conversely, despite the deleterious action of ROS, it becomes evident that they can serve as specific signaling molecules (Darley-Usmar and White, 1997; Hancock, 1997; Suzuki et al., 1997; Finkel, 1998; Saran et al., 1998; Allen and Tresini, 2000).

1.3.4.1 Mitochondrial sources of superoxide

Two principal sites of O_2^- generation in mitochondria have been identified in complex I and complex III (figure 7). Complex III is main producer to the outer side of inner mitochondrial membrane (Boveris et al., 1976; Cadenas et al., 1977; Turrens et al., 1985), but also produces O_2^- to the outer side of the inner mitochondrial membrane (Han et al., 2001; Starkov and Fiskum, 2001). On the other hand, complex I is suggested to produce O_2^- only to the inner side (Turrens and Boveris, 1980; Genova et al., 2001; Kushnareva et al., 2002; St-Pierre et al., 2002) and the iron-sulfur centers (Herrero and Barja, 1997; Herrero and Barja, 1998) or the active site flavin (Liu et al., 2002) are thought to be responsible for superoxide production. Recent studies also suggested that the use of succinate as a main respiratory substrate could lead to O_2^- generation by reverse electron transport from complex II to complex I (Votyakova and Reynolds, 2001; St-Pierre et al., 2002; Han et al., 2003). Moreover, the O_2^- production by complex I during reverse electron transport is higher compared to forward electron transport (Lambert and Brand, 2004b; Lambert and Brand, 2004a).

The relative contribution of every site to the overall O_2^- production varies with experimental conditions and between tissues and species (Turrens, 1997; Barja, 1999; Duchen, 2004). Complex III appears to be responsible for most of the O_2^- production in heart and lung mitochondria (Turrens and Boveris, 1980; Turrens et al., 1982) while complex I is the major source of O_2^- in the brain (Barja and Herrero, 1998; Barja, 1999). Recently, the reverse electron transport from complex II was identified as the main source in the skeletal muscles (Votyakova and Reynolds, 2001; St-Pierre et al., 2002; Han et al., 2003; Lambert and Brand, 2004b).

A high rate of ROS production has also been detected in tissues with high expression of mGPDH: insect fly muscle mitochondria (Bolter and Chefurka, 1990; Sohal, 1991; Miwa et al., 2003), brown adipose tissue mitochondria (Sekhar et al., 1987; Drahota et al., 2002; Drahota et al., 2003) and placental mitochondria (Honzik et al., 2005) with glycerophosphate as a substrate. This suggested that mGPDH is another site of the O_2^- production localized to the outer side of the inner mitochondrial membrane (Drahota et al., 2002; Miwa et al., 2003) (figure 7).

Recently, other possible sites of mitochondrial ROS production were identified (Andreyev et al., 2005). Firstly, isolated succinate dehydrogenase reconstituted into liposomes can produce ROS (Zhang et al., 1998). Furthermore, two recent studies (Starkov et al., 2004; Tretter and Adam-Vizi, 2004) showed that isolated pyruvate dehydrogenase (PDH) and α-ketoglutarate dehydrogenase complex (KGDHC) could also generate superoxide. Nevertheless, it should be noted that the ROS production by these enzymes was observed with isolated enzymes and thus their contribution to mitochondrial ROS production in intact mitochondria is still unclear.

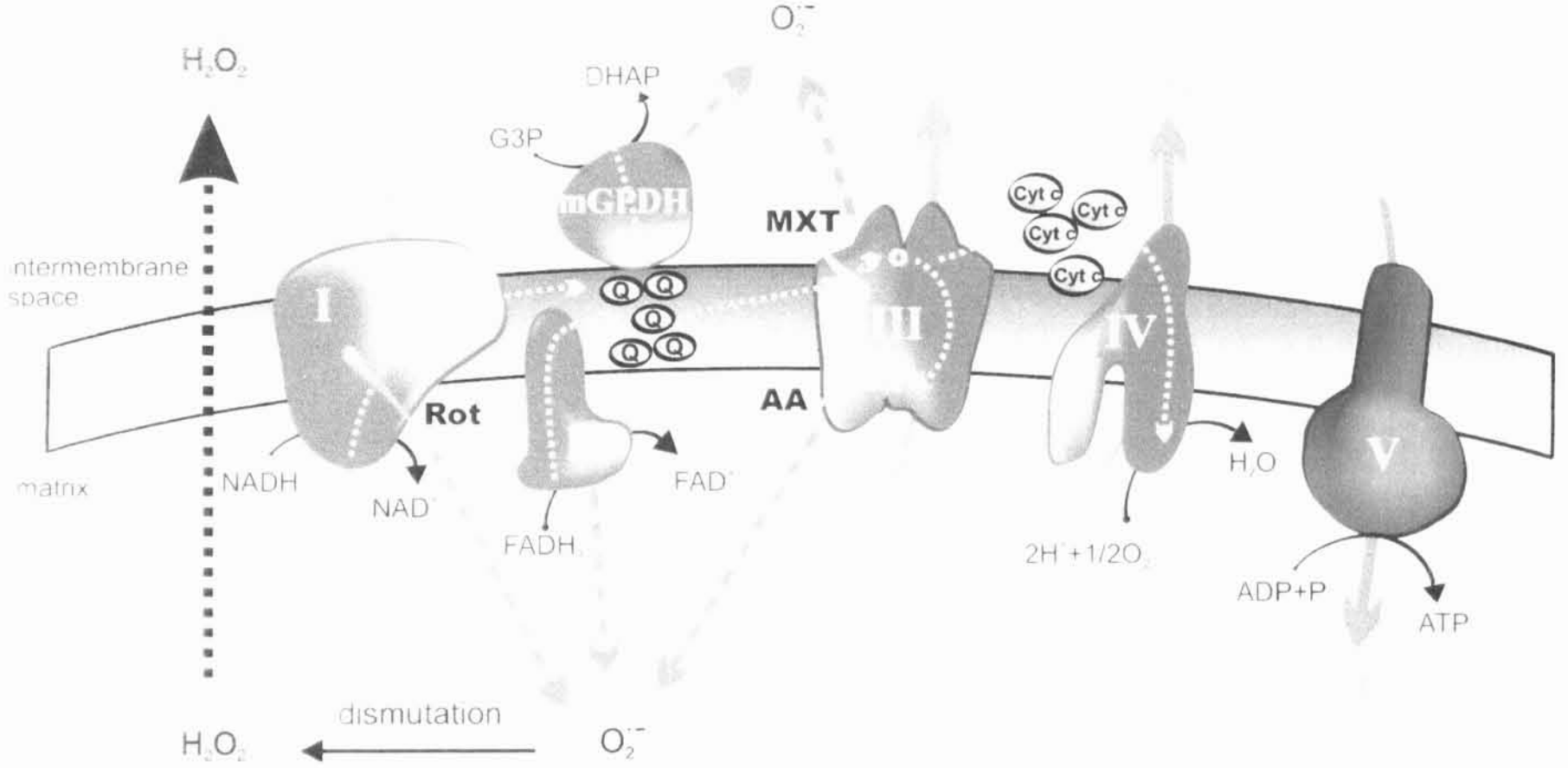

Figure 7
Mitochondrial sources of superoxide production.
mGPDH - mitochondrial glycerophosphate dehydrogenase; Q - ubiquinone; cyt c - cytochrome c; G3P - glycerol-3-phosphate; DHAP - dihydroxyacetone phosphate; I, II, III, IV and V - complexes of respiratory chain. Sites of specific inhibitors are indicated. Inhibitors of complex III - myxothiazol (MXT) and antimycin A (AA); complex I - rotenone (Rot). Blue arrows represent superoxide production, red arrows - proton transport pathways; yellow arrows - electron transport pathways.

1.3.4.2 $\Delta\Psi_m$ and ROS production

Assessments of the O_2^- production in respiring mitochondria vary from 0.1% to 4% of total oxygen consumption depending on the oxygen concentration and respiration state of the mitochondria (Barja, 2002; Nicholls and Ferguson, 2002). It was shown that the rate of O_2^- generation depends on the respiratory state of mitochondria through the values of protonmotive force. In the absence of ADP (state 4), the movement of protons through ATP synthase ceases, the protonmotive force, the membrane potential and ΔpH have the highest values. Under these conditions, electron flow slows down, the respiratory chain becomes more reduced and as a result the formation of O_2^- increases. Transition of respiration state 4 to state 3 (in the presence of ADP) is accompanied by decrease of protonmotive force, which is assumed to alleviate O_2^- generation (Barja, 1999; Staniek and Nohl, 2000). It appears that most of ROS produced by mitochondria *in vivo* is correlated with ΔpH and/or $\Delta\Psi_m$ values.

The O_2^- formation can be also increased by specific inhibitors of respiratory chain complexes (rotenone for complex I, antimycin A for complex III), which stop the electron transport by all upstream carriers (Hansford et al., 1997; Liu et al., 2002; St-Pierre et al., 2002). Under this condition, the protonmotive force is zero. It remains unclear whether this mechanism has any significance for in vivo ROS production. Possibly, structural changes in respiratory chain enzymes blocking the electron transport could be the reason.

It seems that the UCP proteins have an important role in oxidative stress. It was shown that UCP2 expression might limit the free radical generation (Clapham et al., 2000; Lowell and Spiegelman, 2000). Echtay et al. (Echtay et al., 2002a; Echtay et al., 2002b) observed that an increase in superoxide caused activation of UCPs resulting in mild uncoupling. It indicated that the interaction of superoxide with UCPs might be a mechanism for decreasing Δp and thus the ROS production inside mitochondria. They assumed that mainly UCP2 and 3 might be more associated with protection against ROS than with thermogenesis (Echtay et al., 2002b).

The relationship between superoxide production and the components of protonmotive force ($\Delta\Psi_m$ and ΔpH) has been recently studied in detail by Brand's group (Lambert and Brand, 2004b; Lambert and Brand, 2004a). Earlier reports (Korshunov et al., 1997; Liu, 1997; Votyakova and Reynolds, 2001) have used uncouplers and/or inhibitors to show the

sensitivity of the $O_2^{\cdot-}$ formation to the $\Delta\Psi_m$, but under these conditions, the ΔpH and thus Δp were also influenced. Brand's group showed that Δp alters superoxide production mostly by a direct effect on complex I in rat skeletal muscle mitochondria. In particular, they demonstrated that a high ΔpH gradient across the inner mitochondrial membrane is required for high rates of superoxide production by complex I during reverse electron transport (Lambert and Brand, 2004b; Lambert and Brand, 2004a).

1.3.4.3 Antioxidant defenses

Superoxide anion is the precursor for most ROS (figure 8). Its dismutation (spontaneously or by superoxide dismutase) produces hydrogen peroxide (H_2O_2), which can be reduced to water (by catalase or glutathion peroxidase) or to hydroxyl radical OH· (by reduced transition metals), one of the strongest oxidants (Turrens, 2003). Moreover, $O_2^{\cdot-}$ can react with other radicals including nitric oxide (NO·) and the resulting peroxynitrite is also a very powerful oxidant (Beckman and Koppenol, 1996; Radi et al., 2002).

Since superoxide and its derivatives are highly reactive radicals, it is necessary to maintain their concentration at the lowest possible level. Both the cytoplasm and mitochondria are equipped with various antioxidant defenses. Mitochondrial superoxide dismutase with manganese in the active site (MnSOD) converts $O_2^{\cdot-}$ to H_2O_2 in the matrix or in the inner side of the inner mitochondrial membrane (Fridovich, 1995). The $O_2^{\cdot-}$ concentration in the intermembrane space is controlled by several mechanisms. First, an isoform of SOD with copper and zinc (Cu/ZnSOD) is localized there (Okado-Matsumoto and Fridovich, 2001) and it is also found in the cytosol of eukaryotic cells. Cytochrome *c*, which transports one electron from complex III to complex IV, can be reduced by $O_2^{\cdot-}$ (Butler et al., 1975) regenerating oxygen and the reduced form can transfer the electron to the cytochrome *c* oxidase. Thus, $O_2^{\cdot-}$ can contribute to the energy needed to pump protons through complex IV. Finally, lower pH in the intermembrane space facilitates spontaneous dismutation of superoxide (Guidot et al., 1995).

Hydrogen peroxide, the product of $O_2^{\cdot-}$ dismutation, is mostly degraded by glutathione peroxidase, which has very high activity especially in the liver (Chance et al., 1979). Another detoxifying enzyme, catalase that is present in peroxisomes, was found in

heart mitochondria as well (Radi et al., 1991); this enzyme has not been found in other tissues, including skeletal muscles (Phung et al., 1994).

In addition, other electron carriers appear to have detoxifying features. For example, in the presence of the substrate for complex II, succinate, the fully reduced form of coenzyme Q can act as a reducing agent for the elimination of various peroxides, unlike its partially reduced form (semiquinone), which is a source of $O_2^{\cdot-}$ (Beyer, 1990; Eto et al., 1992). Moreover, the inner mitochondrial membrane contains vitamin E, a powerful antioxidant (Ham and Liebler, 1995).

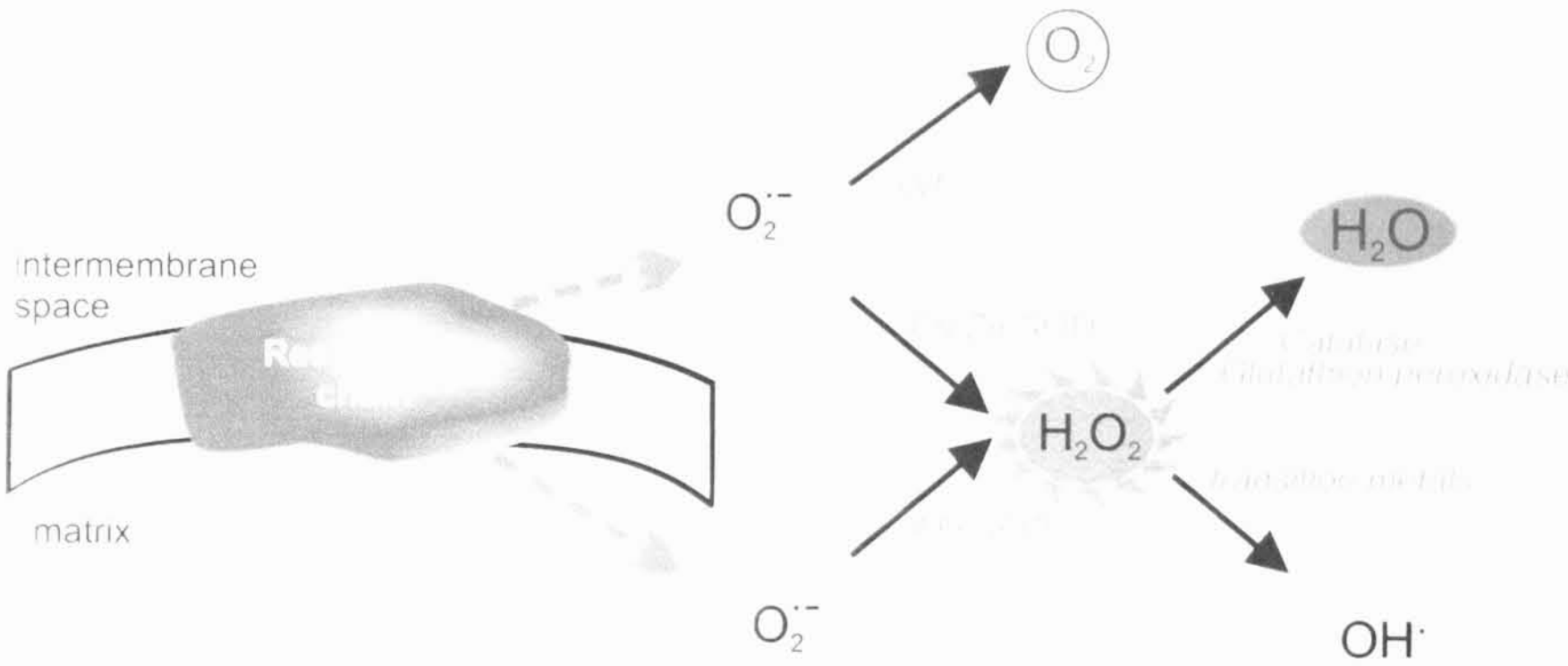

Figure 8
Antioxidant defenses.
Superoxide and its derivatives are shown. Cu/Zn SOD - cytosolic superoxide dismutase, MnSOD - mitochondrial superoxide dismutase, cyt c^3 - cytochome c.

1.3.5 Mitochondria and cell death

Cells die by two main pathways: necrosis associated with the plasma membrane lysis, and apoptosis (programmed cell death) resulting in digestion of cell contents minimizing its leakage (Nicholls and Ferguson, 2002). The family of proteases (caspases) plays a key role of the proteolytic digestion. They exist in non-apoptotic cells as inactive precursors and are activated by proteolytic cleavage. In 1996 it was found that during an activation of caspases cytochrome *c* is released (Green, 2000) and, together with cytoplasmic factor Apaf1 (apoptotic protease activating factor 1) and procaspase 9, it creates 'apoptosome'

capable of activating other caspases (figure 9). A second pathway for caspase activation, sufficient for apoptosis in some cells, is initiated by the binding of ligands to the tumor necrosis factor (TNF) family and this complex is able to activate caspases (Nicholls and Ferguson, 2002).

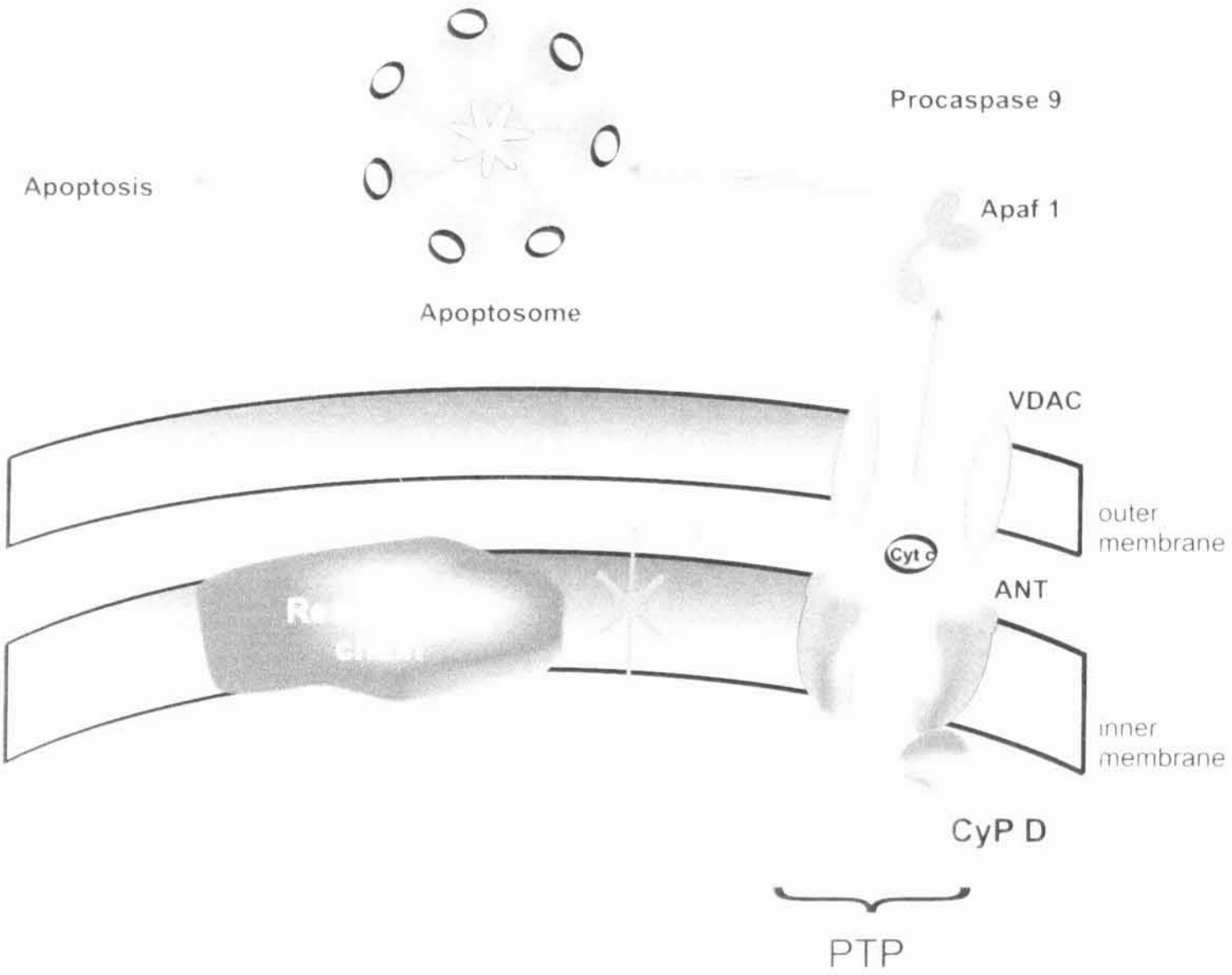

Figure 9
Apoptosis - programmed cell death.
Apaf1 - apoptotic protease activating factor 1; VDAC - voltage-dependent anion channel; ANT - adenine nucleotide transporter; CyP D - cyclophilin D; PTP - permeability transition pore.

The mechanism of cytochrome *c* release is poorly understood. There are two hypotheses: specific proteins form or activate a pore in the outer membrane allowing selective efflux of cytochrome *c* or non-selective rupture of the outer membrane occurring because of osmotic expansion after opening of the permeability transition pore (PTP).

The PTP is a large conductance pore formed by several proteins from both mitochondrial membranes. Its structure seems to include the adenine nucleotide translocator (ANT) in the inner mitochondrial membrane, the voltage-dependent anion channel (VDAC) in the outer membrane and cyclophilin D in the matrix. (Crompton, 2000) (figure 9). The PTP is opened by a combination of high $[Ca^{2+}]_m$, oxidative stress,

ATP depletion, high inorganic phosphate and mitochondrial depolarization (Crompton, 1999) and is non-selectively permeable for solutes up to about 1.5 kDa. The basic consequence of the PTP opening is the loss of the protonmotive force and efflux of mitochondrial calcium (Chernyak, 1997; Brustovetsky and Dubinsky, 2000).

It is clear that the PTP can be activated in cells under specialized conditions but it is currently unknown whether the PTP plays any role in cell physiology or whether it even exists except under pathophysiological conditions. Nevertheless, there is growing evidence suggesting that the PTP opening is a normal feature of mitochondrial physiology. Several groups have reported that transient openings of the PTP are associated with transient changes in the mitochondrial membrane potential (Huser and Blatter, 1999; De Giorgi et al., 2002).

1.3.6 Mitochondrial genetics and biology

Mitochondria retain a number of features that reflect their endosymbiotic origin. It includes a double membrane structure and circular mitochondrial genome with a specific replication, transcription, translation and protein assembly system. During the mammalian mitochondrial evolution, many mitochondrial genes have been transferred to the nucleus and mitochondrial genome has been reduced to about 16,500 base pairs (Wallace, 1982; Adams and Palmer, 2003). It remains unclear, why the mitochondria still retain genomes. A widely discussed hypothesis is that some highly hydrophobic proteins (e.g. COXII or ATP6) are difficult to import across the mitochondrial membrane and sort to the correct location (Popot and de Vitry, 1990).

The mitochondrion encodes only 13 subunits of the OXPHOS enzymes together with 12S and 16S rRNA genes and 22 tRNA genes required for mitochondrial protein synthesis (figure 10) (Wallace, 1999).

The mtDNA is maternally inherited (Giles et al., 1980) and has very high mutation rate. When mutation arises, cells contain a mixture of wild type and mutant mtDNA, which is called heteroplasmy. During cell division the mutant and wild type mtDNA are randomly distributed, which can lead to segregation of any one type of mtDNA (homoplasmy). When the percentage of mutant mtDNA exceeds a certain value, the cellular energy expenditure declines below bioenergetic threshold essential for cell life. Beyond this value, disease symptoms appear (Scriver et al., 1995; Wallace, 1999;

Rossignol et al., 2003). It has been shown that the same mtDNA mutation can cause particularly different symptoms among members of the affected family in association with the heteroplasmy. OXPHOS enzymes can also be affected by mutations in nDNA with phenotypes similar to those of mtDNA origin (Wallace, 1999).

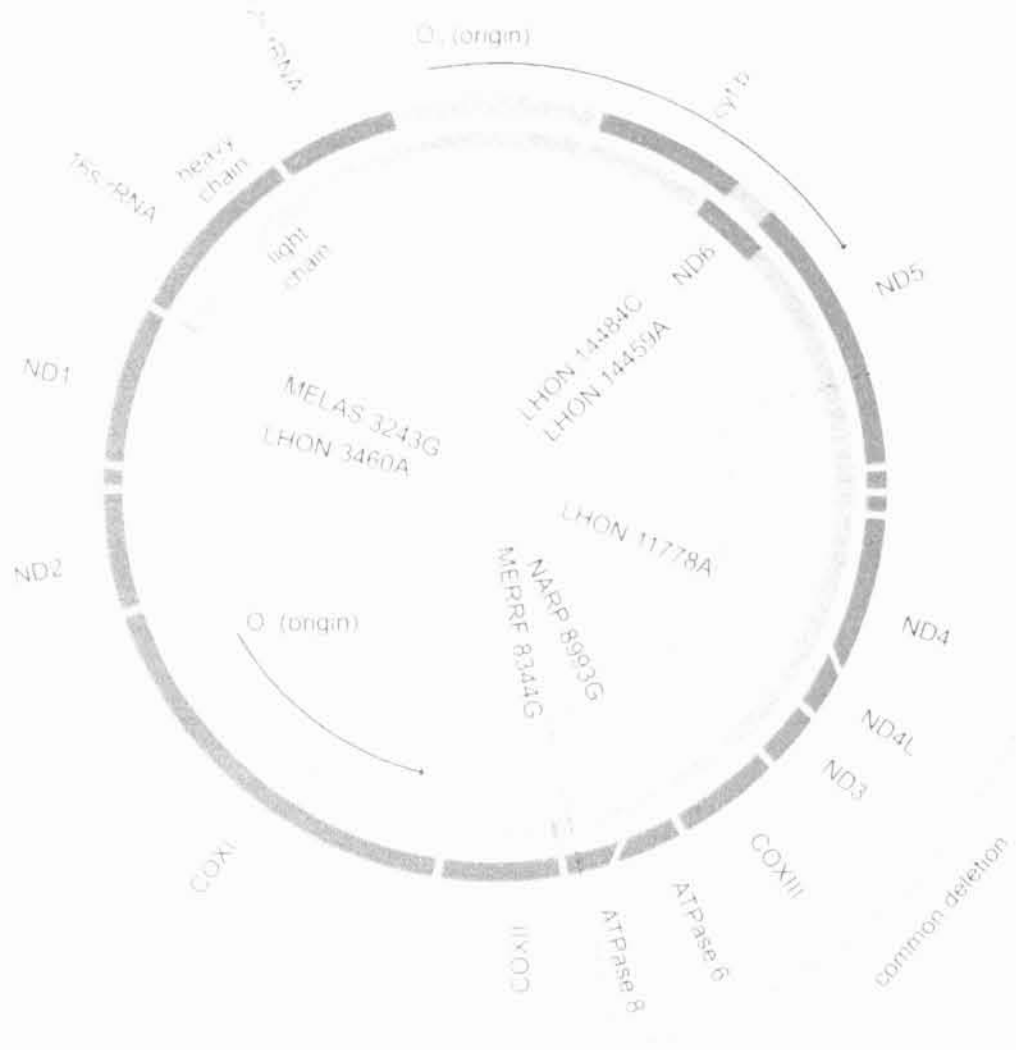

Figure 10
The human mitochondrial genome.
The double helix can be separated into light and heavy chain. Light chain (orange) encodes tRNAse (white boxes) and one complex I subunit (ND6), while the heavy chain (green) encodes six complex I subunits (ND1, ND2, ND3, ND4L, ND4 and ND5), cytochrome b (cyt b), three complex IV subunits (COXI, COXII and COXIII), two ATP synthase subunits (ATPase 6, ATPase 8) and the 14 tRNAse. Sites of point mutation are marked and the region of common deletion is outlined (see text for details).

Three of the most important aspects of the mitochondrial OXPHOS disease pathogenesis are energy deprivation, generation of reactive oxygen species and regulation of apoptosis. Mitochondrial PTP can be initiated by excessive mitochondrial uptake of calcium, increased exposure to ROS or a decline in energetic capacity. The opening of the PTP causes collapse of Δp, swelling of mitochondria and release of death-promoting factors (Zoratti and Szabo, 1995; Liu et al., 1996; Green and Reed, 1998; Crompton, 1999; Susin et al., 1999).

1.3.7 Mitochondrial diseases

Mitochondrial defects occur in a broad variety of degenerative diseases, aging and cancer. More than 200 mtDNA point mutations, deletions and insertion have been identified in a variety of degenerative diseases (MITOMAP: A Human Mitochondrial Genome Database. http://www.mitomap.org). During the last decade, it has been shown that mitochondrial diseases associate also with mutations in nuclear genes that encode subunits of OXPHOS proteins, OXPHOS-specific assembly proteins or different components of mtDNA and protein synthesis machineries (Shoubridge, 2001b).

Oxidative phosphorylation defects can result in a variety of multisystem disorders primarily affecting tissues with high-energy demands. The mitochondrial diseases range from severe encephalopathies of early childhood to milder disorders of adults. Depending on the type of the genetic defects (in mtDNA or nDNA), the mitochondrial disorder transmission can be maternal or Mendelian, some of the most severe disorders are acquired.

1.3.7.1 mtDNA mutations

Pathogenic mutations of mtDNA include point mutations and rearrangement (deletion/duplication, insertion). Point mutations have been identified in tRNA, rRNA and structural genes and are more common than mtDNA rearrangements. Clinical phenotypes of mitochondrial diseases can diverge or overlap because a given mtDNA mutation can produce different phenotypes, while very similar phenotypes can be caused by different mutations.

Mutations in structural genes

The most frequent mtDNA mutations in structural genes associate with complex I and complex V. **LHON** – Leber hereditary optic neuropathy is typically caused by mutations in genes for complex I subunits ND1, ND4 and ND6. These mutations are usually homoplasmic resulting in visual loss due to optic nerve atrophy.

The most common mutation in complex V genes is transition of T to G in position 8993 in *ATP6* gene encoding subunit a, a part of the proton channel in the F_o domain of ATP synthase. Depending on the mutation load the mutations can manifest either as

Leigh's syndrome (nearly homoplasmic mutation load) or as **NARP** (neurogenic muscle weakness, ataxia and retinitis pigmentosa) when less than 75% of mutated mtDNA is present. Leigh's syndrome is an early-onset, neurodegenerative disease characterized by bilateral lesions in the brainstem (Shoffner et al., 1992; Tatuch et al., 1992; Ortiz et al., 1993), which are absent in NARP.

Mutations in tRNA

Mutations in mitochondrial protein synthesis genes can cause different symptoms including encephalopathies or myopathies with ragged red fibers (RRF) (Scriver et al., 1995; Rosenberg et al., 1997; Wallace, 1999) but specific mutations also associate with specific clinical manifestation. For example the mtDNA mutation at position 8344 in $tRNA^{Lys}$ gene results in myoclonical epilepsy and RRF (MERRF) (Wallace et al., 1988; Shoffner IV et al., 1990). Another mutation in $tRNA^{Leu}$ gene at position 3243 associates with stroke-like activity and mitochondrial myopathy (MELAS) when more than 85% of mutated mtDNA is present (Goto et al., 1990) or diabetes mellitus and deafness when the percentage of mutated mtDNA decreases under 30% (Gerbitz et al., 1995; Goto, 1995). Milder mitochondrial protein synthesis mutations can be homoplasmic, affecting only central nervous system such as mutation in $tRNA^{Gln}$ gene at position 4336, which is associated with Alzheimer's disease (Shoffner et al., 1993).

Deletions of mtDNA

Diseases resulting from mtDNA rearrangements include chronic progressive external ophtalmopelia (**CPEO**), Kearns-Sayre syndrome (**KSS**), maternally inherited diabetes mellitus and deafness (Ballinger et al., 1992; Ballinger et al., 1994). CPEO and KSS patients suffer from mitochondrial myopathy ophtalmoplegia and ptosis (droopy lids) and some have cardiac defects, renal problems and other symptoms (Mita et al., 1989; Shoubridge et al., 1990; Heddi et al., 1994).

1.3.7.2 nDNA mutations

Mitochondrial diseases resulting from the mutation in nDNA exhibit Mendelian inheritance patterns but still share many clinical features with the diseases caused by mutations in mtDNA. Mutations affecting several genes essential for mtDNA replication result in multiple mtDNA deletions or decreased cellular content of mtDNA - mtDNA

depletion. In addition, increasing number of mutations has been reported in the last decade that cause specific, isolated defects of individual OXPHOS complexes.

Up to now, specific defects of nuclear origin have been found in all mitochondrial respiratory chain complexes including COX (Shoubridge, 2001a; Pecina et al., 2004) and ATPase (Houstek et al., 1999).

Cytochrome c oxidase deficiencies

COX defects originating from mutations in nuclear genome (Tiranti et al., 1998; Zhu et al., 1998; Papadopoulou et al., 1999; Robinson, 2000; Pecina et al., 2004) often manifest in the first months of life and the prognosis is very serious or fatal. So far, no mutations in the nuclear genes for COX subunits have been located, but numerous mutations in the genes encoding COX assembly proteins have been described. The dysfunction of COX due to these mutations is caused by structural changes and/or changes in the amount of the enzyme. The mutations in *SCO1*, *SCO2* and *COX15* genes are usually manifested as cardiomyopathies (Papadopoulou et al., 1999; Robinson, 2000; Antonicka et al., 2003b), mutation in the *COX10* gene resulted in multiple early-onset clinical phenotypes (Antonicka et al., 2003a). The most common COX assembly disorders are caused by mutations in the *SURF1* gene (Tiranti et al., 1998; Zhu et al., 1998), which are frequently manifested as COX-associated Leigh syndrome – subacute necrotizing encephalopathy (DiMauro et al., 1986).

ATP synthase deficiencies

ATPase defects of nuclear origin are characterized as a selective decrease of ATPase content caused by diminished ATPase biosynthesis. Since 1999 several cases of mitochondrial disorders of nuclear origin were described in the Czech Republic (Houstek et al., 1999; Vojtiskova et al., 2004), Belgium (De Meirleir et al., 2004) and Austria (Mayr et al., 2004). Most of the cases showed reduction of ATPase content below 30% of the control, early onset of the disease, cardiomyopathy and 3 methyl-glutaconic aciduria (Houstek et al., 2004). The possible cause for insufficient ATPase biosynthesis can be a limited production or mutation of some of the ATPase assembly proteins (Atpaf1p, Atpaf2p). The mutation of the *ATPAF2* gene was found in one of the patients from Belgium (De Meirleir et al., 2004), no mutation in structural or assembly genes were identified in other patients (unpublished data).

1.4 Monitoring of mitochondrial function by $\Delta\Psi_m$ measurement

The mitochondrial membrane potential cannot be assessed directly using the microelectrodes because of the size of the mitochondria. Consequently, indirect methods have been employed to monitor $\Delta\Psi_m$ in the cells, especially fluorescence methods. The early methods used radioisotopes, in which case the organelles have to be separated from the medium. Nowadays, the most common methods usually monitor the residual concentration of the membrane-permeable cations (e.g. phosphonium cations) using ion-selective electrodes. An alternative approach is to use membrane-permeable cationic fluorescent probes and monitor the change in their spectral properties. These dyes are also called potentiometric, slow or redistribution membrane-potential fluorescent dyes.

1.4.1 Membrane-permeable cation redistribution

Membrane-permeable cations (either phosphonium cations or cationic fluorochromes) are only suitable for the estimation of $\Delta\Psi_m$ because of the negative charge inside mitochondria. During incubation with mitochondria, they move across membranes until they reach electrochemical equilibrium. Under this condition, the distribution of the probe between aqueous phases at the two sides of the mitochondrial membrane obeys Nernst equation (Ehrenberg et al., 1988; Plasek and Sigler, 1996):

$$\Delta\Psi = -\frac{RT}{zF}\ln\frac{c_o}{c_i} \qquad (4)$$

where c_o and c_i are the concentrations of the cation outside and inside mitochondrion, z is the ion valency and R, T and F are gas constant, absolute temperature and Faraday constant, respectively. Thus, the increase of the cationic dyes concentration in mitochondria indicates hyperpolarization of the mitochondrial membrane.

If we incubate whole cells with the membrane-permeable cations, the voltage-dependent partitioning of the dye between medium, cytosol and matrix is described by the equations:

$$c_i = c_o\exp(-\frac{zF\Delta\Psi_p}{RT}) \qquad (5)$$

$$c_m = c_o\exp(-\frac{zF\Delta\Psi_m}{RT}) \qquad (6)$$

where $\Delta\Psi_p$ and $\Delta\Psi_m$ are plasma and mitochondrial membrane potentials, respectively, c_o, c_i and c_m are the concentrations of the dye in the medium, cytosol and matrix. To avoid the contribution of the plasma membrane potential it is possible to permeabilize cells by detergent, for example digitonin (Floryk and Houstek, 1999). Such treatment has the following advantages: (i) plasma membrane potential is dissipated, (ii) less time is necessary for the accumulation of cationic probes in mitochondria, and (iii) compounds influencing the $\Delta\Psi_m$ have better accessibility to the mitochondrial membrane.

1.4.2 $\Delta\Psi_m$ determination using radioisotopes or ion-selective electrodes

The radioisotope technique is based on the measurement of the distribution of β-emitter $^{86}Rb^+$ that substitutes K^+ in the presence of valinomycin. Isolated mitochondria are incubated with $^{86}Rb^+$, valinomycin and substrate. After centrifugation, the amount of isotope in the pellet is assessed, and the concentration of the isotope calculated. To perform this calculation, another indicator, e.g. [^{14}C] sucrose that cannot permeate the inner mitochondrial membrane, has to be present. The sucrose count indicates the volume of contaminating medium and allows correction of $^{86}Rb^+$ counts. It is also necessary to estimate the matrix volume by determination of the difference between [^{14}C] sucrose-permeable and ^3H_2O-permeable spaces (Rottenberg, 1984; Nicholls and Ferguson, 2002). The disadvantage of this method is the fixed value of the $\Delta\Psi_m$ corresponding to Nernst equilibrium for the pre-existing K^+ gradient across membrane.

This drawback can be avoided by using phosphonium cations, for example TPP^+ (tetraphenyl phosphonium). The positive charge of TPP^+ is shielded by hydrophobic groups and thus it can pass through the inner mitochondrial membrane in dependence on $\Delta\Psi_m$. The cation accumulation can be measured isotopically, or ion-selective electrode can be used. TPP^+-selective electrode allows the continuous monitoring of TPP^+ concentration in the medium and $\Delta\Psi_m$ can be calculated via Nernst-equation (Zolkiewska et al., 1989; Nicholls and Ferguson, 2002). Unfortunately, the $\Delta\Psi_m$ calculation in intact cells requires the values of the mitochondrial volume and the amount of TPP^+ that binds nonspecifically to the various cell membranes. Moreover, relatively high amounts of the sample are necessary.

1.4.3 $\Delta\Psi_m$ determination using fluorescence potentiometric dyes

Fluorescence-based measurements of the mitochondrial membrane potential can be carried out in individual cells using microfluorimetry as well as in cell suspensions using fluorimetry. It is necessary to pay attention to the selection of proper dye and method.

1.4.3.1 General properties of potentiometric dyes

Fluorescent potentiometric dyes used for monitoring of mitochondrial membrane potential are membrane-permeable cationic fluorochromes. It is assumed that their uptake by mitochondria is controlled by the mitochondrial membrane potential in accordance with Nernst equation. Each compound contains quaternary nitrogen with delocalized charge, which can increase their membrane permeability. The dye permeability can be also modified by structural features (e.g. the length of the alkyl chain in case of carbocyanines dyes influences dye hydrophobicity) (Nicholls and Ward, 2000).

The most widely used among fluorescent dyes suitable for the monitoring of membrane potential are carbocyanines and rhodamines. Carbocyanines were very popular in the early period of slow dye application (Plasek and Sigler, 1996). Rhodamines were first used to measure $\Delta\Psi_m$ in cells and can be used in both matrix quenching and non-quenching modes (Johnson et al., 1981). The third class of slow dyes are oxonols - anionic dyes which accumulate in the intracellular space of depolarized cells, but not in mitochondria with high negative-inside potentials. Thus, they are suitable only for monitoring of plasma membrane potential. Some of the redistribution dyes are listed in table 2.

Some groups have also used MitoTracker dyes (table 2) for monitoring of $\Delta\Psi_m$ changes (Macho et al., 1996; Matylevitch et al., 1998; Buckman et al., 2001). The MitoTrackers dyes (MitoTracker Green, MitoTracker Orange CMTMRos or MitoTracker Red CMXRos) contain chloromethyl groups that are thought to react with SH groups within the cell. MitoTracker Green is suggested to be $\Delta\Psi_m$-insensitive and thus it can be suitable for assessing the mitochondrial mass (Poot et al., 1996). On the other hand, MitoTrackers Orange (table 2) and Red are positively charged and it was shown that they can be $\Delta\Psi_m$-sensitive (Macho et al., 1996; Matylevitch et al., 1998), but it depends on the cell types (Buckman et al., 2001; Plasek et al., 2005). In addition, they partially inhibit the

activity of complex I, but these side effects can be reduced by using low dye concentration - less than 100 nM (Scorrano et al., 1999; Degli Esposti, 2001).

	dye	formula	absorption/emission λ_{max} (nm)
Carbocyanines	**$DiOC_6(3)$**	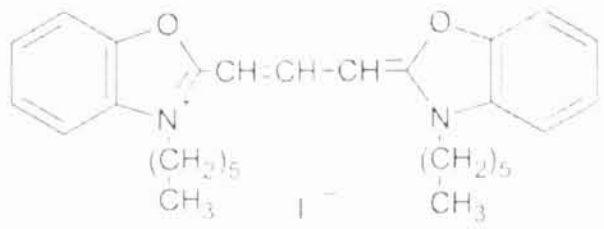	484/501
	JC-1	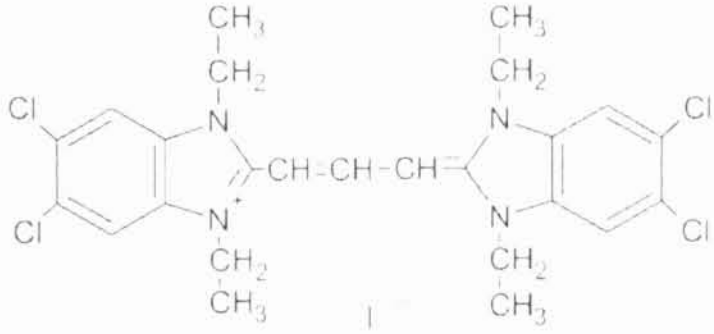	monomers 510/527 J-aggregates 510/590
Rhodamines	**Rhodamine 123**	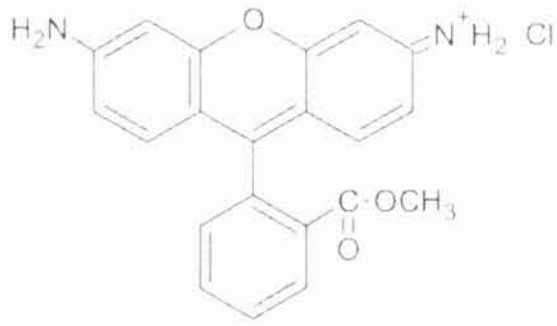	507/529
	TMRM	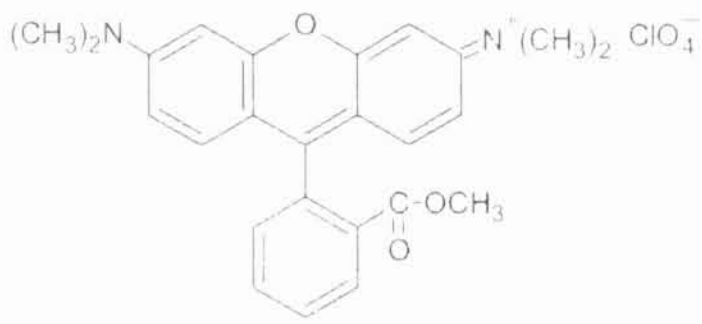	549/573
MitoTrackers	**MitoTracker Orange**	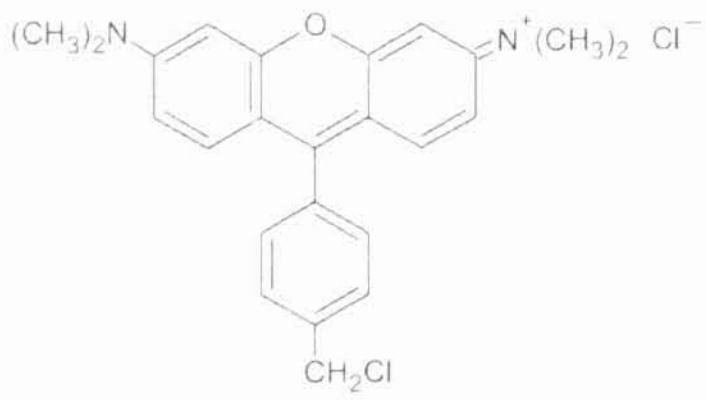	551/576

Table 2
Examples of redistribution dyes for mitochondrial membrane potential and their absorption and emission maxima.

1.4.3.2 Fluorescent properties of potentiometric dyes

After the accumulation of a slow dye in the mitochondria, changes of the probe absorption and fluorescence emission spectra are observed. Usually, the changes in apparent fluorescence intensity are only assessed. Such changes can be caused either by the formation of dye aggregates (dimers or higher aggregates), whose fluorescence emission spectra can be blue-shifted (H-aggregates) or red-shifted (J-aggregates) relative to those ones of monomers, or by the binding of the dye to matrix macromolecules (proteins etc.). The spectral effects are usually accompanied by changes in fluorescence lifetime and quantum yield (Sims et al., 1974; Emaus et al., 1986; Plasek and Hrouda, 1991; Plasek and Sigler, 1996). These changes depend on the properties of a given dye, its concentration, and the cell density, as well as on the fluorimeter set up.

The spectral properties of carbocyanines are controlled by the solvent polarity and by the second heteroatom (i.e. I, O or S). They are also influenced by the number of methine groups in the bridge between the rings. For example carbocyanines with pentamethine bridges ($-C_n(5)$) have a strong tendency to form aggregates contrary to those with trimethine bridges ($-C_n(3)$). On the other hand, carbocyanines are relatively insensitive to the length of alkyl chains (Sims et al., 1974; Tsien and Hladky, 1978).

In rhodamines, a red shift of absorption and fluorescence emission spectra (about 10 nm) is observed. In contrast to carbocyanines, no concentration-dependent formation of aggregates was found with rhodamines (Emaus et al., 1986). Rhodamine 123, tetramethylrhodamine methyl ester (TMRM) and tetramethylrhodamine ethyl ester (TMRE) were considered to be sensitive and specific probes for $\Delta\Psi_m$ in isolated rat liver mitochondria (Emaus et al., 1986; O'Connor et al., 1988; Scaduto and Grotyohann, 1999) and also in permeabilized cells (Floryk and Houstek, 1999).

1.4.3.3 Dye selection

Potentiometric dyes share a number of drawbacks for their use, including self-quenching or toxicity. Before starting the experiment, an optimal dye-loading protocol should be designed for given cell type, cell number and detection technology. The dye concentration should be sufficient to yield optimal signal-to-noise ratio without compromising mitochondrial function. The emphasis should be put on maximizing

detection gain or on increasing amount of the sample rather than increasing dye concentration. However, just increasing the intensity of excitation may cause photobleaching or radical formation. Finally, while selecting appropriate fluorescent probe not only its properties but also compatibility with the technique should be considered (Dykens and Stout, 2001).

$DiOC_6(3)$

3,3′-dihexyloxacarbocyanine iodide [$DiOC_6(3)$] belongs to the large family of carbocyanine dyes. It has been used as an indicator of mitochondrial membrane potential. Unfortunately, $DiOC_6(3)$ also stains endoplasmic reticulum (Dykens and Stout, 2001). According to Rottenberg et al. (Rottenberg and Wu, 1998) $DiOC_6(3)$ staining is selective for mitochondria only at concentrations below 1 nM. $DiOC_6(3)$ may also inhibit mitochondrial respiration (Rottenberg and Wu, 1998; Dykens and Stout, 2001).

JC – 1

JC-1 (5, 5′, 6, 6′- tetrachloro -1, 1′, 3, 3′- tetraethylbenzimidazolylcarbocyanineiodide) differs from the other potentiometric dyes in its ability to display the changes in its $\Delta\Psi_m$-driven mitochondrial accumulation by marked changes in the color of emission. At low concentration or low $\Delta\Psi_m$, JC-1 exhibits green fluorescence, whereas at a higher concentration or higher $\Delta\Psi_m$ the dye forms J-aggregates that emit red fluorescence (Reers et al., 1995). This is in contrast to the self-quenching in rhodamines that occurs upon their aggregation at high concentrations. This means that JC-1 can be used as a ratiometric indicator of mitochondrial membrane potential. Cossarizza et al. (Cossarizza et al., 1996) showed that the ratio of monomer to J-aggregate fluorescence was proportional to $\Delta\Psi_m$ (Reers et al., 1991). Therefore, the spectral properties of JC-1 are suitable for the visualization of mitochondria in living cells using fluorescence microscopy as well as for cytofluorimetric analyses (Smiley et al., 1991; Reers et al., 1995). The main drawback associated with this probe is that fairly complicated instruments are required for ratiometric measurements. With JC-1, a drop in $\Delta\Psi_m$ is theoretically reflected in both the increase in the green fluorescence and the decrease in red fluorescence. Di Lisa et al. (Di Lisa et al., 1995) reported that the primary response to depolarization is a spectral shift to red fluorescence. However, another group has reported that depolarization caused an increase in green fluorescence in the cytosol (Scanlon and Reynolds, 1998).

Rhodamine 123

An alternative to $DiOC_6(3)$ is rhodamine 123 - a very popular probe for monitoring mitochondrial membrane potential. However, it suffers from several limitations associated with the use of slow potentiometric dye. For example, it exhibits an extensive self-quenching, inhibits the respiration and uncouples mitochondria significantly at micromolar probe concentrations, and its non-specific binding to mitochondria compromises its Nernstian distribution (Emaus et al., 1986; Bunting et al., 1989; Scaduto and Grotyohann, 1999). In addition, phototoxicity is another side effect one must take care to avoid with this dye (Nicholls and Ward, 2000).

TMRM and TMRE

Tetramethylrhodamine methyl (or ethyl) ester (TMRM, TMRE) have very similar structure as rhodamine 123 and they were introduced in 1988 by Ehrenberg and colleagues (Ehrenberg et al., 1988). These dyes, especially TMRM, are more permeable than rhodamine 123 (Bunting, 1992; Vergun et al., 1999) and have much lower non-Nerstian binding to the cell than rhodamine 123 due to lower hydrophobicity (Ehrenberg et al., 1988).

It should be noted that TMRM and TMRE also inhibit respiration but at much higher concentration than rhodamine 123 or carbocyanines. The relative degree of respiration inhibition is following: TMRE > rhodamine 123 > TMRM. Summarized, TMRM appears to be the most suitable fluorescence probe for determination of $\Delta\Psi_m$ in a concentration lower than 1 μM (Scaduto and Grotyohann, 1999) using various methods (Floryk and Houstek, 1999; Duchen et al., 2003).

1.4.3.4 Techniques for fluorescence detection of $\Delta\Psi_m$

The $\Delta\Psi_m$ can be measured by fluorescent dyes in either quenching or non-quenching mode. Quenching of the dye fluorescence can be observed in the suspension of mitochondria or whole cells. In this case, dyes are loaded into the cells at relatively high concentrations (~1-20 μM) for a short period (15-20 min). As the dye accumulates into the mitochondria, its concentration exceeds a certain limit and non-fluorescent aggregates occur. Mitochondrial depolarization causes redistribution of the dye into the cytosol that is followed by increase in fluorescence intensity (Duchen et al., 2003). Obviously, the fluorescence signal is a non-linear function of dye concentration in this case, and thus this

approach is useless in attempting to compare $\Delta\Psi_m$ in populations of cells in response to manipulations. Additionally, the concentration is too high and thus could be toxic for the cells (see above).

The non-quenching mode is employed in fluorescence microscopy or flow cytometry and it is possible to use very low concentrations of the dye. In these circumstances, the redistribution of the dye between mitochondria and its environment obeys Nernst equation and the depolarization of mitochondria is indicated by a decrease in probe fluorescence intensity (Fink et al., 1998; Buckman and Reynolds, 2001; Wong and Cortopassi, 2002).

Spectrofluorimetry in suspension

This assay is the easiest and thus very frequent method for the estimation of $\Delta\Psi_m$ in both quenching and non-quenching mode. Great care must be taken in the selection of the fluorescent probe and the experimental conditions because many factors can interfere with $\Delta\Psi_m$ signal, e.g. variations in plasma membrane potential (in the case of intact cells) or the accumulation of the probe in other cell organelles. Moreover, the acquired signal is the average of all the fluorescence changes in the cell suspension. This phenomenon can be avoided by measurement in quenching mode or investigation of isolated mitochondria (Nicholls and Ferguson, 2002).

Flow cytometry

In flow cytometry experiments, the total fluorescence of each individual cell in a large cell population is determined. In most flow cytometers scattered light in both forward and side direction is also estimated, which provides information about cell volume and granularity, respectively. Typically, cell suspension is incubated with fluorescent probe and then the cellular fluorescence as well as scattered light are measured. A typical measurement is displayed in figure 11. Since cytofluorimetric assays of $\Delta\Psi_m$ measure the fluorescence intensities associated with cells, the fluorescence dyes whose response is based on quenching are not suitable. The best dyes for flow cytometry are rhodamine derivates TMRM or TMRE (Floryk and Houstek, 1999). Carbocyanines with trimethine bridges and JC-1 are also suitable (Cossarizza et al., 1993; Plasek and Sigler, 1996).

It should be noted that, in the case of intact cells, the flow cytometry measures the mean signal from the whole cell, i.e. $\Delta\Psi_p$ also contributes to this signal. This means that the fluorescence signal can change after depolarization of plasma membrane without any change in $\Delta\Psi_m$. On the other hand, depolarization of mitochondria causes redistribution of

the dye to cytosol, but the fluorescence signal from the whole does not change (Duchen et al., 2003). To avoid these problems, the cells should be permeabilized by detergent (Floryk and Houstek, 1999).

Figure 11
A typical cytofluorimetric measurement.
Permeabilized human skin fibroblasts were loaded for 15 min by 20 nM TMRM with or without uncoupler (FCCP). Left panel – decrease of TMRM signal after uncoupling; right panel – homogeneous cell population.

Confocal microscopy

For the measurement of $\Delta\Psi_m$ changes by confocal microscopy, both quenching and non-quenching mode can be used. The measurements in the non-quenching mode are based on the principle that, at very low concentration, the dye redistributes according to the Nernst equation (figure 12). High-resolution imaging is necessary for the accurate measurements and it is important to remove out-of-focus signal by de-blurring algorithm. This issue is carefully discussed by Fink et al. (Fink et al., 1998). The approach can be used in dynamics measurements, e.g. $\Delta\Psi_m$ change in response to pharmacological treatment. In such experiments, the dye redistributes to cytosol in response to mitochondrial depolarization, which is followed by dye re-equilibration between cytosol and extracellular environment due to plasma membrane potential (Duchen et al., 2003).

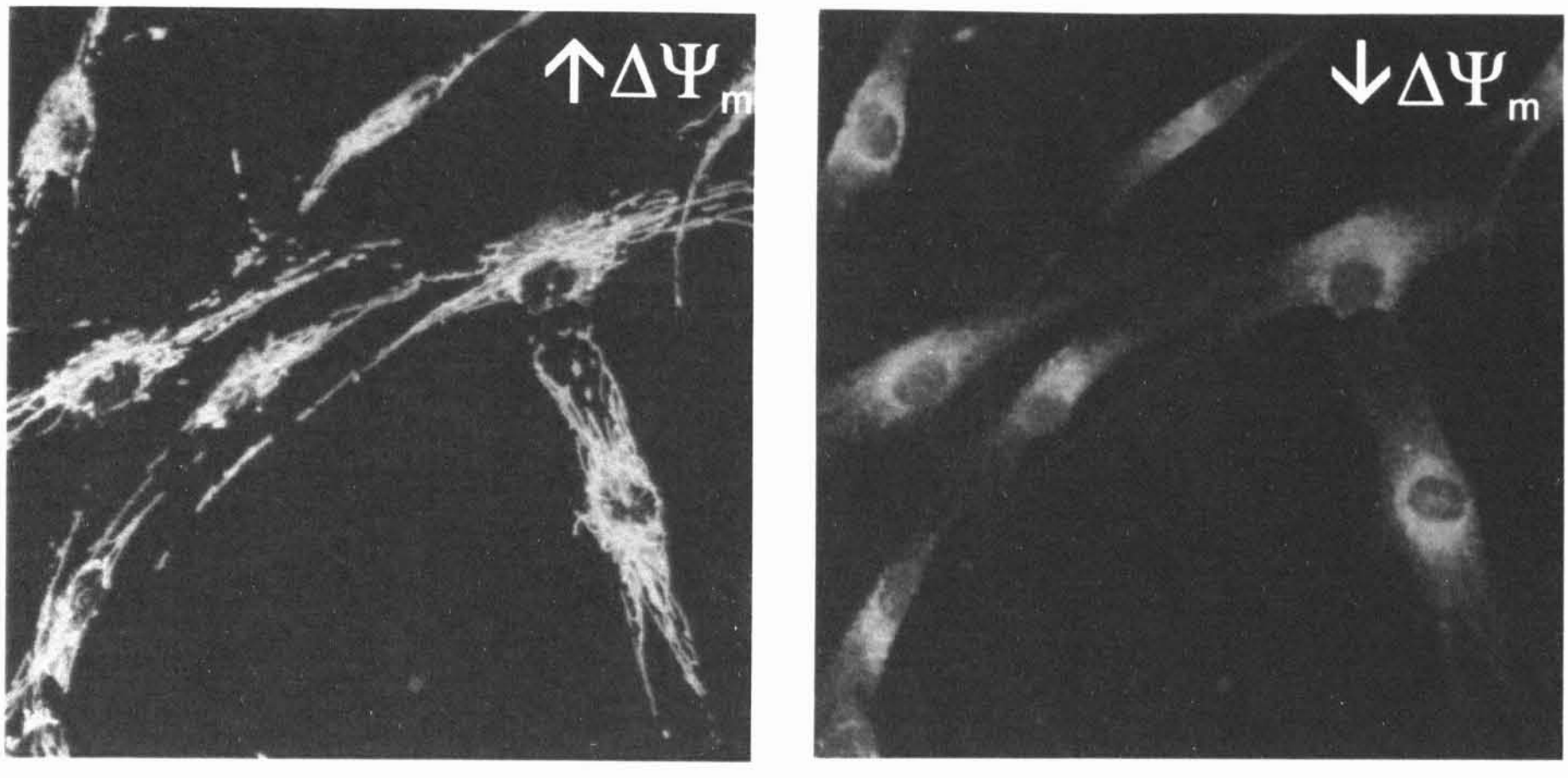

Figure 12
Mitochondrial membrane potential analyzed by confocal microscope.
Intact human skin fibroblasts were labeled with 20 nM TMRM for 30 min. Left panel – TMRM is accumulated in energized mitochondria; right panel - TMRM is released into cytosol after uncoupling.

The problem arises when the average signal across a cell is measured. In this case, the mean signal may not change at all after mitochondrial depolarization. Therefore, several groups used the quenching mode resulting in increase of fluorescence signal after depolarization. As the fluorescence signal is a non-linear function of dye concentration, this approach cannot be used in attempting to compare $\Delta\Psi_m$ in populations of cells (Duchen et al., 2003; Duchen, 2004).

Fluorescence resonance energy transfer (FRET)

In this method, the energy of emission of one dye is transferred to a second dye molecule with no photon emission, resulting in the quenching of the first, along with the corresponding excitation and emission of the second dye. The extent of energy transfer in FRET is altered by numerous factors (e.g. the extent of overlap between emission and excitation spectra of the dye pairs), as well as physical characteristics of the dyes (e.g. dipole orientations). However, the principal factor in defining the efficiency of FRET is the proximity of the exchanging dye molecules.

Dykens and colleagues (Dykens and Stout, 2001) developed the FRET assay for $\Delta\Psi_m$ based on FRET between two dyes, both localized to mitochondria. The excitation dye

is nonyl acridine orange (NAO) which stains cardiolipin (diphosphatidyl glycerol), the mitochondrial specific lipid, and the second dye is TMRM (or TMRE), which is sequestered into the mitochondrial matrix by $\Delta\Psi_m$. FRET between these two dyes occurs only when $\Delta\Psi_m$ exists and TMRM enters the matrix (Dykens and Stout, 2001).

Calibration of probe response

Finally, all the techniques outlined here are designed to measure relative changes in $\Delta\Psi_m$. If an absolute value of $\Delta\Psi_m$ is required, the probe response must be calibrated, which is quite difficult. The most widely used calibration is based on the $\Delta\Psi_m$ clamping to potassium equilibrium diffusion potentials - method described by Di Lisa et al. (Di Lisa et al., 1995). This protocol works only with mitochondria or permeabilized cells (Plasek and Sigler, 1996; Dykens and Stout, 2001).

In this procedure, the cells are measured in the presence of defined potassium concentrations and the potassium diffusion potential is created by the subsequent addition of a saturating amount of valinomycin. The membrane potential is calculated according to the Nernst equation and it is assumed that matrix potassium concentration is equal 120 mM (Rossi and Azzone, 1969; Di Lisa et al., 1995).

2 The aims of the thesis

During studies of molecular mechanisms of mitochondrial dysfunction, the prominent role of Δp becomes evident. This central energetic parameter of the mitochondria may trigger the cascade of cellular events resulting in cellular dysfunction and cell death. Therefore, detailed and sensitive measurements of Δp, mainly by means of $\Delta\Psi_m$ analysis, represent very powerful tool for both research and diagnostic studies of human mitochondrial diseases.

The present thesis was focused on the dynamics of the mitochondrial membrane potential, $\Delta\Psi_m$, and its role in etiopathology of mitochondrial disorders. The primary aim of the study was to develop a cytofluorimetric method for assessment of the changes in $\Delta\Psi_m$ in cultured cells, especially human skin fibroblasts as the most frequent and accessible material for study of mitopathies. The technique was then applied in combination with other functional methods in studies of a number of specific mitochondrial diseases associated with the defects of either $\Delta\Psi_m$ formation or utilization in patients harboring various types of defects in mitochondrial and cellular function.

The method was sensitive enough for detailed characterization of pathogenic mechanisms and proved to be both easy and accessible for diagnostic screening of mitochondrial disorders. All the mitochondrial membrane potential measurements were performed by the author of the thesis.

3 Summary of the results

The thesis consists of seven articles, in which studies of $\Delta\Psi_m$ have been performed on the following pathological models: COX deficiency due to mutations in SURF1 assembly factor, ATPase dysfunction due to mutations in mtDNA or nDNA and changes in mitochondrial biogenesis in cancer cells originating from kidney tumor.

1. Flow-cytometric monitoring of mitochondrial depolarisation: from fluorescence intensities to millivolts, *J. Plášek, A. Vojtíšková and J. Houštěk, Journal of Photochemistry and. Photobiology B: Biology, 78: 99-108, 2005.*

The first article describes the development of the method that makes it possible to measure the $\Delta\Psi_m$ changes in permeabilized cells in an absolute scale of millivolts. It employs the cytofluorimetric measurements of fluorescence of cells labeled with the cationic redistribution dye TMRM. The fluorescence intensity is proportional to TMRM concentration accumulated in mitochondria according to Nernst equation. This fact allows the logarithmic transformation of measured data to a linear scale of mitochondrial membrane potential. The theory was validated using the classical approach for $\Delta\Psi_m$ determination by TPP^+ electrode.

2. Functional alteration of cytochrome *c* oxidase by *SURF1* mutations in Leigh syndrome, *P. Pecina, M. Čapková, S.K.R. Chowdhury, Z. Drahota, A. Dubot, A. Vojtíšková, H. Hansíková, H. Houšťková, J. Zeman, C. Godinot and J. Houštěk, Biochimica et Biophysica Acta, 1639: 53-63, 2003.*

In the second article, the fibroblasts with cytochrome *c* oxidase (COX) deficiency due to mutation in *SURF1* gene were investigated. The *SURF1* gene encodes the assembly factor for COX and its absence results in lower steady-state levels COX and accumulation of incomplete forms of the enzyme. Using cytofluorimetric analysis of $\Delta\Psi_m$, we demonstrated that the proton-pumping activity of incomplete COX assemblies is impaired. This leads to decreased ability of cells to maintain $\Delta\Psi_m$ at functional load, which presents a possible pathogenic mechanism.

The next four articles deal with the defects of ATP synthase. In contrast to the COX deficiencies, ATPase defects are associated with impairment of utilization of $\Delta\Psi_m$ for ATP synthesis.

3. Mitochondrial membrane potential and ATP production in primary disorders of ATP synthase, *A. Vojtíšková, P. Ješina, , M. Kalous, V. Kaplanová M. Tesařová, D. Fornůsková, A. Dubot, J. Zeman, C. Godinot and J. Houštěk, Toxicology Mechanisms and Methods, 14: 7-11, 2004.*

While in the maternally inherited ATPase defects due to mitochondrial DNA (mtDNA) mutations in *ATP6* gene the enzyme is structurally and functionally modified, in ATPase defects of nuclear origin mitochondria contain a decreased amount of otherwise normal enzyme as thoroughly discussed in the third article.

4. GUG is an efficient initiation codon to translate the human mitochondrial *ATP6* gene, *A. Dubot, C. Godinot, V. Dumur, B. Sablonniere,T. Stojkovic, J.M. Cuisset, A. Vojtíšková, P. Pecina, P. Ješina and J. Houštěk, Biochemical and Biophysical Research Communications, 313: 687-693, 2004.*

The fourth paper summarizes our studies on a novel mutation in the initiation codon of *ATP6* gene (8527A>G) coding for subunit a of ATPase, which forms a proton channel and thus is crucial for $\Delta\Psi_m$ utilization. Surprisingly, measurements of $\Delta\Psi_m$ as well as other biochemical and functional analyses of patient cells harboring this mutation showed no differences from the data obtained with control cells. Most importantly, the analysis of mitochondrial protein synthesis using ^{35}S-methionine labeling revealed that despite the change of AUG to GUG initiation codon, the subunit a is present at normal steady-state levels. In accordance with this findings the cell respiration, maintenance of $\Delta\Psi_m$ and ATP synthesis is unchanged from control. The main conclusion of the paper is that, in human mtDNA, GUG can be used as an alternative initiation codon.

5. Diminished synthesis of subunit a (ATP6) and altered function of ATP synthase and cytochrome *c* oxidase due to the mtDNA 2 bp microdeletion of TA at position 9205 and 9206, *P. Ješina, M. Tesařová, D. Fornůsková, A. Vojtíšková, P. Pecina, V. Kaplanová, H. Hansíková, J. Zeman and J. Houštěk, Biochemical Journal, 383: 1-11, 2004.*

In contrast to the mutation in initiation codon, very severe functional changes result from another very rare mutation in *ATP6* gene, namely a two-base microdeletion in the

stop codon (9205ΔTA), which is described in the fifth paper. This mutation interferes with the *ATP6* transcript maturation and leads to its severe reduction. In accordance, the protein content is dramatically decreased and its absence in the assembled ATPase causes profoundly decreased ability of $\Delta\Psi_m$ utilization. This was demonstrated by cytofluorimetric analysis – in state 3, the $\Delta\Psi_m$ was higher in patient cells than in control. Correspondingly, ATP production in patient cells was pronouncedly depressed.

6. Mitochondrial diseases and ATPase defects of nuclear origin, *J. Houštěk, T. Mráček, A. Vojtíšková and J. Zeman, Biochimica et Biophysica Acta, 1658: 115-121, 2004.*

The sixth article describes the etiopathologic mechanisms of ATPase defects of nuclear origin. As mentioned above in these cases the biosynthesis of ATPase is down regulated due to a block at the early stage of enzyme assembly. The decreased amount of the enzyme results in a low capacity for efficient utilization of $\Delta\Psi_m$ and thus in hyperpolarization of the mitochondrial membrane. This article specifically shows that this bioenergetic abnormality leads to a dramatic increase of mitochondrial production of reactive oxygen species (ROS). We conclude that oxidative stress due to increase ROS production might be equally important for the etiopathology of ATPase disorders as the impairment of energy provision.

7. A new role for the von Hippel-Lindau tumor suppressor protein: stimulation of mitochondrial oxidative phosphorylation complex biogenesis, *E. Hervouet, J. Demont, P. Pecina, A. Vojtíšková, J. Houštěk, H. Simonnet and C. Godinot, Carcinogenesis, 26(3): 531-539, 2005.*

The last article deals with mitochondrial function and energetics of clear cell renal carcinoma (CCRC). These cells are characterized by bi-allelic inactivation of the von Hippel-Lindau (*VHL*) tumor suppressor gene, which encodes a protein involved in oxygen signaling to hypoxia-inducible transcription factor (HIF). Although CCRC culture cells suffer from a mitochondrial deficiency common to many types of cancer as originally described by Warburg (Warburg, 1956), our measurements showed that these cells are able to maintain normal values of $\Delta\Psi_m$. This fact indicates that the maintenance of $\Delta\Psi_m$ is essential for cell survival and growth and is achieved even at the cost of suppressed synthesis of ATP. Consequently, mitochondrial energy provision is severely decreased in these cancer cells and they have to rely on ATP supplied from glycolysis. This can be demonstrated by the inability of these cells to grow under the conditions requiring

oxidative phosphorylation, e.g. replacement of glucose by galactose in culture medium. The growth of CCRC cells on galactose could have been only restored after transfection and ectopic expression of wild-type VHL protein. Its expression increased mitochondrial biogenesis – mtDNA content, expression of OXPHOS enzyme and cell respiration. The stimulation of mitochondrial biogenesis described in this paper is a novel function for VHL protein.

4 References

Abramson, J., M. Svensson-Ek, B. Byrne and S. Iwata (2001). "Structure of cytochrome *c* oxidase: a comparison of the bacterial and mitochondrial enzymes." Biochim Biophys Acta **1544**(1-2): 1-9.

Adams, K. L. and J. D. Palmer (2003). "Evolution of mitochondrial gene content: gene loss and transfer to the nucleus." Mol Phylogenet Evol **29**(3): 380-395.

Alexander, C., M. Votruba, U. E. Pesch, D. L. Thiselton, S. Mayer, A. Moore, M. Rodriguez, U. Kellner, B. Leo-Kottler, G. Auburger, S. S. Bhattacharya and B. Wissinger (2000). "OPA1, encoding a dynamin-related GTPase, is mutated in autosomal dominant optic atrophy linked to chromosome 3q28." Nat Genet **26**(2): 211-215.

Allen, R. G. and M. Tresini (2000). "Oxidative stress and gene regulation." Free Radic Biol Med **28**(3): 463-499.

Andreyev, A. Y., Y. E. Kushnareva and A. A. Starkov (2005). "Mitochondrial metabolism of reactive oxygen species." Biochemistry (Mosc) **70**(2): 200-214.

Antonicka, H., S. C. Leary, G. H. Guercin, J. N. Agar, R. Horvath, N. G. Kennaway, C. O. Harding, M. Jaksch and E. A. Shoubridge (2003a). "Mutations in COX10 result in a defect in mitochondrial heme A biosynthesis and account for multiple, early-onset clinical phenotypes associated with isolated COX deficiency." Hum Mol Genet **12**(20): 2693-2702.

Antonicka, H., A. Mattman, C. G. Carlson, D. M. Glerum, K. C. Hoffbuhr, S. C. Leary, N. G. Kennaway and E. A. Shoubridge (2003b). "Mutations in COX15 produce a defect in the mitochondrial heme biosynthetic pathway, causing early-onset fatal hypertrophic cardiomyopathy." Am J Hum Genet **72**(1): 101-114.

Ballinger, S. W., J. M. Shoffner, S. Gebhart, D. A. Koontz and D. C. Wallace (1994). "Mitochondrial diabetes revisited [letter]." Nat.Genet. **7**: 458-459.

Ballinger, S. W., J. M. Shoffner, E. V. Hedaya, I. Trounce, M. A. Polak, D. A. Koontz and D. C. Wallace (1992). "Maternally transmitted diabetes and deafness associated with a 10.4 kb mitochondrial DNA deletion." Nat Genet **1**: 11-15.

Barja, G. (1999). "Mitochondrial oxygen radical generation and leak: sites of production in states 4 and 3, organ specificity, and relation to aging and longevity." J Bioenerg Biomembr **31**(4): 347-366.

Barja, G. (2002). "The quantitative measurement of H2O2 generation in isolated mitochondria." J Bioenerg Biomembr **34**(3): 227-233.

Barja, G. and A. Herrero (1998). "Localization at complex I and mechanism of the higher free radical production of brain nonsynaptic mitochondria in the short-lived rat than in the longevous pigeon." J Bioenerg Biomembr **30**(3): 235-243.

Beckman, J. S. and W. H. Koppenol (1996). "Nitric oxide, superoxide, and peroxynitrite: the good, the bad, and ugly." Am J Physiol **271**(5 Pt 1): C1424-1437.

Beyer, R. E. (1990). "The participation of coenzyme Q in free radical production and antioxidation." Free Radic Biol Med **8**(6): 545-565.

Bleazard, W., J. M. McCaffery, E. J. King, S. Bale, A. Mozdy, Q. Tieu, J. Nunnari and J. M. Shaw (1999). "The dynamin-related GTPase Dnm1 regulates mitochondrial fission in yeast." Nat Cell Biol **1**(5): 298-304.

Bolter, C. J. and W. Chefurka (1990). "Extramitochondrial release of hydrogen peroxide from insect and mouse liver mitochondria using the respiratory inhibitors phosphine, myxothiazol, and antimycin and spectral analysis of inhibited cytochromes." Arch Biochem Biophys **278**(1): 65-72.

Boveris, A. (1984). "Determination of the production of superoxide radicals and hydrogen peroxide in mitochondria." Methods Enzymol **105**: 429-435.

Boveris, A. and E. Cadenas (1975). "Mitochondrial production of superoxide anions and its relationship to the antimycin insensitive respiration." FEBS Lett **54**(3): 311-314.

Boveris, A., E. Cadenas and A. O. Stoppani (1976). "Role of ubiquinone in the mitochondrial generation of hydrogen peroxide." Biochem J **156**(2): 435-444.

Brand, M. D. (1985). "The stoichiometry of the exchange catalysed by the mitochondrial calcium/sodium antiporter." Biochem J **229**(1): 161-166.

Brookes, P. S., Y. Yoon, J. L. Robotham, M. W. Anders and S. S. Sheu (2004). "Calcium, ATP, and ROS: a mitochondrial love-hate triangle." Am J Physiol Cell Physiol **287**(4): C817-833.

Brustovetsky, N. and J. M. Dubinsky (2000). "Dual responses of CNS mitochondria to elevated calcium." J Neurosci **20**(1): 103-113.

Buckman, J. F., H. Hernandez, G. J. Kress, T. V. Votyakova, S. Pal and I. J. Reynolds (2001). "MitoTracker labeling in primary neuronal and astrocytic cultures: influence of mitochondrial membrane potential and oxidants." J Neurosci Methods **104**(2): 165-176.

Buckman, J. F. and I. J. Reynolds (2001). "Spontaneous changes in mitochondrial membrane potential in cultured neurons." J Neurosci **21**(14): 5054-5065.

Bunting, J. R. (1992). "Influx and efflux kinetics of cationic dye binding to respiring mitochondria." Biophys Chem **42**(2): 163-175.

Bunting, J. R., T. V. Phan, E. Kamali and R. M. Dowben (1989). "Fluorescent cationic probes of mitochondria. Metrics and mechanism of interaction." Biophys J **56**(5): 979-993.

Butler, J., G. G. Jayson and A. J. Swallow (1975). "The reaction between the superoxide anion radical and cytochrome *c*." Biochim Biophys Acta **408**(3): 215-222.

Cadenas, E., A. Boveris, C. I. Ragan and A. O. Stoppani (1977). "Production of superoxide radicals and hydrogen peroxide by NADH-ubiquinone reductase and ubiquinol-cytochrome *c* reductase from beef-heart mitochondria." Arch Biochem Biophys **180**(2): 248-257.

Cadenas, E. and K. J. Davies (2000). "Mitochondrial free radical generation, oxidative stress, and aging." Free Radic Biol Med **29**(3-4): 222-230.

Clapham, J. C., J. R. Arch, H. Chapman, A. Haynes, C. Lister, G. B. Moore, V. Piercy, S. A. Carter, I. Lehner, S. A. Smith, L. J. Beeley, R. J. Godden, N. Herrity, M. Skehel, K. K. Changani, P. D. Hockings, D. G. Reid, S. M. Squires, J. Hatcher, B. Trail, J. Latcham, S. Rastan, A. J. Harper, S. Cadenas, J. A. Buckingham, M. D. Brand and A. Abuin (2000). "Mice overexpressing human uncoupling protein-3 in skeletal muscle are hyperphagic and lean." Nature **406**(6794): 415-418.

Collinson, I. R., M. J. Runswick, S. K. Buchanan, I. M. Fearnley, J. M. Skehel, M. J. van Raaij, D. E. Griffiths and J. E. Walker (1994). "Fo membrane domain of ATP synthase from bovine heart mitochondria: purification, subunit composition, and reconstitution with F1-ATPase." Biochemistry **33**: 7971-7978.

Cossarizza, A., M. Baccarani-Contri, G. Kalashnikova and C. Franceschi (1993). "A new method for the cytofluorimetric analysis of mitochondrial membrane potential using the J-aggregate forming lipophilic cation 5,5',6,6'-tetrachloro-1,1',3,3'-tetraethylbenzimidazolcarbocyanine iodide (JC-1)." Biochem Biophys Res Commun **197**: 40-45.

Cossarizza, A., D. Ceccarelli and A. Masini (1996). "Functional heterogeneity of an isolated mitochondrial population revealed by cytofluorometric analysis at the single organelle level." Exp Cell Res **222**: 84-94.

Crompton, M. (1999). "The mitochondrial permeability transition pore and its role in cell death." Biochem J **341 (Pt 2)**: 233-249.

Crompton, M. (2000). "Mitochondrial intermembrane junctional complexes and their role in cell death." J Physiol **529 (Pt 1)**: 11-21.

Darley-Usmar, V. and R. White (1997). "Disruption of vascular signalling by the reaction of nitric oxide with superoxide: implications for cardiovascular disease." Exp Physiol **82**(2): 305-316.

De Giorgi, F., L. Lartigue, M. K. Bauer, A. Schubert, S. Grimm, G. T. Hanson, S. J. Remington, R. J. Youle and F. Ichas (2002). "The permeability transition pore signals apoptosis by directing Bax translocation and multimerization." Faseb J **16**(6): 607-609.

De Meirleir, L., S. Seneca, W. Lissens, I. De Clercq, F. Eyskens, E. Gerlo, J. Smet and R. Van Coster (2004). "Respiratory chain complex V deficiency due to a mutation in the assembly gene ATP12." J Med Genet **41**(2): 120-124.

Degli Esposti, M. (2001). "Assessing functional integrity of mitochondria in vitro and in vivo." Methods Cell Biol **65**: 75-96.

Delettre, C., G. Lenaers, J. M. Griffoin, N. Gigarel, C. Lorenzo, P. Belenguer, L. Pelloquin, J. Grosgeorge, C. Turc-Carel, E. Perret, C. Astarie-Dequeker, L. Lasquellec, B. Arnaud, B. Ducommun, J. Kaplan and C. P. Hamel (2000). "Nuclear gene OPA1, encoding a mitochondrial dynamin-related protein, is mutated in dominant optic atrophy." Nat Genet **26**(2): 207-210.

Di Lisa, F., P. S. Blank, R. Colonna, G. Gambassi, H. S. Silverman, M. D. Stern and R. G. Hansford (1995). "Mitochondrial membrane potential in single living adult rat cardiac myocytes exposed to anoxia or metabolic inhibition." J Physiol (Lond) **486**: 1-13.

DiMauro, S., M. Zeviani, S. Servidei, E. Bonilla, A. F. Miranda, A. Prelle and E. A. Schon (1986). "Cytochrome oxidase deficiency: clinical and biochemical heterogeneity." Ann NY Acad Sci **488**: 19-32.

Diwan, J. J., T. Haley and D. R. Sanadi (1988). "Reconstitution of transmembrane K+ transport with a 53 kilodalton mitochondrial protein." Biochem Biophys Res Commun **153**(1): 224-230.

Drahota, Z., S. K. Chowdhury, D. Floryk, T. Mracek, J. Wilhelm, H. Rauchova, G. Lenaz and J. Houstek (2002). "Glycerophosphate-dependent hydrogen peroxide production by brown adipose tissue mitochondria and its activation by ferricyanide." J Bioenerg Biomembr **34**(2): 105-113.

Drahota, Z., H. Rauchova, P. Jesina, A. Vojtiskova and J. Houstek (2003). "Glycerophosphate-dependent peroxide production by brown fat mitochondria from newborn rats." Gen Physiol Biophys **22**(1): 93-102.

Duchen, M. R. (1992). "Ca(2+)-dependent changes in the mitochondrial energetics in single dissociated mouse sensory neurons." Biochem J **283 (Pt 1)**: 41-50.

Duchen, M. R. (2004). "Mitochondria in health and disease: perspectives on a new mitochondrial biology." Mol Aspects Med **25**(4): 365-451.

Duchen, M. R., A. Surin and J. Jacobson (2003). "Imaging mitochondrial function in intact cells." Methods Enzymol **361**: 353-389.

Dykens, J. A. and A. K. Stout (2001). "Assessment of mitochondrial membrane potential in situ using single potentiometric dyes and a novel fluorescence resonance energy transfer technique." Methods Cell Biol **65**: 285-309.

Ehrenberg, B., V. Montana, M. D. Wei, J. P. Wuskell and L. M. Loew (1988). "Membrane potential can be determined in individual cells from the nernstian distribution of cationic dyes." Biophys J **53**: 785-794.

Echtay, K. S., M. P. Murphy, R. A. Smith, D. A. Talbot and M. D. Brand (2002a). "Superoxide Activates Mitochondrial Uncoupling Protein 2 from the Matrix Side. Studies using targeted antioxidants." J Biol Chem **277**(49): 47129-47135.

Echtay, K. S., D. Roussel, J. St-Pierre, M. B. Jekabsons, S. Cadenas, J. A. Stuart, J. A. Harper, S. J. Roebuck, A. Morrison, S. Pickering, J. C. Clapham and M. D. Brand (2002b). "Superoxide activates mitochondrial uncoupling proteins." Nature **415**(6867): 96-99.

Emaus, R. K., R. Grunwald and J. J. Lemasters (1986). "Rhodamine 123 as a probe of transmembrane potential in isolated rat- liver mitochondria: spectral and metabolic properties." Biochim Biophys Acta **850**: 436-448.

Estabrook, R. W. and B. Sacktor (1958). "alpha-Glycerophosphate oxidase of flight muscle mitochondria." J Biol Chem **233**: 1014-1019.

Eto, Y., D. Kang, E. Hasegawa, K. Takeshige and S. Minakami (1992). "Succinate-dependent lipid peroxidation and its prevention by reduced ubiquinone in beef heart submitochondrial particles." Arch Biochem Biophys **295**(1): 101-106.

Fink, C., F. Morgan and L. M. Loew (1998). "Intracellular fluorescent probe concentrations by confocal microscopy." Biophys J **75**(4): 1648-1658.

Finkel, T. (1998). "Oxygen radicals and signaling." Curr Opin Cell Biol **10**(2): 248-253.

Floryk, D. and J. Houstek (1999). "Tetramethyl Rhodamine Methyl Ester (TMRM) is Suitable for Cytofluorometric Measurements of Mitochondrial Membrane Potential in Cells Treated with Digitonin." Bioscience Reports **19**(1): 27-34.

Frank, V. and B. Kadenbach (1996). "Regulation of the H+/e- stoichiometry of cytochrome *c* oxidase from bovine heart by intramitochondrial ATP/ADP ratios." FEBS Lett **382**(1-2): 121-124.

Fridovich, I. (1995). "Superoxide radical and superoxide dismutases." Annu Rev Biochem **64**: 97-112.

Garlid, K. D. and P. Paucek (2003). "Mitochondrial potassium transport: the K(+) cycle." Biochim Biophys Acta **1606**(1-3): 23-41.

Genova, M. L., B. Ventura, G. Giuliano, C. Bovina, G. Formiggini, G. Parenti Castelli and G. Lenaz (2001). "The site of production of superoxide radical in mitochondrial Complex I is not a bound ubisemiquinone but presumably iron-sulfur cluster N2." FEBS Lett **505**(3): 364-368.

Gerbitz, K. D., J. M. van den Ouweland, J. A. Maassen and M. Jaksch (1995). "Mitochondrial diabetes mellitus: a review." Biochim Biophys Acta **1271**: 253-260.

Giles, R. E., H. Blanc, H. M. Cann and D. C. Wallace (1980). "Maternal inheritance of human mitochondrial DNA." Proc Natl Acad Sci USA **77**: 6715-6719.

Goto, Y. (1995). "Clinical features of MELAS and mitochondrial DNA mutations." Muscle Nerve **3**: S107-112.

Goto, Y., I. Nonaka and S. Horai (1990). "A mutation in the $tRNA^{Leu(UUR)}$ gene associated with the MELAS subgroup of mitochondrial encephalomyopathies." Nature **348**: 651-653.

Green, D. R. (2000). "Apoptotic pathways: paper wraps stone blunts scissors." Cell **102**(1): 1-4.

Green, D. R. and J. C. Reed (1998). "Mitochondria and apoptosis." Science **281**(5381): 1309-1312.

Guidot, D. M., J. E. Repine, A. D. Kitlowski, S. C. Flores, S. K. Nelson, R. M. Wright and J. M. McCord (1995). "Mitochondrial respiration scavenges extramitochondrial superoxide anion via a nonenzymatic mechanism." J Clin Invest **96**(2): 1131-1136.

Halliwell, B. and J. M. Gutteridge (1999). Free radicals in biology and medicine, Oxford University Press.

Ham, A. J. and D. C. Liebler (1995). "Vitamin E oxidation in rat liver mitochondria." Biochemistry **34**(17): 5754-5761.

Han, D., R. Canali, D. Rettori and N. Kaplowitz (2003). "Effect of glutathione depletion on sites and topology of superoxide and hydrogen peroxide production in mitochondria." Mol Pharmacol **64**(5): 1136-1144.

Han, D., E. Williams and E. Cadenas (2001). "Mitochondrial respiratory chain-dependent generation of superoxide anion and its release into the intermembrane space." Biochem J **353**(Pt 2): 411-416.

Hancock, J. T. (1997). "Superoxide, hydrogen peroxide and nitric oxide as signalling molecules: their production and role in disease." Br J Biomed Sci **54**(1): 38-46.

Hansford, R. G., B. A. Hogue and V. Mildaziene (1997). "Dependence of H2O2 formation by rat heart mitochondria on substrate availability and donor age." J Bioenerg Biomembr **29**(1): 89-95.

Heaton, G. M., R. J. Wagenvoord, A. Kemp, Jr. and D. G. Nicholls (1978). "Brown-adipose-tissue mitochondria: photoaffinity labelling of the regulatory site of energy dissipation." Eur J Biochem **82**(2): 515-521.

Heddi, A., P. Lestienne, D. C. Wallace and G. Stepien (1994). "Steady state levels of mitochondrial and nuclear oxidative phosphorylation transcripts in Kearns-Sayre syndrome." Biochim Biophys Acta **1226**: 206-212.

Hermann, G. J., J. W. Thatcher, J. P. Mills, K. G. Hales, M. T. Fuller, J. Nunnari and J. M. Shaw (1998). "Mitochondrial fusion in yeast requires the transmembrane GTPase Fzo1p." J Cell Biol **143**(2): 359-373.

Herrero, A. and G. Barja (1997). "Sites and mechanisms responsible for the low rate of free radical production of heart mitochondria in the long-lived pigeon." Mech Ageing Dev **98**(2): 95-111.

Herrero, A. and G. Barja (1998). "H2O2 production of heart mitochondria and aging rate are slower in canaries and parakeets than in mice: sites of free radical generation and mechanisms involved." Mech Ageing Dev **103**(2): 133-146.

Honzik, T., Z. Drahota, M. Bohm, P. Jesina, T. Mracek, J. Paul, J. Zeman and J. Houstek (2005). "Specific Properties of Heavy Fraction of Mitochondria from Human-term Placenta - Glycerophosphate-dependent Hydrogen Peroxide Production." Placenta **in press**.

Houstek, J., P. Klement, D. Floryk, H. Antonicka, J. Hermanska, M. Kalous, H. Hansikova, H. Hout'kova, S. K. Chowdhury, t. Rosipal, S. Kmoch, L. Stratilova and J. Zeman (1999). "A novel deficiency of mitochondrial ATPase of nuclear origin." Hum Mol Genet **8**(11): 1967-1974.

Houstek, J., T. Mracek, A. Vojtiskova and J. Zeman (2004). "Mitochondrial diseases and ATPase defects of nuclear origin." Biochim Biophys Acta **1658**(1-2): 115-121.

Huser, J. and L. A. Blatter (1999). "Fluctuations in mitochondrial membrane potential caused by repetitive gating of the permeability transition pore." Biochem J **343 Pt 2**: 311-317.

Huttemann, M., V. Frank and B. Kadenbach (1999). "The possible role of isoforms of cytochrome *c* oxidase subunit VIa in mammalian thermogenesis." Cell Mol Life Sci **55**(11): 1482-1490.

Chance, B., H. Sies and A. Boveris (1979). "Hydroperoxide metabolism in mammalian organs." Physiol Rev **59**(3): 527-605.

Chen, H., S. A. Detmer, A. J. Ewald, E. E. Griffin, S. E. Fraser and D. C. Chan (2003). "Mitofusins Mfn1 and Mfn2 coordinately regulate mitochondrial fusion and are essential for embryonic development." J Cell Biol **160**(2): 189-200.

Chernyak, B. V. (1997). "Cyclosporin A-sensitive release of Ca2+ from mitochondria in intact thymocytes." FEBS Lett **418**(1-2): 131-134.

Imoto, M., I. Tachibana and R. Urrutia (1998). "Identification and functional characterization of a novel human protein highly related to the yeast dynamin-like GTPase Vps1p." J Cell Sci **111**(Pt 10): 1341-1349.

Johnson, L. V., M. L. Walsh, B. J. Bockus and L. B. Chen (1981). "Monitoring of relative mitochondrial membrane potential in living cells by fluorescence microscopy." J Cell Biol **88**: 526-535.

Jouaville, L. S., P. Pinton, C. Bastianutto, G. A. Rutter and R. Rizzuto (1999). "Regulation of mitochondrial ATP synthesis by calcium: evidence for a long-term metabolic priming." Proc Natl Acad Sci U S A **96**(24): 13807-13812.

Jung, D. W., K. Baysal and G. P. Brierley (1995). "The sodium-calcium antiport of heart mitochondria is not electroneutral." J Biol Chem **270**(2): 672-678.

Kadenbach, B., M. Huttemann, S. Arnold, I. Lee and E. Bender (2000). "Mitochondrial energy metabolism is regulated via nuclear-coded subunits of cytochrome *c* oxidase." Free Radic Biol Med **29**(3-4): 211-221.

Karbowski, M. and R. J. Youle (2003). "Dynamics of mitochondrial morphology in healthy cells and during apoptosis." Cell Death Differ **10**(8): 870-880.

Kirichok, Y., G. Krapivinsky and D. E. Clapham (2004). "The mitochondrial calcium uniporter is a highly selective ion channel." Nature **427**(6972): 360-364.

Klingenberg, M. (1970). "Localization of the glycerol-phosphate dehydrogenase in the outer phase of the mitochondrial inner membrane." Eur J Biochem **13**: 247-252.

Korshunov, S. S., V. P. Skulachev and A. A. Starkov (1997). "High protonic potential actuates a mechanism of production of reactive oxygen species in mitochondria." FEBS Lett **416**(1): 15-18.

Kushnareva, Y., A. N. Murphy and A. Andreyev (2002). "Complex I-mediated reactive oxygen species generation: modulation by cytochrome *c* and NAD(P)+ oxidation-reduction state." Biochem J **368**(Pt 2): 545-553.

Lambert, A. J. and M. D. Brand (2004a). "Inhibitors of the quinone-binding site allow rapid superoxide production from mitochondrial NADH:ubiquinone oxidoreductase (complex I)." J Biol Chem **279**(38): 39414-39420.

Lambert, A. J. and M. D. Brand (2004b). "Superoxide production by NADH:ubiquinone oxidoreductase (complex I) depends on the pH gradient across the mitochondrial inner membrane." Biochem J **382**(Pt 2): 511-517.

Liu, S. S. (1997). "Generating, partitioning, targeting and functioning of superoxide in mitochondria." Biosci Rep **17**(3): 259-272.

Liu, X., C. N. Kim, J. Yang, R. Jemmerson and X. Wang (1996). "Induction of apoptotic program in cell-free extracts: requirement for dATP and cytochrome *c*." Cell **86**(1): 147-157.

Liu, Y., G. Fiskum and D. Schubert (2002). "Generation of reactive oxygen species by the mitochondrial electron transport chain." J Neurochem **80**(5): 780-787.

Lowell, B. B. and B. M. Spiegelman (2000). "Towards a molecular understanding of adaptive thermogenesis." Nature **404**(6778): 652-660.

Ludwig, B., E. Bender, S. Arnold, M. Huttemann, I. Lee and B. Kadenbach (2001). "Cytochrome *c* oxidase and the regulation of oxidative phosphorylation." Chembiochem Europ J Chem Biol **2**(6): 392-403.

Macho, A., D. Decaudin, M. Castedo, T. Hirsch, S. A. Susin, N. Zamzami and G. Kroemer (1996). "Chloromethyl-X-Rosamine is an aldehyde-fixable potential- sensitive fluorochrome for the detection of early apoptosis [see comments]." Cytometry **25**: 333-340.

Matylevitch, N. P., S. T. Schuschereba, J. R. Mata, G. R. Gilligan, D. F. Lawlor, C. W. Goodwin and P. D. Bowman (1998). "Apoptosis and accidental cell death in cultured human keratinocytes after thermal injury." Am J Pathol **153**(2): 567-577.

Mayr, J. A., J. Paul, P. Pecina, P. Kurnik, H. Förster, U. Fötschl, W. Sperl and J. Houstek (2004). "Reduced Respiratory Control with ADP and Changed Pattern of Respiratory Chain Enzymes due to Selective Deficiency of the Mitochondrial ATP Synthase." Pediatr Res **55**(6): 1-7.

McCormack, J. G., A. P. Halestrap and R. M. Denton (1990). "Role of calcium ions in regulation of mammalian intramitochondrial metabolism." Physiol Rev **70**(2): 391-425.

Mironova, G. D., N. I. Fedotcheva, P. R. Makarov, L. A. Pronevich and G. P. Mironov (1981). "[Protein from beef heart mitochondria inducing the potassium channel conductivity of bilayer lipid membrane]." Biofizika **26**(3): 451-457.

Mita, S., B. Schmidt, E. A. Schon, S. DiMauro and E. Bonilla (1989). "Detection of "deleted" mitochondrial genomes in cytochrome-*c* oxidase-deficient muscle fibers of a patient with Kearns-Sayre syndrome." Proc Natl Acad Sci USA **86**: 9509-9513.

Mitchell, P. (1961). "Coupling of phosphorylation to electron and hydrogen transfer by a chemi-osmotic type of mechanism." Nature **191**: 144-148.

MITOMAP: A Human Mitochondrial Genome Database. http://www.mitomap.org.

Miwa, S., J. St-Pierre, L. Partridge and M. D. Brand (2003). "Superoxide and hydrogen peroxide production by Drosophila mitochondria." Free Radic Biol Med **35**(8): 938-948.

Murphy, M. P. and M. D. Brand (1987). "Variable stoichiometry of proton pumping by the mitochondrial respiratory chain." Nature **329**(6135): 170-172.

Murphy, M. P. and M. D. Brand (1988). "Membrane-potential-dependent changes in the stoichiometry of charge translocation by the mitochondrial electron transport chain." Eur J Biochem **173**(3): 637-644.

Nicholls, D. G. and S. J. Ferguson (2002). Bioenergetics 3. London, Academic Press.

Nicholls, D. G. and M. W. Ward (2000). "Mitochondrial membrane potential and neuronal glutamate excitotoxicity: mortality and millivolts." Trends Neurosci **23**(4): 166-174.

Nisoli, E., E. Clementi, S. Moncada and M. O. Carruba (2004). "Mitochondrial biogenesis as a cellular signaling framework." Biochem Pharmacol **67**(1): 1-15.

O'Connor, J. E., J. L. Vargas, B. F. Kimler, J. Hernandez-Yago and S. Grisolia (1988). "Use of rhodamine 123 to investigate alterations in mitochondrial activity in isolated mouse liver mitochondria." Biochem Biophys Res Commun **151**: 568-573.

Okado-Matsumoto, A. and I. Fridovich (2001). "Subcellular distribution of superoxide dismutases (SOD) in rat liver: Cu,Zn-SOD in mitochondria." J Biol Chem **276**(42): 38388-38393.

Olichon, A., L. J. Emorine, E. Descoins, L. Pelloquin, L. Brichese, N. Gas, E. Guillou, C. Delettre, A. Valette, C. P. Hamel, B. Ducommun, G. Lenaers and P. Belenguer (2002). "The human dynamin-related protein OPA1 is anchored to the mitochondrial inner membrane facing the inter-membrane space." FEBS Lett **523**(1-3): 171-176.

Ortiz, R. G., N. J. Newman, J. M. Shoffner, A. E. Kaufman, D. A. Koontz and D. C. Wallace (1993). "Variable retinal and neurologic manifestations in patients harboring the mitochondrial DNA 8993 mutation." Arch Ophthalmol **111**: 1525-1530.

Papadopoulou, L. C., C. M. Sue, M. M. Davidson, K. Tanji, I. Nishino, J. E. Sadlock, S. Krishna, W. Walker, J. Selby, D. M. Glerum, R. V. Coster, G. Lyon, E. Scalais, R. Lebel, P. Kaplan, S. Shanske, D. C. De Vivo, E. Bonilla, M. Hirano, S. DiMauro and E. A. Schon (1999). "Fatal infantile cardioencephalomyopathy with COX deficiency and mutations in SCO2, a COX assembly gene." Nat Genet **23**(3): 333-337.

Pecina, P., H. Houstkova, H. Hansikova, J. Zeman and J. Houstek (2004). "Genetic defects of cytochrome *c* oxidase assembly." Physiol Res **53 Suppl 1**: S213-223.

Phung, C. D., J. A. Ezieme and J. F. Turrens (1994). "Hydrogen peroxide metabolism in skeletal muscle mitochondria." Arch Biochem Biophys **315**(2): 479-482.

Plasek, J. and V. Hrouda (1991). "Assessment of membrane potential changes using the carbocyanine dye, diS-C3-(5): synchronous excitation spectroscopy studies." Eur Biophys J **19**(4): 183-188.

Plasek, J. and K. Sigler (1996). "Slow fluorescent indicators of membrane potential: a survey of different approaches to probe response analysis." J Photochem Photobiol B **33**(2): 101-124.

Plasek, J., A. Vojtiskova and J. Houstek (2005). "Flow-cytometric monitoring of mitochondrial depolarisation: from fluorescence intensities to millivolts." J Photochem Photobiol B **78**(2): 99-108.

Poot, M., Y. Z. Zhang, J. A. Kramer, K. S. Wells, L. J. Jones, D. K. Hanzel, A. G. Lugade, V. L. Singer and R. P. Haugland (1996). "Analysis of mitochondrial morphology and function with novel fixable fluorescent stains." J Histochem Cytochem **44**(12): 1363-1372.

Popot, J. L. and C. de Vitry (1990). "On the microassembly of integral membrane proteins." Annu Rev Biophys Biophys Chem **19**: 369-403.

Poyton, R. O. and J. E. McEwen (1996). "Crosstalk between nuclear and mitochondrial genomes." Annu Rev Biochem **65**: 563-607.

Pralong, W. F., L. Hunyady, P. Varnai, C. B. Wollheim and A. Spat (1992). "Pyridine nucleotide redox state parallels production of aldosterone in potassium-stimulated adrenal glomerulosa cells." Proc Natl Acad Sci U S A **89**(1): 132-136.

Radi, R., A. Cassina, R. Hodara, C. Quijano and L. Castro (2002). "Peroxynitrite reactions and formation in mitochondria." Free Radic Biol Med **33**(11): 1451-1464.

Radi, R., J. F. Turrens, L. Y. Chang, K. M. Bush, J. D. Crapo and B. A. Freeman (1991). "Detection of catalase in rat heart mitochondria." J Biol Chem **266**(32): 22028-22034.

Rapaport, D., M. Brunner, W. Neupert and B. Westermann (1998). "Fzo1p is a mitochondrial outer membrane protein essential for the biogenesis of functional mitochondria in Saccharomyces cerevisiae." J Biol Chem **273**(32): 20150-20155.

Reers, M., S. T. Smiley, C. Mottola-Hartshorn, A. Chen, M. Lin and L. B. Chen (1995). "Mitochondrial membrane potential monitored by JC-1 dye." Methods of Enzymol **260**: 406-417.

Reers, M., T. W. Smith and L. B. Chen (1991). "J-aggregate formation of a carbocyanine as a quantitative fluorescent indicator of membrane potential." Biochemistry **30**: 4480-4486.

Rizzuto, R., M. R. Duchen and T. Pozzan (2004). "Flirting in little space: the ER/mitochondria Ca2+ liaison." Sci STKE **2004**(215): re1.

Robinson, B. H. (2000). "Human cytochrome oxidase deficiency." Pediatr Res **48**(5): 581-585.

Rosenberg, R. N., S. B. Prusiner, S. DiMauro, R. L. Barchi and G. Fenichel (1997). The Molecular and Genetic Basis of Neurological Disease, Butterworth-Heinemann.

Rossi, E. and G. F. Azzone (1969). "Ion transport in liver mitochondria. Energy barrier and stoicheometry of aerobic K+ translocation." Eur J Biochem **7**(3): 418-426.

Rossignol, R., B. Faustin, C. Rocher, M. Malgat, J. P. Mazat and T. Letellier (2003). "Mitochondrial threshold effects." Biochem J **370**(Pt 3): 751-762.

Rottenberg, H. (1984). "Membrane potential and surface potential in mitochondria: uptake and binding of lipophilic cations." J Membr Biol **81**(2): 127-138.

Rottenberg, H. and S. Wu (1998). "Quantitative assay by flow cytometry of the mitochondrial membrane potential in intact cells." Biochim Biophys Acta **1404**(3): 393-404.

Saran, M., C. Michel and W. Bors (1998). "Radical functions in vivo: a critical review of current concepts and hypotheses." Z Naturforsch [C] **53**(3-4): 210-227.

Scaduto, R. C., Jr. and L. W. Grotyohann (1999). "Measurement of mitochondrial membrane potential using fluorescent rhodamine derivatives." Biophys J **76**(1 Pt 1): 469-477.

Scanlon, J. M. and I. J. Reynolds (1998). "Effects of oxidants and glutamate receptor activation on mitochondrial membrane potential in rat forebrain neurons." J Neurochem **71**(6): 2392-2400.

Scorrano, L., V. Petronilli, R. Colonna, F. Di Lisa and P. Bernardi (1999). "Chloromethyltetramethylrosamine (Mitotracker Orange) induces the mitochondrial permeability transition and inhibits respiratory complex I. Implications for the mechanism of cytochrome *c* release." J Biol Chem **274**(35): 24657-24663.

Scriver, C. R., A. L. Beaudet, W. S. Sly and D. Valle (1995). The methabolic and molecular basis of inherited disease. New York, McGraw-Hill, Inc. Health Profession Division.

Sekhar, B. S., C. K. Kurup and T. Ramasarma (1987). "Generation of hydrogen peroxide by brown adipose tissue mitochondria." J Bioenerg Biomembr **19**(4): 397-407.

Shoffner IV, J. M., M. T. Lott, A. M. S. Lezza, P. Seibel, S. W. Ballinger and D. C. Wallace (1990). "Myoclonic Epilepsy and Ragged-Red Fibers Disease (MERRF) Is Associated with a Mitochondrial DNA $tRNA^{Lys}$ Mutation." Cell **61**: 931-937.

Shoffner, J. M., M. D. Brown, A. Torroni, M. T. Lott, M. F. Cabell, S. S. Mirra, M. F. Beal, C. C. Yang, M. Gearing, R. Salvo, et al. (1993). "Mitochondrial DNA variants observed in Alzheimer disease and Parkinson disease patients." Genomics **17**: 171-184.

Shoffner, J. M., P. M. Fernhoff, N. S. Krawiecki, D. B. Caplan, P. J. Holt, D. A. Koontz, Y. Takei, N. J. Newman, R. G. Ortiz, M. Polak, et al. (1992). "Subacute necrotizing encephalopathy: oxidative phosphorylation defects and the ATPase 6 point mutation." Neurology **42**: 2168-2174.

Shoubridge, E. A. (2001a). "Cytochrome *c* oxidase deficiency." Am J Med Genet **106**(1): 46-52.

Shoubridge, E. A. (2001b). "Nuclear genetic defects of oxidative phosphorylation." Hum Mol Genet **10**(20): 2277-2284.

Shoubridge, E. A., G. Karpati and K. E. Hastings (1990). "Deletion mutants are functionally dominant over wild-type mitochondrial genomes in skeletal muscle fiber segments in mitochondrial disease." Cell **62**(1): 43-49.

Sims, P. J., A. S. Waggoner, C. H. Wang and J. F. Hoffman (1974). "Studies on the mechanism by which cyanine dyes measure membrane potential in red blood cells and phosphatidylcholine vesicles." Biochemistry **13**(16): 3315-3330.

Smiley, S. T., M. Reers, C. Mottola-Hartshorn, M. Lin, A. Chen, T. W. Smith, G. D. Steele, Jr. and L. B. Chen (1991). "Intracellular heterogeneity in mitochondrial

membrane potentials revealed by a J-aggregate-forming lipophilic cation JC-1." Proc Natl Acad Sci USA **88**: 3671-3675.

Sohal, R. S. (1991). "Hydrogen peroxide production by mitochondria may be a biomarker of aging." Mech Ageing Dev **60**(2): 189-198.

Staniek, K. and H. Nohl (2000). "Are mitochondria a permanent source of reactive oxygen species?" Biochim Biophys Acta **1460**(2-3): 268-275.

Starkov, A. A. and G. Fiskum (2001). "Myxothiazol induces H(2)O(2) production from mitochondrial respiratory chain." Biochem Biophys Res Commun **281**(3): 645-650.

Starkov, A. A., G. Fiskum, C. Chinopoulos, B. J. Lorenzo, S. E. Browne, M. S. Patel and M. F. Beal (2004). "Mitochondrial alpha-ketoglutarate dehydrogenase complex generates reactive oxygen species." J Neurosci **24**(36): 7779-7788.

Stock, D., C. Gibbons, I. Arechaga, A. G. Leslie and J. E. Walker (2000). "The rotary mechanism of ATP synthase." Curr Opin Struct Biol **10**(6): 672-679.

St-Pierre, J., J. A. Buckingham, S. J. Roebuck and M. D. Brand (2002). "Topology of superoxide production from different sites in the mitochondrial electron transport chain." J Biol Chem **277**(47): 44784-44790.

Susin, S. A., H. K. Lorenzo, N. Zamzami, I. Marzo, B. E. Snow, G. M. Brothers, J. Mangion, E. Jacotot, P. Costantini, M. Loeffler, N. Larochette, D. R. Goodlett, R. Aebersold, D. P. Siderovski, J. M. Penninger and G. Kroemer (1999). "Molecular characterization of mitochondrial apoptosis-inducing factor." Nature **397**(6718): 441-446.

Suzuki, Y. J., H. J. Forman and A. Sevanian (1997). "Oxidants as stimulators of signal transduction." Free Radic Biol Med **22**(1-2): 269-285.

Tatuch, Y., J. Christodoulou, A. Feigenbaum, J. T. Clarke, J. Wherret, C. Smith, N. Rudd, R. Petrova Benedict and B. H. Robinson (1992). "Heteroplasmic mtDNA mutation (T--->G) at 8993 can cause Leigh disease when the percentage of abnormal mtDNA is high." Am J Hum Genet **50**: 852-858.

Tiranti, V., K. Hoertnagel, R. Carrozzo, C. Galimberti, M. Munaro, M. Granatiero, L. Zelante, P. Gasparini, R. Marzella, M. Rocchi, M. P. Bayona-Bafaluy, J. A. Enriquez, G. Uziel, E. Bertini, C. Dionisi-Vici, B. Franco, T. Meitinger and M. Zeviani (1998). "Mutations of SURF-1 in Leigh disease associated with cytochrome *c* oxidase deficiency." Am J Hum Genet **63**(6): 1609-1621.

Tretter, L. and V. Adam-Vizi (2004). "Generation of reactive oxygen species in the reaction catalyzed by alpha-ketoglutarate dehydrogenase." J Neurosci **24**(36): 7771-7778.

Tsien, R. Y. and S. B. Hladky (1978). "A quantitative resolution of the spectra of a membrane potential indicator, diS-C3-(5), bound to cell components and to red blood cells." J Membr Biol **38**(1-2): 73-97.

Tsukihara, T., H. Aoyama, E. Yamashita, T. Tomizaki, H. Yamaguchi, K. Shinzawa-Itoh, R. Nakashima, R. Yaono and S. Yoshikawa (1996). "The whole structure of the 13-subunit oxidized cytochrome *c* oxidase at 2.8 A [see comments]." Science **272**(5265): 1136-1144.

Turrens, J. F. (1997). "Superoxide production by the mitochondrial respiratory chain." Biosci Rep **17**(1): 3-8.

Turrens, J. F. (2003). "Mitochondrial formation of reactive oxygen species." J Physiol **552**(Pt 2): 335-344.

Turrens, J. F., A. Alexandre and A. L. Lehninger (1985). "Ubisemiquinone is the electron donor for superoxide formation by complex III of heart mitochondria." Arch Biochem Biophys **237**(2): 408-414.

Turrens, J. F. and A. Boveris (1980). "Generation of superoxide anion by the NADH dehydrogenase of bovine heart mitochondria." Biochem J **191**(2): 421-427.

Turrens, J. F., B. A. Freeman, J. G. Levitt and J. D. Crapo (1982). "The effect of hyperoxia on superoxide production by lung submitochondrial particles." Arch Biochem Biophys **217**(2): 401-410.

Vergun, O., J. Keelan, B. I. Khodorov and M. R. Duchen (1999). "Glutamate-induced mitochondrial depolarisation and perturbation of calcium homeostasis in cultured rat hippocampal neurones." J Physiol **519 Pt 2**: 451-466.

Vojtiskova, A., P. Jesina, M. Tesarova, M. Kalous, A. Dubot, C. Godinot, D. Fornuskova, V. Kaplanova, J. Zeman and J. Houstek (2004). "Mitochondrial membrane potential and ATP production in primary disorders of ATP synthase." Toxicol Mech Meth **14**: 7-11.

Votyakova, T. V. and I. J. Reynolds (2001). "DeltaPsi(m)-Dependent and -independent production of reactive oxygen species by rat brain mitochondria." J Neurochem **79**(2): 266-277.

Walker, J. E. (1998). "ATP synthesis by rotary catalysis (Nobel lecture)." Engew Chem Int Ed **37**: 2308-2319.

Wallace, D. C. (1982). "Structure and evolution of organelle genomes." Microbiol Rev **46**(2): 208-240.

Wallace, D. C. (1999). "Mitochondrial diseases in man and mouse." Science **283**(5407): 1482-1488.

Wallace, D. C., X. Zheng, M. T. Lott, J. M. Shoffner IV, J. A. Hodge, R. I. Kelley, C. M. Epstein and L. C. Hopkins (1988). "Familial mitochondrial encephalomyopathy (MERRF): Genetic, pathophysiological, and biochemical characterization of a mitochondrial DNA disease." Cell **55**: 601-610.

Warburg, O. (1956). "On respiratory impairment in cancer cells." Science **124**(3215): 269-270.

Wikstrom, M. K. and H. T. Saari (1977). "The mechanism of energy conservation and transduction by mitochondrial cytochrome *c* oxidase." Biochim Biophys Acta **462**(2): 347-361.

Wong, A. and G. A. Cortopassi (2002). "High-throughput measurement of mitochondrial membrane potential in a neural cell line using a fluorescence plate reader." Biochem Biophys Res Commun **298**(5): 750-754.

Wong, E. D., J. A. Wagner, S. W. Gorsich, J. M. McCaffery, J. M. Shaw and J. Nunnari (2000). "The dynamin-related GTPase, Mgm1p, is an intermembrane space protein required for maintenance of fusion competent mitochondria." J Cell Biol **151**(2): 341-352.

Zhang, L., L. Yu and C. A. Yu (1998). "Generation of superoxide anion by succinate-cytochrome *c* reductase from bovine heart mitochondria." J Biol Chem **273**(51): 33972-33976.

Zhu, Z., J. Yao, T. Johns, K. Fu, I. De Bie, C. Macmillan, A. P. Cuthbert, R. F. Newbold, J. Wang, M. Chevrette, G. K. Brown, R. M. Brown and E. A. Shoubridge (1998). "SURF1, encoding a factor involved in the biogenesis of cytochrome *c* oxidase, is mutated in Leigh syndrome." Nat Genet **20**(4): 337-343.

Zolkiewska, A., B. Zablocka, J. Duszynski and L. Wojtczak (1989). "Resting state respiration of mitochondria: reappraisal of the role of passive ion fluxes." Arch Biochem Biophys **275**(2): 580-590.

Zoratti, M. and I. Szabo (1995). "The mitochondrial permeability transition." Biochim Biophys Acta **1241**(2): 139-176.

Article 1

Available online at www.sciencedirect.com
SCIENCE DIRECT
Journal of Photochemistry and Photobiology B: Biology 78 (2005) 99–108
Journal of Photochemistry and Photobiology B:Biology
www.elsevier.com/locate/jphotobiol

Flow-cytometric monitoring of mitochondrial depolarisation: from fluorescence intensities to millivolts

J. Plášek [a,*], A. Vojtíšková [a,b], J. Houštěk [b]

[a] Faculty of Mathematics and Physics, Institute of Physics, Charles University, Ke Karlovu 5, 121 16 Prague, Czech Republic
[b] Institute of Physiology and Center for Integrated Genomics, Academy of Sciences of the Czech Republic, Vídeňská 1083, 142 20 Prague, Czech Republic

Received 21 July 2004; received in revised form 23 September 2004; accepted 24 September 2004
Available online 2 December 2004

Abstract

Redistribution potentiometric dyes represent a powerful tool for monitoring membrane potential of mitochondria, especially when these dyes are used with flow cytometry. In particular, tetramethylrhodamine methyl ester proved to be suitable for the screening of mitochondrial membrane potential in cultured human skin fibroblasts from patients suffering from different defects of oxidative phosphorylation. We have developed a method that makes it possible to measure the changes in mitochondrial membrane potential, or to assess the differences between respective mitochondrial membrane potentials in investigated cells and controls in the absolute scale of millivolts. Our approach employs the fact that a logarithmic transformation of Nernst equation-controlled intensity of fluorescence from potentiometric dyes accumulated in mitochondria leads to a linear scale for mitochondrial membrane potentials.

Keywords: Fluorescent probes; Mitochondrial membrane potential; mV-scale calibration

1. Introduction

The membrane potential in many cell types, as well as in their organelles such as mitochondria, has been successfully monitored using potentiometric fluorescent probes that can be classified as lipophilic cations, or redistribution dyes [1–3]. The latter name refers to the fact that these dyes redistribute between an external aqueous medium and cell (and/or the interior of cell organelles) until an equilibrium state is reached. Under this condition the ratio of respective probe concentrations in the cell/organelle and their medium obeys Nernst equation. The most popular dyes for monitoring mitochondrial membrane potential are rhodamine 123, tetramethylrhodamine methyl ester (TMRM), tetramethylrhodamine ethyl ester (TMRE), DiOC6(3) and JC-1.

Cationic redistribution dyes tend to accumulate within mitochondria. Thus the intensity of probe fluorescence can be used as a measure of mitochondrial membrane potential (for review see [1]). A fluorescent probe experiment can be performed, and mitochondrial membrane potential measured, in either non-quenching or quenching mode. The former one is employed with fluorescence microscopy, flow cytometry, and plate readers. With these high-sensitivity techniques it is possible to use very low dye concentrations. Then the apparent fluorescence intensity follows satisfactorily a Nernstian distribution of the probe between mitochondria and their environment, and a mitochondrial depolarisation is indicated by a decrease in probe fluorescence intensity, see for example [4–6]. Moreover,

* Corresponding author. Tel.: +420 221911349; fax: +420 224922797.
E-mail address: plasek@karlov.mff.cuni.cz (J. Plášek).

1011-1344/$ - see front matter
doi:10.1016/j.jphotobiol.2004.09.011

due to low dye concentration the effect of the dye on membrane potential can be minimised.

A reverse probe response can be observed in the suspensions of isolated mitochondria (or whole cell suspensions with mitochondria examined in situ) when their fluorescence intensity is measured by standard fluorimetry in the quenching mode. In this case a mitochondrial depolarisation is followed by an increase in fluorescence intensity. The cause of such a disparity between the non-quenching and quenching modes is the formation of non-fluorescent aggregates of probe molecules in the latter case, which happens when the dye concentration in mitochondria exceeds a certain critical limit [7].

Most published assays of mitochondrial membrane potential were carried out at a qualitative level, thus yielding only information on whether or not a depolarisation happened, and/or which experimental condition was able to enhance the apparent depolarisation. Relatively few studies only employed Nernst equation to transform raw changes in probe fluorescence intensity to a graded measure of underlying mitochondrial membrane potential variations. Obviously, the development of quantitative membrane potential studies was hampered by the need to correct the raw fluorescence intensities for a non-Nernstian binding of the dye to mitochondria before using Nernst equation [7–10].

Moreover, the quantification of mitochondrial membrane potential in whole cells is hampered by a few additional technical problems. First, the actual accumulation of cationic dye in mitochondria is controlled by both the plasmalemmal and the mitochondrial membrane potentials because probe molecules enter mitochondria in a two-step process (including the membrane potential-driven flow of probe molecules from the medium to cytosol that is followed by their further distribution to mitochondrial matrix). Second, the mitochondria within cells are morphologically and functionally heterogeneous [11]. To cope successfully with the latter challenge, microfluorimetry seems to be a choice. Microfluorimetric assays must be supported by advanced methods of image processing whenever a reliable quantification of individual mitochondrial contributions is a priority [4]. With detection techniques that integrate mitochondrial responses from whole cells, such as flow cytometry, any information on the above heterogeneity is obviously lost, and cell-averaged values of mitochondrial membrane potential can only be assessed. Furthermore, to avoid the above sequential response of redistribution dyes to the chain of membrane potentials, the plasmalemmal potential has to be first collapsed, e.g., by permeabilizing the plasma membrane with digitonin [6,12].

A theoretical framework is presented in this paper that shows how raw flow-cytometric intensities of probe fluorescence from mitochondria in permeabilised cell can be scaled in millivolts. To demonstrate this approach, we employed TMRM since a number of recent studies proved this potentiometric dye to be a reliable reporter of mitochondrial membrane potential ($\Delta\Psi$). In particular, the advantage of TMRM over other redistribution dyes is its relatively low level of non-Nernstian binding [13], though TMRM can be still toxic to mitochondria and/or affect their normal functions when used at high concentrations, see e.g., [7]. JC-1, another popular redistribution dye that is suitable for monitoring mitochondrial membrane potential, forms red-fluorescence dimmers upon accumulation in energised mitochondria. Therefore it is usually used as a ratiometric probe [14] and cannot be treated in terms of our theoretical framework.

Examples of the recent studies carried out with TMRM cover its use for a discrimination of depolarised from polarised mitochondria [15], especially in apoptotic cells [16–18]. TMRM was also broadly used in monitoring mitochondrial depolarisation events [5,19–25], with particular illustrations including, for example, the depolarising effect of nitric oxide [26], ROS-mediated $\Delta\Psi$ flickering [27], the effect of glutamate exposure [28], or mitochondrial changes associated with Ca^{2+} depletion of the sarcoplasmic reticulum [29] and changes in $\Delta\Psi$ in different types of mitochondrial diseases caused by dysfunction of oxidative phosphorylation enzymes due to mutations in nuclear or mitochondrial DNA [30–35].

2. Materials and methods

2.1. Cell cultures

Human skin fibroblasts from control, healthy individual were cultured in DMEM medium (SEVAC, Prague, Czech Republic) with 10% foetal calf serum (Sigma, St. Louis, USA) at 37 °C in 5% CO_2 in air. Cells were grown to approximately 90% confluence and harvested using 0.05% trypsin and 0.02% EDTA. Detached cells were diluted with ice-cold culture medium, sedimented by centrifugation ($600 \times g$) and washed twice in cold phosphate-buffered saline (PBS). The cells were resuspended in a KCl medium (80 mM KCl, 10 mM Tris HCl, 3 mM $MgCl_2$, 5 mM KH_2PO_4, 1 mM EDTA, pH 7.4) to a protein concentration 1 mg/ml. The protein concentration was measured by the method of Bradford [36] in samples sonicated for 20 s.

2.2. Isolation of rat liver mitochondria

The liver tissue was homogenised in 0.25 M sucrose, 10 mM Tris–HCl, 1 mM EDTA medium, pH 7.4, and mitochondria were isolated by a standard differential centrifugation method as described by Schneider and Hogeboom [37].

2.3. Measurement of $\Delta\Psi$

Flow cytometry. Aliquots of cells (0.1 mg of protein) were diluted in 0.5 ml of KCl medium and incubated with 20 nM TMRM (Molecular Probes, Eugene, USA) and with 1 μl of digitonin (Fluka, Buchs, Switzerland), stock solution 10 mg/ml in DMSO (final concentration 0.1 mg digitonin/mg protein), for 15 min at room temperature. Before starting mitochondrial membrane potential assays we also tested whether the apparent probe fluorescence intensity from individual cells is actually proportional to the added TMRM concentration, which is a basic prerequisite for the application of the model presented below. It was found that even with fully polarised mitochondria this condition is satisfied up to the dye concentration of 100 nM (data not shown). When studying uncoupler- or ADP-induced depolarisation, carbonylcyanide-*p*-trifluoromethoxyphenylhydrazone (FCCP, 1 μM) or 0.1 mM ADP was added to the cells 1 min before measuring TMRM fluorescence intensity.

Mitochondria were stained with MitoTracker Green (MTG, Molecular Probes, Eugene, USA) by incubating the cells with 20 nM probe for 15 min at room temperature. In MTG assays, FCCP was added in two different ways, both prior to and after their incubation with the mitochondrial marker.

Cytofluorimetric analysis was performed using FACSort flow cytometer (Becton Dickinson, San Jose, USA) equipped with an argon laser tuned to 488 nm. TMRM fluorescence was analysed in the FL2 channel (band-pass filter 580 ± 30 nm) and MTG fluorescence in the FL1 channel (band-pass filter 530 ± 15 nm). A minimum of 10,000 cells were used for each measurement. Data were acquired in logarithmic-scale mode using a CellQuest software and analysed with free-ware Summit™ Software (www.cytomation.com). Arithmetic mean value of the fluorescence intensity (measured in relative units, hereafter denoted as rel.u.) was determined for each sample.

TPP^+-sensitive electrode. $\Delta\Psi$ of rat liver mitochondria was measured using TPP^+-sensitive electrode according to [38] at 25 °C in a final volume of 2 ml. Before addition of mitochondria the electrode was calibrated with increasing concentration of TPP^+; the final TPP^+ concentration was 6 μM. Values of $\Delta\Psi$ were corrected for TPP^+ binding according to [39]. The mitochondrial concentration was 0.5 mg/ml as assessed by the Bradford method [36] and assumed matrix volume was 1.1 μl/mg protein [40].

3. Theory

The theory presented in this paper has been tailored to the flow-cytometric monitoring of the mitochondrial membrane potential in cells with their plasmalemmal potential collapsed, e.g., by permeabilizing them with digitonin. An inherent feature of flow cytometry is that the observed fluorescence intensity is a real attribute of a particular cell, free of any undesirable fluorescence contribution from the cell medium. Therefore, no terms due to the extracellular fluorescence need to be considered in the theory of flow-cytometric assays of mitochondrial membrane potential.

3.1. The case of ideal Nernstian accumulation of cationic redistribution dyes in mitochondria

Let us assume that a cationic redistribution dye enters mitochondria whose membrane potential is $\Delta\Psi$. If an equilibrium redistribution of the dye has been achieved, its respective concentrations in mitochondria and their medium, c_{in} and c_{out}, obey Nernst equation

$$c_{in} = c_{out} \exp(-F\Delta\Psi/RT), \tag{1}$$

where F, R and T is Faraday constant, gas constant and absolute temperature, respectively. To make quantitative aspects of later formulas more clear, we will replace the RT/F product by its particular value corresponding to somewhat arbitrary room temperature of 23 °C, for which $RT/F = 25.5$ mV.

Any information about the concentration of fluorescent probe within an individual organelle (and thus about the mitochondrial potential $\Delta\Psi$) is reported by I, the intensity of probe fluorescence, which is proportional to the following factors:

- c_{in} the actual concentration of dye in the mitochondrion,
- V_m the mitochondrion inner volume in which the dye is accumulated,
- I_{exc} the intensity of excitation laser beam,
- $\varepsilon(\lambda)$ molar absorption coefficient of the dye,
- Q fluorescence quantum yield,
- S_D the overall sensitivity of fluorimeter detection system.

Using the above symbols, we get

$$I = c_{in} V_m I_{exc} \varepsilon(\lambda) Q S_D. \tag{2}$$

To learn more about the meaning of the above terms, as well as about the theoretical background of fluorimetry, see for example [41]. Next we will replace for practical reasons the product of the photophysical parameters of the dye ($\varepsilon(\lambda)$ and Q) and the instrument parameters (I_{exc} and S_D) by a single multiplicative constant, hereafter denoted as P. After substituting this renamed product into Eq. (1) we get

$$I_\Psi = c_{out} \exp(-\Delta\Psi/25.5) V_m P. \tag{3}$$

where I_Ψ is the fluorescence intensity corresponding to the mitochondrial membrane potential $\Delta\Psi$. Moreover, we can employ a trivial fact that the concentration, c_{in}, of free dye in mitochondria is expected to equal c_{out} if $\Delta\Psi = 0$. The fluorescence intensity from uncoupled mitochondria, I_0, can be then written as

$$I_0 = c_{out} V_m P \tag{4}$$

and accordingly I_Ψ expressed in terms of $\Delta\Psi$ and I_0 as follows:

$$I_\Psi = I_0 \exp(-\Delta\Psi/25.5). \tag{5}$$

3.2. The effect of non-Nernstian accumulation of the fluorescent probe in the mitochondria

The Nernst equation-based formula (5) is only rigorous for dyes that redistribute between two compartments of very similar physico-chemical properties. Unfortunately, this is not the case of mitochondria whose interior is heavily loaded with various proteins. Thus the total intra-mitochondrial dye concentration can be considerably enhanced in a non-Nernstian way, i.e., due to its binding to matrix macromolecules [1,7]. According to paper by Scaduto [7], the total amount of TMRM in matrix space would be about 33-fold higher than the amount predicted from the direct application of Nernst equation. Therefore, we must add to the Nernst equation-based formula (5) a term quantifying the contribution of bound dye fluorescence.

A reasonable mathematical treatment of a resultant complex model is possible as long as c_{in} (the dye concentration in mitochondria) is negligible compared to the concentration of macromolecular binding sites in the mitochondrial matrix [1,42]. Under this condition the amount of dye that binds to macromolecules is to a good approximation proportional to c_{in}. Then the expression for I_Ψ is

$$I_\Psi = c_{in} V_m P + c_{in} K \gamma V_m P, \tag{6}$$

where K is the equilibrium ratio of bound-to-free dye concentrations, and γ is the ratio of bound-to-free dye fluorescence quantum yields. A similar equation can also be written for I_0 in which case it holds $c_{in} = c_{out}$. One can easily show that upon replacing P by $P^* = (1 + \gamma K)P$, the Eq. (5) becomes applicable even to the case of non-Nernstian accumulation of the probe in mitochondria.

The applicability of the above linear approximation can easily be tested in practice. Such a test consists in finding the range of dye concentrations for which the apparent fluorescence intensity from mitochondria is proportional to the probe concentration in their medium. For obvious reasons, this test should be performed with highly energised mitochondria when the concentration of accumulated dye is expected to reach its maximal value. Note also that at high dye concentrations an immediate sensitivity of TMRM response to $\Delta\Psi$ changes can be lost [26].

3.3. A linear scale for measuring mitochondrial membrane potential

Upon a simple logarithmic transformation of the exponential formula (5) we obtain

$$\Delta\Psi = 25.5 \ln(I_0/I_\Psi) \quad \text{or} \quad \Delta\Psi = 58.7 \log(I_0/I_\Psi), \tag{7}$$

which suggests that a linear scale for measuring mitochondrial membrane potential can be constructed if the probe fluorescence intensity, I_Ψ, is expressed in terms of an I_Ψ/I_0 ratio. Then, we can assess for any experimental I_Ψ a corresponding $\Delta\Psi$ value in units of mV, provided that we are able to determine I_0 in a calibration experiment with $\Delta\Psi$ set to zero. Note, however, that even if the above calibration cannot be done, it is still possible to employ (7) for quantifying a difference between mitochondrial membrane potentials in two distinct states.

Let us assume that the mitochondrial membrane potential changed from $\Delta\Psi_1$ to $\Delta\Psi_2$, and thus the flow-cytometric assay gave fluorescence intensities $I_{\Psi 1}$ and $I_{\Psi 2}$, respectively. In case that I_0 can be treated as a constant, Eq. (7) results in a simple formula

$$\Delta\Psi_{12} = \Delta\Psi_1 - \Delta\Psi_2 = 58.7 \log(I_{\Psi 2}/I_{\Psi 1}), \tag{8}$$

where a symbol $\Delta\Psi_{12}$ is used to denote the potential difference $\Delta\Psi_1 - \Delta\Psi_2$.

The above assumption of a constant I_0 value is justified if we deal with well-defined cell specimens of constant mitochondrial volumes. For cells of different origin, however, their actual mitochondrial volumes need to be determined, and the experimental probe fluorescence intensities normalised relative to some reference value before using (8). To achieve this, we will combine the measurement of probe fluorescence intensity I_Ψ with a MitoTracker Green assay; this approach is based on assumption that a MitoTracker dye accumulates in mitochondria in a potential-independent way [43]. Under this condition its fluorescence intensity, I_M, can be treated as proportional to the total mitochondrial volume in examined cells (see Section 4), i.e.,

$$I_M = c_M^* V_m, \tag{9}$$

where c_M^* is a multiplicative constant. When combined with (4), this equation yields

$$I_0 = c_{out} c_M I_M / c_M^*. \tag{10}$$

Finally, we will substitute (10) into (7) to get a formula suitable for the assessment of the difference between mitochondrial membrane potentials in two distinct cell populations

$$\Delta\Psi_{12} = 58.7 \log(I_{\Psi 2} I_{M1} / I_{M2} I_{\Psi 1}), \quad (11)$$

where I_{M1} and I_{M2} are the MitoTracker fluorescence intensities measured in cells that exhibit the mitochondrial membrane potentials $\Delta\Psi_1$ and $\Delta\Psi_2$, respectively.

3.4. The effect of probe accumulation in cell cytosol

A probe fluorescence signal from whole cells, I_{Ψ}^{tot}, comprises the pure emission from mitochondria, I_{Ψ}, plus the contributions of I^{out} and I^{cyt} fluorescence intensities, which are due to a dye bound to the outer face of the mitochondrial membrane and accumulated within the cell cytoplasm, respectively. Then we have

$$I_{\Psi}^{tot} = I_{\Psi} + I^{out} + I^{cyt}. \quad (12)$$

Hereafter, we will denote the sum of I^{out} and I^{cyt} as I_B (background fluorescence) and get the Nernstian part of measured fluorescence intensity as follows

$$I_{\Psi} = I_{\Psi}^{tot} - I_B. \quad (13)$$

Unfortunately, no cytofluorimetric assay can directly discriminate between I_{Ψ} and I_B. Therefore, we need some additional information before processing the measured data quantitatively. To get it we will take into account that both I^{out} and I^{cyt} in digitonin-treated cells are independent of $\Delta\Psi$; this assumption is practically equivalent to c_{out} being independent of $\Delta\Psi$ changes. Obviously, this can happen if the total volume of mitochondria in the analysed cell suspension is negligible as compared to the suspension total volume. If it is so, the accumulation of the dye in mitochondria cannot reduce considerably the dye concentration in the medium. Then both c_{out} and I_B can be treated as constants.

In such circumstances, I_B can be determined after dissipating mitochondrial potential with an uncoupler (state 3 – uncoupled), e.g., FCCP. In the literature, the value of $\Delta\Psi$ in energised mitochondria (state 4) varies from 150 to 200 mV depending on cell type or the experimental method [9,40,44–49]. We used $\Delta\Psi_{cal} = 150$ mV, but as demonstrated in Table 3, this value is accurate enough for many experimental situations. Then two reference values for the estimation of background intensity can be used – the fluorescent intensity in state 4 (cells with substrate and without ADP) and the intensity in the state 3 – uncoupled with collapsed $\Delta\Psi$ (cells with substrate and an uncoupler FCCP). If we denote the fluorescence intensity measured with energised and uncoupled mitochondria as I_4^{tot} and I_U^{tot}, respectively, the Eq. (8) combined with Eq. (13) yields

$$\Delta\Psi_{cal} = 58.7 \log((I_4^{tot} - I_B)/(I_U^{tot} - I_B)), \quad (14)$$

which represents a theoretical basis for correcting raw fluorescence intensities I_{Ψ}^{tot} for the contribution of background fluorescence.

4. Results and discussion

4.1. The monitoring of mitochondrial mass/volume with mitotracker green fluorescence

To assess in relative units the total mass of mitochondria in investigated cells, we used the mitochondria-selective probe MitoTracker Green (MTG). This dye is non-fluorescent in aqueous solutions and becomes fluorescent once in the mitochondrial lipid environment. According to Molecular Probes Handbook by Haugland MTG probe appears to accumulate in mitochondria of certain cell types regardless of the mitochondrial membrane potential [43].

In contrast to the Molecular Probes Handbook some authors reported that the MTG accumulation in mitochondria is sensitive to $\Delta\Psi$ changes [50,51], and/or can vary owing to the fact that MTG is a P-glycoprotein substrate [52]. Buckman and co-workers [51] found that MTG may be used for measurements of mitochondrial mass at low concentrations only ($\leq$50 nM). Therefore, we tested the sensitivity of MTG fluorescence intensity to $\Delta\Psi$ in our particular cell model (human skin fibroblasts) at the dye concentration of 20 nM.

This test consisted in comparing respective MTG fluorescence intensities from cells with and without FCCP. No difference was observed between respective MTG fluorescence intensities from energised and uncoupled mitochondria when FCCP was added to MTG stained cells. When the cells were uncoupled prior to their staining with MTG, the resultant fluorescence intensity was about 10% lower than that one from energised mitochondria (data not shown). This difference is small enough in the logarithmic scale that is to be used to quantify the measured fluorescence intensities in terms of $\Delta\Psi$. In theory, the apparent insensitivity of MTG fluorescence to mitochondrial membrane potential could be an artefact indicating that a binding capacity of mitochondria has been exceeded. To exclude this eventuality we measured also the dependence of fluorescence intensity on the concentration of MTG added to cells. It was found that the MTG fluorescence intensity from coupled cells is proportional to the probe concentration up to 100 nM, Fig. 1. Since we always added the dye to the investigated cells at a concentration of 20 nM, a contribution of the above artefact to the data presented below is practically excluded.

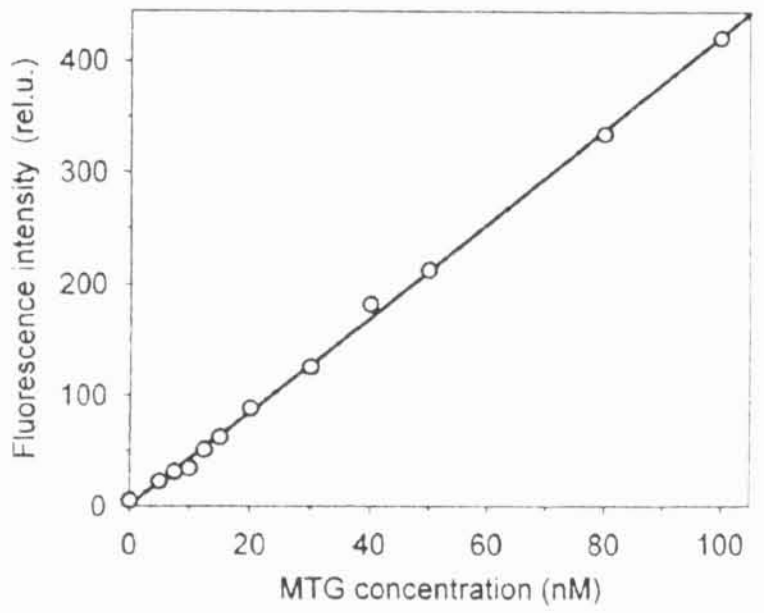

Fig. 1. The dependence of Mitotracker Green fluorescence intensity from polarised mitochondria of human skin fibroblasts on the tracer concentration.

In summary, the intensity of MTG fluorescence from human skin fibroblasts can be accepted as a suitable measure of the total mass of their mitochondria, and hence also of their total volume, which proportionality is justified until we are not dealing with conditions resulting in swelling or contraction.

4.2. Calibration procedure

To assess the contribution of I_B to raw fluorescence intensities I_Ψ^{tot} we used Eq. (14) with $\Delta\Psi_{cal}$ set at 150 mV. The assay was performed with cells withdrawn from the same fibroblast cell culture on four different days over the period of four weeks; for two of these four cell preparations the flow cytometric assay was repeated three times. Data are shown in Table 1.

While the individual values of I_4^{tot}, I_U^{tot} and I_M varied only moderately within the sets of data measured on a particular day, their day-to-day variations were not negligible. Regardless of these variations, a data processing that consisted in

(i) the determination of I_B value using Eq. (14),
(ii) the calculation of I_4 and I_U using Eq. (13),
(iii) correcting both I_4 and I_U for the relative volume of mitochondria in examined cells resulted in a relatively uniform set of I_4/I_M and I_U/I_M ratios. A crucial question is how reproducible the monitoring of mitochondrial membrane potentials is when it is based on such I_4/I_M values. We analysed therefore observed probe fluorescence intensities I_{4k} in terms of fluctuations of TMRM-reported membrane potentials $\Delta\Psi_{4k}$ relative to their mean value $\overline{\Delta\Psi_4}$, i.e., in terms $\Delta\Psi_{4k} - \overline{\Delta\Psi_4}$, hereafter denoted as $\delta(\Delta\Psi)_{4k}$. Note that such fluctuations can be determined even if the $\Delta\Psi_{4k}$ values themselves cannot be assessed. This amazing fact results from the logarithmic relationship between I_{4k} and $\Delta\Psi_{4k}$ as involved in Eqs. (7) and (8). Owing to this relationship the arithmetic mean $\overline{\Delta\Psi_4}$ of a certain set of $\Delta\Psi_{4k}$ values can be expressed in terms of the geometrical mean of corresponding probe fluorescence intensities I_{4k}, i.e., in terms of $\bar{I}_4 = (I_{41}I_{42}\cdots I_{4n})^{\frac{1}{n}}$. It can be easily shown that Eq. (8) when applied to $\bar{I}_4$ and I_{4k} pairs yields $\Delta\Psi_{4k} - \overline{\Delta\Psi_4}$.

We found that a standard deviation of these $\delta(\Delta\Psi)_{4k}$ fluctuations was 4.62 mV when the experimental data were not corrected for the relative volume of mitochondria. When corrected probe fluorescence intensities I_4/I_M were used to calculate $\delta(\Delta\Psi)_k$ fluctuations, the standard deviation decreased to 1.63 mV. This indicates that, despite its known drawbacks, MTG probing of relative mitochondrial volumes can improve the precision of TMRM-based assays.

Another interesting finding concerns the size of I_B. For the particular case of human skin fibroblasts the experimental I_B values are comparable to their corresponding I_U^{tot} values, which indicate that the assumption of negligibly small I_B, as used by O'Reilly et al. [10], should not be routinely taken as justified for any cell type.

Table 1
Cytofluorimetric monitoring of $\Delta\Psi$ in human skin fibroblasts: the fluctuations in the set of data collected during the period of four weeks

Day	Measured data			Calculated values					
	I_4^{tot} (rel.u.)	I_U^{tot} (rel.u.)	I_M (rel.u.)	I_B (rel.u.)	I_4 (rel.u.)	I_4/I_M	I_U (rel.u.)	$\delta(\Delta\Psi)$ (mV)	$\delta(\Delta\Psi)_{corr}$ (mV)
1	505[a]	104[a]	75.2	102.9	402.1	5.35	1.10	−3.98	1.93
8	653	97	117.9	95.4	557.6	4.73	1.60	4.20	−1.14
16	626	107	107.9	105.5	520.5	4.82	1.50	2.48	−0.65
	664	97	112.2	95.4	568.6	5.07	1.60	4.69	0.59
	677	92	132.4	90.4	586.6	4.43	1.60	5.47	−2.77
27	473	98	78.5	97.0	376.0	4.79	1.00	−5.65	−0.82
	485	79	77.7	77.9	407.1	5.24	1.10	−3.67	1.42
	491	83	77.7	81.9	409.1	5.27	1.10	−3.54	1.54
Geometrical means	566				471.4	4.95			
Standard deviations								4.62	1.63

[a] For controls the halfwidths (FWHM) of experimental peaks were typically about ±35% of the peak mean value in fully energised mitochondria. In the resultant mV scale this has corresponded to about ±8 mV. In FCCP treated cells the peaks were about 1.5-fold broader in the mV scale.

Table 2
The simulation of calibration-induced errors in the $\Delta\Psi_{12}$ assessment: model pairs of $I_{\Psi 1}$ and $I_{\Psi 2}$ fluorescence intensities calculated for the series of hypothetical $\Delta\Psi_{12}$ differences (see text)

$\Delta\Psi_{12}$ (mV)	20	40	60	80	100	120
$I_{\Psi 1}$ (rel.u.)	451.3	451.3	451.3	451.3	451.3	451.3
$I_{\Psi 2}$ (rel.u.)	206.0	94.0	42.9	19.6	8.9	4.1

4.3. Practical limits of $\Delta\Psi_{12}$ measurements

The logarithmic relationship between measured probe fluorescence intensities and underlying mitochondrial membrane potentials has got a trivial consequence concerning apparent errors in $\Delta\Psi_{12}$ assessment: if scaled in millivolts, they appear acceptably low even at rather high $I_{\Psi 2}/I_{\Psi 1}$ fluctuations. For example, the $\Delta\Psi_{12}$ errors do not exceed 1, 3 and 5 mV levels if relative $I_{\Psi 2}/I_{\Psi 1}$ errors are less then 4%, 12% and 22%, respectively.

The most problematical aspect of the $I_{\Psi 2}/I_{\Psi 1}$ measurement is the I_B assessment, which is affected by the uncertainty about the true $\Delta\Psi_{cal}$ value. To understand when this uncertainty becomes a serious limit to the reliable estimation of $\Delta\Psi_{12}$ we performed a series of computer simulations. We used typical values of I_4^{tot} and I_U^{tot} intensities of TMRM fluorescence as found in control cells from healthy donors. In the particular case of human skin fibroblasts we have got I_4^{tot} and I_U^{tot} of 550 and 100 rel.u., respectively. We calculated I_B and I_4 fluorescence intensities for these data using $\Delta\Psi_{cal} = 150$ mV, and got $I_B = 98.7$ rel.u. and I_4 of 451.3 rel.u. Second, $I_4 = 451.3$ rel.u. was introduced into Eq. (8) as $I_{\Psi 1}$, and simulated $I_{\Psi 2}$ fluorescence intensities were calculated that are to be observed if the underlying mitochondrial membrane potential drops from $\Delta\Psi_1$ to $\Delta\Psi_2$ by $\Delta\Psi_{12} = 20$, 40, 60, 80, 100, or 120 mV, Table 2. Then we simulated an effect of incorrect calibration, having assumed that the actual depolarisation of control mitochondria due to the effect of FCCP on the control mitochondria is weaker than expected, and thus the actual $\Delta\Psi_{cal} = \Delta\Psi_4 - \Delta\Psi_U$ difference is less than 150 mV. In these circumstances, the $I_B(150)$ values calculated with Eq. (14) and $\Delta\Psi_{cal} = 150$ mV are higher than the true background $I_B(\Delta\Psi_{cal})$; hereafter such a model-dependent deviation from the true background intensity, $I_B(150) - I_B(\Delta\Psi_{cal})$, will be denoted δI_B. Then the assessment of $\Delta\Psi_{12}$ values based on experimental $I_{\Psi 2}^{tot}$ and $I_{\Psi 1}^{tot}$ fluorescence intensities shall be flawed because it is not obtained with true probe fluorescence intensities $I_{\Psi 2}$ and $I_{\Psi 1}$, but with their overcorrected counterparts $I_{\Psi 2} - \delta I_B$ and $I_{\Psi 1} - \delta I_B$. Considering this we can simulate the effect of overestimated I_B backgrounds for the model data of Table 2 using a wide range of $\Delta\Psi_{cal}$ values. The results are presented in Fig. 2, with $\delta(\Delta\Psi_{12})$ representing the difference between respective $\Delta\Psi_{12}$ values calculated for overcorrected and true data.

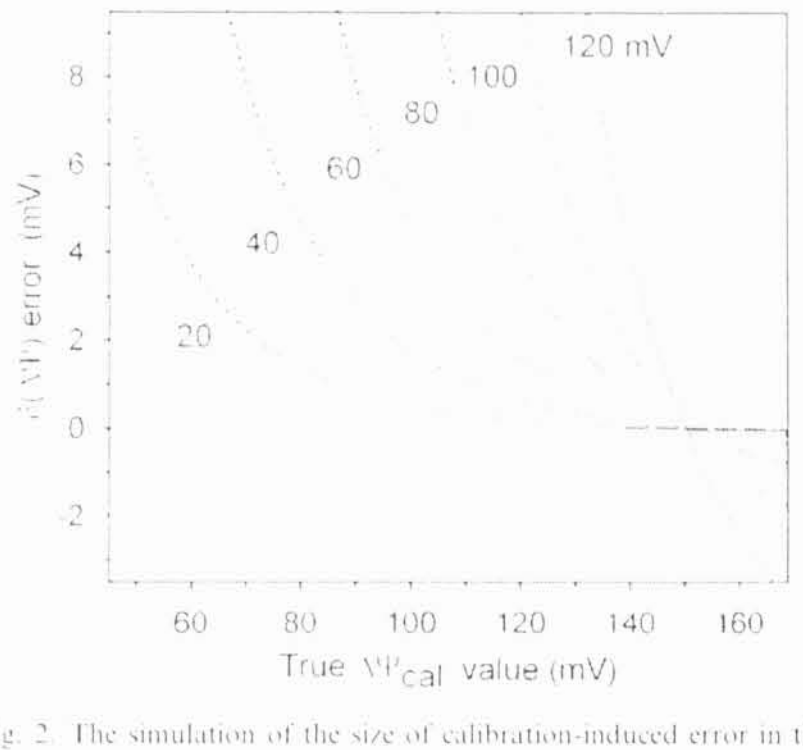

Fig. 2. The simulation of the size of calibration-induced error in the $\Delta\Psi_{12}$ assessment. Individual curves represent $\delta(\Delta\Psi_{12})$ for simulated $\Delta\Psi_{12}$ ranging from 20 to 120 mV (see attached labels). Thick lines indicate the limits within which $\delta(\Delta\Psi_{12})$ is less than 10% of $\Delta\Psi_{12}$ value.

The size of $\delta(\Delta\Psi_{12})$ error in our simulated data remains acceptably low for a wide range of potentially important experimental situations. In particular, in case of moderate depolarisation ($\Delta\Psi_{12} \leqslant 20$ mV) it is less than 3.5 mV even if erroneous $\Delta\Psi_{cal}$ is as low as 70 mV. With increasing magnitude of mitochondrial depolarisation the tolerable uncertainty in $\Delta\Psi_{cal}$ value becomes obviously more narrow: for example, with $\Delta\Psi_{12} = 80$ mV the error in setting $\Delta\Psi_{cal}$ values should not exceed 25 mV to yield $\delta(\Delta\Psi_{12}) \leqslant 3.5$ mV. Though much less than in the preceding case, this uncertainty is still acceptable from the point of real FCCP calibration experiment. Finally, an extreme situation is represented by nearly uncoupled mitochondria with $\Delta\Psi_{12}$ value close to 150 mV. In this case, $I_{\Psi 2}$ fluorescence intensity will become very low, and hence the calculation of $\Delta\Psi_{12}$ extremely sensitive to even moderate errors in the I_B assessment.

The above simulated data are not adequate for I_4^{tot} and I_U^{tot} fluorescence intensities that differ considerably from those we found in our controls. However, one can easily perform similar simulation test, and thus check the limits of reliable $\Delta\Psi_{12}$ assessments for any particular assay performed with a redistribution dye and flow cytometry.

4.4. ADP induced depolarisation: an example of moderate changes in mitochondrial membrane potential

It is known that upon adding ADP to mitochondria that are at state 4 (with substrate, without ADP) their membrane potential drops by about 20–30 mV because

Table 3
ADP-induced depolarisation in mitochondria of human skin fibroblasts measured by flow cytometry and in rat liver mitochondria measured by TPP$^+$ electrode

Flow cytometry									TPP$^+$ electrode	
Raw data			Calculated data: $\Delta\Psi_{cal}$ = 150 mV			Calculated data: $\Delta\Psi_{cal}$ = 180 mV			$\Delta\Psi_4$ (mV)	$\Delta\Psi_{4\,ADP}$ (mV)
I_4^{tot} (rel.u.)	I_U^{tot} (rel.u.)	I_{ADP}^{tot} (rel.u.)	I_B (rel.u.)	I_4 (rel.u.)	I_{ADP} (rel.u.)	$\Delta\Psi_{4\,ADP}$ (mV)	I_B (rel.u.)	I_4 (rel.u.)	I_{ADP} (rel.u.)	$\Delta\Psi_{4\,ADP}$ (mV)		
1263	169	599	166	1097	433	−23.7	168	1095	431	−23.8	184	154
1211	160	596	157	1054	439	−22.3	159	1052	437	−22.5	181	154
1214	178	541	175	1039	366	−26.6	177	1037	364	−26.8	178	157
1338	199	647	196	1142	451	−23.7	198	1140	449	−23.8	184	161
1478	212	746	209	1270	538	−21.9	211	1267	535	−22.0	187	163
1477	229	697	226	1252	472	−24.9	230	1252	472	−24.9		
$\Delta\Psi_{4\,ADP}$ mean value ± SD			−24.2 ± 1.6 mV				−24.4 ± 1.6 mV				25.0 ± 3.5 mV	

The concentration of ADP was 0.1 mM.

of an increased energy demand when ATP is synthesised [40,47]. This value matches well the $\Delta\Psi_{12}$ range for which the flow-cytometric probing of mitochondrial membrane potential should be relatively robust with respect to the possible uncertainty in the $\Delta\Psi_{cal}$ value.

We measured the 0.1 mM ADP-induced depolarisation (state 3 → ADP) in cultured human skin fibroblasts by flow cytometry (six independent measurements) and also in isolated rat liver mitochondria by TPP$^+$-sensitive electrode (five measurements). Using cytofluorimetric analysis we obtained the values I_4^{tot} and I_U^{tot}, which were then used to calculate I_B values. To test how robust our method is we fixed $\Delta\Psi_{cal}$ to either 150 or 180 mV. After correcting raw fluorescence intensities I_4^{tot} and I_{ADP}^{tot} for corresponding I_B values, the ADP-induced changes in mitochondrial membrane potential, $\Delta\Psi_{4\,ADP}$, were calculated (Table 3). Mean $\Delta\Psi_{4\,ADP}$ values in human fibroblasts were −24.2 ± 1.6 and −24.4 ± 1.6 mV for $\Delta\Psi_{cal}$ = 150 and 180 mV, respectively. These values match perfectly the values obtained from the TPP$^+$ electrode −25.0 ± 3.5 mV which confirms the robustness of the $\Delta\Psi$ calculation from TMRM fluorescence intensities.

5. Conclusions

The mathematical formulas presented in this paper provide a framework for assigning TMRM (or other redistribution dye, expect JC-1) fluorescence intensities, as measured by flow cytometry in digitonin-treated cells, to the underlying changes of mitochondrial membrane potential in the absolute scale of millivolts. In order to correct for cellular content of mitochondria, the TMRM fluorescence intensities are normalised using specific mitochondrial probe MTG. In summary, the main steps of this procedure are:

- The measurements of $\Delta\Psi$ changes are performed with mitochondria in permeabilised cells, in which the plasma membrane-potential-driven dye uptake is absent.
- Prior to any routine use of this method, the dye concentration and incubation period must be optimised with respect to the actual range of linear fluorescence response in the particular cells.
- Probe fluorescence intensity from mitochondria in digitonin-treated cells is then measured using flow cytometry, and quantified in terms of its mean value.
- The fluorescence intensity is measured in the cells in state 4 and in state 3 – uncoupled, yielding I_4^{tot} and I_U^{tot}, respectively.
- A background fluorescence intensity I_B is assessed using I_4^{tot}, I_U^{tot} and Eq. (14) with properly chosen $\Delta\Psi_{cal}$ value.

- Corrected fluorescence intensities $I_{\Psi 1} = I_{\Psi 1}^{\text{tot}} - I_{\text{B}}$ and $I_{\Psi 2} = I_{\Psi 2}^{\text{tot}} - I_{\text{B}}$ are then determined for mitochondrial states of interest, and $\Delta\Psi_{12}$ is calculated with Eq. (8).
- MTG fluorescence intensities, I_{M}, should be measured to normalize fluorescence intensities $I_{\Psi 1}$ and $I_{\Psi 2}$ equal mitochondrial volumes.
- Finally, $\Delta\Psi_{12}$ is calculated using these normalised fluorescence intensities and Eq. (11).

Acknowledgments

This work was supported by 113200001 and 5011922 institutional grants from The Ministry of Education, Youth and Sports of the Czech Republic, the Grant Agency of the Charles University (grant no. 166/2002) and a grant from the Grant Agency of the Ministry of Health of the Czech Republic (NR/7790-3).

References

[1] J. Plasek, K. Sigler, Slow fluorescent indicators of membrane potential: a survey of different approaches to probe response analysis, J. Photochem. Photobiol. B 33 (2) (1996) 101–124.
[2] L.B. Chen, Mitochondrial membrane potential in living cells, Annu. Rev. Cell Biol. 4 (1988) 155–181.
[3] J.C. Smith, Potential-sensitive molecular probes in membranes of bioenergetic relevance, Biochim. Biophys. Acta 1016 (1) (1990) 1–28.
[4] C. Fink, F. Morgan, L.M. Loew, Intracellular fluorescent probe concentrations by confocal microscopy, Biophys. J. 75 (4) (1998) 1648–1658.
[5] J.F. Buckman, I.J. Reynolds, Spontaneous changes in mitochondrial membrane potential in cultured neurons, J. Neurosci. 21 (14) (2001) 5054–5065.
[6] A. Wong, G.A. Cortopassi, High-throughput measurement of mitochondrial membrane potential in a neural cell line using a fluorescence plate reader, Biochem. Biophys. Res. Commun. 298 (5) (2002) 750–754.
[7] R.C. Scaduto Jr., L.W. Grotyohann, Measurement of mitochondrial membrane potential using fluorescent rhodamine derivatives, Biophys. J. 76 (1 Pt 1) (1999) 469–477.
[8] H. Rottenberg, S. Wu, Quantitative assay by flow cytometry of the mitochondrial membrane potential in intact cells, Biochim. Biophys. Acta 1404 (3) (1998) 393–404.
[9] D.G. Nicholls, M.W. Ward, Mitochondrial membrane potential and neuronal glutamate excitotoxicity: mortality and millivolts, Trends Neurosci. 23 (4) (2000) 166–174.
[10] C.M. O'Reilly, K.E. Fogarty, R.M. Drummond, R.A. Tuft, J.V. Walsh Jr., Quantitative analysis of spontaneous mitochondrial depolarizations, Biophys. J. 85 (5) (2003) 3350–3357.
[11] T.J. Collins, M.J. Berridge, P. Lipp, M.D. Bootman, Mitochondria are morphologically and functionally heterogeneous within cells, EMBO J. 21 (7) (2002) 1616–1627.
[12] D. Floryk, J. Houstek, Tetramethyl rhodamine methyl ester (TMRM) is suitable for cytofluorometric measurements of mitochondrial membrane potential in cells treated with digitonin, Biosci. Reports 19 (1) (1999) 27–34.
[13] B. Ehrenberg, V. Montana, M.D. Wei, J.P. Wuskell, L.M. Loew, Membrane potential can be determined in individual cells from the nernstian distribution of cationic dyes, Biophys. J. 53 (1988) 785–794.
[14] M. Reers, S.T. Smiley, C. Mottola-Hartshorn, A. Chen, M. Lin, L.B. Chen, Mitochondrial membrane potential monitored by JC-1 dye, Meth. Enzymol. 260 (1995) 406–417.
[15] S.P. Elmore, Y. Nishimura, T. Qian, B. Herman, J.J. Lemasters, Discrimination of depolarized from polarized mitochondria by confocal fluorescence resonance energy transfer, Arch. Biochem. Biophys. 422 (2) (2004) 145–152.
[16] W.X. Ding, H.M. Shen, C.N. Ong, Critical role of reactive oxygen species and mitochondrial permeability transition in microcystin-induced rapid apoptosis in rat hepatocytes, Hepatology 32 (3) (2000) 547–555.
[17] B. Qu, Q.T. Li, K.P. Wong, T.M. Tan, B. Halliwell, Mechanism of clofibrate hepatotoxicity: mitochondrial damage and oxidative stress in hepatocytes, Free Radic. Biol. Med. 31 (5) (2001) 659–669.
[18] A. Rasola, M. Geuna, A flow cytometry assay simultaneously detects independent apoptotic parameters, Cytometry 45 (2) (2001) 151–157.
[19] S.K. Chowdhury, Z. Drahota, D. Floryk, P. Calda, J. Houstek, Activities of mitochondrial oxidative phosphorylation enzymes in cultured amniocytes, Clin. Chim. Acta 298 (1–2) (2000) 157–173.
[20] M. Facompre, N. Wattez, J. Kluza, A. Lansiaux, C. Bailly, Relationship between cell cycle changes and variations of the mitochondrial membrane potential induced by etoposide, Mol. Cell Biol. Res. Commun. 4 (1) (2000) 37–42.
[21] V. Petronilli, D. Penzo, L. Scorrano, P. Bernardi, F. Di Lisa, The mitochondrial permeability transition release of cytochrome c and cell death. Correlation with the duration of pore openings in situ, J. Biol. Chem. 276 (15) (2001) 12030–12034.
[22] C.J. Feeney, P.S. Pennefather, A.V. Gyulkhandanyan, A cuvette-based fluorometric analysis of mitochondrial membrane potential measured in cultured astrocyte monolayers, J. Neurosci. Methods 125 (1–2) (2003) 13–25.
[23] D.D. Kindler, C. Thiffault, N.J. Solenski, J. Dennis, V. Kostecki, R. Jenkins, P.M. Keeney, J.P. Bennett Jr., Neurotoxic nitric oxide rapidly depolarizes and permeabilizes mitochondria by dynamically opening the mitochondrial transition pore, Mol. Cell Neurosci. 23 (4) (2003) 559–573.
[24] Y.O. Kweon, Y.H. Paik, B. Schnabl, T. Qian, J.J. Lemasters, D.A. Brenner, Gliotoxin-mediated apoptosis of activated human hepatic stellate cells, J. Hepatol. 39 (1) (2003) 38–46.
[25] S.A. Andrabi, I. Sayeed, D. Siemen, G. Wolf, T.F. Horn, Direct inhibition of the mitochondrial permeability transition pore: a possible mechanism responsible for anti-apoptotic effects of melatonin, Faseb. J. 18 (7) (2004) 869–871.
[26] R.M. Bell, H.L. Maddock, D.M. Yellon, The cardioprotective and mitochondrial depolarising properties of exogenous nitric oxide in mouse heart, Cardiovasc. Res. 57 (2) (2003) 405–415.
[27] F. De Giorgi, L. Lartigue, F. Ichas, Electrical coupling and plasticity of the mitochondrial network, Cell Calcium 28 (5–6) (2000) 365–370.
[28] M.W. Ward, A.C. Rego, B.G. Frenguelli, D.G. Nicholls, Mitochondrial membrane potential and glutamate excitotoxicity in cultured cerebellar granule cells, J. Neurosci. 20 (19) (2000) 7208–7219.
[29] M. Jaconi, C. Bony, S.M. Richards, A. Terzic, S. Arnaudeau, G. Vassort, M. Puceat, Inositol 1,4,5-trisphosphate directs Ca(2+) flow between mitochondria and the Endoplasmic/Sarcoplasmic reticulum: a role in regulating cardiac autonomic Ca(2+) spiking, Mol. Biol. Cell 11 (5) (2000) 1845–1858.
[30] H. Antonicka, D. Floryk, P. Klement, L. Stratilova, J. Hermanska, H. Houstkova, M. Kalous, Z. Drahota, J. Zeman,

J. Houstek, Defective kinetics of cytochrome c oxidase and alteration of mitochondrial membrane potential in fibroblasts and cytoplasmic cells with the mutation for myoclonus epilepsy with ragged-red fibres ('MERRF') at position 8344 nt, Biochem. J. 342 (3) (1999) 537–544.

[31] J. Houstek, P. Klement, D. Floryk, H. Antonicka, J. Hermanska, M. Kalous, H. Hansikova, H. Hout'kova, S.K. Chowdhury, t. Rosipal, S. Kmoch, L. Stratilova, J. Zeman, A novel deficiency of mitochondrial ATPase of nuclear origin, Hum. Mol. Genet. 8 (11) (1999) 1967–1974.

[32] P. Pecina, M. Capkova, S.K. Chowdhury, Z. Drahota, A. Dubot, A. Vojtiskova, H. Hansikova, H. Houst'kova, J. Zeman, C. Godinot, J. Houstek, Functional alteration of cytochrome c oxidase by SURF1 mutations in Leigh syndrome, Biochim. Biophys. Acta 1639 (1) (2003) 53–63.

[33] A. Dubot, C. Godinot, V. Dumur, B. Sablonniere, T. Stojkovic, J.M. Cuisset, A. Vojtiskova, P. Pecina, P. Jesina, J. Houstek, GUG is an efficient initiation codon to translate the human mitochondrial ATP6 gene, Biochem. Biophys. Res. Commun. 313 (3) (2004) 687–693.

[34] A. Vojtiskova, P. Jesina, M. Tesarova, M. Kalous, A. Dubot, C. Godinot, D. Fornuskova, V. Kaplanova, J. Zeman, J. Houstek, Mitochondrial membrane potential and ATP production in primary disorders of ATP synthase, Toxicol. Mech. Meth. 14 (2004) 7–11.

[35] J. Houstek, T. Mracek, A. Vojtiskova, J. Zeman, Mitochondrial diseases and ATPase defects of nuclear origin, Biochim. Biophys. Acta 1658 (1-2) (2004) 115–121.

[36] M.M. Bradford, A rapid and sensitive method for the quantitation of microgram quantities of protein utilizing the principle of protein dye binding, Anal. Biochem. 72 (1976) 248–254.

[37] W.C. Schneider, D.A. Hogeboom, Intracellular distribution of enzymes. V. Further studies on the distribution of cytochrome c in rat liver homogenates, J. Biol. Chem. 183 (1950) 1123–1128.

[38] N. Kamo, M. Muratsugu, R. Hongoh, Y. Kobatake, Membrane potential of mitochondria measured with an electrode sensitive to tetraphenyl phosphonium and relationship between proton electrochemical potential and phosphorylation potential in steady state, J. Membr. Biol. 49 (2) (1979) 105–121.

[39] A. Zolkiewska, B. Zablocka, J. Duszynski, L. Wojtczak, Resting state respiration of mitochondria: reappraisal of the role of passive ion fluxes, Arch. Biochem. Biophys. 275 (2) (1989) 580–590.

[40] A. Cossarizza, D. Ceccarelli, A. Masini, Functional heterogeneity of an isolated mitochondrial population revealed by cytofluorometric analysis at the single organelle level, Exp. Cell Res. 222 (1996) 84–94.

[41] J.R. Lakowicz, Principles of Fluorescence Spectroscopy, second ed., Kluwer Academic/Plenum Publishers, New York, 1999.

[42] J. Plasek, R.F. Dale, K. Sigler, G. Laskay, Transmembrane potentials in cells: a diS-C3(3) assay for relative potentials as an indicator of real changes, Biochim. Biophys. Acta 1196 (2) (1994) 181–190.

[43] R.P. Haugland, Handbook of Fluorescent Probes and Research Products, ninth ed., Molecular Probes, Eugene, 2002.

[44] D.G. Nicholls, The influence of respiration and ATP hydrolysis on the proton-electrochemical gradient across the inner membrane of rat-liver mitochondria as determined by ion distribution, Eur. J. Biochem. 50 (1) (1974) 305–315.

[45] J.B. Hoek, D.G. Nicholls, J.R. Williamson, Determination of the mitochondrial protonmotive force in isolated hepatocytes, J. Biol. Chem. 255 (1980) 1458–1464.

[46] H. Rottenberg, Membrane potential and surface potential in mitochondria: uptake and binding of lipophilic cations, J. Membr. Biol. 81 (2) (1984) 127–138.

[47] J. Sanchez Olavarria, C. Galindo, M. Montero, Y. Baquero, J. Victorica, J. Satrustegui, Measurement of 'in situ' mitochondrial membrane potential in Ehrlich ascites tumor cells during aerobic glycolysis, Biochim. Biophys. Acta 935 (3) (1988) 322–332.

[48] K. Bogucka, A. Wroniszewska, M. Bednarek, J. Duszynski, L. Wojtczak, Energetics of Ehrlich ascites mitochondria: membrane potential of isolated mitochondria and mitochondria within digitonin-permeabilized cells, Biochim. Biophys. Acta 1015 (3) (1990) 503–509.

[49] M.R. Duchen, A. Surin, J. Jacobson, Imaging mitochondrial function in intact cells, Methods Enzymol. 361 (2003) 353–389.

[50] J.F. Keij, C. Bell-Prince, J.A. Steinkamp, Staining of mitochondrial membranes with 10-nonyl acridine orange, MitoFluor Green, and MitoTracker Green is affected by mitochondrial membrane potential altering drugs, Cytometry 39 (3) (2000) 203–210.

[51] J.F. Buckman, H. Hernandez, G.J. Kress, T.V. Votyakova, S. Pal, I.J. Reynolds, MitoTracker labeling in primary neuronal and astrocytic cultures: influence of mitochondrial membrane potential and oxidants, J. Neurosci. Methods 104 (2) (2001) 165–176.

[52] L.F. Marques-Santos, J.G. Oliveira, R.C. Maia, V.M. Rumjanek, Mitotracker green is a P-glycoprotein substrate, Biosci. Rep. 23 (4) (2003) 199–212.

Article 2

Available online at www.sciencedirect.com
SCIENCE DIRECT®
Biochimica et Biophysica Acta 1639 (2003) 53–63
BBA
www.bba-direct.com

Functional alteration of cytochrome *c* oxidase by *SURF1* mutations in Leigh syndrome

Petr Pecina[a], Markéta Čapková[b], Subir K.R. Chowdhury[a], Zdeněk Drahota[a], Audrey Dubot[c], Alena Vojtíšková[a], Hana Hansíková[b], Hana Houšťková[b], Jiří Zeman[b], Catherine Godinot[c], Josef Houštěk[a,*]

[a] *Institute of Physiology and Centre for Integrated Genomics, Academy of Sciences of the Czech Republic, Vídeňská 1083, 142 20 Prague 4-Krč, Czech Republic*
[b] *Department of Paediatrics, 1st Faculty of Medicine, Charles University, Ke Karlovu 2, 129 08 Prague, Czech Republic*
[c] *Center of Molecular and Cellular Genetics, UMR 5534, CNRS, Claude-Bernard University of Lyon 1, 69 622 Villeurbanne, France*

Received 10 March 2003; accepted 21 July 2003

Abstract

Subacute necrotising encephalomyopathy (Leigh syndrome) due to cytochrome *c* oxidase (COX) deficiency is often caused by mutations in the *SURF1* gene, encoding the Surf1 protein essential for COX assembly. We have investigated five patients with different *SURF1* mutations resulting in the absence of Surf1 protein. All of them presented with severe and generalised COX defect. Immunoelectrophoretic analysis of cultured fibroblasts revealed 85% decrease of the normal-size COX complexes and significant accumulation of incomplete COX assemblies of 90–120 kDa. Spectrophotometric assay of COX activity showed a 70–90% decrease in lauryl maltoside (LM)-solubilised fibroblasts. In contrast, oxygen consumption analysis in whole cells revealed only a 13–31% decrease of COX activity, which was completely inhibited by detergent in patient cells but not in controls. In patient fibroblasts ADP-stimulated respiration was 50% decreased and cytofluorometry showed a significant decrease of mitochondrial membrane potential $\Delta\Psi_m$ in state 4, as well as a 2.4-fold higher sensitivity of $\Delta\Psi_m$ to uncoupler. We conclude that the absence of the Surf1 protein leads to the formation of incomplete COX complexes, which in situ maintain rather high electron-transport activity, while their H^+-pumping is impaired. Enzyme inactivation by the detergent in patient cells indicates instability of incomplete COX assemblies.

Keywords: Cytochrome *c* oxidase; *SURF1*; Leigh syndrome; Mitochondrial disorder

1. Introduction

The Leigh syndrome (LS) is a subacute necrotising encephalopathy characterised by bilaterally symmetrical necrotic lesions in subcortical brain regions with onset early in infancy [1]. Heterogeneous genetic defects of both mitochondrial and nuclear origin have been described as a cause of LS [2]. The autosomal recessive LS associated with isolated cytochrome *c* oxidase (COX) deficiency (LS^{COX}) is the most common form of COX disorders [3] and one of the most frequently occurring respiratory chain defects in infancy and childhood. It was genetically confirmed that LS^{COX} is caused by a nuclear gene disorder [4,5]. Furthermore, many of the cases studied belonged to a single complementation group [6,7], suggesting one major locus to be responsible for the disease.

Human COX is composed of 13 subunits: mtDNA genes encode the 3 subunits forming the catalytic core of the enzyme; the other 10 subunits are encoded by the nuclear genome [8]. In addition, numerous nucleus encoded factors are required for efficient assembly and maintenance of the COX holoenzymes that are similar in yeast and human [9,10]. Using different experimental techniques, two groups identified mutations in *SURF1* gene to be responsible for LS^{COX} [11,12]. *SURF1* encodes a protein homologous to

Abbreviations: CS, citrate synthase; COX, cytochrome *c* oxidase; GCCR, glycerophosphate cytochrome *c* reductase; SCCR, succinate cytochrome *c* reductase; LS, Leigh syndrome; LS^{COX}, LS associated with isolated cytochrome *c* oxidase deficiency; LM, lauryl maltoside; $\Delta\Psi_m$, mitochondrial membrane potential; TMRM, tetramethylrhodamine methyl ester

* Corresponding author. Tel.: +42-24106-2434; fax: +42-24106-2149.
E-mail address: houstek@biomed.cas.cz (J. Houštěk).

0925-4439/$ - see front matter © 2003 Elsevier B.V. All rights reserved.
doi:10.1016/S0925-4439(03)00127-3

yeast Shy1p, which is required for efficient assembly of COX [13].

The domain structure of this 30-kDa inner mitochondrial membrane protein is well conserved among eukaryotes and also prokaryotes which underlines its necessity for the function of the respiratory chain [14]. To date, about 30 different pathogenic mutations in *SURF1* have been described [15]. Most of them are nonsense mutations inducing the formation of a premature stop codon; missense and splicing-site mutations are less common. It has been proposed that the severe isolated COX defects result from impaired assembly of the complex, which stops at the S2 intermediate before insertion of subunits II and III into the heterodimer of subunits I and IV [16–18]. The decreased steady-state level of COX subunits [19], pointing to a lesser amount of the COX holoenzyme, is consistent with severely decreased COX activity measured spectrophotometrically [11]. Recent studies on calcium homeostasis in fibroblasts of LS^{COX} patients suggest a decreased mitochondrial membrane potential [20], which might be an important factor negatively affecting the ATP synthesis ability, leading to severe pathological phenotype of the disease. Another analysis revealed increased thermosensitivity and greater susceptibility to detergent inactivation of the COX from LS^{COX} fibroblasts [21], resulting probably from the decreased stability of partially or improperly assembled COX complexes. However, neither the exact role of *SURF1* in COX assembly nor detailed characterisation of the functional consequences of the defect has been reported.

In this paper we analysed fibroblasts from five LS^{COX} patients with *SURF1* mutation combining several experimental techniques novel to LS^{COX} study. Our aim was to gain further insight into the functional consequences of *SURF1* mutations on cell energetics.

2. Materials and methods

2.1. Ethics

This study was carried out in accordance with the Declaration of Helsinki of the World Medical Association and was approved by the Committees of Medical Ethics at all collaborating institutions. Informed consent was obtained from parents.

2.2. Patients

All five children were born in term after an uncomplicated pregnancy with birth weight 3180–3500 g and length 49–52 cm. Their parents and siblings are healthy. In all children, the postnatal adaptation and early psychomotor development were normal in the first months of life, but failure to thrive, progressive muscle hypotonia, hypertrichosis and severe delay in developmental milestones with strabismus (patient 2 and 4), nystagmus (patient 3) or amaurosis (patient 1) were observed at the end of the first year of life, followed by a total arrest of psychomotor development. Biochemical analyses revealed hyperlactacidemia (blood-lactate 2.1–4.9 mmol/l; controls < 2.1) with elevated lactate pyruvate ratio (20–50; controls 10–18) and increased lactate in cerebrospinal fluid (CSF-lactate 3.7–5.8 mmol/l; controls < 2.3). The MRI of the brain (in one case CT) demonstrated symmetrical necrotic lesions in basal ganglia corresponding to LS in all affected children. Four children died after repeated respiratory infection due to cardio-respiratory failure at the age between 3 and 5 years; only one 11-year-old girl with prolonged course of the disease (patient 3) is alive.

2.3. Cell cultures, mitochondria

Human skin fibroblasts were cultured in Dulbecco's modified Eagle's medium (Sevac, Czech Republic) with 10% foetal calf serum (Sigma, Czech Republic). Cells were grown to approximately 90% confluence and harvested using 0.05% trypsin and 0.02% EDTA. Detached cells were diluted with ice-cold culture medium, sedimented by centrifugation and washed twice in phosphate-buffered saline (PBS).

Mitochondria-enriched fractions (mitochondria) were prepared from fibroblasts as before [22]. In brief, trypsinised cells resuspended in 0.25 M sucrose, 10 mM Tris, 1 mM EDTA, pH 7.4 (STE medium) were treated for 15 min with digitonin (0.4 mg/mg protein; Fluka, Switzerland) at 0 °C. The suspension was 10-fold diluted with STE and centrifuged at 12,000 × *g* for 10 min. The pellet was resuspended in STE, washed by centrifugation and resuspended to a final concentration of 1–2 mg protein/ml. Based on immunodetection and enzyme activity measurements, more than 95% of the inner mitochondria membrane proteins were recovered in this fraction.

2.4. DNA analysis and sequencing

All nine exons of *SURF1* were amplified using high-fidelity KlenTaq polymerase (Gene Age Technologies, Prague) in five separate PCR reactions with the intronic primer pairs as described in Table 1. PCR products were extracted from the gel and purified using QIAquick Gel Extraction Kit (Qiagen). PCR products containing exons 1 and 2, very rich in GC, were amplified in the presence of 7-deazadGTP and dGTP (3:1), as described by Zhu et al. [11]. Automated cycle sequencing was performed on Alf express (Amersham Pharmacia Biotech) using AmpliTaq polymerase (Applied Biosystems) and cy5-labeled sequencing primers.

2.5. Bacterial expression and purification of human Surf1 protein

A human *SURF1* cDNA fragment (amino acids 51 to 300 of human Surf1) lacking its natural stop codon and its

Table 1
Primers for PCR amplification of exons 1 to 9 of *SURF1*

Exon(s)	Oligonucleotide sequences[1]	Fragment size (bp)	PCR cycle
1 and 2	sense: 5′-taatacgactcactatagggGCCCCGGCAACTCGCTCATGG-3′ antisense: 5′-caggaaacagctatgacCGCTCAGCCGGCAGTTGGTTCAT-3′	501	94 °C, 10 s, 68 °C, 30 s, 72 °C, 1 min
3 and 4	sense: 5′-taatacgactcactatagggGCTCTAGGCAGCAGGTTTTGATT-3′ antisense: 5′-caggaaacagctatgacGGCAGTGACTAAAAGTCCCACCA-3′	556	94 °C, 10 s, 62 °C, 30 s, 72 °C, 1 min
5	sense: 5′-taatacgactcactatagggCCCTTTGCCTTTCTCCTTCACTT-3′ antisense: 5′-caggaaacagctatgacTCCTACCAAGGTTGGGGATTGT-3′	442	94 °C, 10 s, 62 °C, 30 s, 72 °C, 1 min
6 and 7	sense: 5′-taatacgactcactatagggCCTATGGGTGCCTGAGTGAC-3′ antisense: 5′-caggaaacagctatgacGAGGGTTAGGAGGAAGGACAGTA-3′	508	94 °C, 10 s, 62 °C, 30 s, 72 °C, 1 min
8 and 9	sense: 5′-taatacgactcactatagggAAGGCCATACAGGACTTCCAAC-3′ antisense: 5′-caggaaacagctatgacACTGAAACCAAGCCAGGATTTTA-3′	526	94 °C, 10 s, 62 °C, 30 s, 72 °C, 1 min

[1] *SURF1* sequence is in capital letters, additional sequence complementary to the sequencing primers is in lowercase letters.

presumed mitochondrial signal sequence was inserted by TA cloning into the plasmid pet-15B containing upstream to the N-terminal Surf1p sequence a 6-His sequence and a thrombin site (to cleave the 6-His sequence). The plasmid was used to transform bacteria JM109 (DE3) (Promega) made competent by $CaCl_2$ treatment. The protein was overexpressed in these bacteria by IPTG induction and purified on an affinity nickel column following the QIA expressionist™ protocol and using 8 M urea, 10 mM sodium phosphate, 10 mM Tris and 0.25 M imidazole (pH 4.5) as elution buffer.

2.6. Electrophoretic and Western blot analysis

The samples for Blue-Native-polyacrylamide gel electrophoresis (BN-PAGE) were prepared as described [23]. Mitochondrial protein (150 μg) derived from control and patient fibroblasts was solubilised by digitonin (2 g/g protein) in 50 mM NaCl, 5 mM 6-aminohexanoic acid, 50 mM imidazole/HCl buffer (pH 7.0) and centrifuged at 20,000 × *g* for 20 min. The supernatants were collected and the Serva Blue G dye was added in concentration of 0.1 g/g detergent. Protein aliquots (10 μg) of these samples were separated on a 6–18% gradient polyacrylamide slab gel prepared according to Schagger [23] in Mini Protean system (BioRad). The electrophoretic run was performed at 90 V for 3.5 h.

The samples of fibroblasts and derived mitochondria for SDS-PAGE were boiled for 3 min in a sample lysis buffer (2% mercaptoethanol, 4% SDS, 10 mM Tris–HCl, 10% glycerol). SDS-Tricine electrophoresis [24] was performed on 10% or 12.5% polyacrylamide slab gels (Mini Protean, BioRad). The same protein aliquots (10–15 μg/slot) of control and patient samples of mitochondria or original fibroblasts (10) were loaded.

For immunodetection of Surf1 protein, proteins from the gel were blotted onto a Schleicher and Schuell™ nitrocellulose membrane (0.2-μm pores) by semidry electrotransfer at 0.7 mA/cm^2 for 1 h. The membranes were blocked with PBS containing 5% defatted milk and 0.1% Tween 20, incubated with polyclonal anti-human Surf1 antibody (1:200 dilution, a generous gift from Dr. E.A. Shoubridge, McGill University, Montreal, Canada) and then with goat anti-rabbit IgG conjugated with horseradish peroxidase (1:20,000, BioRad). The blots were developed using Super Signal West Femto substrate (Pierce), essentially as described by Yao and Shoubridge [19].

For immunodetection of respiratory chain enzymes, proteins from the BN-PAGE or SDS-PAGE gels were blotted onto Hybond C-extra nitrocellulose membrane (Amersham) as above and the membrane was blocked in PBS with 0.2% Tween 20 (PBST). The membranes from BN-PAGE were used as a whole; the membranes from SDS-PAGE were cut according to MW markers into parts containing individual subunits. These parts were incubated for 2.5 h with corresponding primary antibodies (monoclonal antibodies against COX I (1:330), COX IV (1:670), COX VIc (1:200) and F_1-ATPase α subunit (1:250) from Molecular Probes diluted in PBST containing 2% bovine serum albumin (PBSTA), followed by incubation for 1.5 h with peroxidase labelled goat anti-mouse IgG (Sigma) diluted 1:1000 in PBSTA. The chemiluminescent reaction using ECL kit (Amersham) was detected on LAS 1000 (Fuji, Japan) and the signal was quantified using Aida 2.11 Image Analyser software.

2.7. Spectrophotometric measurements of respiratory chain enzymes activities

COX, succinate-cytochrome *c* reductase (SCCR), glycerophosphate-cytochrome *c* reductase (GCCR) and citrate synthase (CS) were assayed at 30 °C as previously [25]. In brief, samples of 0.1 mg protein of cultured cells were solubilised with 4 mg lauryl maltoside (LM)/mg protein in 1 ml of 20 mM phosphate buffer at pH 7.4 and the COX reaction was started by addition of 40 μM reduced cytochrome *c*. SCCR and GCCR were measured in a medium containing 10 mM potassium phosphate (pH 7.8), 2 mM EDTA, 0.01% bovine serum albumin (fatty-acid-free), 0.2 mM ATP, 1 mM KCN, 5 μM rotenone and 10 mM succinate or 20 mM glycerophosphate. Cells (0.2 mg protein) were incubated with 1 mg digitonin/mg protein in 1 ml of the medium for 2 min at 30 °C, then the reaction was started by 40 μM oxidised cytochrome *c* and assayed for 5 min. CS

was determined at 30 °C in a medium containing 150 mM Tris–HCl (pH 8.2), 4 mg LM/mg protein, 0.1 mM dithionitrobenzoic acid and 0.2 mg protein of fibroblasts/ml. The reaction was started with 5 μM acetyl CoA and changes of absorbance at 412 nm were read for 1 min. This value was subtracted from the rate obtained after subsequent addition of 0.5 mM oxaloacetic acid.

2.8. Polarographic measurements

Oxygen consumption by fibroblasts was determined at 30 °C as described before [25] using the OROBOROS oxygraph (Innsbruck, Austria). Freshly harvested fibroblasts were resuspended in a KCl medium (80 mM KCl, 10 mM Tris–HCl, 3 mM $MgCl_2$, 1 mM EDTA, 5 mM potassium phosphate, pH 7.4) and cells (1 mg protein/ml) were permeabilised by digitonin using 0.05 mg/mg protein. Various respiratory substrates and inhibitors were used as indicated. Oxygen consumption was expressed in pmol oxygen/s/mg protein. COX activity was measured with 5 mM ascorbate, 0.2 or 1 mM TMPD and 40 μM cytochrome *c*, and it was corrected for autooxidation, which was determined as 0.33 mM KCN-insensitive oxygen uptake.

2.9. Cytofluorometric analysis of mitochondrial membrane potential

Mitochondrial membrane potential ($\Delta\Psi_m$) measurements were performed on the FACSort flow cytometer (Becton Dickinson, San Jose, CA, USA) according to Floryk and Houstek [26]. Fibroblasts were resuspended in the KCl medium containing 10 mM succinate at a protein concentration of 1 mg/ml and permeabilised by 0.1 mg digitonin/mg protein. Permeabilised fibroblasts were resuspended in the KCl medium at 0.2 mg protein/ml and incubated with 20 nM tetramethylrhodamine methyl ester (TMRM, Molecular Probes, USA). A minimum of 5000 cells was used for each FACS measurement. Data were acquired on a log scale using CellQuest (Becton Dickinson) and analysed with WinMDI 2.8 software (Trotter, J., TSRI, La Jolla, USA). Arithmetic mean values of fluorescence signal in arbitrary units were determined for each sample for subsequent graphic representation.

2.10. Protein determination

The protein content was measured according to the method of Bradford [27] or by the Micro BCA protein kit (BioRad), using bovine serum albumin as a standard. Cell samples were sonicated for 20 s prior to protein determination.

2.11. Statistics

Data are presented as mean ± S.D. values derived from parallel measurements in both patients and controls. Standard *t* test or Mann–Whitney *U* test was used for significance calculations ($P < 0.05$).

3. Results

3.1. SURF1 mutations

DNA analysis revealed different mutations of *SURF1* gene in the investigated patients (Table 2). Patient 1 was homozygous for the frameshift mutation 841delCT that introduces a premature stop codon in exon 9. This mutation, first described by Tiranti et al. [28], has already been reported for several other patients (for review see Ref. [15]). Patient 2 exhibited mutation 312insAT/del10 which occurs at high frequency in LS^{COX} patients and a 821del18 mutation which results in the removal of exon 8 [29]. Patient 3, who is the only one surviving at the age of 11 years, was heterozygous, carrying the 841delCT mutation (see above) and a new C574T missense mutation in exon 6 that changed the arginine at position 192 to a tryptophan [30]. Interestingly, the Arg^{192} is conserved in all eukaryots but *Arabidopsis thaliana* while it is only occasionally found in bacterial Surf1 homologs [14]. Patient 4 is homozygous for the previously described mutation C688T changing the arginine in position 230 into a stop codon [18,31]. Patient 5 carried the 841delCT mutation. No other mutation could be detected in patient 5, similarly as in several other published cases [32].

3.2. Absence of Surf1 protein

Fig. 1 shows that the Surf1 protein could not be detected in fibroblast mitochondria of any of the five LS^{COX} patients by Western blot analysis, using rabbit anti-human Surf1 antibody, although the antibody reacted well with isolated Surf1 protein and clearly detected the Surf1 protein in mitochondria from control fibroblasts.

3.3. Changes in COX activity and respiratory control

Fibroblasts from all LS^{COX} patients exhibited severely decreased COX activity in comparison with control cells

Table 2
Mutations in *SURF1* in five patients with Leigh syndrome due to COX deficiency

Patient	Exon	Mutations	Mutation type
P1	9/9	841 delCT/841 delCT	frameshift/frameshift: stop codon 870–872
P2	4/8–9	312 insATdel10/821 del18	frameshift: stop codon 316–318/exon 8 removal
P3	6/9	C574>T/841 delCT	Arg192>Trp/frameshift: stop codon 870–872
P4	7/7	C688>T/C688>T	Arg230>stop/Arg230>stop
P5	9/–	841 delCT/–	frameshift: stop codon 870–872/–

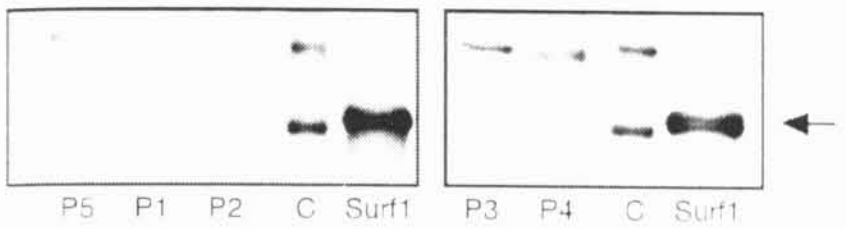

Fig. 1. Surf1 protein content in fibroblasts of patients with different *SURF1* mutations. Surf1, 20 ng of recombinant Surf1 protein (amino acids 50 to 300, about 30 kDa); C, controls; P1–P5, patients 1 to 5. For analysis 15 μg protein of mitochondria from patient and control fibroblasts was used. The arrow marks the position of Surf1 protein antigen.

when using the standard diagnostic spectrophotometric assay (Table 3). In the group of five patients the COX was decreased approximately to 20% of the controls (the mean values were 7.34 and 36.41 nmol cytochrome *c* oxidised/min/mg protein in LS^{COX} patients and control fibroblasts, respectively). We found similar decrease of COX activity in all of our patients, despite the differences in the course of the disease. Activities of other mitochondrial enzymes, SCCR, GCCR and CS, were the same as in control cells. Thus, the COX activity related to CS, a mitochondrial matrix marker, was fourfold decreased (0.14 in the LS^{COX} patients and 0.57 in the controls, respectively) (Table 3).

By spectrophotometric analysis of COX using permeabilised mitochondria, a maximum activity is achieved which is known to be in excess over the other components of the respiratory chain; however, when the COX activity is determined as oxygen consumption with TMPD + ascorbate in whole cells with intact mitochondria, the activity of COX exceeds only by 1.5–2.5-fold the activity of respiratory chain dehydrogenases [33,34]. When we measured the oxygen consumption by LS^{COX} fibroblasts in the presence of FCCP, the activity of succinate oxidase accounted for 80% of the activity of controls (Fig. 2, Table 4). Similarly, we found that COX activity in LS^{COX} fibroblasts with *SURF1* mutations was 69–87% of activity in control cells, depending on the concentration of TMPD used. Thus, in contrast to spectrophotometric measurements, the COX activity in patient fibroblasts was much less decreased when measured polarographically in cells containing intact mitochondria.

Oxygraphic analysis further showed significantly lower activation of respiration by ADP (Fig. 2), both absolutely and in relation to state 3 uncoupled respiration. When using succinate as a substrate, the ADP-stimulated respiration in the patient cells was 50% decreased compared to control fibroblasts (Table 4) and consequently, the ratio between state 3-ADP and state 3-uncoupled respiration was 1.6-fold lower in patient cells.

As shown in Fig. 3, the discrepancy between the spectrophotometric and polarographic detection of COX activity in LS^{COX} fibroblasts resulted from a different sensitivity of COX in LS^{COX} and control cells to detergent action. Addition of 0.012% LM to the polarographic assay completely inhibited the COX activity in LS^{COX} fibroblasts but it was without any effect on the COX activity in control cells. When we titrated the COX activity in LS^{COX} patients by sequential additions of LM we found pronounced COX inactivation already at about 0.009% of LM (Fig. 3). The effect of LM was the same when using 0.2 mM TMPD (Fig. 3) or 1 mM TMPD (not shown). As solubilisation by LM is routinely used in COX activity measurements in most studies, it is highly probable that the very low COX activity described in the literature in LS^{COX} patients reflects the higher sensitivity of COX in LS^{COX} patients with *SURF1* mutations to detergents.

3.4. The content and subunit composition of COX complexes

To assess the amount and composition of COX complexes in patient versus control mitochondria isolated from fibroblasts, we analysed digitonin-solubilised samples (2 mg mg protein) by the BN-PAGE and Western blotting using monoclonal antibody against subunit COX I (Molecular Probes A6404) (Fig. 4A). Such analysis detects not only the COX monomers but also supramolecular structures containing COX [35] and assembly intermediates accumulating due to alteration of assembly of the enzyme, because COX I is the subunit starting the assembly process [16]. In LS^{COX} mitochondria compared to controls, the quantification revealed only a 30% content of the total COX I signal and pronounced changes of its distribution among several distinct structures. Only half of the signal in LS^{COX} mitochondria comes from COX assemblies found in control mitochondria, existing either as COX monomers or COX-containing supramolecular structures with other respiratory chain enzymes. The other half of the signal in LS^{COX} mitochondria was found in assembly intermediates ranging in size from 90 to 120 kDa, which were absent in controls. Quantitatively, the COX I in incomplete forms of patient COX made up about 15% of the total COX I signal in controls.

In order to further characterize the respiratory chain supramolecular structures according to Schagger's nomenclature [35], we performed detection with antibody against NADH39 subunit of complex I. Unlike to COX, the sum of

Table 3
Spectrophotometric determination of enzyme activities in cultured fibroblasts of LS^{COX} patients

	Controls	LS^{COX} patients	Percent controls
COX	36.41 ± 9.73	7.43 ± 3.60	20.4*
SCCR	8.73 ± 1.80	8.57 ± 4.08	98.2
GCCR	7.83 ± 0.96	9.28 ± 2.77	118.6
CS	66.31 ± 35.72	63.94 ± 8.61	96.4
COX/CS	0.57 ± 0.25	0.14 ± 0.03	24.6*

Specific activities of cytochrome *c* oxidase (COX), succinate cytochrome *c* reductase (SCCR), glycerophosphate cytochrome *c* reductase (GCCR) and citrate synthase (CS) are expressed in nmol/min/mg protein. Values are the mean ± S.D. of measurements performed in 5 LS^{COX} and 5–30 control fibroblast cultures.

* $P < 0.01$.

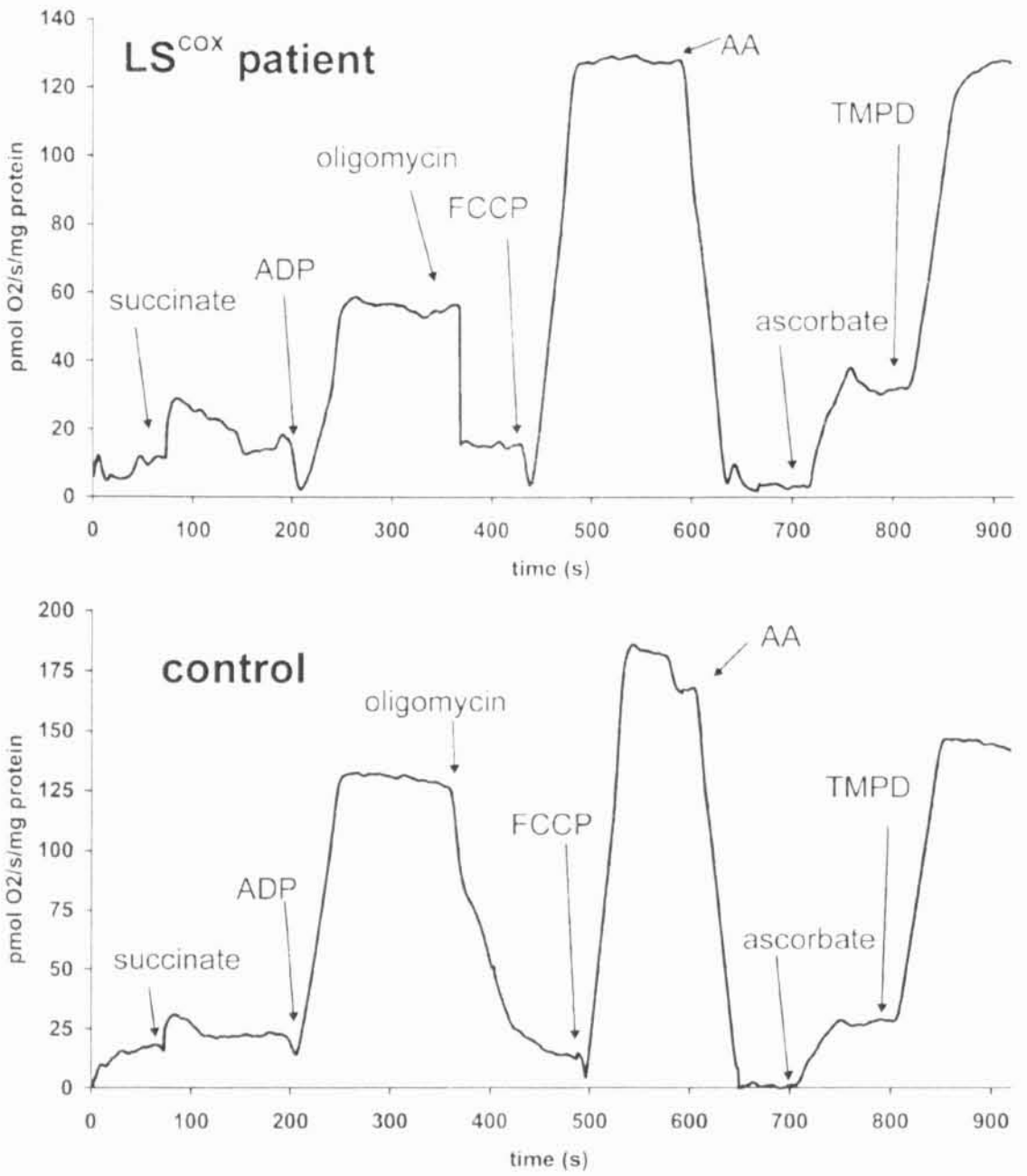

Fig. 2. Oxygen consumption by digitonin-permeabilised fibroblasts. Measurements were performed using 1.0 mg cell protein/ml and 0.05 mg digitonin/mg protein. Subsequent additions of 10 mM succinate, 0.5 mM ADP, 1 μM oligomycin, 1 μM FCCP, 0.2 μg/ml antimycin A (AA), 5 mM ascorbate, 0.2 mM TMPD are indicated. Oxygen consumption is expressed as negative values of the 1st time derivative of changes in oxygen concentration (pmol O_2/s/mg protein).

the NADH39 signal in patient mitochondria was elevated (Fig. 4A) and complexes III and V were also increased (data not shown). In control mitochondria about 60% of COX and virtually all complex I were associated in supracomplex b

Table 4
Polarographic determination of succinate oxidase and COX activities in fibroblasts of controls and LS^{COX} patients

Additions	LS^{COX} patients	Controls	Percent controls
10 mM succinate + 0.5 mM ADP	64.25 ± 16.72 (n = 5)	129.34 ± 27.97 (n = 12)	50*
10 mM succinate + 1 μM FCCP	142.61 ± 52.03 (n = 5)	179.31 ± 45.94 (n = 11)	80
5 mM ascorbate + 0.2 mM TMPD + 1 μM FCCP	52.14 ± 14.69 (n = 5)	65.83 ± 13.74 (n = 12)	87
5 mM ascorbate + 1 mM TMPD + 1 μM FCCP	191.39 ± 21.12 (n = 4)	275.84 ± 30.06 (n = 3)	69*

Activities are expressed in pmol oxygen/s/mg protein. Measurements of oxygen consumption induced by ascorbate + TMPD represent KCN-sensitive activities. Values are the mean ± S.D., n — number of experiments.
* $P < 0.05$

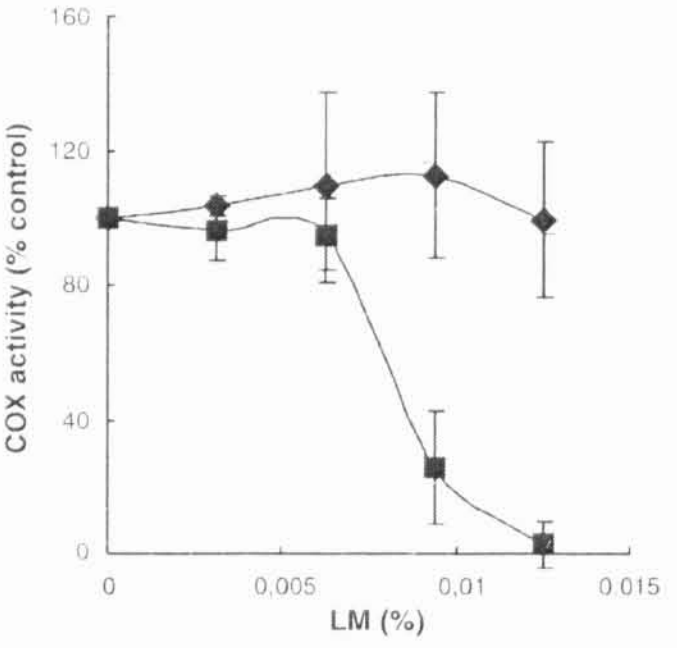

Fig. 3. The effect of lauryl maltoside on COX activity in LS^{COX} and control fibroblasts. COX activity measured polarographically with 5 mM ascorbate and 0.2 mM TMPD is expressed in percent of the values obtained in the absence of lauryl maltoside. Data are the mean ± S.D. of measurements performed in control (F, n = 7) and LS^{COX} (■, n = 5) fibroblasts.

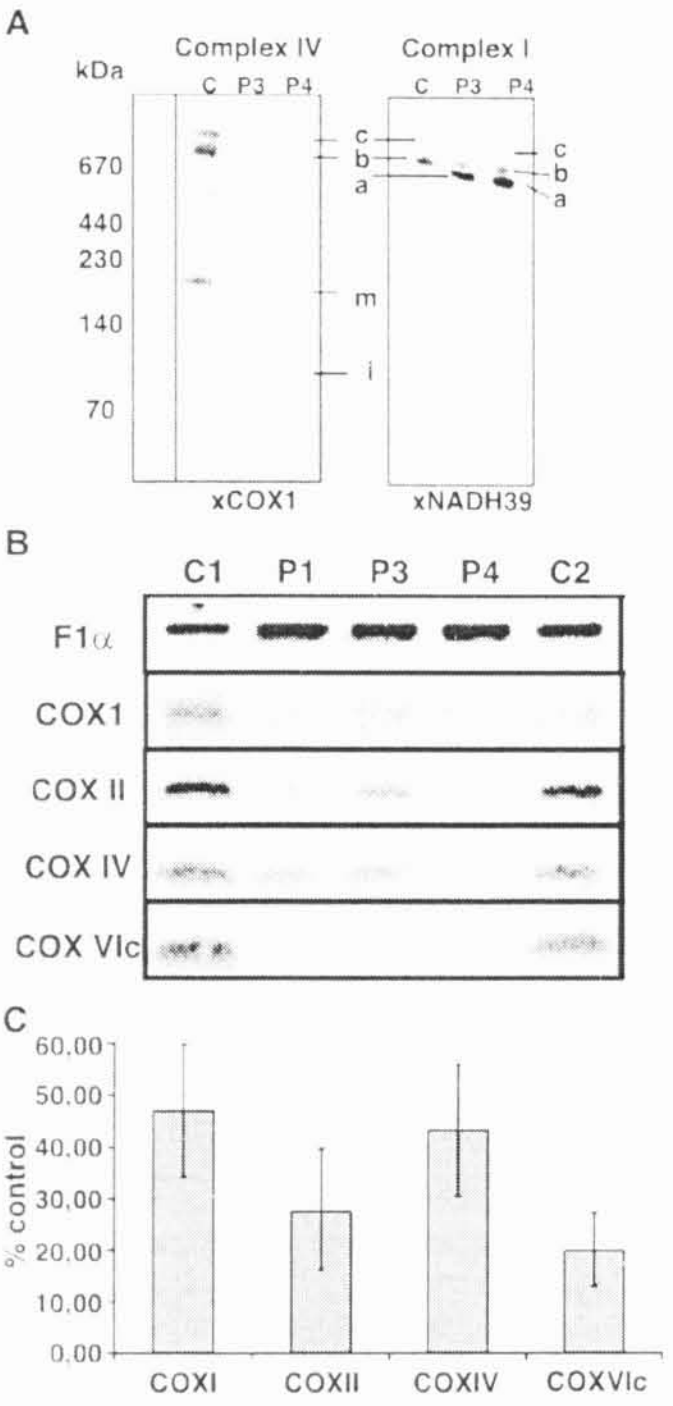

Fig. 4. Electrophoretic analysis of COX in fibroblasts with *SURF1* mutations. (A) BN-PAGE Western blot developed with anti COX I or anti NADH39 monoclonal antibodies. Ten-microgram protein aliquots from control (C) and patients 3 and 4 (P3 and P4) were loaded. Legend to marks: i stands for incomplete COX assemblies, m stands for COX monomer, and a, b, and c mark the respiratory supracomplexes I_1III_2, $I_1III_2IV_1$, and $I_1III_2IV_2$, respectively. (B) SDS-PAGE Western blot of the COX subunits content. Ten-microgram protein aliquots of mitochondria from control fibroblasts (C) and from fibroblasts of LS^{COX} patients P1, P3, and P4 were used for analysis. Detection was done with monoclonal antibodies to the α subunit of F_1-ATPase (F1 α) and COX subunits I, II, IV, and VIc. (C) The graph shows the mean + S.D. values of the content of COX subunits determined in three LS^{COX} patients, expressed in percent of controls.

($I_1III_2IV_1$) and to a lesser extent in supracomplex c ($I_1III_2IV_2$). The levels of both these structures were pronouncedly decreased in samples from patients, where most of the complex I was found in COX-lacking supracomplex a (I_1III_2), most likely due to lack of complex IV needed for stoichiometric assembly of greater structures.

To determine the composition of COX complexes in LS^{COX} fibroblasts with *SURF1* mutation, we performed SDS-PAGE and Western blot analysis using commercially available specific monoclonal antibodies against four different COX subunits, COX I, COX II, COX IV, COX VIc, and against subunit α of F_1-ATPase (Molecular Probes, antibodies A6403,IIIkk A6404, A6409, A6401 and A11144) (Fig. 4B). The detection with monoclonal antibodies revealed about twofold decrease in the content of COX I and COX IV subunits in mitochondria from LS^{COX} patients (Fig. 4C). Even lower was the content of COX II subunit (28% of the control) and the most reduced was the content of COX VIc subunit (20% of the control). In contrast, the content of the F_1-ATPase α subunit was by about 50% higher, this result together with the above BN-PAGE data perhaps pointing to a compensatory mechanism induced by impaired energy provision. The same results were obtained when using whole fibroblasts (not shown).

These electrophoretic data indicate a substantial decrease of the content of normal COX assemblies (monomer and supracomplexes) in fibroblasts of our LS^{COX} patients.

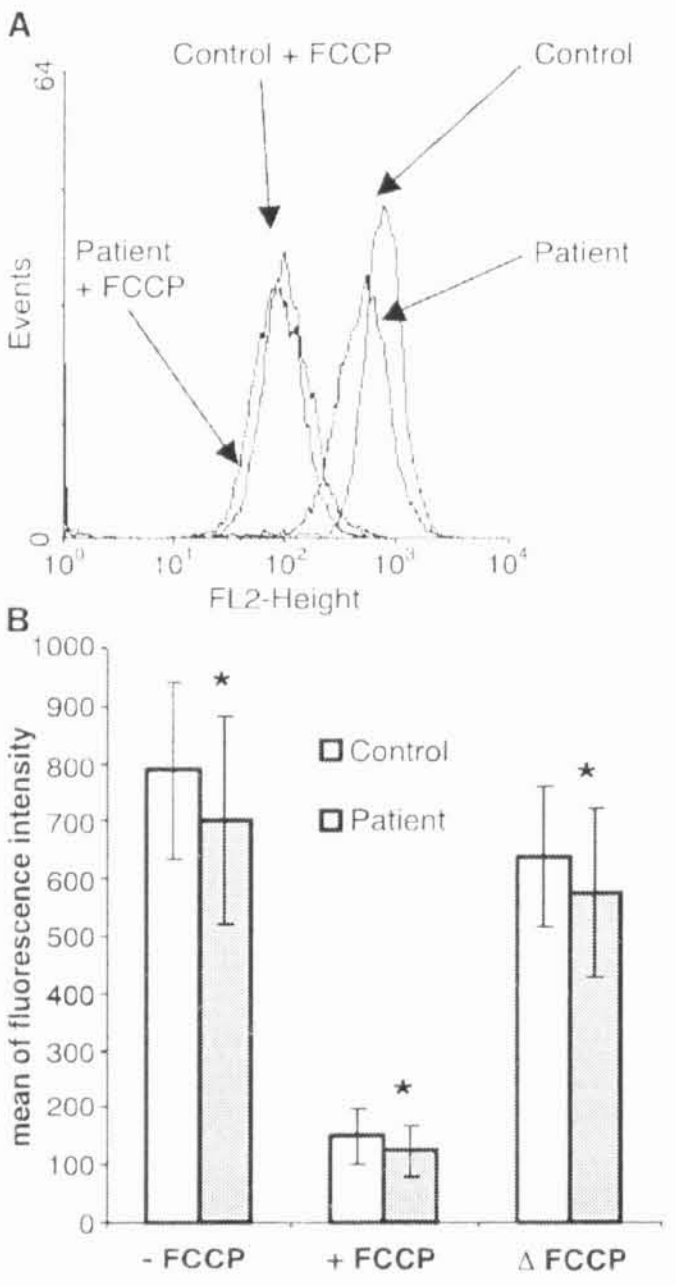

Fig. 5. Cytofluorometric detection of mitochondrial $\Delta\Psi_m$ with TMRM. Fibroblasts from control and LS^{COX} patients were permeabilised with digitonin (0.1 mg/mg protein of cells) and stained with 20 nM TMRM in a KCl medium containing 10 mM succinate. (A) Typical reading of TMRM fluorescence in the presence and absence of 1 μM FCCP is shown. Intensity of fluorescence (FL2 height) on the abscissa; cell number (events) on the ordinate. (B) The mean ± S.D. (n = 35–39) and statistical significance (*) of data evaluated using the Mann–Whitney U test is shown.

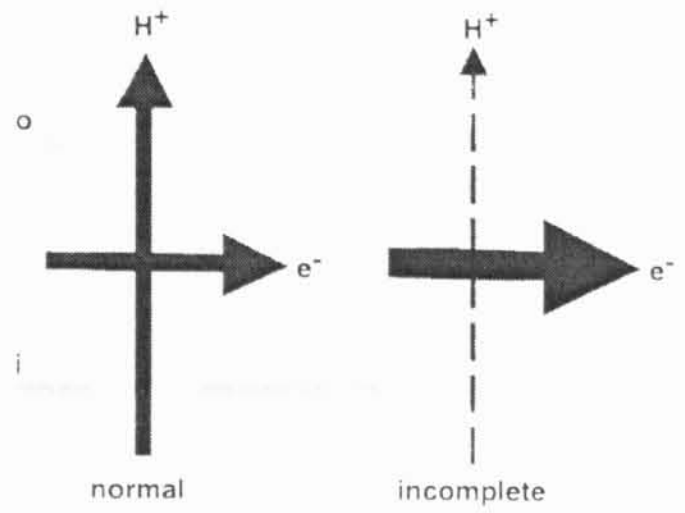

Fig. 7. The schematic drawing of the hypothesised COX complexes present in LS^{COX} patients. The complete COX enzyme present in 15% quantity compared with control has normal electron-transport and proton-pumping activity. The accumulated incomplete COX assemblies lacking small nucleus-encoded subunits have up-regulated electron-transport activity, but their proton-pumping ability is impaired.

succinate oxidase activities compared to controls, although the COX activity of LS^{COX} cells was highly reduced in the spectrophotometric measurement in the presence of a detergent. This discrepancy between spectrophotometric and polarographic data could be explained by different sensitivity of COX to the detergent in patient cells. In spectrophotometric measurement of COX, the mitochondrial membrane has to be disrupted or solubilised to ensure penetration of exogenous cytochrome *c* but when the COX activity is measured as oxygen uptake, ascorbate and TMPD are used as electron donors that freely react with an endogenous cytochrome *c* in intact mitochondria. We found that COX activity measured polarographically in control fibroblasts is quite resistant to increasing concentrations of LM, whereas in fibroblasts with *SURF1* mutation the COX activity was highly decreased by the detergent (Fig. 3). Importantly, we used the conditions (0.2–1 mM TMPD + 5 mM ascorbate), when the COX activity corresponds well with oxidation of endogenous substrates in intact cells or has only slight excess capacity, thus exhibiting substantial control strength over the respiratory rate [33,34,42]. Indeed, these recent experiments of Attardi's laboratory are in agreement with the concept of a "second mechanism of respiratory control" postulated by Kadenbach [43,44] that is based on regulation of COX activity and H^+/e^- ratios in vivo and contrast with the original studies suggesting negligible control strength by COX (for review see Ref. [45]). Similarly to our spectrophotometric assay, usage of sonication instead of detergent also leads to detection of only residual COX activity in patient cells [46]. Increased sensitivity of COX to LM in the case of LS^{COX} has been reported before [47]. While in control cells they found a biphasic, activatory and inhibitory dependence of COX activity, only the inhibitory phase was found in LS^{COX} fibroblasts which contained reduced amount of several nucleus-encoded subunits. Interestingly, the monophasic COX dependence was also present in structurally simple COX from *Paracoccus denitrificans* [48] which lacks homologues of the most of mammalian subunits encoded in the nucleus.

These data indicate that in accordance with delayed manifestation of clinical symptoms, the metabolic consequence of *SURF1* mutation might be in fact milder than generally expected from routine COX measurements. Polarographic oxygen consumption studies of respiratory chain enzymes thus may better mirror the in vivo conditions because the oxidative phosphorylation is fully functional, while spectrophotometric analysis is advantageous in diagnostics of the COX defect due to unmasking of the lability of the enzyme complex.

Based on significant decrease in ADP-stimulated respiration and energy coupling in LS^{COX} fibroblasts, our characterisation of the functional changes of COX due to *SURF1* mutations was further aimed at the H^+-translocating activity of the respiratory chain. We used an indirect approach—the cytofluorometric measurements of the mitochondrial membrane potential $\Delta\Psi_m$ in permeabilised cells using TMRM as fluorescent probe. In our previous studies this method proved useful to detect the decrease in steady-state level of $\Delta\Psi_m$ in fibroblasts and cybrids with a pronounced COX defect due to A8344G MERRF mutation [49]. In the case of LS^{COX} fibroblasts with various *SURF1* mutations compared with control cells, we found a small but significant decrease in $\Delta\Psi_m$ at state 4 (Fig. 5) when the use of the proton gradient is minimised. Furthermore, titrations with FCCP, which simulate the functional load that must be compensated for by increased proton pumping from the matrix, showed much higher sensitivity of patients' fibroblasts to the uncoupling effect of FCCP. This indicates a decrease of proton pumping activity of COX in patient cells. Interestingly, it has been suggested by Wasniewska et al. [20] on the basis of calcium homeostasis studies that the LS^{COX} fibroblasts with *SURF1* mutations may have a decreased $\Delta\Psi_m$.

These functional changes should be related to changes in the amount and composition of COX molecules in LS^{COX} cells. Tiranti et al. [17] found that *SURF1* mutation interferes with assembly of COX subunits at the level of S2 subcomplex. They also detected only a small residual portion of fully assembled enzyme complex, which agrees very well with our results of 15% content of normal COX assemblies in patient mitochondria. Interestingly, this estimate corresponds well with the remaining COX activity in LS^{COX} determined spectrophotometrically (Table 3). Based on our BN-PAGE analysis, half of the total sum of COX complexes in LS^{COX} exists as incomplete assemblies. It is well established that LS^{COX} cells with *SURF1* mutations contain decreased amounts of various COX subunits, coded for by mitochondrial and nuclear DNA, but the data differ in various studies [19,31,50–53]. Our quantification in mitochondria from cultured fibroblasts showed an approximately 50% decrease of the content of subunits I and IV, a 70% decrease of the subunit II and 80% decrease of the level of VIc subunit, a pattern that was quite similar to the results of

Yao and Shoubridge [19] or von Kleist-Retzow et al. [52]. The differential decrease of individual COX subunits in patients with *SURF1* mutations detected by us and in the above-mentioned studies further indicates that incomplete COX assemblies would preferentially lack some of the small nucleus-encoded subunits. These findings, together with the polarographic measurements of COX activity, showing that half reduction of subunit I and IV and 70% reduction of subunit II may still allow for a near-normal function of respiratory chain-linked dehydrogenases in situ, are opening the question to what extent and how the partially assembled COX subcomplexes can operate. As hemes *a* and a_3 are present in COX subunit I, and assuming that also subcomplexes containing COX I + COX II are capable of electron transfer activity, these incomplete COX assemblies must contribute substantially to oxygen consumption determined in polarographic experiments. This would be possible if some of the incomplete, but functional, COX assemblies are more active in electron transport but less in H^+ pumping activity than the complete COX complexes (Fig. 7). It has been shown by Kadenbach's group that the activity of COX is increased upon removal or dissociation of subunit COX VIb [54] or COX VIa [48], in accordance with the hypothesis that small nucleus-encoded subunits physiologically down-regulate the activity of the mammalian enzyme [43,48].

It would be thus possible that the absence of some of the nucleus-encoded subunits, as is generally found in *SURF1* patients, may in fact paradoxically serve as some kind of a rescue mechanism that keeps the COX electron transport activity in situ only mildly decreased. This would provide near-normal electron flux through the respiratory chain and allow proton pumping at complexes I and III ensuring at least decreased level of ATP synthesis.

Acknowledgements

The expert technical assistance of V. Brozková and V. Fialová is gratefully acknowledged. This work was supported by grants from the Charles University (8/2000/C), the Grant Agency of the Czech Republic (303/03/0749), the Ministry of Health of the Czech Republic (NE 6533-3), the institutional projects VZ111100003 and AVOZ5011922, the Barrande Grant 2001-028-1 and the AFM grant (dDT2001).

References

[1] S. DiMauro, M. Zeviani, S. Servidei, E. Bonilla, A.F. Miranda, A. Prelle, E.A. Schon, Cytochrome oxidase deficiency: clinical and biochemical heterogeneity, Ann. N.Y. Acad. Sci. 488 (1986) 19–32.
[2] S. Rahman, R.B. Blok, H.H. Dahl, D.M. Danks, D.M. Kirby, C.W. Chow, J. Christodoulou, D.R. Thorburn, Leigh syndrome: clinical features and biochemical and DNA abnormalities, Ann. Neurol. 39 (1996) 343–351.
[3] B.H. Robinson, Human cytochrome oxidase deficiency, Pediatr. Res. 48 (2000) 581–585.
[4] A.F. Miranda, S. Ishii, S. DiMauro, J.W. Shay, Cytochrome *c* oxidase deficiency in Leigh's syndrome: genetic evidence for a nuclear DNA-encoded mutation, Neurology 39 (1989) 697–702.
[5] V. Tiranti, M. Munaro, D. Sandona, F. Lamantea, M. Rimoldi, S. DiDonato, R. Bisson, M. Zeviani, Nuclear DNA origin of cytochrome *c* oxidase deficiency in Leigh's syndrome: genetic evidence based on patient's-derived rho degrees transformants, Hum. Mol. Genet. 4 (1995) 2017–2023.
[6] M. Munaro, V. Tiranti, D. Sandona, F. Lamantea, G. Uziel, R. Bisson, M. Zeviani, A single cell complementation class is common to several cases of cytochrome *c* oxidase-defective Leigh's syndrome, Hum. Mol. Genet. 6 (1997) 221–228.
[7] R.M. Brown, G.K. Brown, Complementation analysis of systemic cytochrome oxidase deficiency presenting as Leigh syndrome, J. Inherit. Metab. Dis. 19 (1996) 752–760.
[8] J.W. Taanman, Human cytochrome *c* oxidase: structure, function, and deficiency, J. Bioenerg. Biomembranes 29 (1997) 151–163.
[9] R.O. Poyton, J.E. McEwen, Crosstalk between nuclear and mitochondrial genomes, Ann. Rev. Biochem. 65 (1996) 563–607.
[10] L.A. Grivell, M. Artal-Sanz, G. Hakkaart, L. de Jong, I.G. Nijtmans, K. van Oosterum, M. Siep, H. van der Spek, Mitochondrial assembly in yeast, FEBS Lett. 452 (1999) 57–60.
[11] Z. Zhu, J. Yao, T. Johns, K. Fu, I. De Bie, C. Macmillan, A.P. Cuthbert, R.F. Newbold, J. Wang, M. Chevrette, G.K. Brown, R.M. Brown, E.A. Shoubridge, SURF1, encoding a factor involved in the biogenesis of cytochrome *c* oxidase, is mutated in Leigh syndrome, Nat. Genet. 20 (1998) 337–343.
[12] V. Tiranti, K. Hoertnagel, R. Carrozzo, C. Galimberti, M. Munaro, M. Granatiero, L. Zelante, P. Gasparini, R. Marzella, M. Rocchi, M.P. Bayona-Bafaluy, J.A. Enriquez, G. Uziel, F. Bertini, C. Dionisi-Vici, B. Franco, T. Meitinger, M. Zeviani, Mutations of SURF-1 in Leigh disease associated with cytochrome *c* oxidase deficiency, Am. J. Hum. Genet. 63 (1998) 1609–1621.
[13] I.G. Nijtmans, M. Artal Sanz, M. Bucko, M.H. Farhoud, M. Feenstra, G.A. Hakkaart, M. Zeviani, L.A. Grivell, Shy1p occurs in a high molecular weight complex and is required for efficient assembly of cytochrome *c* oxidase in yeast, FEBS Lett. 498 (2001) 46–51.
[14] A. Poyau, K. Buchet, C. Godinot, Sequence conservation from human to prokaryotes of Surf1, a protein involved in cytochrome *c* oxidase assembly, deficient in Leigh syndrome, FEBS Lett. 462 (1999) 416–420.
[15] M.O. Pequignot, R. Dey, M. Zeviani, V. Tiranti, C. Godinot, A. Poyau, C. Sue, S. Di Mauro, M. Abitbol, C. Marsac, Mutations in the SURF1 gene associated with Leigh syndrome and cytochrome *c* oxidase deficiency, Human Mutat. 17 (2001) 374–381.
[16] L.G. Nijtmans, J.W. Taanman, A.O. Muijsers, D. Speijer, C. Van den Bogert, Assembly of cytochrome-*c* oxidase in cultured human cells, Eur. J. Biochem. 254 (1998) 389–394.
[17] V. Tiranti, C. Galimberti, L. Nijtmans, S. Bovolenta, M.P. Perini, M. Zeviani, Characterization of SURF-1 expression and Surf-1p function in normal and disease conditions, Hum. Mol. Genet. 8 (1999) 2533–2540.
[18] M.J. Coenen, L.P. van den Heuvel, L.G. Nijtmans, E. Morava, I. Marquardt, H.J. Girschick, F.J. Trijbels, L.A. Grivell, J.A. Smeitink, SURFEIT-1 gene analysis and two-dimensional blue native gel electrophoresis in cytochrome *c* oxidase deficiency, Biochem. Biophys. Res. Commun. 265 (1999) 339–344.
[19] J. Yao, E.A. Shoubridge, Expression and functional analysis of SURF1 in Leigh syndrome patients with cytochrome *c* oxidase deficiency, Hum. Mol. Genet. 8 (1999) 2541–2549.
[20] M. Wasniewska, E. Karczmarewicz, M. Pronicki, D. Piekutowska-Abramczuk, K. Zablocki, E. Popowska, E. Pronicka, J. Duszynski, Abnormal calcium homeostasis in fibroblasts from patients with Leigh disease, Biochem. Biophys. Res. Commun. 283 (2001) 687–693.

[21] S. Possekel, A. Lombes, H. Ogier de Baulny, M.A. Cheval, M. Fardeau, B. Kadenbach, N.B. Romero, Immunohistochemical analysis of muscle cytochrome *c* oxidase deficiency in children, Histochem. Cell Biol. 103 (1995) 59–68.
[22] P. Klement, L.G. Nijtmans, C. Van den Bogert, J. Houstek, Analysis of oxidative phosphorylation complexes in cultured human fibroblasts and amniocytes by blue-native-electrophoresis using mitoplasts isolated with the help of digitonin, Anal. Biochem. 231 (1995) 218–224.
[23] H. Schagger, Blue-native gels to isolate protein complexes from mitochondria, Methods Cell Biol. 65 (2001) 231–244.
[24] H. Schagger, G. von Jagow, Tricine-sodium dodecyl sulfate-polyacrylamide gel electrophoresis for the separation of proteins in the range from 1 to 100 kDa, Anal. Biochem. 166 (1987) 368–379.
[25] S.K. Chowdhury, Z. Drahota, D. Floryk, P. Calda, J. Houstek, Activities of mitochondrial oxidative phosphorylation enzymes in cultured amniocytes, Clin. Chim. Acta 298 (2000) 157–173.
[26] D. Floryk, J. Houstek, Tetramethyl rhodamine methyl ester (TMRM) is suitable for cytofluorometric measurements of mitochondrial membrane potential in cells treated with digitonin, Biosci. Rep. 19 (1999) 27–34.
[27] M.M. Bradford, A rapid and sensitive method for the quantitation of microgram quantities of protein utilizing the principle of protein dye binding, Anal. Biochem. 72 (1976) 248–254.
[28] V. Tiranti, L. D'Agruma, D. Pareyson, M. Mora, F. Carrara, L. Zelante, P. Gasparini, M. Zeviani, A novel mutation in the mitochondrial tRNA(Val) gene associated with a complex neurological presentation, Ann. Neurol. 43 (1998) 98–101.
[29] S.L. Williams, J.W. Taanman, H. Hansikova, H. Houst'kova, S. Chowdhury, J. Zeman, J. Houstek, A Novel Mutation in SURF1 Causes Skipping of Exon 8 in a Patient with Cytochrome *c* Oxidase-Deficient Leigh Syndrome and Hypertrichosis, Mol. Genet. Metab. 73 (2001) 340–343.
[30] M. Capkova, H. Hansikova, C. Godinot, H. Houst'kova, J. Houstek, J. Zeman, A new missense mutation of 574C>T in the SURF1 gene—biochemical and molecular genetic study in seven children with Leigh syndrome, Cas. Lek. Ces. 141 (2002) 636–641.
[31] A. Poyau, K. Buchet, M.F. Bouzidi, M.T. Zabot, B. Echenne, J. Yao, E.A. Shoubridge, C. Godinot, Missense mutations in SURF1 associated with deficient cytochrome *c* oxidase assembly in Leigh syndrome patients, Hum. Genet. 106 (2000) 194–205.
[32] V. Tiranti, M. Jaksch, S. Hofmann, C. Galimberti, K. Hoertnagel, L. Lulli, P. Freisinger, L. Bindoff, K.D. Gerbitz, G.P. Comi, G. Uziel, M. Zeviani, T. Meitinger, Loss-of-function mutations of SURF-1 are specifically associated with Leigh syndrome with cytochrome *c* oxidase deficiency [see comments], Ann. Neurol. 46 (1999) 161–166.
[33] G. Villani, G. Attardi, In vivo control of respiration by cytochrome *c* oxidase in wild-type and mitochondrial DNA mutation-carrying human cells, Proc. Natl. Acad. Sci. U. S. A. 94 (1997) 1166–1171.
[34] W.S. Kunz, A. Kudin, S. Vielhaber, C.E. Elger, G. Attardi, G. Villani, Flux control of cytochrome *c* oxidase in human skeletal muscle, J. Biol. Chem. 275 (2000) 27741–27745.
[35] H. Schagger, K. Pfeiffer, Supercomplexes in the respiratory chains of yeast and mammalian mitochondria, EMBO J. 19 (2000) 1777–1783.
[36] D.M. Glerum, A. Tzagoloff, Isolation of a human cDNA for heme A farnesyltransferase by functional complementation of a yeast cox10 mutant, Proc. Natl. Acad. Sci. U. S. A. 91 (1994) 8452–8456.
[37] N. Bonnefoy, F. Chalvet, P. Hamel, P.P. Slonimski, G. Dujardin, OXA1, a *Saccharomyces cerevisiae* nuclear gene whose sequence is conserved from prokaryotes to eukaryotes controls cytochrome oxidase biogenesis, J. Mol. Biol. 239 (1994) 201–212.
[38] V. Petruzzella, V. Tiranti, P. Fernandez, P. Ianna, R. Carrozzo, M. Zeviani, Identification and characterization of human cDNAs specific to BCS1, PET112, SCO1, COX15, and COX11, five genes involved in the formation and function of the mitochondrial respiratory chain, Genomics 54 (1998) 494–504.
[39] G. Mashkevich, B. Repetto, D.M. Glerum, C. Jin, A. Tzagoloff, SHY1, the yeast homolog of the mammalian SURF-1 gene, encodes a mitochondrial protein required for respiration, J. Biol. Chem. 272 (1997) 14356–14364.
[40] H. Antonicka, A. Mattman, C.G. Carlson, D.M. Glerum, K.C. Hoffbuhr, S.C. Leary, N.G. Kennaway, E.A. Shoubridge, Mutations in COX15 produce a defect in the mitochondrial heme biosynthetic pathway, causing early-onset fatal hypertrophic cardiomyopathy, Am. J. Hum. Genet. 72 (2003) 101–114.
[41] E.A. Shoubridge, Cytochrome *c* oxidase deficiency, Am. J. Med. Genet. 106 (2001) 46–52.
[42] G. Villani, M. Greco, S. Papa, G. Attardi, Low reserve of cytochrome *c* oxidase capacity in vivo in the respiratory chain of a variety of human cell types, J. Biol. Chem. 273 (1998) 31829–31836.
[43] B. Kadenbach, M. Huttemann, S. Arnold, I. Lee, F. Bender, Mitochondrial energy metabolism is regulated via nuclear-coded subunits of cytochrome *c* oxidase, Free Radic. Biol. Med. 29 (2000) 211–221.
[44] B. Ludwig, F. Bender, S. Arnold, M. Huttemann, I. Lee, B. Kadenbach, Cytochrome *c* oxidase and the regulation of oxidative phosphorylation, Chem. Biochem. Eur. J. Chem. Biol. 2 (2001) 392–403.
[45] R. Rossignol, B. Faustin, C. Rocher, M. Malgat, J.P. Mazat, T. Letellier, Mitochondrial threshold effects, Biochem. J. 6 (2002).
[46] D. Piekutowska-Abramczuk, E. Popowska, E. Pronicka, E. Karczmarewicz, M. Pronicki, T. Kmiec, M. Krajewska-Walasek, SURF1 gene mutations in Polish patients with COX-deficient Leigh syndrome, J. Appl. Genet. 42 (2001) 103–108.
[47] P. Zimmermann, B. Kadenbach, Modified structure and kinetics of cytochrome *c* oxidase in fibroblasts from patients with Leigh syndrome, Biochim. Biophys. Acta 1180 (1992) 99–106.
[48] B. Kadenbach, A. Stroh, F.J. Huther, A. Reimann, D. Steverding, Evolutionary aspects of cytochrome *c* oxidase, J. Bioenerg. Biomembranes 23 (1991) 321–334.
[49] H. Antonicka, D. Floryk, P. Klement, I. Stratilova, J. Hermanska, H. Houstkova, M. Kalous, Z. Drahota, J. Zeman, J. Houstek, Defective kinetics of cytochrome *c* oxidase and alteration of mitochondrial membrane potential in fibroblasts and cytoplasmic cells with the mutation for myoclonus epilepsy with ragged-red fibres ('MERRF') at position 8344 nt, Biochem. J. 342 (1999) 537–544.
[50] C.M. Sue, C. Karadimas, N. Checcarelli, K. Tanji, L.C. Papadopoulou, F. Pallotti, F.L. Guo, S. Shanske, M. Hirano, D.C. De Vivo, R. Van Coster, P. Kaplan, E. Bonilla, S. DiMauro, Differential features of patients with mutations in two COX assembly genes, SURF-1 and SCO2, Ann. Neurol. 47 (2000) 589–595.
[51] B.J. Hanson, R. Carrozzo, F. Piemonte, A. Tessa, B.H. Robinson, R.A. Capaldi, Cytochrome *c* oxidase-deficient patients have distinct subunit assembly profiles, J. Biol. Chem. 276 (2001) 16296–16301.
[52] J.C. von Kleist-Retzow, J. Yao, J.W. Taanman, K. Chantrel, D. Chretien, V. Cormier-Daire, A. Rotig, A. Munnich, P. Rustin, E.A. Shoubridge, Mutations in SURF1 are not specifically associated with Leigh syndrome, J. Med. Genet. 38 (2001) 109–113.
[53] S.L. Williams, H.R. Scholte, R.G. Gray, J.V. Leonard, A.H. Schapira, J.W. Taanman, Immunological phenotyping of fibroblast cultures from patients with a mitochondrial respiratory chain deficit, Lab. Invest. 81 (2001) 1069–1077.
[54] A. Weishaupt, B. Kadenbach, Selective removal of subunit VIb increases the activity of cytochrome *c* oxidase, Biochemistry 31 (1992) 11477–11481.

Article 3

Toxicology Mechanisms and Methods 14:7–11, 2004
Copyright © Taylor & Francis Inc.
ISSN: 1537-6524 print / 1537-6516 online
DOI: 10.1080/15376520490257527

Taylor & Francis
healthsciences

Mitochondrial Membrane Potential and ATP Production in Primary Disorders of ATP Synthase

Alena Vojtíšková, Pavel Ješina, Martin Kalous, Vilma Kaplanová, and Josef Houštěk

Institute of Physiology and Centre for Integrated Genomics, Academy of Sciences of the Czech Republic, Prague, Czech Republic

Markéta Tesařová, Daniela Fornusková, and Jiří Zeman

Department of Pediatrics, First Faculty of Medicine, Charles University, Prague, Czech Republic

Audrey Dubot and Catherine Godinot

Centre of Molecular and Cellular Genetics, Claude Bernard University of Lyon, Villeurbanne, France

Studies of fibroblasts with primary defects in mitochondrial ATP synthase (ATPase) due to heteroplasmic mtDNA mutations in the *ATP6* gene, affecting protonophoric function or synthesis of subunit a, show that at high mutation loads, mitochondrial membrane potential $\Delta\Psi_m$ at state 4 is normal, but ADP-induced discharge of $\Delta\Psi_m$ is impaired and ATP synthesis at state 3-ADP is decreased. Increased $\Delta\Psi_m$ and low ATP synthesis is also found when the ATPase content is diminished by altered biogenesis of the enzyme complex. Irrespective of the different pathogenic mechanisms, elevated $\Delta\Psi_m$ in primary ATPase disorders could increase mitochondrial production of reactive oxygen species and decrease energy provision.

Keywords ATP Synthase, *ATP6*, Flow Cytometry, Membrane Potential, Mitochondrial diseases, mtDNA

Mitochondrial encephalomyopathies due to defects in mitochondrial F_0F_1-adenosine 5'-triphosphate (ATP) synthase (ATPase) are less common than disorders of the respiratory-chain complexes, but they are usually very severe and can be caused by mitochondrial DNA (mtDNA) mutations or by mutations in nuclear genes. Mitochondrial ATPase is the key enzyme of cellular energy conversion. By means of a fascinating rotary motor mechanism (Kinosita et al. 1998; Stock et al. 2000), it couples the H^+ gradient generated by the respiratory chain to the synthesis of ATP from adenosine 5'-diphosphate (ADP) and phosphate. The ATPase complex comprises 16 different subunits (Walker and Collinson 1994). It is composed of the globular F_1 catalytic part, which is connected by two stalks to the membrane-embedded F_0 moiety; the latter translocates protons across the inner mitochondrial membrane. Two F_0 subunits, subunit a (*ATP6*) and subunit A6L, are coded by mtDNA (Anderson et al. 1981); all other subunits are nuclearly encoded.

The most common cause of ATPase defects are missense heteroplasmic mtDNA mutations in the *ATP6* gene, which affect the protonophoric function of subunit a, an essential component, together with multiple copies of subunit c of the ATPase proton channel (Hutcheon et al. 2001; Stock et al. 1999). Higher prevalence show T8993G(C) mutations (Crafaloni et al. 1993; Holt et al. 1990; Puddu et al. 1993; Shoffner et al. 1992; Tatuch et al. 1994) which change Leu^{156} to Arg or Pro. At a lower mutation load, they manifest as neurogenic muscle weakness, ataxia, and retinitis pigmentosa (NARP syndrome); at heteroplasmy exceeding 90% they present as maternally inherited Leigh syndrome (severe and fatal encephalopathy). Less common are T9176G(C) mutations, which change Leu^{217} (Carrozzo et al. 2001; Dionisi-Vici et al. 1998; Thyagarajan et al. 1995), or a T8851G mutation (De Meirleir et al. 1995) that changes Trp^{109}, all manifesting also as striatal necrosis syndromes (Schon et al. 2001). Impairment of the ATPase H^+ channel results often, but not always, in decreased ATP production, whereas the ATPase hydrolytic activity remains largely unchanged (Houstek et al. 1995; Tatuch and Robinson 1993). A different type of pathogenic mechanism represents mtDNA 2bp microdeletion 9205delTA, which was found in a newborn with transient lactic acidosis (Seneca et al. 1996) and also in a child with encephalopathy and severe psychomotor retardation (Fornuskova et al. 2003).

Received 1 July 2003; accepted 10 July 2003.
This work was supported by Grant Agency of Ministry of Health of the Czech Republic (NE6533-3) and institutional projects AVOZ5011922 and VZ111100003.

Address correspondence to Josef Houštěk, Institute of Physiology, Academy of Sciences of the Czech Republic, Vídeňská 1083, 14220 Prague, Czech Republic. E-mail: houstek@biomed.cas.cz

A 9205delTA mutation removes the stop codon of the *ATP6* gene and affects the cleavage site between the *ATP6* and *COXIII* transcripts. Most recently, a new mutation, in which A8527G changes the ATPase 6 initiation codon AUG into GUG (Met → Val), has been found in an adult patient with neuropathy, mental retardation, myopathy, suprarenal peripheral insufficiency, and retinopathy (Dubot et al. 2003).

ATPase defects due to nuclear genome mutations are very rare and appear to be caused by diminished biosynthesis of the ATPase complex. ATPase deficiency of possible nonmitochondrial origin was first described in a child with 3-methylglutaconic aciduria and severe lactic acidosis (Holme et al. 1992). Extremely low ATPase activity and low, tightly coupled respiration rates were observed in muscle mitochondria, but no mutation was found in mtDNA genes encoding ATPase subunits. A nuclear origin of ATP synthase deficiency was demonstrated for the first time in 1999 (Houstek et al. 1999) in a new type of fatal mitochondrial disorder; a child with severe lactic acidosis, cardiomegaly, and hepatomegaly died 2 days after birth. 70 to 80% decrease in ATPase activity and ATP production was associated with a corresponding selective decrease in the ATPase complex, which had normal size and subunit composition. Increased biosynthesis of the β subunit with a very short half-life contrasted with decreased biosynthesis of the assembled ATPase and indicated assembly defect at the level of F_1-ATPase. Cybrid cells made of patient fibroblasts fully complemented the ATPase defect and confirmed the nuclear origin of impaired biogenesis of the enzyme complex (Houstek et al. 1999). Later on several other selective ATPase defects of varying severity have been found, including a fatal ATPase defect described in Belgium (Van Coster et al. 2001); a milder case of ATPase deficiency found in an Austrian patient (Mayr et al. 2002); and two new families with ATPase deficiency of nuclear origin found in the Czech Republic. In this article, we summarize our studies of the functional consequences of various types of primary ATPase defects at the level of mitochondrial ATP synthesis and maintenance and discharge of the mitochondrial membrane potential.

MATERIALS AND METHODS

Cell Cultures

Human skin fibroblasts were cultured in Dulbecco's Modified Eagle's Medium (DMEM) medium with 10% fetal calf serum at 37 C in 5% carbondioxide in air to approximately 90% confluence. Cells were harvested using 0.05% trypsin and 0.02% ethylenediaminetetraacetic acid (EDTA). Previously established fibroblast cultures with different heteroplasmic mtDNA mutations in the *ATP6* gene (Table 1), and fibroblast cultures with selective ATPase deficiency of nuclear origin from three unrelated Czech families (Table 2) were used for the experiments. Derived transmitochondrial cybrids were prepared as before by the method of Tiranti and colleagues (1995).

TABLE 1
ATP production in fibroblasts with different mtDNA mutations in the *ATP6* gene

Mutation	Mutation type	Heteroplasmy	ATP production[a]
T8993G	Missense Leu → Arg	97%	35–54%
9205delTA	Stop codon → Lys	86%	20–40%
A8527G	Met → Val, change of initiation codon AUG → GUG	97%	90–100%

[a] Antimycin A–sensitive production using succinate or pyruvate + malate as a substrate.

Cytofluorometric Analysis

Freshly harvested fibroblasts were resuspended in 80 mM KCl; 10 mM Tris Cl pH 7.4; 3 mM $MgCl_4$; 1 mM EDTA; 5 mM KH_2PO_4; and 10 mM succinate at a protein concentration of 1 mg/mL. Cells were permeabilized by 0.1 mg digitonin per mg protein (Sigma Chemical, St. Louis, MO) and stained with 20 nM tetramethylrhodamine methyl ester (TMRM, Molecular Probes, Eugene, OR) for 15 min at room temperature. ADP, inhibitors, or both were added at indicated concentrations 1 min before cytofluorometric measurements, which were performed as described elsewhere (Floryk and Houstek 1999) on a FACSort flow cytometer (Becton Dickinson, San Jose, CA) equipped with an argon laser, 488 nm. The TMRM signal was analyzed in the FL2 channel, equipped with a band pass filter 585 ± 21 nm; the photomultiplier value of the detector was at 631 V in FL2. Data were acquired in log scale using CellQuest (Becton Dickinson, San Jose, CA) and analyzed with WinMDI 2.8 software (TSRI, La Jolla, CA). Arithmetic mean values of the fluorescence signal in arbitrary units were determined for each sample for the purpose of subsequent graphic representation.

ATP Production Measurements

The rate of ATP synthesis (Wanders et al. 1993) was measured in 150 mM KCl; 25 mM Tris/HCl; 10 mM KPi; 2 mM EDTA; 1% BSA, pH 7.2; using 0.5 mM ADP and succinate, ketglutarate + malate, or pyruvate + malate as a substrate, all in 10 mM concentration. For permeabilization of fibroblasts and cybrids, 0.1 and 0.03 mg digitonin per mg protein, respectively, was used. ATP was determined in DMSO-quenched aliquots according to Ouhabi and colleagues (1998) by a luciferase assay.

Ethics

The described studies were carried out in accordance with the Declaration of Helsinki of the World Medical Association and were approved by the Committees of Medical Ethics at all collaborating institutions. Informed consent was obtained from investigated individuals or their parents.

TABLE 2
ATP production in fibroblasts from three patients with selective deficiency of ATP synthase

Case	I	II	III
Phenotype	LA, CM, H	LA, CM	LA, CM, EM, dev. delay
Onset/survival	Newborn/2 days	Newborn/32 days	Neonate/7 years
ATPase activity in fibroblasts (% of control)[a]	30%	20%	30%
ATP production in fibroblasts (% of control)[b]	28–32%	32–47%	18–23%
ATP production in cybrids (% of control)[b]	102–116%	220–380%	230%

[a]Oligomycin-sensitive ATPase activity.
[b]Antimycin A–sensitive production using succinate, ketoglutarate + malate, or glutamate + malate as a substrate.
CM, cardiomyopathy; EM, encephalomyopathy; H, hepatomegaly; LA, lactic acidosis.
Note: The data for Case I are from the work of Houstek and colleagues (1999); the data for Cases II and III are from two new patients from unrelated families.

RESULTS AND DISCUSSION

The pathogenic mechanisms underlying different types of ATPase defects and disorders seem to range from a dysfunction of mutated subunit a, through insufficient or altered biosynthesis of subunit a, to a diminished production of otherwise normal ATPase complex. With the aim of assessing how these different ATPase defects influence the mitochondrial energy provision, mitochondrial membrane potential $\Delta\Psi_m$ and ATP production were studied. As summarized in Table 1, three types of heteroplasmic mutations in the *ATP6* gene, all present in high mutation loads (86 to 97%), affected substrate-supported ATP production to different extents. The most pronounced decrease in ATP synthesis was in 9205delTA cells; higher rates were found in T8993G fibroblasts; the A8527G mutation was without any effect. Flow cytometry using TMRM as a fluorescent probe further showed that these mutations have varying influences on the $\Delta\Psi_m$. Steady-state levels of $\Delta\Psi_m$ were determined under state 4 conditions, when no ADP is available and $\Delta\mu H^+$ cannot be utilized for ATP synthesis. In all types of fibroblasts, the state 4 $\Delta\Psi_m$ values were within the control range, and the addition of an uncoupler, FCCP, similarly decreased the TMRM signal, indicating that none of the *ATP6* mutations studied increases the passive H^+ flow at state 4. The addition of ADP (state 3-ADP) caused a significant decrease of $\Delta\Psi_m$ in both the control and the A8527G cells, and this ADP-dependent decrease was fully prevented by the ATPase inhibitor oligomycin (Fig. 1). A much smaller, although fully reversible, effect of ADP was seen in 9205delTA cells, and only a minute effect was found in T8993G fibroblasts. Both types of studies, thus, convincingly showed that near-homoplasmic T8993G mutation largely, but not completely, prevented the discharge of $\Delta\Psi_m$ and the synthesis of ATP by mitochondrial ATPase.

It is interesting to note that the behavior of cells with 9205delTA is very similar, and alteration of the *ATP6* stop codon probably interferes with the synthesis of subunit a; or an elongated form of subunit a could be produced, resulting in nonfunctional ATP synthase. In the first case, some incomplete, subunit a–lacking ATPase complexes would be formed. In the second case, the subunit a would be modified in the C-terminal part, where several AA residues that are involved in H^+-translocation are located (Schon et al. 2001). Both types of measurements also clearly showed that A8527G mutation is without detectable effect on mitochondrial ATP synthesis and, very likely, the GUG initiation codon, replacing the canonical AUG, is somehow operative in human mitochondrial *ATP6* mRNA translation, as is the case of *COXI* and *COXII* in some vertebrates (Johansen et al. 1990; Pan et al. 1993).

A completely different pathogenic mechanism is associated with primary ATPase defects of nuclear origin (Houstek et al. 1999), where the mitochondrial content of ATPase complex is selectively reduced relative to the content of respiratory-chain enzymes, while the subunit composition and the hydrolytic as well as the synthetic function of the remaining ATPase complexes are normal. This relative lack of ATPase was found to cause an increase in membrane potential at state 4 (Houstek et al. 1999), which is indicative of decreased passive H^+ leak and which resulted in a pronounced decrease in ATP production (see Table 2 and Houstek et al. 1999). As is shown in Table 2, a similarly pronounced decrease of ATP production was found in two new patients from different families, in whom a 70–80% decrease of mitochondrial ATPase was found. Their clinical presentations also included lactic acidosis and cardiomyopathy. In one case the patient survived for several weeks; the other case was milder and presented with lactic acidosis, cardiomyoptahy, encephalopathy, and developmental delay. In order to find out the genetic origin of these new ATPase defects, transmitochondrial cybrids were prepared by fusing enucleated patient fibroblasts with mtDNA-less (ρ^0) 143B.TK$^-$ osteosarcoma cells. As shown in Table 2, the ATP synthesis was fully restored in both types of cybrids, indicating again that the underlying genetic defect is not a mtDNA mutation.

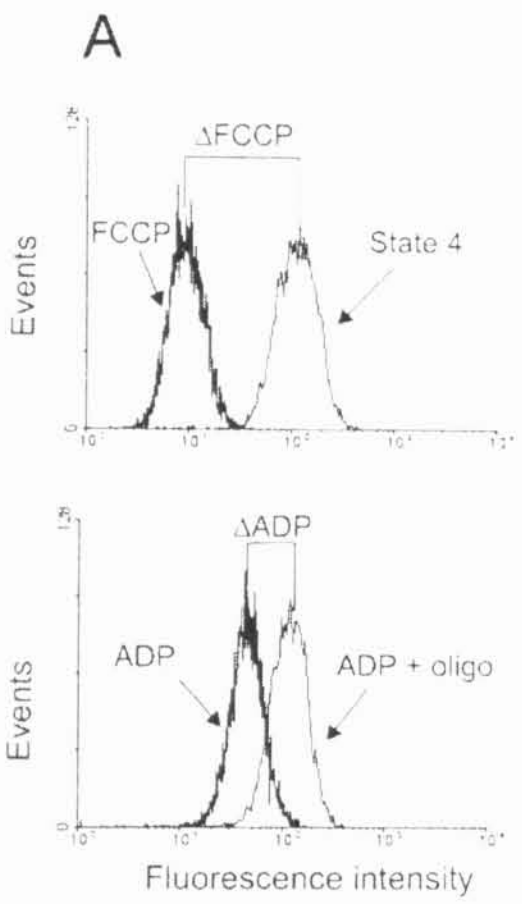

B

Fibroblast	ΔADP/ΔFCCP
Control	0.69-0.73
T8993G	0.09
9205delTA	0.49
A8527G	0.70

FIG. 1. Changes in the mitochondrial membrane potential $\Delta\Psi_m$ in fibroblasts with different *ATP6* mutations. Cytofluorometric analysis of the mitochondrial membrane potential by TMRM fluorescence was performed in a digitonin-permeabilized fibroblast supplied with 10 mM succinate. (A) The effect of 1 μM FCCP, 0.1 mM ADP, and ADP followed by 1 μM oligomycin (oligo) in control cells. (B) The ADP-induced decrease of TMRM fluorescence relative to the FCCP-induced decrease was analyzed in cells with indicated mtDNA mutations.

All the known primary deficiencies of mitochondrial ATPase can significantly affect the mitochondrial ATP production, irrespective of whether the cause is an insufficient amount of normal enzyme or altered properties of ATPase complex that is present in normal quantities. It is also quite clear that in all types of ATPase defects, the production of ATP is only partly inhibited, even in very severe cases. It is difficult to understand how only a partial decline of energy provision (sometimes only 50% or less) can have such serious and often fatal effects. All ATP synthesis data are based on cell cultures, and the situations in the most commonly affected tissues, which have high energy demands, such as brain, heart, and skeletal muscle, can be completely different. On the other hand, inhibitor titration studies in muscle tissue (Rossignol et al. 1999, 2003) show an especially high threshold for ATPase, indicating that some 10% of the normal activity of the enzyme is sufficient for more than 50% functionality of the whole respiratory chain.

It is well established that along with energy shortage, other metabolic consequences, in particular the production of reactive oxygen species (ROS) and the induction of apoptosis and tissue necrosis, are major components of the pathogenic mechanism in mitochondrial OXPHOS diseases (Lenaz et al. 2002; Wallace 1999). An exponential increase in mitochondrial ROS production has been demonstrated at levels of $\Delta\Psi_m$ above 140 mV (Korshunov et al. 1997; Liu 1999), whereas a decrease in $\Delta\Psi_m$ via stimulation of ATP synthase activity, a low ATP/ADP ratio, substrate limitation, or increased proton permeability due to external or internal uncoupling lower the amount of ROS produced (Kadenbach 2003). The main conclusion we draw from our cytofluorometric studies is that in ATPase disorders, higher levels of $\Delta\Psi_m$ can be expected because a low amount of enzyme or altered function of the F_0 proton channel apparently limit the physiological discharge of respiration-generated $\Delta\mu H^+$. If this is the case, increased and unbalanced ROS production, rather than diminished energy provision, would be the key pathogenic process in primary ATPase diseases.

REFERENCES

Anderson, S., Bankier, A. T., Barrell, B. G., de Bruijn, M. H. L., Coulson, A. R., Drouin, J., Eperon, I. C., Nierlich, D. P., Roe, B. A., Sanger, F., Schreier, P. H., Smith, A. J. H., Staden, R., and Young, I. G. 1981. Sequence and organization of the human mitochondrial genome. *Nature* 290:457–465.

Carrozzo, R., Tessa, A., Vazquez-Memije, M. E., Piemonte, F., Patrono, C., Malandrini, A., Dionisi-Vici, C., Vilarinho, L., Villanova, M., Schagger, H., Federico, A., Bertini, E., and Santorelli, F. M. 2001. The T9176G mtDNA mutation severely affects ATP production and results in Leigh syndrome. *Neurology* 56:687–690.

Ciafaloni, E., Santorelli, F. M., Shanske, S., Deonna, T., Roulet, E., Janzer, C., Pescia, G., and DiMauro, S. 1993. Maternally inherited Leigh syndrome. *J. Peidatr.* 122:419–422.

De Meirleir, L., Seneca, S., Lissens, W., Schoentjes, E., and Desprechins, B. 1995. Bilateral striatal necrosis with a novel point mutation in the mitochondrial ATPase 6 gene. *Pediatr. Neurol.* 13:242–246.

Dionisi-Vici, C., Seneca, S., Zeviani, M., Fariello, G., Rimoldi, M., Bertini, E., and De Meirleir, L. 1998. Fulminant Leigh syndrome and sudden unexpected

death in a family with the T9176C mutation of the mitochondrial ATPase 6 gene. *J. Inherit. Metab. Dis.* 21:2–8.

Dubot, A., Godinot, C., Vojtiskova, A., Pecina, P., Jesina, P., and Houstek, J. 2003. Use of GUG as initiation codon for the human mitochondria-encoded ATP6 subunit. In *Functional Genomics and Disease*. European Science Foundation, PD4/171. http://www.esffg2003.org.

Floryk, D., and Houstek, J. 1999. Tetramethyl rhodamine methyl ester (TMRM) is suitable for cytofluorometric measurements of mitochondrial membrane potential in cells treated with digitonin. *Biosci. Rep.* 19:27–34.

Fornuskova, D., Tesarova, M., Hansikova, H., and Zeman, J. 2003. New mtDNA mutation 9204delTA in a family with mitochondrial encephalopathy and ATP-synthase defect. *Cas. Lek. Cesk.* 142:313.

Holme, E., Greter, J., Jacobson, C. E., Larsson, N. G., Lindstedt, S., Nilsson, K. O., Oldfors, A., and Tulinius, M. 1992. Mitochondrial ATP-synthase deficiency in a child with 3-methylglutaconic aciduria. *Pediatr. Res.* 32:731–735.

Holt, I. J., Harding, A. E., Petty, R. K. H., and Morgan-Hughes, J. A. 1990. A new mitochondrial disease associated with mitochondrial DNA heteroplasmy. *Am. J. Hum. Genet.* 46:428–433.

Houstek, J., Klement, P., Floryk, D., Antonicka, H., Hermanska, J., Kalous, M., Hansikova, H., Hout'kova, H., Chowdhury, S. K., Rosipal, T., Kmoch, S., Stratilova, L., and Zeman, J. 1999. A novel deficiency of mitochondrial ATPase of nuclear origin. *Hum. Mol. Genet.* 8:1967–1974.

Houstek, J., Klement, P., Hermanska, J., Houstkova, H., Hansikova, H., van den Bogert, C., and Zeman, J. 1995. Altered properties of mitochondrial ATP-synthase in patients with a T → G mutation in the ATPase 6 (subunit a) gene at position 8993 of mtDNA. *Biochim. Biophys. Acta* 1271:349–357.

Hutcheon, M. L., Duncan, T. M., Ngai, H., and Cross, R. L. 2001. Energy-driven subunit rotation at the interface between subunit a and the c oligomer in the F(O) sector of *Escherichia coli* ATP synthase. *Proc. Natl. Acad. Sci. USA* 98:8519–8524.

Johansen, S., Guddal, P. H., and Johansen, T. 1990. Organization of the mitochondrial genome of Atlantic cod, *Gadus morhua*. *Nucleic Acids Res.* 18:411–419.

Kadenbach, B. 2003. Intrinsic and extrinsic uncoupling of oxidative phosphorylation. *Biochim. Biophys. Acta* 1604:77–94.

Kinosita, K., Jr., Yasuda, R., Noji, H., Ishiwata, S., and Yoshida, M. 1998. F1-ATPase: a rotary motor made of a single molecule. *Cell* 93:21–24.

Korshunov, S. S., Skulachev, V. P., and Starkov, A. A. 1997. High protonic potential actuates a mechanism of production of reactive oxygen species in mitochondria. *FEBS Lett.* 416:15–18.

Lenaz, G., Bovina, C., D'Aurelio, M., Fato, R., Formiggini, G., Genova, M. L., Giuliano, G., Pich, M. M., Paolucci, U., Castelli, G. P., and Ventura, B. 2002. Role of mitochondria in oxidative stress and aging. *Ann. N.Y. Acad. Sci.* 959:199–213.

Liu, S. S. 1999. Cooperation of a "reactive oxygen cycle" with the Q cycle and the proton cycle in the respiratory chain: superoxide generating and cycling mechanisms in mitochondria. *J. Bioenerg. Biomembr.* 31:367–376.

Mayr, J. A., Paul, J., Kurnik, P., Fotschl, U., Houstek, J., and Sperl, W. 2002. Increased uncoupling in a patient with a quantitative defect of the F0F1-ATP-synthase. *J. Inherit. Metab. Dis.* 25(suppl. 1):178.

Ouhabi, R., Boue-Grabot, M., and Mazat, J. P. 1998. Mitochondrial ATP synthesis in permeabilized cells: assessment of the ATP/O values in situ. *Anal. Biochem.* 263:169–175.

Pan, Y. F., Lee, Y. W., Wei, Y. H., and Chiang, A. N. 1993. A gene for cytochrome c oxidase subunit II in duck mitochondrial DNA: structural features and sequence evolution. *Biochem. Mol. Biol. Int.* 30:479–489.

Puddu, P., Barboni, P., Mantovani, V., Montagna, P., Cerullo, A., Braghiani, M., Molinotti, C., and Caramazza, R. 1993. Retinitis pigmentosa, ataxia, and mental retardation associated with mitochondrial DNA mutation in an Italian family. *Br. J. Ophthalmol.* 77:84–88.

Rossignol, R., Faustin, B., Rocher, C., Malgat, M., Mazat, J. P., and Letellier, T. 2003. Mitochondrial threshold effects. *Biochem. J.* 370:751–762.

Rossignol, R., Malgat, M., Mazat, J. P., and Letellier, T. 1999. Threshold effect and tissue specificity: implication for mitochondrial cytopathies. *J. Biol. Chem.* 274:33426–33432.

Schon, E. A., Santra, S., Pallotti, F., and Girvin, M. E. 2001. Pathogenesis of primary defects in mitochondrial ATP synthesis. *Semin. Cell Dev. Biol.* 12:441–448.

Seneca, S., Abramowicz, M., Lissens, W., Muller, M. F., Vamos, E., and de Meirleir, L. 1996. A mitochondrial DNA microdeletion in a newborn girl with transient lactic acidosis. *J. Inherit. Metab. Dis.* 19:115–118.

Shoffner, J. M., Fernhoff, P. M., Krawiecki, N. S., Caplan, D. B., Holt, P. J., Koontz, D. A., Taket, Y., Newman, N. J., Ortiz, R. G., Polak, M., Baflinger, S. W., Lott, M. T., and Wallace, D. C. 1992. Subacute necrotizing encephalopathy: oxidative phosphorylation defects and the ATPase 6 point mutation. *Neurology* 42:2168–2174.

Stock, D., Gibbons, C., Arechaga, I., Leslie, A. G., and Walker, J. E. 2000. The rotary mechanism of ATP synthase. *Curr. Opin. Struct. Biol.* 10:672–679.

Stock, D., Leslie, A. G., and Walker, J. E. 1999. Molecular architecture of the rotary motor in ATP synthase. *Science* 286:1700–1705.

Tatuch, Y., Pagon, R. A., Vleek, B., Roberts, R., Korson, M., and Robinson, B. H. 1994. The 8993mtDNA mutation: heteroplasmy and clinical presentation in three families. *Eur. J. Hum. Genet.* 2:35–43.

Tatuch, Y., and Robinson, B. H. 1993. The mitochondrial DNA mutation at 8993 associated with NARP slows the rate of ATP synthesis in isolated lymphoblast mitochondria. *Biochem. Biophys. Res. Commun.* 192:124–128.

Thyagarajan, D., Shanske, S., Vazquez Memije, M., De Vivo, D., and DiMauro, S. 1995. A novel mitochondrial ATPase 6 point mutation in familial bilateral striatal necrosis. *Ann. Neurol.* 38:468–472.

Tiranti, V., Munaro, M., Sandona, D., Lamantea, E., Rimoldi, M., DiDonato, S., Bisson, R., and Zeviani, M. 1998. Nuclear DNA origin of cytochrome c oxidase deficiency in Leigh's syndrome: Genetic evidence based on patient-derived rho degrees transformants. *Hum. Mol. Genet.* 4:2017–2023.

Van Coster, R., Smet, J., and Eyskens, F. 2001. Severe complex V deficiency with fatal outcome in neonatal period. In *Society for the Study of Inborn Errors of Metabolism*, ed. G. T. N. Besley, 24, p. 83. Prague, Czech Republic: Kluwer Academic.

Walker, J. E., and Collinson, I. R. 1994. The role of the stalk in the coupling mechanism of F1F0-ATPases. *FEBS Lett.* 346:39–43.

Wallace, D. C. 1999. Mitochondrial diseases in man and mouse. *Science* 283:1482–1488.

Wanders, R. J., Ruiter, J. P., and Wijburg, F. A. 1993. Studies on mitochondrial oxidative phosphorylation in permeabilized human skin fibroblasts: application to mitochondrial encephalomyopathies. *Biochim. Biophys. Acta* 1181:219–222.

Article 4

Available online at www.sciencedirect.com
SCIENCE DIRECT®
Biochemical and Biophysical Research Communications 313 (2004) 687–693
BBRC
www.elsevier.com/locate/ybbrc

GUG is an efficient initiation codon to translate the human mitochondrial *ATP6* gene

A. Dubot,[a] C. Godinot,[a,*] V. Dumur,[b] B. Sablonnière,[b] T. Stojkovic,[c] J.M. Cuisset,[d] A. Vojtiskova,[e] P. Pecina,[e] P. Jesina,[e] and J. Houstek[e]

[a] *Centre National de la Recherche Scientifique, Université Claude Bernard de Lyon I, 69622 Villeurbanne France*
[b] *Département de Biochimie et Biologie moléculaire, Centre Hospitalier Régional Universitaire, Hôpital R.Salengro, Bd du Pr Emile Laine, 59037 Lille Cedex, France*
[c] *Service de Neurologie, Centre Hospitalier Régional Universitaire, Hôpital R.Salengro, Bd du Pr Emile Laine, 59037 Lille Cedex, France*
[d] *Service de Neuropédiatrie, Centre Hospitalier Régional Universitaire, Hôpital R.Salengro, Bd du Pr Emile Laine, 59037 Lille Cedex, France*
[e] *Department of Bioenergetics, Institute of Physiology and Centre for Integrated Genomics, Academy of Sciences of the Czech Republic, CZ 142 20 Prague, Czech Republic*

Received 27 November 2003

Abstract

A maternally inherited and practically homoplasmic mitochondrial (mtDNA) mutation, 8527A > G, changing the initiation codon AUG into GUG, normally coding for a valine, was observed in the *ATP6* gene encoding the ATPase subunit a. No alternate Met codon could replace the normal translational initiator. The patient harboring this mutation exhibited clinical symptoms suggesting a mitochondrial disease but his mother who carried the same mtDNA mutation was healthy. The mutation was absent from 100 controls and occurred once amongst 44 patients suspected of Leber Hereditary Optic Neuropathy (LHON) but devoid of typical LHON mutations. In patient fibroblasts, no effect of 8527A > G mutation could be demonstrated on the biosynthesis of mtDNA-encoded proteins, on size and the content of ATPase subunit a, on ATP hydrolysis and on mitochondrial membrane potential. In addition, ATP synthesis was barely decreased. Therefore, GUG is a functional initiation codon for the human *ATP6* gene.

Keywords: ATPase-ATPsynthase; ATPase subunit a; *ATP6* gene; Mitochondrial diseases; Leber's hereditary optic neuropathy; Mitochondrial initiation codon; Human

Mitochondrial diseases associated with defects in oxidative phosphorylation (OXPHOS) complexes due to mutations in mitochondrial DNA (mtDNA) are generally multisystemic diseases affecting predominantly brain and muscle but they can also involve many organs [1]. Up to now, more than 70 different point mutations in mtDNA causing defects in protein-coding genes of complex I, III, IV or V have been described [2]. In complex V, the resulting diseases can be severe as is NARP (neuropathy, ataxia, and retinitis pigmentosa, OMIM 535000) or MILS (maternally inherited case of Leigh syndrome, OMIM 516069) that are associated with the mtDNA 8993T > G or C point mutation in ATPase subunit a, depending on the percentage of mutated mtDNA. Another type of disease is the Leber's hereditary optic neuropathy (LHON) characterized by blindness generally appearing in midlife and associated with mtDNA mutations on genes mainly encoding complex I subunits. Although these mutations are generally homoplasmic, the disease has incomplete penetrance. This has suggested the influence of either environmental factors or the occurrence of additional genetic factors [3].

mtDNA mutations modifying the initiation codon are rare in human diseases. A mutation 3308T > C (M to T) at the initiation codon of ND1 (NADH

* Corresponding author. Fax: +33-4-72-44-05-55.
E-mail address: godinot@univ-lyon1.fr (C. Godinot).

0006-291X/$ - see front matter © 2003 Elsevier Inc. All rights reserved.
doi:10.1016/j.bbrc.2003.12.013

dehydrogenase subunit 1) has been identified in a MELAS patient [4]. However, the complex I activity and the synthesis of the ND1 polypeptide were normal. The authors suggested that another Met codon located close to the 5′ end of mitochondrial mRNAs could be used as translational initiator. On the contrary, the mutation 7587T > C, similarly replacing Thr for the initiator Met in cytochrome *c* oxidase subunit II (COII) [5], resulted in negligible synthesis of COII, probably because there is no in-frame Met codon in the vicinity of the 5′ end of *COII* [6]. This suggested that AUG was the only efficient initiation codon in human mtDNA. We describe here a new mutation in the *ATP6* initiation codon and show that this neither affected the size nor the amount of ATPase subunit a synthesized, in spite of the absence of an alternative Met close-by the 5′-end of the *ATP6* gene, downstream from the initiation codon. We hypothesize that other features than the initiator AUG in the human mtDNA sequence must be used for selection of the proper initiation site.

Patients and methods

Patients. Patient P was the fifth child born to consanguineous parents. Suprarenal insufficiency appeared early after birth and hypotonia later on. He had delayed milestones, walking difficulties, and psychomotor retardation of unknown cause. A peroxisomal disorder was excluded [7]. At the age of 22 years, he remained ambulatory with canes and the main clinical features were mental retardation, sensory axonal neuropathy, ophthalmoplegia, retinopathy, and suprarenal gland insufficiency. Histochemical analysis in muscle revealed a few ragged red fibers with modified Gomori's trichrome and lipid storage with black Sudan stain. Electron microscopy disclosed abnormal mitochondria accumulated under the sarcolemma.

Patient L suddenly became almost blind at the age of 8 years and exhibited an acute peripapillary microangiopathy typical of Leber disease [3]. His grandparents were first cousins and no other family member was blind.

Skin fibroblasts from NARP patients were also used in this study. They were obtained from patients previously described by Parfait et al. [8].

Informed consent was obtained from all investigated individuals or from their parents.

Cell culture. Skin fibroblasts from patient P, from NARP patients harboring more than 90% of mutant mtDNA (8993T > G), and from control subjects were cultured under standard conditions [8]. Fibroblast mitochondria were isolated by hypoosmotic shock [9].

Mitochondrial enzyme assays. ATP synthesis was measured as described [10] in fibroblasts permeabilized in the presence of 0.1 mg digitonin/mg protein. ATP was determined in DMSO-quenched aliquots using a luciferase assay [11]. Respiratory chain and citrate synthase activities were determined as described for muscle homogenates [12] and for fibroblasts [13]. The oligomycin-sensitive ATPase activity was measured by the spectrophotometric assay [14] after treating fibroblasts with digitonin and removing contaminating NADH oxidase by 10% Percoll treatment [15]. Protein contents were measured using the Bradford assay (Bio-Rad) with bovine serum albumin as standard.

Cytofluorometric analysis. Mitochondrial membrane potential ($\Delta\Psi_m$) was performed with freshly harvested fibroblasts permeabilized with digitonin and stained with 20 nM tetramethylrhodamine methyl ester (TMRM, Molecular Probes, USA) on the FACS Calibur flow cytometer (Becton Dickinson, San Jose, California, USA) [16].

DNA analysis. mtDNA-encoded ATPase genes were sequenced using the following primers: For 8196–8214, Rev 8799–8780, For 8540–8560, Rev 9300–9282 [17]. The percentage of mutated 8527A > G was estimated by PCR and restriction analysis: a 104-bp fragment DNA was amplified using (AAATAGAATGATCAG TACTGCG) as reverse primer and (AATTATAACAAACCaTGA GAACCtA) as forward primer that was mismatched to create a single *Dde*I restriction site only in the presence of the mutation. After 35 PCR cycles, 2 μCi of [α^{32}P]dCTP (3000 Ci/mmol) was added and one additional cycle was performed with a 5-min denaturation and a 10-min elongation time. The PCR products were incubated with *Dde*I for 3 h at 37 °C and submitted to electrophoresis through a 12% polyacrylamide gel. The dried gel was scanned with a phosphorimager and the proportion of mutated mtDNA was estimated with Image Quant software.

Western blot analysis. Proteins separated by Tricine SDS PAGE [18] on 10% polyacrylamide gels were blotted onto Hybond C-extra nitrocellulose membrane (Amersham Biosciences) by semidry electrotransfer (0.8 mA/cm^2, 1 h). The primary antibodies against the ATPase F_1-α subunit, (20D6, 1:20,000, [19]) and ATPase subunit c (1:900, [20]) were used. The anti-ATPase a antibody was prepared by Dr. MF Bouzidi using a peptide corresponding to the N-terminal 10 amino-acids of the human ATPase subunit a to which a tyrosine was added for coupling to bovine serum albumin (BSA) in the presence of bisdiazobenzidine [21]. Before use, the rabbit serum was incubated overnight at 4 °C with 5% BSA and the immunoprecipitated anti-serum albumin antibodies were removed by centrifugation at 20,000*g* for 30 min. This step was repeated twice. The specificity of the antibody was checked by verifying that the 20 kDa band corresponding to the ATPase subunit a was specifically absent in HeLa S3 rho^0 cells devoid of mtDNA [14]. It was diluted (1:500) before use.

Biosynthesis of mitochondrial proteins. Fibroblasts were cultured in Gibco medium 21013 devoid of methionine and cystein plus 10% extensively dialyzed fetal calf serum, 1 mM pyruvate, 2 mM glutamine, 30 mg cystein/L, and 100 μg emetine/ml, as described by Chomyn [22]. They were labeled for 3 h with 375 μCi/ml L-[^{35}S]methionine. Products were separated through a 4% stacking gel and a 15–20% gradient SDS PAGE. Gels were incubated with Amplify (Amersham Biosciences) according to the manufacturer's protocol, dried, and exposed to Hyperfilm MP (Amersham Biosciences) films for one week.

Results

Identification of the 8527A > G mutation and of its level of heteroplasmy

Fig. 1 (top) shows that patient P carried the mutation 8527A > G (GenBank Accession No.: AY370877) in the mitochondrial *ATP6* gene encoding ATPase subunit a. Amplification of a mtDNA fragment encompassing this mutation, using a mismatch primer that created a *Dde*I restriction site only when the mutation was present: (Fig. 1 bottom), showed that *Dde*I cleaved more than 97% mtDNA from muscle or from fibroblasts. Analysis of DNA from the blood of the patient and of his mother gave

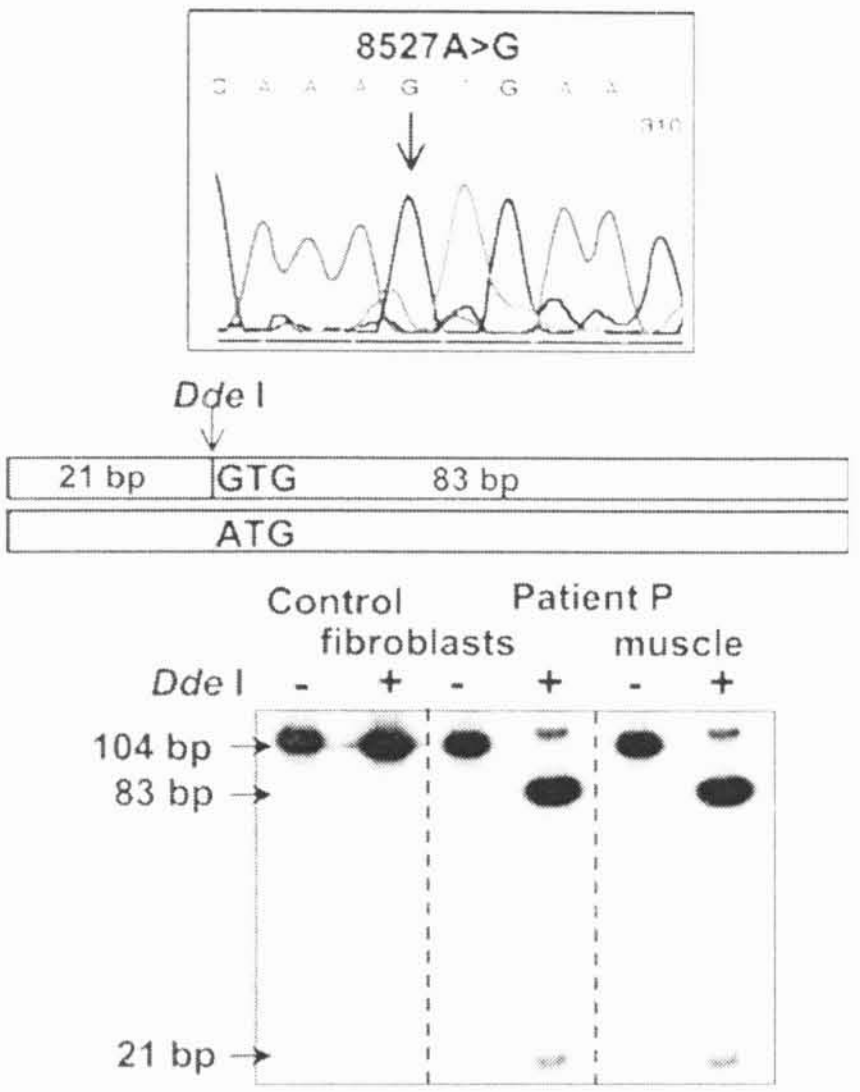

Fig. 1. Mutation in the mitochondrial *ATP6* initiation codon: Top, 8527A > G mutation observed by sequencing the patient *ATP6* gene. Bottom, restriction fragment analysis by *Dde*I of DNA extracted from control and patient P fibroblasts and muscle biopsy.

similar results (not shown), but the 8527A > G mutation was not detected in the father's blood. The mutation was therefore inherited from the mother who did not present any apparent clinical symptom. The normal ATG initiation codon is highly conserved in *ATP6* all over the phylogenic scale. The *ATP6* showed a 8932C > T homoplasmic polymorphism changing a Pro into Ser (this Pro is not conserved in all mammals) that was described in healthy subjects [23]. In this patient, no other mutation has been found in the ATPase *A6L* or in the close-by $tRNA^{Lys}$ genes.

The 8527A > G mutation was not found in a series of DNA samples of 100 healthy unrelated controls with no identified mitochondrial disease and in 43 out of 44 patients suspected of Leber's Hereditary Optic Neuropathy (LHON), but in which none of the most frequent LHON mutations (11778G > A, 4216T > C, 4917A > G, 3460G > A, 14482C > G, 14484T > C, 15257G > A) could be detected. The LHON patient carrying this mutation was patient L who also harbored the 8932C > T polymorphism, that may be related to North African origin of both P and L patients.

Table 1
Control and patient P oxidative phosphorylation complex activities

	Muscle homogenate		Skin fibroblasts	
	Controls	Patient P	Controls	Patient P
Complex I	3–11	6		
Complex I + III	3–9	9	11–38	21
Complex II	19–40	55	8–28	14
Complex II + III	4–12	4	16–40	24
Complex IV	40–100	127	50–120	72
ATPase (oligomycin-sensitive)			127–166	143–199
ATP synthesis (succinate)			37–51	31–42
			(46 ± 8)	(37 ± 6)
ATP synthesis (P + M)			37–48	30–37
			(44 ± 6)	(34 ± 3)
Citrate synthase	91–200	120	27–81	48

Values for controls: range of values observed for 100–150 control muscle homogenates or for 8 skin fibroblast cultures taken between 5 and 8 passages. For patient P the data represent the mean of 2 measurements. Activities are expressed as nmol substrate transformed/min/mg of protein and substrate transformations are as follows: citrate synthase, 5-thio-2-nitrobenzoate; complex I, rotenone-sensitive NADH ubiquinone oxidoreduction; complex II, 2,6-dichlorophenolindophenol reduction; complex IV, reduced cytochrome *c* oxidation; complex I + III, antimycin-sensitive NADH-cytochrome *c* reduction; complex II + III, succinate-cytochrome *c* reduction; and oligomycin-sensitive ATPase, ATP hydrolyzed, the rate of ATP hydrolysis was first measured in the absence of oligomycin and then after addition of 1 μg of oligomycin in digitonin- and Percoll-treated cells, as described in Patients and methods; oligomycin inhibited the rate of ATP hydrolysis by 61% (control fibroblasts) and 60% (patient fibroblasts). ATP synthesis: ATP synthesized in the presence of succinate or pyruvate + malate (P + M). In the case of ATP synthesis, the second line indicates the means ± SD of 3 experiments.

Activities of oxidative phosphorylation complexes

Table 1 shows that in patient P, all tested respiratory chain activities in muscle and fibroblasts were within the range of control values. Similarly, the oligomycin-sensitive ATPase hydrolytic activity was normal in patient P cells. The 8527A > G cells were capable of a near normal ATP synthesis (using either succinate or pyruvate and malate as a substrate) that was about 20% decreased compared with control cells. Fig. 2 shows that the 8527A > G cells displayed normal values of the TMRM fluorescence, which is proportional to the mitochondrial membrane potential ($\Delta\Psi_m$), at state 4 (completely sensitive to an uncoupler FCCP) and the state 4 $\Delta\Psi_m$ was decreased by ADP (state 3 ADP) equally in patient cells and in controls. ADP-induced decrease of TMRM fluorescence was fully prevented by 1 μM oligomycin (Fig. 2), 10 μM carboxyatractyloside or 3 μM aurovertin (not shown) indicating fully operational $\Delta\Psi_m$ discharge by ATP synthase. This contrasted with a diminished effect of ADP on $\Delta\Psi_m$ in the NARP cells carrying the

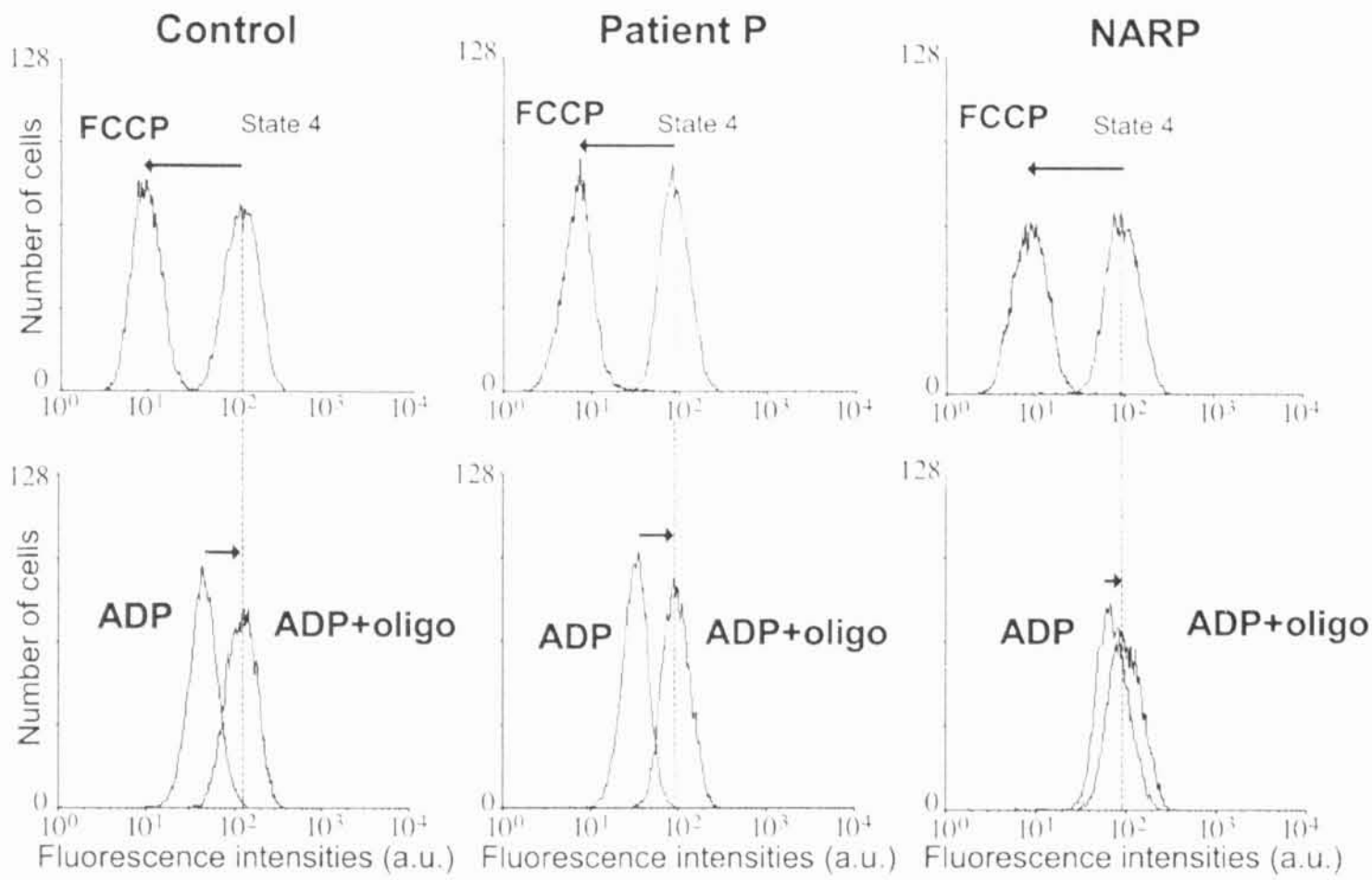

Fig. 2. Mitochondrial membrane potential analyzed by TMRM fluorescence in control cells, P patient cells and NARP cells. Upper panels show the cytofluorometric analysis at state 4 in the presence of succinate and effect of 1 μM FCCP, lower panels show effect of 0.1 mM ADP and its sensitivity to 1 μM oligomycin. Fluorescence intensities are displayed in arbitrary units.

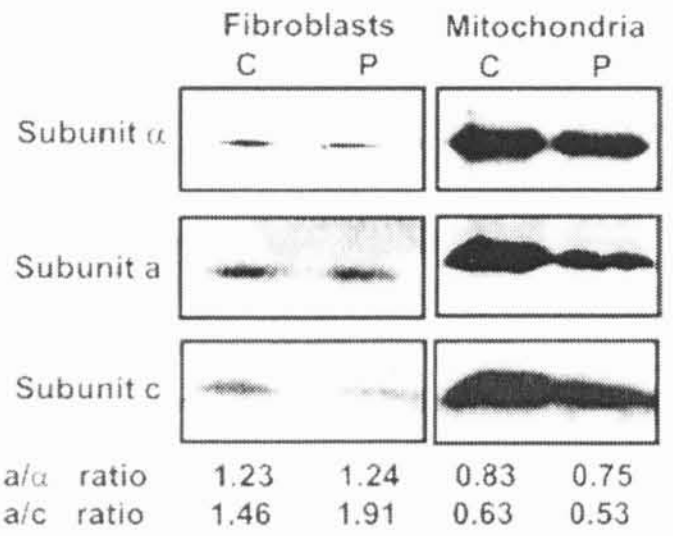

Fig. 3. Western blot analysis of ATPase subunits α, a, and c in P patient and control fibroblasts and isolated fibroblast mitochondria. Relative ratios of ATPase subunit a/subunit α and subunit a/subunit c are shown.

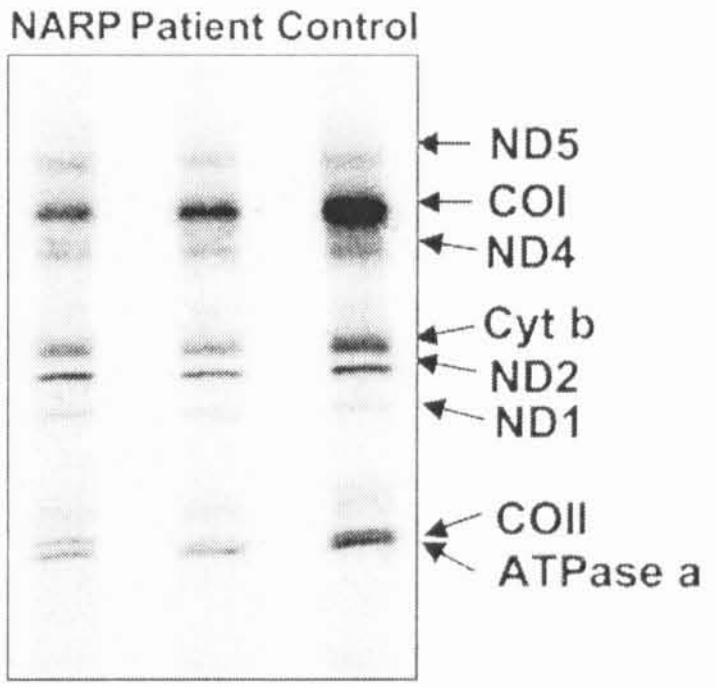

Fig. 4. Incorporation of [^{35}S]methionine into proteins encoded by mtDNA in control, NARP and patient P fibroblasts.

8993T > G mutation that have highly decreased ability to synthesize ATP [24].

Amounts of ATPase subunits and synthesis of mtDNA encoded proteins

Western blot analysis of ATPase subunits (Fig. 3) in 8527A > G fibroblasts and isolated fibroblast mitochondria showed that mtDNA-encoded ATPase subunit a was present with a normal size and that the relative amount of subunit a to nucleus-encoded ATPase subunits α and c was present in similar proportions in patient P and in control fibroblasts. Also analysis of lauryl maltoside-solubilized mitochondrial proteins by Blue Native gel electrophoresis revealed normal size of ATPase complex from 8527A > G fibroblasts (not shown). Fig. 4 further shows that [^{35}S]methionine was apparently incorporated into ATPase subunit a in

similar proportions as for other mtDNA-encoded proteins of control or NARP patient cells. Therefore, the mutation in the *ATP6* initiation codon did not decrease the biosynthesis and the steady state amount of this subunit in fibroblasts.

Discussion

This study demonstrates that the mutation 8527A > G changing the AUG initiation codon of the *ATP6* into GUG (normally encoding a valine) did not prevent the synthesis of the ATPase a subunit, did not change its size, and did not decrease its content relative to other ATPase subunits. This part of the mtDNA sequence encodes two ATPase subunits, the subunit a and the subunit A6L (also called subunit 8). The 8527A > G mutation did not change the sequence of the latter because it was a silent mutation on the third position of the codon. To our knowledge, the only known mutations modifying initiation codons in the human mtDNA are the 3308T > C and 7587T > C mutations located in the genes coding for ND1 and COII, respectively. Both are predicted to change Met to Thr. In the case of the *ND1* gene, it has initially been identified in a MELAS patient [4]. However, the complex I activity of cells bearing this mutation was normal, since the mutation did not produce any detectable alteration in mitochondrial ND1 polypeptide synthesis, at least in skin fibroblasts, and since the mutation was also present in healthy individuals carrying the West African haplogroup L1b [25]. Fernandez-Moreno et al. [6] have suggested that the AUG codon specifying Met present on the third triplet in-frame with the 5′ end of the ND1 mRNA is used as translational initiator. The two missing N-terminal amino acids would not prevent ND1 from being functional.

In the *COII* case, the initiation codon ACG was not functional since the mutation 7587T > C resulted in a mitochondrial encephalomyopathy and in lower levels of COX observed in fibers or cells containing less than 55–65% of wild type mtDNA [5].

In the case of the *ATP6*, no Met codon able to replace the normal initiation codon in the vicinity of the 5′ end of ATPase 6 mRNA is present in the sequence [17], ruling out the possibility that an alternate Met could replace the normal translational initiator. The first patient in which this mutation was observed presents multi-organ deficiency reminiscent of mitochondrial diseases, and the ability of patient fibroblasts to synthesize ATP in the presence of either succinate or malate and pyruvate, was at most decreased by 20%, as measured by sensitive luciferase assay. On the other hand, ATP hydrolysis and ADP-induced decrease of mitochondrial membrane potential were equal to controls, and all attempts to demonstrate a deficiency of the ATPase subunit a, and putative change in the assembly and cellular content of the ATPase complex have been unsuccessful.

The very low residual amount of mtDNA amplified as the wild type (less than 3%) is not likely to provide enough normal *ATP6* mRNA to compensate for the defect if AUG was the only active initiation codon. Moreover, the small percentage of DNA amplified as normal mtDNA in the patient may be of nuclear origin. Indeed, during evolution, mtDNA has been integrated on several chromosomes of the nuclear genome. A Blast study in GenBank revealed at least seven DNA fragments (in chromosomes 1, 2, 5, 6, 7, 10, and 17 of the human genome) that could be amplified with the primers used to detect heteroplasmy in the patient mtDNA and exhibited homology with ATPase subunit a. Therefore, it is likely that the mitochondrial mutation is homoplasmic in the patient P's mtDNA and in that of his healthy mother.

One cannot ascertain that the clinical symptoms observed in this patient are related to the mutation 8527A > G because his mother is healthy and carries the same practically homoplasmic mutation load, unless this is a new example of incomplete penetrance of mtDNA mutation, as observed in LHON [26]. The only other individual in whom the mutation has been observed became suddenly blind at the age of 8 years, presenting an optic atrophy similar to what is observed in patients suffering from LHON. This might suggest that this mutation could induce some negative consequences at least in some specific tissues. The most likely explanation is that the mutated initiation codon GUG must be somehow functional, as it has been observed in other eukaryotic mtDNA [27] and in *Escherichia coli* [28]. This mutation might eventually bring on some negative consequences that would induce the disease, when conjugated to another factor, genetic or environmental. The fact that both patients P and L carrying the same two mutations on *ATP6* are consanguineous suggests that an unidentified nuclear gene might contribute to the disease.

The main conclusion of this paper is that, in human mtDNA, GUG can be used as an alternative initiation codon to produce a normal amount of ATPase subunit a. To our knowledge, GUG has never been reported to be able to initiate the translation of human mtDNA-encoded proteins. In *Saccharomyces cerevisiae*, when AUG was mutated to AUA in *COII* mRNA, the translation occurred at this codon at a reduced rate and not at the next downstream AUG [29,30]. Although the mechanism of start site selection in mitochondrial translation is not well understood, studies made in yeast have shown the involvement of mRNA-specific activator proteins, such as MRP21 and MRP51 [31], eventually after binding to specific sequences present on mRNAs or 5′-untranslated regions [32].

We propose as a working hypothesis that, in the case of human *ATP6*, a protein, yet to be identified, might bind upstream the AUG (or GUG) initiation codon at the level of the *ATP8* coding sequence, to position the mRNA on the ribosome. To induce the disease, such a protein should carry a mutation that would decrease ribosome binding efficiency and lower ATPase subunit a synthesis when AUG is mutated to GUG. This could be harmful mainly in tissues requiring a high rate of ATP synthesis.

Acknowledgments

This work was supported by the "Fondation Jerome Lejeune," the "Centre National de la Recherche Scientifique," the Rhone-Alpes Région, the Grant Agency of Ministry of Health of the Czech Republic (NE6533-3), and institutional projects AVOZ5011922 and VZ111100003.

References

[1] D.C. Wallace, Mitochondrial disease in man and mouse, Science 283 (1999) 1482–1488.

[2] D.C. Wallace, M.T. Lott, MITOMAP: "A Human Mitochondrial Genome Database" 2003; Available from http://www.mitomap.org.

[3] N. Howell, Leber hereditary optic neuropathy: respiratory chain dysfunction and degeneration of the optic nerve, Vis. Res. 38 (1998) 1495–1504.

[4] Y. Campos, M.A. Martin, J.C. Rubio, M.C. Gutierrez del Olmo, A. Cabello, J. Arenas, Bilateral striatal necrosis and MELAS associated with a new T3308C mutation in the mitochondrial ND1 gene, Biochem. Biophys. Res. Commun. 238 (1997) 323–325.

[5] K.M. Clark, R.W. Taylor, M.A. Johnson, P.F. Chinnery, Z.M. Chrzanowska-Lightowlers, R.M. Andrews, I.P. Nelson, N.W. Wood, P.J. Lamont, M.G. Hanna, R.N. Lightowlers, D.M. Turnbull, An mtDNA mutation in the initiation codon of the cytochrome *c* oxidase subunit II gene results in lower levels of the protein and a mitochondrial encephalomyopathy, Am. J. Hum. Genet. 64 (1999) 1330–1339.

[6] M.A. Fernandez-Moreno, B. Bornstein, N. Petit, R. Garesse, The pathogenic role of point mutations affecting the translational initiation codon of mitochondrial genes, Mol. Genet. Metab. 70 (2000) 238–240.

[7] R.J.A. Wanders, Peroxisomal disorders: clinical, biochemical and molecular aspects, Neurochem. Res. 24 (1999) 565–580.

[8] B. Parfait, P. de Lonlay, J.C. von Kleist-Retzow, V. Cormier-Daire, D. Chretien, A. Rotig, D. Rabier, J.M. Saudubray, P. Rustin, A. Munnich, The neurogenic weakness, ataxia and retinitis pigmentosa (NARP) syndrome mtDNA mutation (T8993G) triggers muscle ATPase deficiency and hypocitrullinaemia, Eur. J. Pediatr. 158 (1999) 55–58.

[9] H.A. Bentlage, U. Wendel, H. Schägger, H.J. ter Laak, A.J. Janssen, J.M. Trijbels, Lethal infantile mitochondrial disease with isolated complex I deficiency in fibroblasts but with combined complex I and IV deficiencies in muscle, Neurology 47 (1996) 243–248.

[10] R.J. Wanders, J.P. Ruiter, F.A. Wijburg, J. Zeman, P. Klement, J. Houstek, Prenatal diagnosis of systemic disorders of the respiratory chain in cultured chorionic villus fibroblasts by study of ATP-synthesis in digitonin-permeabilized cells, J. Inherit. Metab. Dis. 19 (1996) 133–136.

[11] R. Ouhabi, M. Boue-Grabot, J.P. Mazat, Mitochondrial ATP synthesis in permeabilized cells: assessment of the ATP/O values in situ, Anal. Biochem. 263 (1998) 169–175.

[12] T. Letellier, M. Malgat, M. Coquet, B. Moretto, F. Parrot-Roulaud, J.P. Mazat, Mitochondrial myopathy studies on permeabilized muscle fibers, Pediatric Res. 32 (1992) 17–22.

[13] P. Rustin, D. Chretien, T. Bourgeron, B. Gérard, A. Rotig, J.M. Saudubray, A. Munnich, Biochemical and molecular investigations in respiratory chain deficiencies, Clin. Chim. Acta 228 (1994) 35–51.

[14] K. Buchet, C. Godinot, Functional F1-ATPase essential in maintaining growth and membrane potential of human mitochondrial DNA-depleted rho° cells, J. Biol. Chem. 273 (1998) 22983–22989.

[15] D. Chretien, P. Benit, M. Chol, S. Lebon, A. Rotig, A. Munnich, P. Rustin, Assay of mitochondrial respiratory chain complex I in human lymphocytes and cultured skin fibroblasts, Biochem. Biophys. Res. Commun. 301 (2003) 222–224.

[16] D. Floryk, J. Houstek, Tetramethyl rhodamine methyl ester (TMRM) is suitable for cytofluorometric measurements of mitochondrial membrane potential in cells treated with digitonin, Biosci. Rep. 19 (1999) 27–34.

[17] S. Anderson, A.T. Bankier, B.G. Barrell, M.H. de Bruijn, A.R. Coulson, J. Drouin, I.C. Eperon, D.P. Nierlich, B.A. Roe, F. Sanger, P.H. Schreier, A.J. Smith, R. Staden, I.G. Young, Sequence and organization of the human mitochondrial genome, Nature 290 (1981) 457–465.

[18] H. Schägger, G. von Jagow, Tricine-sodium dodecyl sulfate polyacrylamide gel electrophoresis for the separation of proteins in the range from 1 to 100 kDa, Anal. Biochem. 166 (1987) 368–379.

[19] M. Moradi-Améli, C. Godinot, Characterisation of monoclonal antibodies against mitochondrial F1-ATPase, Proc. Natl. Acad. Sci. USA 80 (1983) 6167–6171.

[20] J. Houstek, U. Andersson, P. Tvrdik, J. Nedergaard, B. Cannon, The expression of subunit c correlates with and thus may limit the biosynthesis of the mitochondrial F0F1-ATPase in brown adipose tissue, J. Biol. Chem. 270 (1995) 7689–7694.

[21] J. Johnson, Production and assay of murine anti-allotype antisera, in: I. Letkovitz, B. Perris (Eds.), Immunological Methods I, Academic Press, Orlando, USA, 1985, p. 202.

[22] A. Chomyn, In vivo labeling and analysis of human mitochondrial translation products, Methods Enzymol. 264 (1996) 197–211.

[23] K. Polyak, B. Vogelstein, MITOMAP mtDNA sequence data, 1999; Available from http://www.mitomap.org/mitomap/mitomapmutant.

[24] J. Houstek, P. Klement, J. Hermanska, H. Houstkova, H. Hansikova, C. Van den Bogert, J. Zeman, Altered properties of mitochondrial ATP-synthase in patients with a T > G mutation in the ATPase 6 (a subunit) gene at position 8993 of mtDNA, Biochim. Biophys. Acta 1271 (1995) 349–357.

[25] H. Rocha, C. Flores, Y. Campos, J. Arenas, L. Vilarinho, F.M. Santorelli, A. Torroni, About the pathological role of the mtDNA T3308C mutation ellipsis, Am. J. Hum. Genet. 65 (1999) 1457–1459.

[26] P.Y. Man, D.M. Turnbull, P.F. Chinnery, Leber hereditary optic neuropathy, J. Med. Genet. 39 (2002) 162–169.

[27] Mitbase: Available from http://www3.ebi.ac.uk/Research/Mitbase/trans_tabs.html.

[28] C.O. Gualerzi, C.L. Pon, Initiation of mRNA translation in prokaryotes, Biochemistry 29 (1990) 5881–5889.

[29] J.J. Mulero, T.D. Fox, Reduced but accurate translation from a mutant AUA initiation codon in the mitochondrial COX2 mRNA

of *Saccahromyces cerevisiae*, Mol. Gen. Genet. 242 (1994) 383–390.

[30] N. Bonnefoy, T.D. Fox, In vivo analysis of mutated initiation codons in the mitochondrial COX2 gene of *Saccharomyces cerevisiae* fused to the reporter gene ARG8m reveals lack of downstream reinitiation, Mol. Gen. Genet. 262 (2000) 1036–1046.

[31] N.S. Green-Wilms, T.D. Fox, M.C. Costanzo, Functional interactions between yeast mitochondrial ribosomes and mRNA 5′ untranslated leaders, Mol. Cell. Biol. 18 (1998) 1826–1834.

[32] H.M. Dunstan, N.S. Green-Wilms, T.D. Fox, In vivo analysis of *Saccharomyces cerevisiae* COX2 mRNA 5′ untranslated leader function in mitochondrial translation initiation and translational activation, Genetics 147 (1997) 87–100.

Article 5

Biochem. J. (2004) **383**, 561–571 (Printed in Great Britain)

Diminished synthesis of subunit a (ATP6) and altered function of ATP synthase and cytochrome *c* oxidase due to the mtDNA 2 bp microdeletion of TA at positions 9205 and 9206

Pavel JEŠINA*[1], Markéta TESAŘOVÁ†[1], Daniela FORNŮSKOVÁ†, Alena VOJTÍŠKOVÁ*, Petr PECINA*, Vilma KAPLANOVÁ*, Hana HANSÍKOVÁ†, Jiří ZEMAN† and Josef HOUŠTĚK*[2]

*Department of Bioenergetics, Institute of Physiology and Centre for Integrated Genomics, Academy of Sciences of the Czech Republic, Videnska 1083, 142 20 Prague, Czech Republic, and †Department of Pediatrics and Institute for Inherited Metabolic Disorders, 1st Faculty of Medicine, Charles University, 120 00 Prague, Czech Republic

Dysfunction of mitochondrial ATPase (F_1F_o-ATP synthase) due to missense mutations in ATP6 [mtDNA (mitochondrial DNA)-encoded subunit a] is a frequent cause of severe mitochondrial encephalomyopathies. We have investigated a rare mtDNA mutation, i.e. a 2 bp deletion of TA at positions 9205 and 9206 (9205ΔTA), which affects the STOP codon of the *ATP6* gene and the cleavage site between the RNAs for *ATP6* and *COX3* (cytochrome *c* oxidase 3). The mutation was present at increasing load in a three-generation family (in blood: 16 %/82 %/> 98 %). In the affected boy with severe encephalopathy, a homoplasmic mutation was present in blood, fibroblasts and muscle. The fibroblasts from the patient showed normal aurovertin-sensitive ATPase hydrolytic activity, a 70 % decrease in ATP synthesis and an 85 % decrease in COX activity. ADP-stimulated respiration and the ADP-induced decrease in the mitochondrial membrane potential at state 4 were decreased by 50 %. The content of subunit a was decreased 10-fold compared with other ATPase subunits, and [^{35}S]-methionine labelling showed a 9-fold decrease in subunit a biosynthesis. The content of COX subunits 1, 4 and 6c was decreased by 30–60 %. Northern Blot and quantitative real-time reverse transcription–PCR analysis further demonstrated that the primary ATP6–COX3 transcript is cleaved to the ATP6 and COX3 mRNAs 2–3-fold less efficiently. Structural studies by Blue-Native and two-dimensional electrophoresis revealed an altered pattern of COX assembly and instability of the ATPase complex, which dissociated into subcomplexes. The results indicate that the 9205ΔTA mutation prevents the synthesis of ATPase subunit a, and causes the formation of incomplete ATPase complexes that are capable of ATP hydrolysis but not ATP synthesis. The mutation also affects the biogenesis of COX, which is present in a decreased amount in cells from affected individuals.

Key words: *ATP6*, ATP synthase, *COX3*, cytochrome *c* oxidase, mitochondrial disease, mitochondrial DNA (mtDNA).

INTRODUCTION

The mammalian ATPase (F_1F_o-ATP synthase) complex catalyses the synthesis of ATP from ADP and P_i, the final step of the OXPHOS (oxidative phosphorylation) pathway. The ATPase complex consists of 16 different subunits [1], and is composed of the globular F_1 catalytic part connected by two stalks to the membrane-embedded F_o moiety that translocates protons across the mitochondrial inner membrane. Only two F_o subunits, subunit a (ATP6) and A6L (ATP8), are encoded by mtDNA (mitochondrial DNA) [2]. Both are essential for the biogenesis and assembly of the ATPase complex [3].

Mutations in mtDNA represent a frequent cause of mitochondrial diseases. They can involve tRNAs, rRNAs or protein-encoding genes (for review see [4]) and are associated with a wide variety of clinical pictures, ranging from isolated myopathy to multisystem disorders, affecting primarily tissues with high energy demands, such as skeletal muscle, heart and nervous system. Most pathogenic mtDNA mutations are in tRNAs. Mutations in protein-encoding genes are much less frequent, with the exception of those associated with complex I or ATPase dysfunction. All maternally inherited ATPase diseases are caused by mutations in the *ATP6* gene; no mutation has been reported in the *ATP8* (*A6L*) gene. Mutations in the *ATP6* gene disturb the function of the ATPase proton channel, which consists of subunit a and multiple copies of subunit c. The most frequent are heteroplasmic T8993G [5] or less severe T8993C mutations [6], which result in replacement of Leu^{156} by Arg or Pro in subunit a, and often present as a NARP (neurogenic muscle weakness, ataxia, retinitis pigmentosa) [5] or MILS (maternally inherited Leigh syndrome) [7] phenotype. Several other, less frequent, mutations of *ATP6* at positions 9176 or 8851 have also been described (for review see [8]), resulting in similar lesions in brain, particularly in the striatum (familiar bilateral striatal necrosis). The T8993G mutation results in a decrease in mitochondrial ATP production [9] without a significant effect on ATP hydrolysis [7], and in structural changes in the ATPase complex [10], which, however, could not be found in some cases [11]. It has been observed that the ATPase deficiency is associated with a decreased ability of cells from affected individuals to assemble correctly the ATPase complex, which shows instability in BN-PAGE (Blue-Native PAGE) experiments [10,12].

Abbreviations used: ATPase, F_1F_o-ATP synthase; BN-PAGE, Blue-Native PAGE; COX, cytochrome *c* oxidase; CS, citrate synthase; 2D, two-dimensional; DDM, dodecyl maltoside; FCCP, carbonyl cyanide 4-trifluoromethoxyphenylhydrazone; LRPPRC, leucine-rich pentatricopeptide repeat cassette; mtDNA, mitochondrial DNA; OXPHOS, oxidative phosphorylation; $\Delta\Psi_m$, mitochondrial membrane potential; RFLP, restriction fragment length polymorphism; RT-PCR, reverse transcription–PCR; SDH, succinate dehydrogenase; TMPD, *N,N,N′,N′*-tetramethyl-*p*-phenylenediamine; TMRM, tetramethylrhodamine methyl ester; WB, Western blot.

[1] These authors contributed equally to this work.

[2] To whom correspondence should be addressed (email houstek@biomed.cas.cz).

In the present paper we have studied a very rare mtDNA mutation in the *ATP6* gene – a 2 bp microdeletion at positions 9205 and 9206 (9205ΔTA). This mutation cancels the STOP codon of *ATP6* gene and changes the cleavage site between the ATP6 and COX3 (cytochrome *c* oxidase subunit 3) transcripts. It was originally discovered in a newborn with transient lactic acidosis [13]. Recently we found a second case of a 9205ΔTA mutation that was present in a child with severe encephalopathy and hyperlactacidaemia [14]. Here we present the results of molecular and biochemical studies of ATPase and COX that focus on the biosynthesis of ATPase subunit a and the structural and functional consequences of the 9205ΔTA mutation.

EXPERIMENTAL

Ethics

This study was carried out in accordance with the Declaration of Helsinki of the World Medical Association, and was approved by the Committees of Medical Ethics at all collaborating institutions. Informed consent was obtained from the parents of the child.

Case report

The boy was born at term from a second, uncomplicated pregnancy, with birth weight 3450 g and length 52 cm. Failure to thrive, spastic quadruparesis and microcephalia were observed from the 3rd month of life, followed by practical arrest of any psychomotor development. Metabolic investigations revealed intermittent hyperlactacidaemia (B-lactate, 0.95–3.4 mmol/l; controls < 2.1 mmol/l), with increased levels of lactate and alanine in the cerebrospinal fluid [lactate, 4.8 mmol/l (controls < 1.8 mmol/l); alanine, 36 μmol/l (controls < 34 μmol/l)]. He is 5 years old at present. Both parents are healthy, but an older brother (from the first marriage of the mother) died due to a respiratory failure at the age of 3 years. He presented with fatal infantile encephalopathy, severe psychomotor delay, frontal lobe atrophy and lactic acidosis.

Cell cultures and isolation of mitochondria

Fibroblast cultures were established from skin biopsies, and cells were grown in Dulbecco's modified Eagle's medium supplemented with 10 % (v/v) fetal calf serum (Sigma) at 37 °C in 5 % CO_2 in air. Cells were grown to approx. 90 % confluence and harvested using 0.05 % (w/v) trypsin and 0.02 % (w/v) EDTA. Detached cells were diluted with an ice-cold culture medium, sedimented by centrifugation and washed twice in PBS.

Mitochondria were isolated from fibroblasts by a hypo-osmotic shock method [15]. The freshly harvested cells were disrupted in 10 mM Tris buffer (pH 7.4) and quickly homogenized in a Teflon/glass homogenizer at 4 °C. Sucrose was added to a final concentration of 0.25 M immediately after homogenization. The nuclei were removed by centrifugation for 10 min at 4 °C and 600 ***g*** and the mitochondrial fraction was isolated from the postnuclear supernatant by centrifugation for 10 min at 4 °C and 10000 ***g***. The mitochondrial pellet was washed and finally resuspended in 0.25 M sucrose, 2 mM EGTA, 40 mM KCl and 20 mM Tris, pH 7.4, and stored at −70 °C.

Mitoplasts were prepared from fibroblasts as described previously [16]. In brief, trypsinized cells suspended in an STE medium (0.25 M sucrose, 10 mM Tris, 1 mM EDTA, pH 7.4) were treated with digitonin (0.4 mg/mg of protein; Fluka) on ice for 15 min. The suspension was diluted 10-fold with STE and centrifuged for 10 min at 4 °C and 12000 ***g***. The pellet was washed by centrifugation and resuspended in STE to a final concentration of 1–2 mg of protein/ml. Based on immunodetection and enzyme activity measurements, > 95 % of the mitochondrial inner membrane proteins were recovered in this fraction.

Muscle mitochondria were isolated according to [17], but without use of protease. Tissue samples were homogenized at 4 °C in a KCl medium (100 mM KCl, 50 mM Tris, 2 mM EDTA, 10 mg/ml aprotinin, pH 7.5). The homogenate was centrifuged for 10 min at 4 °C and 600 ***g***, the supernatant was filtered through a 100 μm nylon screen, and mitochondria were sedimented by centrifugation for 10 min at 4 °C and 10000 ***g***. The mitochondrial pellet was washed by centrifugation and resuspended to a final protein concentration of 20–25 mg/ml.

DNA analysis and sequencing

Total genomic DNA from muscle and cultured fibroblasts was isolated by phenol extraction. The entire mtDNA was amplified in six overlapping fragments by PCR (7–3148, 2073–5719, 5645–8815, 8403–11132, 11005–14684 and 13863–136). Purified fragments were sequenced on the automatic sequencer ALFExpress II (Amersham Biosciences) using cycle sequencing with 41 Cy5-labelled internal sequencing primers.

Restriction analysis

To determine the amount of mtDNA containing the microdeletion, the PCR/RFLP (restriction fragment length polymorphism) analysis method was performed according to [18] using the mismatched (bold) primers 5′-CCT CTA CCT GCA CGA CAA **TG**C A-3′ (forward) and 5′-CGT TAT GCA **TT**G GAA GTG AAA TCA C-3′ (reverse), which introduce two novel *Nsi*I restriction sites in the case of the wild-type mtDNA and one *Nsi*I restriction site in the case of mutant mtDNA. PCR products were radioactively labelled with [α-^{32}P]dCTP in the final cycle of PCR and run on a non-denaturing 13 % (w/v) polyacrylamide gel after complete digestion. The proportions of wild-type and mutant mtDNA were measured using a PhosphorImager and ImageQuant software (Molecular Dynamics).

Northern blot analysis

Total RNA was isolated from cultured fibroblasts by phenol/guanidium thiocyanate/chloroform extraction [19]. Approx. 20 μg of total RNA per lane was separated through a 1.2 % (w/v) agarose/formaldehyde gel and transferred to a Hybond-N nylon membrane (Amersham) in 20 × SSC (1 × SSC is 0.15 M NaCl/0.015 M sodium citrate). The membrane was prehybridized for 2 h at 45 °C in 5 × SSC, Denhardt's solution, 0.5 % SDS and 100 μg/ml sonicated herring sperm. The membranes were hybridized overnight at 45 °C with [α-^{32}P]dCTP-labelled probes corresponding to regions of the genes *ATP6* (8361–9060), *COX3* (9269–9912), *ND1* (3313–4252) and *COX1* (6120–6960). The radioactivity was detected by phosphor imaging (as above).

Quantitative RT-PCR (reverse transcription–PCR) analysis

Total RNA was isolated from cultured fibroblasts using RNA Blue reagent (Top-Bio, Prague, Czech Republic). Following DNase I treatment (Invitrogen), first-strand cDNA was synthesized from 1 μg RNA aliquots with 200 units SuperScript II reverse transcriptase using either 200 ng of random hexamer primers or 500 ng of oligo(dT)$_{12-18}$ (all Invitrogen) according to the manufacturer's instructions. Real-time quantitative RT-PCR was performed on a LightCycler instrument (Roche Diagnostics) using a QuantiTect SYBR Green PCR kit (Qiagen). PCR reactions were performed

on cDNAs using primer pairs specific for the *ATP6* gene transcript (forward, 5′-CCT TAT GAG CGG GCA CAG T-3′; reverse, 5′-CAG GGC TAT TGG AA-3′; nt 8846–8994), for the *COX3* gene transcript (forward, 5′-GCC CTC TCA GCC CTC CTA ATG-3′; reverse, 5′-GTG GCC TTG GTA TGT GCT TTC TCG-3′; nt 9267–9416), for the *ATP6–COX3* gene transcript (forward, 5′-AAT CCA AGC CTA CGT TTT CAC ACT-3′; reverse, 5′-TAG GCC GGA GGT CAT TAG G-3′; nt 9150–9299), for the *CYTB* gene transcript (forward, 5′-GAC CTC CCC ACC CCA TCC A-3′; reverse, 5′-AAA GGC GGT TGA GGC GTC TG-3′; nt 14804–14935) and for the *ND1* gene transcript (forward, 5′-CAA CCT CAA CCT AGG CCT CCT-3′; reverse, 5′-ACG GCT AGG CTA GAG GTG GC-3′; nt 3595–3644). The primer pair for *ATP6–COX3* was designed to flank the splice site of the ATP6–COX3 transcript. Amplified regions of the ATP6 or COX3 transcript were present in both processed and unprocessed RNAs. All reactions were run at an annealing temperature of 60 °C. The PCR mixture contained 5 μl of 2 × SYBR Green PCR Master Mix, 2 μl of 100 × diluted reverse transcription product and 200 nM of each primer in a total volume of 10 μl. All reactions were performed in triplicate. For each primer pair, non-template controls were included to check for the absence of contaminants and primer-dimers that would interfere with quantification when SYBR Green is used. The external standard curve was generated in parallel for all reactions using serial dilutions of cDNA synthesized from control RNA. For each sample, the relative amounts of ATP6, COX3, CYTB, ND1 and unprocessed ATP6–COX3 transcripts were determined from the standard curves. Each sample was analysed in two separate experiments.

Electrophoresis and WB (Western blot) analysis

BN-PAGE [20] was used for the separation of native mitochondrial OXPHOS complexes on 6–15% (w/v) polyacrylamide gradient minigels (Mini Protean system; Bio-Rad) as described previously [16]. Mitoplasts were pelleted by centrifugation for 10 min at 4 °C and 10000 **g**, and solubilized using 1 g of DDM (dodecyl maltoside)/g of protein for 20 min on ice in a buffer containing 1.75 M aminocaproic acid, 2 mM EDTA and 75 mM Bis-Tris (pH 7.0). Samples were centrifuged for 20 min at 20000 **g** and Serva Blue G dye was added to collected supernatants at a concentration of 0.1 g/g of detergent. Electrophoresis was performed at 50 V for 30 min and then at 90 V.

SDS/PAGE [21] was performed on 10% (w/v) polyacrylamide slab minigels, and analysis of [^{35}S]methionine-labelled proteins was performed on a 16 cm long 15–20% (w/v) gradient polyacrylamide slab gels (Protean system; Bio-Rad). The samples were boiled for 3 min in sample lysis buffer [2% (v/v) mercaptoethanol, 4% (w/v) SDS, 10 mM Tris/HCl, 10% (v/v) glycerol]. For 2D (two-dimensional) analysis, strips of the first-dimension BN-PAGE gel were incubated for 1 h in 1% (w/v) SDS and 1% (v/v) mercaptoethanol and then subjected to SDS/PAGE (10% polyacrylamide) for separation in the second dimension [21].

Gels were blotted on to Hybond C-extra nitrocellulose membranes (Amersham) by semi-dry electrotransfer for 1 h at 0.8 mA/cm^2 and the membrane was blocked in PBS containing 0.2% (v/v) Tween 20 (PBST). The membranes were used whole or were cut according to molecular mass markers into portions containing individual OXPHOS complexes or their subunits. Membranes were incubated for 3 h with primary antibodies diluted in PBS containing 2% (w/v) BSA (PBSTA). Previously characterized polyclonal antibodies were used at the indicated titres: those against the F_1c subunit of ATPase (1:900) [22] and those against the F_1a (ATP6) subunit of ATPase (1:500) [23]. In addition, we used monoclonal antibodies against subunits COX1 (1:330; Molecular Probes A-6403), COX4 (1:670; Molecular Probes A-6409), COX6c (1:200; Molecular Probes A-6401), NADH39 (1:250; Molecular Probes A-11140), SDH70 (succinate dehydrogenase 70 kDa subunit; 1:2000; Molecular Probes A-11142) and subunit α of F_1-ATPase (1:200000; lot 20D6 [24]). Incubation with peroxidase-labelled secondary antibodies in PBSTA was performed for 1 h using either goat anti-mouse IgG (1:1000; Sigma A8924) or goat anti-rabbit IgG (1:1000; Sigma F0382). The chemiluminescence reaction with an ECL$^+$ kit (Amersham) was detected on an LAS 1000 instrument (Fuji) and the signal was quantified using Aida 2.11 Image Analyser software.

Spectrophotometric assays

The activities of the mitochondrial enzymes NADH:CoQ reductase (complex I), succinate:CoQ reductase (complex II), CoQ:cytochrome *c* reductase (complex III), COX (complex IV), NADH:cytochrome *c* reductase (complex I + III), succinate:cytochrome *c* reductase (complex II + III) and CS (citrate synthase) were measured spectrophotometrically by standard methods at 37 °C in muscle homogenate and isolated muscle mitochondria [17,25–28] or in cultured fibroblasts [29].

ATPase hydrolytic activity was measured in a ATP-regenerating system as described in [30]. Mitochondria (8–22 μg of protein/ml) were incubated in a medium containing 40 mM Tris (pH 7.4), 5 mM $MgCl_2$, 10 mM KCl, 2 mM phosphoenolpyruvate, 0.2 mM NADH, 1 μg/ml rotenone, 0.1% (w/v) BSA, 5 units of pyruvate kinase and 5 units of lactate dehydrogenase for 2 min. The reaction was started by the addition of 1 mM ATP and the rate of NADH oxidation, equimolar to ATP hydrolysis, was monitored as the decrease in absorbance at 340 nm. Sensitivity to aurovertin was determined by parallel measurements in the presence of 2 μM inhibitor.

High-resolution oxygraphy

Oxygen consumption by cultured fibroblasts was determined at 30 °C as described previously [29,31] using an Oxygraph-2k (Oroboros, Innsbruck, Austria). Freshly harvested fibroblasts were suspended in a KCl medium (80 mM KCl, 10 mM Tris/HCl, 3 mM $MgCl_2$, 1 mM EDTA, 5 mM potassium phosphate, pH 7.4) and cells were permeabilized by digitonin (0.1 mg of detergent/mg of protein). Respiratory substrates and inhibitors were used at the concentrations indicated. Oxygen consumption was expressed in pmol of oxygen/s per mg of protein. COX activity was measured with 5 mM ascorbate and 1 mM TMPD (*N*,*N*,*N*′,*N*′-tetramethyl-*p*-phenylenediamine), and was corrected for substrate autooxidation (determined as oxygen uptake insensitive to 0.33 mM KCN).

Cytofluorimetric analysis of $\Delta\Psi_m$ (mitochondrial membrane potential)

Cytofluorimetric measurements were performed on a FACSort flow cytometer (Becton Dickinson) according to [32]. Fibroblasts were suspended in a KCl medium containing 10 mM succinate to a protein concentration of 1 mg/ml and permeabilized by 0.1 mg of digitonin/mg of protein. Permeabilized fibroblasts were diluted to 0.2 mg of protein/ml and incubated with 20 nM TMRM (tetramethylrhodamine methyl ester; Molecular Probes) for 15 min. OXPHOS inhibitors and ADP at the concentrations indicated were added 1 min before cytofluorimetric analysis. Approx. 10000 cells were used for each measurement. Data were acquired on a logarithmic scale using CellQuest (Becton Dickinson) and analysed with WinMDI 2.8 software (J. Trotter, TSRI, La Jolla, CA, U.S.A.). Arithmetic mean values of fluorescence signal in

Table 1 Respiratory chain enzyme and mitochondrial ATPase activities in isolated muscle mitochondria and cultured skin fibroblasts

SCCR, succinate:cytochrome *c* reductase; NCCR, NADH:cytochrome *c* reductase; SQR, succinate:CoQ reductase; QCCR, CoQ:cytochrome *c* reductase; NQR, NADH:CoQ reductase; ND, not determined. Values for age-related controls are presented as means ± S.D. and as a confidence interval (in parentheses).

(A)

	Activity (nmol/min per mg of protein)					
	Muscle homogenate		Muscle mitochondria		Fibroblasts (mitochondria*)	
Enzyme	Patient	Controls ($n = 20$)	Patient	Controls ($n = 20$)	Patient	Controls ($n = 30$)
COX	122	125 ± 72 (53–197)	331	682 ± 395 (287–1077)	5.1	29 ± 11 (18–40)
CS	241	114 ± 29 (85–143)	284	419 ± 221 (200–640)	40.9	58 ± 12 (46–70)
COX/CS	0.50	1.04 ± 0.44 (0.60–1.48)	1.16	1.66 ± 0.57 (1.09–2.23)	0.12	0.51 ± 0.18 (0.33–0.69)
SCCR	ND		98	127 ± 77 (50–206)	ND	
NCCR	ND		76	99 ± 57 (42–156)	16.3	28 ± 14 (14–42)
SQR	ND		43	64 ± 44 (20–108)	10.6	13 ± 8 (5–21)
QCCR	ND		54	178 ± 79 (100–257)	14.1	17 ± 10 (7–27)
NQR	ND		192	274 ± 80 (194–354)	33.8	23 ± 10 (15–50)
ATPase	ND		ND		320 ± 33.1*	254 ± 16.0*

(B)

	Activity (nmol/min per mg of protein)				
	Patient		Mother	Grandmother	Controls ($n = 30$)
Enzyme	Expt 1	Expt 2			
COX	7.9	2.4	16.9	34.4	29 ± 11
CS	45.5	33.8	50.5	52.2	58 ± 12
COX/CS	0.17	0.07	0.33	0.66	0.51 ± 0.18

arbitrary units were determined for each sample for subsequent graphic presentation.

ATP synthesis

The rate of ATP synthesis was measured at 37 °C in 150 mM KCl, 25 mM Tris/HCl, 10 mM potassium phosphate, 2 mM EDTA and 1% (w/v) BSA, pH 7.2, using 0.5 mM ADP and 10 mM succinate or 10 mM pyruvate + 10 mM malate as substrate, as described previously [33]. Protein concentration was 1 mg/ml. For permeabilization of fibroblasts, 0.1 mg of digitonin/mg of protein was used. The reaction was started by addition of fibroblasts and performed for the indicated time intervals. Reaction mixture aliquots of 200 μl were added to 200 μl of DMSO, and ATP content was determined in DMSO-quenched samples by a luciferase assay according to [34]. ATP production was expressed in nmol of ATP/min per mg of protein.

Biosynthesis of mitochondrial proteins

Growth medium was removed from cultured fibroblasts, and the cells were rinsed with methionine-free medium without serum (Gibco medium 21013; 1 mM pyruvate, 2 mM glutamine and 30 mg/l cysteine) and incubated in the same medium containing 10% (v/v) dialysed fetal calf serum and 100 μg/ml emetine for 10 min. The cells were labelled for 3 h with 300 μCi/ml L-[^{35}S]methionine, as described in [35]. The products were separated by 15–20% (w/v) polyacrylamide gradient SDS/PAGE. A small aliquot of the samples prepared for electrophoresis was used to measure the total incorporation of radioactivity in the mitochondrial fraction as trichloroacetic acid-precipitable counts. The radioactivity of proteins was quantified in dried gels using a BAS-5000 system (Fuji). Labelled proteins were identified according to their molecular mass as reported previously in *ex vivo* translation assays [35].

Protein determination

The protein content was measured by the Bradford or Micro BCA protein kit assays (Bio-Rad), using BSA as a standard. Samples were sonicated for 20 s prior to protein determination.

RESULTS

Activities of respiratory chain enzymes and mitochondrial ATPase

The activities of respiratory chain enzymes (Table 1A) in a muscle homogenate from a patient with encephalopathy and lactic acidosis showed a decrease in the COX/CS ratio. In isolated muscle mitochondria, both COX activity and the COX/CS ratio were at the lower end of the control range, complex I activity was below the control range and complex III activity was moderately decreased. In fibroblasts from the patient, we found a pronounced decrease in COX activity to 15% of the control, CS was just below the control range, and the activities of other respiratory chain enzymes were normal. ATPase hydrolytic activity was determined in isolated mitochondria from the patient's fibroblasts. It was measured as aurovertin-sensitive activity at a constant ATP concentration and was found to be normal.

When COX activity was measured in fibroblasts from the patient's asymptomatic mother and grandmother, decreased COX activity and a COX/CS ratio near the lower limit of the reference range were found in the mother, but not in the grandmother (Table 1B).

mtDNA 9205ΔTA mutation in the affected family

Sequencing of the patient's mtDNA revealed a very rare mtDNA mutation – a heteroplasmic 2 bp deletion TA at positions 9205 and 9206 (9205ΔTA) in the *ATP6–COX3* genes. Analysis of mutation heteroplasmy in tissues of the affected boy by radioactive RFLP (using *Nsi*I restrictase; Table 2) showed practically homoplasmic

Table 2 9205ΔTA mutation load in family members

Sample	mtDNA heteroplasmy (%)
mtDNA	
Grandmother – blood DNA	16
Grandmother – fibroblast DNA	6
Mother – blood DNA	82
Mother – fibroblast DNA	82
Patient – blood DNA	> 98
Patient – muscle DNA	> 98
Patient – fibroblasts DNA	> 98
cDNA	
Patient – fibroblasts cDNA oligo(dT)	> 98
Patient – fibroblasts cDNA oligo(dT) + random primers	> 98

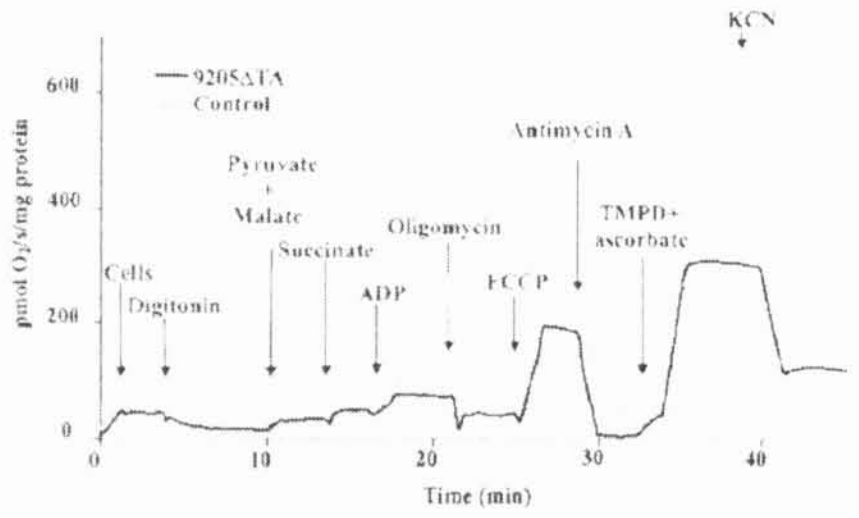

Figure 1 Oxygen consumption by digitonin-permeabilized skin fibroblasts

Measurements were performed using 0.45–0.62 mg of cell protein/ml and 0.1 mg of digitonin/mg of protein. Subsequent additions of pyruvate (5 mM), malate (1.5 mM), succinate (10 mM), ADP (0.5 mM), oligomycin (1 μM), FCCP (1 μM), antimycin A (0.2 μg/ml), ascorbate (5 mM), TMPD (1 mM) and KCN (0.33 mM) are indicated. Oxygen consumption is expressed as negative values of the first time derivative of changes in oxygen tension (pmol of O_2/s per mg of protein).

9205ΔTA mtDNA mutation in fibroblasts, muscle and blood (> 98%). Analysis of blood DNA confirmed the presence of the 9205ΔTA mutation at lower loads both in the mother (82%) and in the grandmother (16%). Interestingly, a similar mutation load was found in their fibroblasts (mother 92%; grandmother 9%), in correspondence with the observed decrease in COX activity in the mother's fibroblasts (see above).

An equal mutation load in the patient's fibroblasts was found using RFLP of isolated DNA as well as of cDNA reverse-transcribed from isolated RNA using either oligo(dT) or oligo (dT) + random primers, indicating that the mutation is fully retained in ATP6–COX3 RNA and poly(A) RNA (Table 2).

Oxygraphic analysis of cultured fibroblasts

The functional consequences of the 9205ΔTA mutation were analysed by high-resolution oxygraphy of the patient's fibroblasts that had been permeabilized by a low concentration of digitonin. The 9205ΔTA cells showed a pronounced decrease in ADP-stimulated oxygen consumption using pyruvate, malate and succinate as substrate, which contrasted with a normal rate of state 3 respiration in the presence of the uncoupler FCCP (carbonyl cyanide 4-trifluoromethoxyphenylhydrazone). We also observed a decrease in COX activity determined with TMPD and ascorbate (Figure 1). In 9205ΔTA cells from the patient, ADP-stimulated respiration

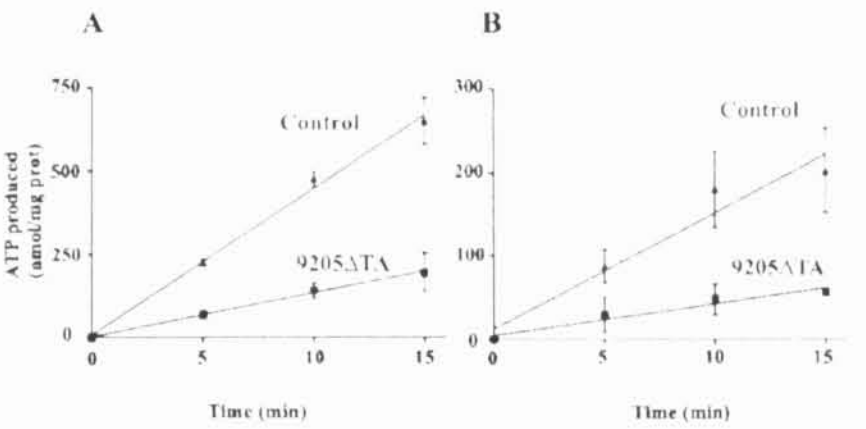

Figure 2 Production of ATP by control and 9205ΔTA fibroblasts

The rate of ATP synthesis was measured in the presence of 0.5 mM ADP in 9205ΔTA (■) and control (▲) digitonin-permeabilized fibroblasts treated with 0.1 mg of digitonin/mg of protein. Substrates were 10 mM pyruvate + 10 mM malate (**A**) or 10 mM succinate (**B**). ATP was determined in DMSO-quenched aliquots by a luciferase assay. Data represent means ± S.D. for three experiments.

was 50–60%, FCCP-stimulated respiration was 100–110% and COX activity was 40–50% of values in control cells. Although well coupled, the mitochondria of 9205ΔTA cells thus showed a strongly impaired effect of ADP, indicating a decreased ability to synthesize ATP.

Low ATP production in 9205ΔTA cells

The ability of fibroblasts to synthesize ATP by the mitochondrial OXPHOS pathway was measured directly in cells suspended in mitochondrial medium, permeabilized by digitonin and supplied with respiratory substrates and ADP, as in the oxygraphic experiments. With either succinate or pyruvate + malate as substrate, linear production of ATP was observed in control cells for 15 min, corresponding to ATP production of 16.4 ± 1.8 and 45.4 ± 1.5 nmol/min per mg of protein respectively, in accordance with the oxygraphic measurements. In 9205ΔTA fibroblasts, a steadily diminished ATP production was observed during the 15 min interval with both types of substrate, giving values of 4.8 ± 0.7 and 13.7 ± 0.4 nmol/min per mg of protein respectively, which are approx. 30% of control values (Figure 2).

Changes in $\Delta\Psi_m$

$\Delta\Psi_m$ was analysed cytofluorimetrically in digitonin-permeabilized fibroblasts using the membrane potential-sensitive cationic probe TMRM. We found that the $\Delta\Psi_m$ of the patient's fibroblasts was practically normal at state 4 using succinate as a substrate, but the effect of the addition of ADP on $\Delta\Psi_m$ was significantly decreased in 9205ΔTA cells (Figure 3). Whereas in control cells the TMRM fluorescence was decreased by the addition of ADP (state 3 ADP) to approx. 28% of the state 4 value, in the 9205ΔTA cells the TMRM fluorescence decreased to only 50%. The observed 2-fold difference in TMRM fluorescence would correspond to an even more pronounced difference in $\Delta\Psi_m$ values in mV, because the accumulation of the fluorophore obeys the Nernst equation and depends exponentially on $\Delta\Psi_m$ [36]. In both types of cells, the effect of ADP was fully reversible by oligomycin (Figure 3), atractyloside or aurovertin (results not shown), indicating that the effect of ADP requires the transport of ADP to the mitochondrial matrix as well as the catalytic activity of ATPase. In accordance with the measurements of ATP production and respirometry, these results suggest that ATP synthesis by mitochondrial ATPase is strongly impaired in 9205ΔTA cells from the affected individual.

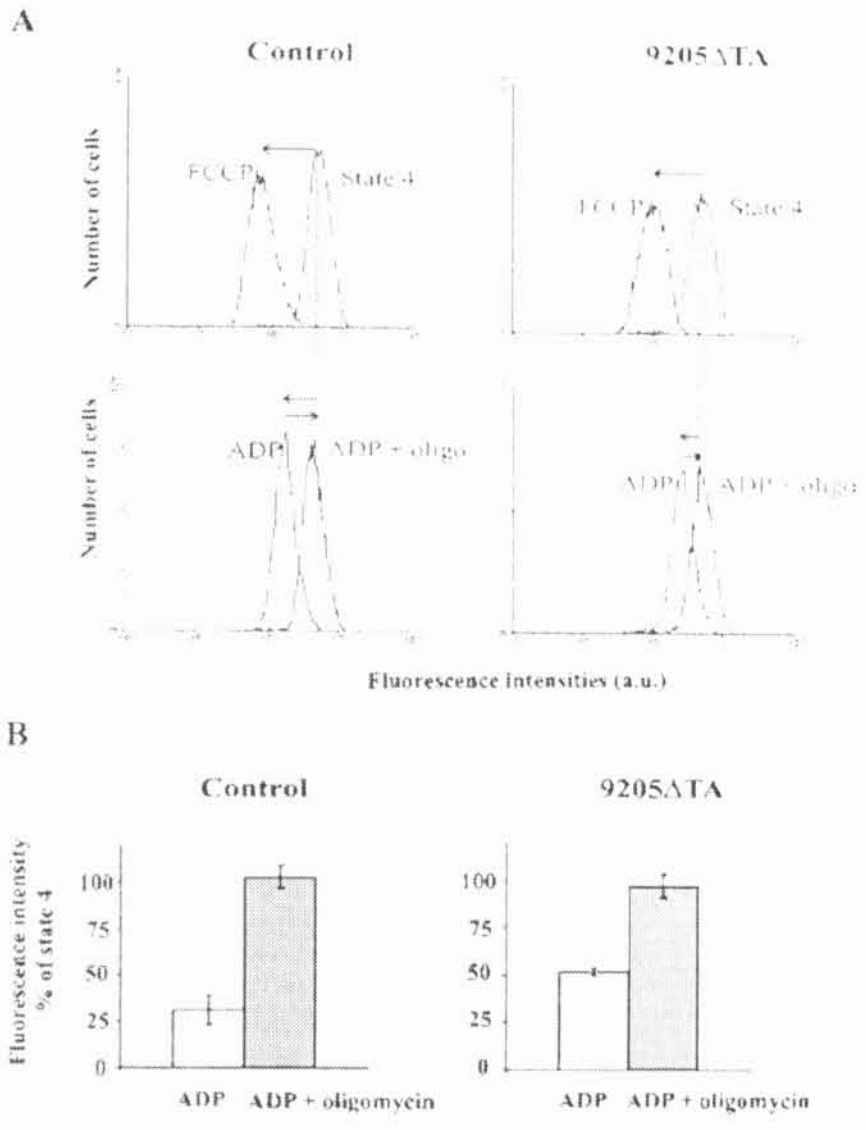

Figure 3 Cytofluorimetric analysis of control and 9205ΔTA fibroblasts

Cytofluorimetric analysis was performed in digitonin-treated fibroblasts (0.1 mg of digitonin/mg of protein) and stained with 20 nM TMRM in a KCl medium containing 10 mM succinate. (**A**) Typical reading of TMRM fluorescence at state 4 and effect of 1 μM FCCP is shown in the upper panels. Lower panels show the effect of 0.1 mM ADP and its sensitivity to 1 μM oligomycin (oligo). (**B**) TMRM fluorescence of state 3-ADP and effect of oligomycin is expressed as percentage of the state 4 signal. The $\Delta\Psi_m$-independent signal (after addition of FCCP) was subtracted from all data. The data represent means ± S.D. for four independent experiments.

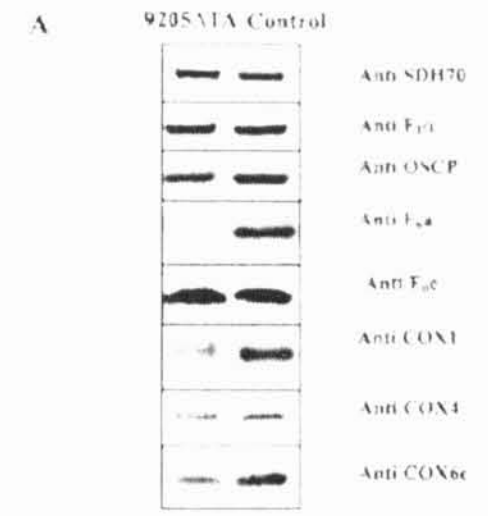

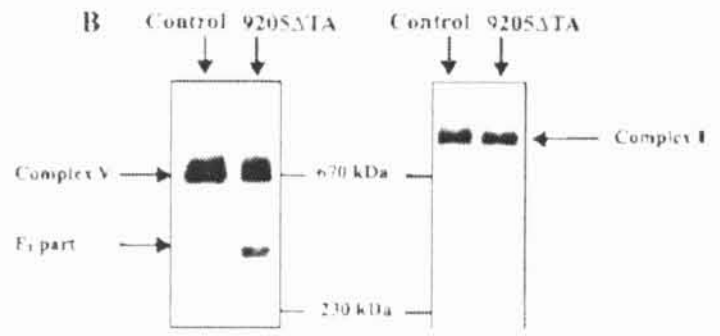

Figure 4 Electrophoretic analysis of OXPHOS complexes

(**A**) SDS/PAGE WB of ATPase, COX and SDH subunits was performed using aliquots of 7.5 μg of protein of mitochondria from control and 9205ΔTA cells. Detection was done with monoclonal antibodies against subunits SDH70, F-α, OSCP (oligomycin-sensitivity conferring protein), COX1, COX4 and COX6c, and with polyclonal antibodies against ATPase subunits F_0a and F_0c. (**B**) BN-PAGE WB with monoclonal antibody against F-α and NADH39 subunit was performed using 15 μg aliquots of protein solubilized using 1 g of DDM/g of protein from mitoplasts of control and 9205ΔTA cells. The migration of molecular mass standards is indicated.

Altered composition and increased lability of ATPase and COX

In order to assess the cellular content of ATPase and COX subunits, we analysed the mitochondrial proteins of isolated fibroblasts by SDS/PAGE and WB. It is clearly apparent from Figure 4(A) that 9205ΔTA fibroblasts had a selectively diminished content of ATPase subunit a and a significantly decreased content of COX subunits. In comparison with control cells, 9205ΔTA mitochondria contained 11 ± 5.9% of F_0 subunit a, 127 ± 13.0% of F_1 α subunit, 85% of OSCP (oligomycin-sensitivity-conferring protein), 108 ± 18.0% of F_0 subunit c, 47 ± 2.8% of COX1 subunit, 69 ± 8.5% of COX4 subunit and 36 ± 21.2% of COX6c subunit (average values of four experiments; data normalized to the content of the SDH 70 kDa subunit). The same pattern was obtained when analysing complete cell protein extracts (results not shown).

To resolve the native ATPase complex, we solubilized mitochondrial OXPHOS complexes from mitoplasts by DDM and analysed them by BN-PAGE and WB using an antibody against ATPase F_1 α subunit. As shown in Figure 4(B), in 9205ΔTA cells we found a decreased content of the full-size ATPase and the accumulation of an incomplete form of the ATPase with a molecular mass of approx. 390 kDa. A parallel WB analysis of complex I using an antibody to the NADH39 subunit showed an identical pattern in control and 9205ΔTA cells – we observed only intact complex with a molecular mass above 800 kDa (Figure 4B) that was present in the same amounts in 9205ΔTA and control cells.

2D electrophoretic analysis of ATPase and COX

Detailed analysis of the different forms of ATPase present in DDM-solubilized enzyme complexes was performed by 2D electrophoresis, whereby proteins resolved by BN-PAGE in the first dimension were separated by SDS/PAGE in the second dimension and detected by WB. The ATPase complex with an apparent molecular mass of approx. 620 kDa was significantly decreased in 9205ΔTA cells, but several other, smaller ATPase subcomplexes were detected by F_1 subunit α- and F_0 subunit c-immunoreactive signals (Figure 5A). In addition to the 390 kDa F_1 subcomplex containing the α subunit, which was present in the 9205ΔTA cells in increased amounts, a larger 460 kDa complex containing both subunits α and c was also found in the 9205ΔTA cells. Moreover, an additional, subunit c-containing complex with a molecular mass of approx. 120 kDa and a markedly increased amount of free subunit α (approx. 60 kDa) were seen. However, none of the above complexes showed a detectable reaction with an antibody against subunit a in the 9205ΔTA cells.

2D analysis of COX was performed using antibodies to COX1 and COX4 subunits (Figure 5B). A pronounced decrease in the amount of COX was observed in the DDM solubilizate of 9205ΔTA cells. In control cells, most of the COX was present as a monomer, but a significant amount of COX dimers (approx. 420–440 kDa) and small amounts of COX supercomplex (approx.

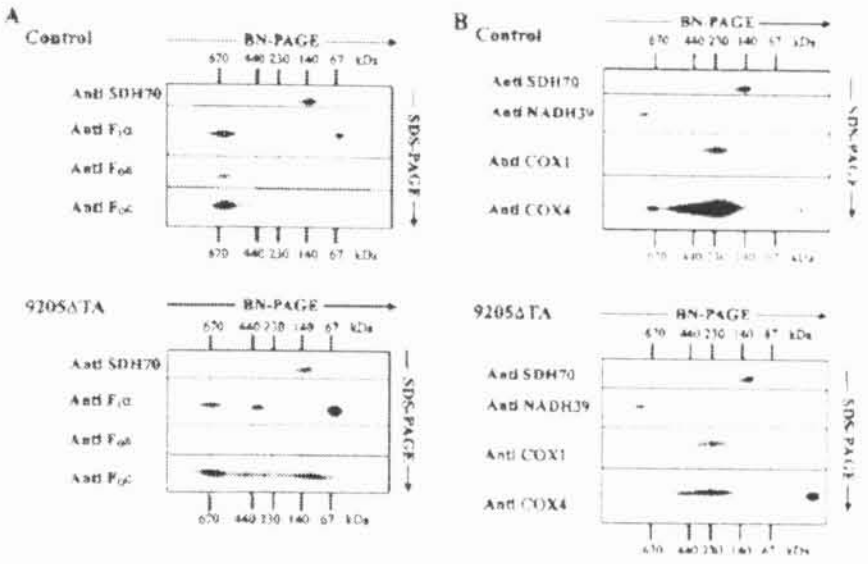

Figure 5 2D electrophoretic analysis and immunodetection of OXPHOS complexes

Aliquots (15 μg of protein) of DDM-solubilized mitoplasts from 9205ΔTA and control fibroblasts were separated in the first dimension by BN-PAGE and in the second dimension by SDS/PAGE. WB analysis was performed with an antibody against the SDH70 subunit and with antibodies (**A**) against ATPase subunits $F_1\alpha$, F_{o6} and F_{oC} or (**B**) against complex I subunit NADH39 and against COX subunits COX1 and COX4. The migration of molecular mass standards is indicated.

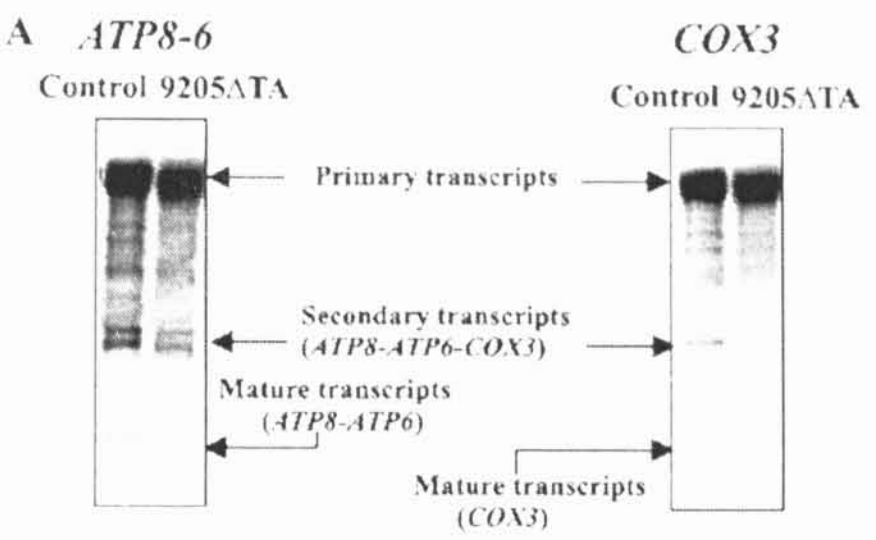

Figure 6 Northern blot analysis of ATP6 and COX3 transcripts

Northern blot analysis of COX3, ATP8–ATP6 and ND1 transcripts was performed in control and 9205 ΔTA cells. The mRNA species representing (**A**) the primary mtDNA polycistronic transcript, partially processed ATP8–ATP6–COX3 transcripts and mature COX3 and ATP8–ATP6 transcripts and (**B**) mature ND1 and ATP8–ATP6 transcripts are indicated.

670 kDa; probably COX-bc_1 supercomplex) as well as some monomeric COX4 subunits were clearly seen. In the 9205ΔTA cells the pattern was different. An additional band of molecular mass approx. 100 kDa was present, and the relative content of the free COX4 subunit was much higher (approx. 15-fold) than in control cells.

WB analysis of complex I on 2D gels using a monoclonal antibody to the NADH39 subunit showed no difference between control and 9205ΔTA cells. Only the full-size, assembled complex I was found, and was present in similar amounts in both types of cells. No assembly intermediates were detected. Similarly, no difference was found in the case of complex II using the anti-SDH70 antibody. Thus, unlike ATPase and COX, the biosynthesis and/or stability of complex I were not affected by the 9205ΔTA mutation.

Steady-state levels and processing of ATP6 and COX3 mRNAs

The 9205ΔTA microdeletion is situated between the genes *ATP6* and *COX3*, which are transcribed in one polycistronic transcript that is subsequently cleaved stepwise and polyadenylated into mature mRNA. Therefore we studied the steady-state levels and processing of ATP6 and COX3 mRNAs. Northern blot analysis using cDNA complementary to mtDNA sequences 8361–9060 and 9269–9912 as a probe was performed to determine whether the mutation disturbs the RNA processing of ATP6 and COX3 transcripts (Figure 6A). The primary, unprocessed, and the secondary ATP8–ATP6–COX3 transcripts occurred in both 9205ΔTA cells and control cells in similar amounts. The steady-state levels of processed COX3 and ATP8–ATP6 transcripts were decreased in 9205ΔTA cells. The relative values of the ATP8–ATP6/ATP8–ATP6–COX3 and COX3/ATP8–ATP6–COX3 RNA ratios revealed approx. 40% and 50% decreases respectively in ATP8–ATP6 and COX3 RNA levels. In parallel, we also determined the steady-state levels of the transcripts of two other genes encoded by mtDNA, i.e. *ND1* and *COX1*. We observed the same content of the mature ND1 transcript (Figure 6B) in control and 9205ΔTA cells. Similarly, there was no difference in the content of COX1 transcripts (results not shown).

These Northern blot data were fully confirmed by quantitative RT-PCR experiments (Figure 7). Using PCR products corresponding to *ATP6* (nt 8846–8994), *COX3* (nt 9267–9416) and the *ATP6–COX3* cleavage site (nt 9150–9299), we found that ATP6 as well as COX3 RNA levels were decreased 2–3-fold relative to those of the uncleaved polycistronic ATP8–ATP6–COX3 transcript. The decrease was also confirmed when relating ATP6 and COX3 RNA levels to *CYTB* and *ND1* expression (PCR product of 14804–14935 for *CYTB* and 3595–3644 for *ND1*). As also shown in Figure 7, similar results were obtained using cDNA prepared by oligo(dT) or random primers, indicating that polyadenylation is neither impaired nor affects transcript processing.

Specific decrease in the biosynthesis of ATPase subunit a

To assess how the 9205ΔTA mutation affects the biosynthesis of subunit a and other mtDNA-encoded proteins, [^{35}S]methionine labelling of proteins in 9205ΔTA cells was performed in the presence of emetine (an inhibitor of cytosolic proteosynthesis). The extent of labelling (Figure 8) was comparable in 9205ΔTA and control cells, and the pattern of labelled proteins was also similar, with two exceptions – markedly decreased labelling of a band of approx. 22 kDa and increased labelling of a band of approx. 12 kDa. The first band was identified as ATPase subunit a, based on WB analysis performed on the same gel with an antibody against subunit a (Figure 8), in accordance with the size and mobility of subunit a in this type of SDS/PAGE [37]. On the basis of its size, the second band was identified as ATPase subunit 8 (A6L). The COX3 subunit was weakly labelled in both types of

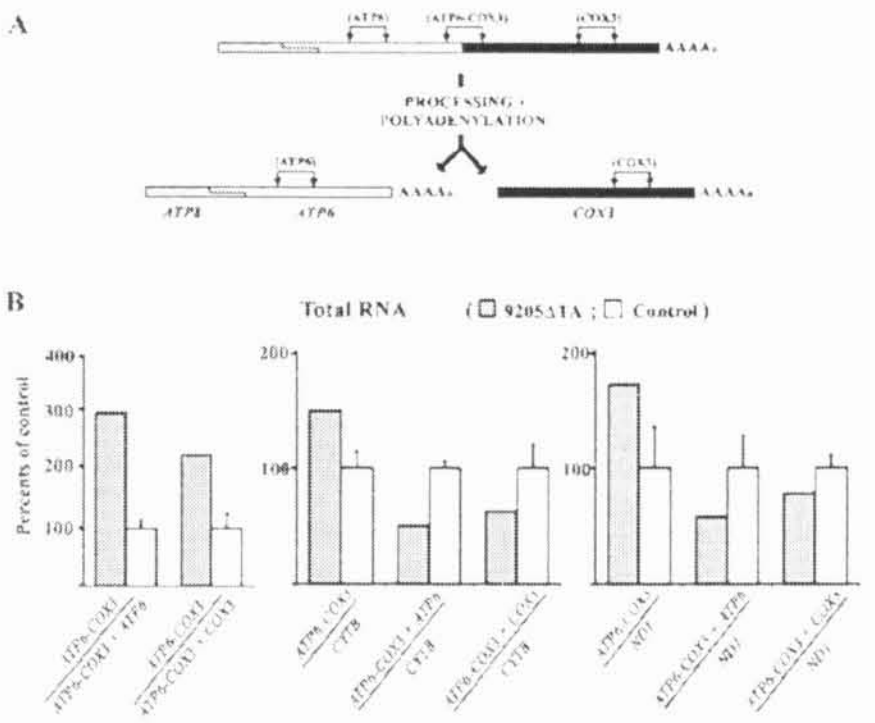

Figure 7 Quantitative real-time RT-PCR analysis of ATP6, COX3, cytochrome *b* and ND1 transcripts

(**A**) Scheme of ATP6–COX3 RNA processing and PCR products analysed. For experiments, cDNAs obtained from (**B**) total RNA (reverse transcription with random primers) or (**C**) mRNA (reverse transcription with oligo(dT) primers) were used. The relative amount of uncleaved ATP6–COX3 transcript and the amounts of all ATP6 or COX3 transcripts present either in unprocessed form or in mature form were measured and correlated. The values were also correlated to the expression of mitochondrial *CYTB* and *ND1* as reference genes. Graphs depict results obtained in 9205ΔTA fibroblasts expressed as a percentage of the mean ± S.D. for three controls.

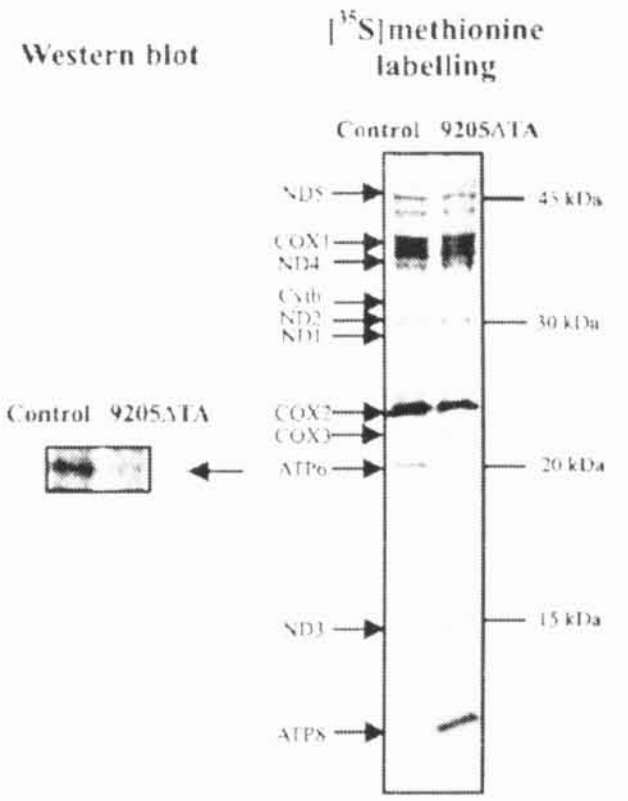

Figure 8 Incorporation of [^{35}S]methionine into proteins encoded by mtDNA

mtDNA-specific translation was performed in control and 9205ΔTA fibroblasts in the presence of emetine. Radioactive proteins were separated by SDS/PAGE on a 15–20% (w/v) gradient polyacrylamide gel and detected by phosphorimaging. On the left side, the WB from the same SDS/PAGE run using an antibody against subunit $F_1\alpha$ is shown. The migration of mtDNA-encoded polypeptides and of molecular mass standards is indicated.

cells, and no significant difference could be seen between the 9205ΔTA and control cells. Three independent experiments gave essentially the same result, and clearly showed, in accordance with all WB data, that mutation of the *ATP6* STOP codon greatly decreases the synthesis of ATPase subunit a (to 12.7 ± 0.73% of the control). In turn, up-regulation of ATP8 synthesis is apparent.

DISCUSSION

We present a detailed analysis of the impact of a maternally inherited 2 bp microdeletion TA at position 9205 and 9206 in the mtDNA (9205ΔTA) on the respiratory chain complexes, with the aim of disclosing the pathogenic mechanism in a patient with severe encephalomyopathy, spastic quadruparesis, microcephalia and hyperlactacidaemia.

Biochemically, the patient presented with a pronounced selective decrease in COX activity in his fibroblasts (15% of control), while a lowered COX/CS ratio and a mild decrease in complex III activity were found in muscle. Sequencing of mtDNA revealed a 2 bp microdeletion, which disrupts the STOP codon of the *ATP6* gene. This mutation has been described only once previously, in a patient with seizures and repetitive bouts of lactic acidaemia [13]. It was reported as being homoplasmic (lymphocytes and fibroblasts), but was not detected in that patient's mother or grandmother. In our patient, the mutation was also found to be homoplasmic (>98%) in all tissues tested. In addition, the heteroplasmic mutation 9205ΔTA was present in the asymptomatic mother (82%) and grandmother (16%). Importantly, a high mutation load in the mother's fibroblasts was also associated with a decrease in COX activity.

The mtDNA mutation 9205ΔTA lies on the boundary of two genes, *ATP6* and *COX3*, and it is highly probable that it influences the transcription and post-transcriptional modification of these genes. Assuming that this is the main cause of the patient's phenotype, insufficient energy provision is to be expected in the tissues, particularly in brain (explaining the dominating encephalopathy). Our measurements in the patient's fibroblasts showed a 3-fold decrease in mitochondrial ATP production. In fact, the observed decrease was even higher than that observed in cases of missense mutations in the *ATP6* gene (T9176G, T8993G and T8993C), where higher values of residual mitochondrial ATP production have been reported [10–12,38]. By analogy with these mutations, we found completely normal ATPase hydrolytic activity. Thus it appears that only a fraction of ATPase complexes can utilize $\Delta\Psi_m$ to drive ATP synthesis in 9205ΔTA cells. This view is further supported by the normal $\Delta\Psi_m$ observed at state 4 and its decrease by FCCP, while ADP (state 3-ADP) caused a much smaller decrease in $\Delta\Psi_m$ in the patient. These data indicate that mitochondria in 9205ΔTA cells can be fully energized and that the mutation does not enhance the passive H^+ transport at state 4 via the F_o proton channel of the ATPase complexes, which are known to contribute to the proton conductivity of the mitochondrial inner

membrane [39]. When, however, ADP becomes available, the discharge by ATP synthesis of $\Delta\Psi_m$ in 9205ΔTA cells is significantly decreased.

Our functional data support the view that the F_o part has an altered function in the majority of ATPase complexes of the patient's fibroblasts, due to the absence of subunit a (an essential component of the ATPase proton channel) or an alteration of its structure (for review, see [40]). The absence of the *ATP6* STOP codon could interfere with synthesis of the subunit by decreasing the translational efficacy of the ATP6 mRNA, resulting in a low amount of subunit a being produced and in the formation of ATPase complexes lacking subunit a and incapable of synthesizing ATP. Another possibility might be production of subunit a modified in the C-terminal part, as a poly(A) tail in the absence of a regular STOP codon could cause extension of several lysine residues at the C-terminus. Indeed, several amino acid residues involved in H^+ translocation are located in this part of the protein [8].

To delineate the subunit composition and native structure of ATPase, we employed electrophoretic/WB analysis using subunit-specific antibodies, including a polyclonal antibody against subunit a [23]. We have found that the content of subunit a is greatly decreased (to 11% of control) in the patient's fibroblasts, whereas other ATPase subunits are unchanged. The antibody was raised against 10 amino acids at the N-terminal part of human subunit a, and most probably would react with a putative form of subunit a elongated at the C-terminus. However, no larger forms of subunit a could be detected by WB. A low content of subunit a was confirmed by 9-fold decreased labelling of this subunit by [^{35}S]methionine, and the labelling pattern also did not indicate the accumulation of a larger form of this subunit in 9205ΔTA cells.

Under native electrophoretic conditions, we found in the 9205ΔTA cells a decreased content of DDM-solubilized, normal-sized F_1F_o-ATPase, together with an increased content of an F_1 subcomplex of 390 kDa. There was no apparent difference between the mobility of the 620 kDa ATPase complex in the 9205ΔTA and control samples; however, subunit a, present in the ATPase in one copy, represents only 4% of the total ATPase mass, and the expected difference in mobility of the whole, subunit a-lacking complex is below the resolution of BN-PAGE. Furthermore, we found yet another larger, F_1-containing subcomplex of 460 kDa that consists of F_1-ATPase and some F_o subunits, including subunit c. This pattern closely resembles that in cells with a T8993G mutation in the *ATP6* gene [10,12], or in cells with doxycycline-inhibited mitochondrial protein synthesis [3]. Interestingly, these three different mechanisms that affect the biosynthesis of subunit a gave a very similar picture at the level of ATPase structure. In the case of the 9205ΔTA mutation, the ATPase complexes exert lability upon DDM extraction that is not observed in those from control cells; however, even the subunit a-lacking ATPase complexes maintain structural interactions between the F_1 and F_o parts of the enzyme, although these are weaker. It appears that incomplete F_o is also able to 'gate' the F_1 in these complexes, as no H^+ leak has been detected by measurement of membrane potential.

In addition to changes in ATPase, we also found changes in the structure and function of COX. The pronounced decrease in COX activity observed in spectrophotometric assays was confirmed by the oxidation of TMPD + ascorbate in 9205ΔTA cells. The remaining COX activity, however, did not limit the generation of $\Delta\Psi_m$, and it was also sufficient for substrate oxidation in the uncoupled state. The functional consequences at the level of COX resembled to some extent COX assembly defects due to *SURF1* mutations [41]. The total amount of COX subunits detected by WB was also decreased, indicating a 30–50% decrease in enzyme content. Some of the COX complexes showed a normal size, but some COX subunits detected by 2D/WB analysis were found to be present in COX subcomplexes or as free subunits. The 2D pattern resembled the pattern observed in cells with a 15 bp deletion (9480Δ15) in *COX3* [37] that show a failure to assemble the holoenzyme complex and instability of the COX1–COX2 interaction [42].

When comparing the changes in ATPase and COX, it appears that 9205ΔTA cells contain approx. 10% of the control content of normal ATPase complexes and 30–50% of that of normal COX complexes. Both enzymes are present in mitochondria at normal, physiological conditions in excess in most tissues, and their threshold values are known to vary in individual cell types [43]. With regard to the dominating encephalopathy in our patient, it is interesting that the reserve capacity of COX appears to be rather high in brain, while the reserve capacity of ATPase appears to be much lower.

All of the data presented herein are in accordance with the hypothesis that the mechanism by which the 9205ΔTA mutation affects mitochondrial function is associated with changes in the transcription of the *ATP6* and *COX3* genes and their translational competence and efficacy. Using two independent approaches, i.e. Northern blot and quantitative real-time PCR analysis of cDNA, we found that processing of the primary ATP8–ATP6–COX3 transcript is impaired in our patient. Both methods revealed a 2–3-fold decrease in the content of mature ATP6 and COX3 transcripts, while the content of ND1 and COX1 transcripts was unaffected. The same picture emerged when analysing polyadenylated forms of ATP6 and COX3 RNAs. These differences found in the patient's cells were also confirmed when relating the steady-state levels of ATP6 and COX3 RNAs and mRNAs to the levels of CYTB or ND1 transcripts.

The decrease in the amount of the mature ATP6 transcript agreed well with the decreased synthesis and content of subunit a. Interestingly, the labelling of subunit 8 was increased, indicating up-regulated translation of the *ATP8* gene, which precedes and partially overlaps the *ATP6* gene. The translation of the ATP8 and ATP6 mRNAs is well described in yeast, but the structure of these genes and its regulation differs completely from that in mammalian mitochondria, where the mechanism of ATP8 and ATP6 biosynthesis is largely unknown. The question arises whether increased labelling of subunit 8 could be caused by translation of *ATP8* from an unspliced form of the ATP8–ATP6–COX3 transcript, part of which is, according to our results, polyadenylated [cDNA synthesis with random primers and oligo(dT) primer] and could be therefore subjected to translation.

Recently, Seneca and co-workers continued an analysis of the fibroblasts from the first patient identified with the 9205ΔTA deletion [18,44]. They investigated the levels and fate of ATP6 and COX3 mRNAs and did not find any difference in primary transcript processing in their patient, but some differences in the deadenylation of mRNAs were present. In the second paper they investigated the biochemical consequences of the mutation, and the only difference they found was an accumulation of the F_1-ATPase intermediate and increased ATP8 labelling. Therefore two patients with the same 9205ΔTA homoplasmic mutation differ dramatically, and this difference is difficult to understand. There appears to be a good correlation between changes in mature transcripts, pronounced biochemical consequences and severe encephalopathy in our patient, compared with unchanged RNA processing, insignificant biochemical changes and much weaker clinical presentation in the Seneca study. On the other hand, both patients harbour the same homoplasmic 9205ΔTA mutation. Thus in one case the mutation is pathogenic, and in the other it has little effect. We have no explanation for this difference at the

moment, but several aspects might be important. In both cases numerous other changes in mtDNA sequence were found. In our case all were identified as more or less frequent polymorphisms, one of which was present in the *ATP6* gene (A8860G) and one in the *COX3* gene (G9477A). In the Seneca case mtDNA sequencing revealed 42 changes from the revised Cambridge Reference Sequence, including three rare polymorphisms (C9335T, A11362G and A12822G) and two novel transitions (T15287C and T15705C) in the *CYTB* gene. The two types of mtDNA also belong to different haplogroups.

The question arises as to whether in the Seneca case the absence of pathogenicity might be due to some compensatory mechanism affecting the post-transcriptional processing and translation of the ATP6 and COX3 mRNAs. Two revertants have been described in human mtDNA, in cells carrying tRNA mutations. A suppressor mutation at position 12300 was found, generating $tRNA^{Leu}$ (CUN), which compensated for the 3243 (MELAS; mitochondrial encephalomyopathy, lactic acidosis and stroke-like episodes) mutation of $tRNA^{Leu}$ (UUR) [45]. In the second case, a G5703A mutation in $tRNA^{Asn}$ was functionally rescued without changes in mtDNA upon cultivation in a galactose medium [46]. A compensatory import of surrogate tRNA due to nuclear mutation was proposed, but not shown. Moreover, a similar compensatory import of RNAs or proteins is highly unlikely in 9205ΔTA cells.

A possible compensatory mechanism could be connected with factors that affect (and/or correct) the processing of mitochondrial transcripts and their translation in 9205ΔTA cells. Interestingly, several nuclear-encoded factors have been described in yeast (NCA2, NCA3, NAM1/MTF2, Aep3p) that are essential for proper processing of mitochondrial RNAs, namely the ATP8–ATP6 co-transcript (for references see [47]), but their mammalian orthologues have not been found, possibly reflecting differences in the structure of mitochondrial RNAs between yeast and mammals. Another group of factors is represented by proteins mediating the mRNA–ribosome interaction. The search for mammalian orthologues in this group was more successful. A LRPPRC (leucine-rich pentatricopeptide repeat cassette) protein was identified using a functional genomics approach [48], and it was shown that mutation in the *LRPPRC* gene causes the Leigh syndrome of French–Canadian type, which is a human mitochondrial COX deficiency [49]. However, the divergence of the LRPPRC protein sequence from that of the analogous yeast protein is very large and, therefore, it has not yet been possible to identify other mammalian proteins by a sequence similarity approach.

This work was supported by grants from the Grant Agency of the Ministry of Health of the Czech Republic (NR/7790-3, 8065-3), the Grant Agency of Charles University (GAUK 14/2004), the Grant Agency of the Czech Republic (303/03/0749) and by institutional projects (AVOZ5011922, VZ 111100003). The expert technical assistance of V. Fialova and V. Brozkova is gratefully acknowledged.

REFERENCES

1 Walker, J. E. and Collinson, I. R. (1994) The role of the stalk in the coupling mechanism of F_1F_0-ATPases. FEBS Lett. **346**, 39–43
2 Anderson, S., Bankier, A. T., Barrell, B. G., de Bruijn, M. H. L., Coulson, A. R., Drouin, J., Eperon, I. C., Nierlich, D. P., Roe, B. A., Sanger, F. et al. (1981) Sequence and organization of the human mitochondrial genome. Nature (London) **290**, 457–465
3 Nijtmans, L. G., Klement, P., Houstek, J. and van den Bogert, C. (1995) Assembly of mitochondrial ATP synthase in cultured human cells: implications for mitochondrial diseases. Biochim. Biophys. Acta **1272**, 190–198
4 DiMauro, S. and Schon, E. A. (2001) Mitochondrial DNA mutations in human disease. Am. J. Med. Genet. **106**, 18–26
5 Holt, I. J., Harding, A. E., Petty, R. K. H. and Morgan-Hughes, J. A. (1990) A new mitochondrial disease associated with mitochondrial DNA heteroplasmy. Am. J. Hum. Genet. **46**, 428–433
6 de Vries, D. D., van Engelen, B. G., Gabreels, F. J., Ruitenbeek, W. and van Oost, B. A. (1993) A second missense mutation in the mitochondrial ATPase 6 gene in Leigh's syndrome. Ann. Neurol. **34**, 410–412
7 Tatuch, Y., Christodoulou, J., Feigenbaum, A., Clarke, J. T., Wherret, J., Smith, C., Rudd, N., Petrova-Benedict, R. and Robinson, B. H. (1992) Heteroplasmic mtDNA mutation (T→G) at 8993 can cause Leigh disease when the percentage of abnormal mtDNA is high. Am. J. Hum. Genet. **50**, 852–858
8 Schon, E. A., Santra, S., Pallotti, F. and Girvin, M. E. (2001) Pathogenesis of primary defects in mitochondrial ATP synthesis. Semin. Cell Dev. Biol. **12**, 441–448
9 Tatuch, Y. and Robinson, B. H. (1993) The mitochondrial DNA mutation at 8993 associated with NARP slows the rate of ATP synthesis in isolated lymphoblast mitochondria. Biochem. Biophys. Res. Commun. **192**, 124–128
10 Houstek, J., Klement, P., Hermanska, J., Houstkova, H., Hansikova, H., van den Bogert, C. and Zeman, J. (1995) Altered properties of mitochondrial ATP-synthase in patients with a T→G mutation in the ATPase 6 (subunit a) gene at position 8993 of mtDNA. Biochim. Biophys. Acta **1271**, 349–357
11 Garcia, J. J., Ogilvie, I., Robinson, B. H. and Capaldi, R. A. (2000) Structure, functioning, and assembly of the ATP synthase in cells from patients with the T8993G mitochondrial DNA mutation. Comparison with the enzyme in Rho^0 cells completely lacking mtDNA. J. Biol. Chem. **275**, 11075–11081
12 Nijtmans, L. G., Henderson, N. S., Attardi, G. and Holt, I. J. (2001) Impaired ATP synthase assembly associated with a mutation in the human ATP synthase subunit 6 gene. J. Biol. Chem. **276**, 6755–6762
13 Seneca, S., Abramowicz, M., Lissens, W., Muller, M. F., Vamos, E. and de Meirleir, L. (1996) A mitochondrial DNA microdeletion in a newborn girl with transient lactic acidosis. J. Inherit. Metab. Dis. **19**, 115–118
14 Fornuskova, D., Tesarova, M., Hansikova, H. and Zeman, J. (2003) New mtDNA mutation 9204delTA in a family with mitochondrial encephalopathy and ATP synthase defect. Cas. Lek. Cesk. **142**, 313
15 Bentlage, H. A., Wendel, U., Schagger, H., ter Laak, H. J., Janssen, A. J. and Trijbels, J. M. (1996) Lethal infantile mitochondrial disease with isolated complex I deficiency in fibroblasts but with combined complex I and IV deficiencies in muscle. Neurology **47**, 243–248
16 Klement, P., Nijtmans, L. G., Van den Bogert, C. and Houstek, J. (1995) Analysis of oxidative phosphorylation complexes in cultured human fibroblasts and amniocytes by blue-native-electrophoresis using mitoplasts isolated with the help of digitonin. Anal. Biochem. **231**, 218–224
17 Makinen, M. and Lee, C. P. (1968) Biochemical studies of skeletal muscle mitochondria. I. Microanalysis of cytochrome content, oxidative and phosphorylative activities of mammalian skeletal muscle mitochondria. Arch. Biochem. Biophys. **126**, 75–82
18 Chrzanowska-Lightowlers, Z. M., Temperley, R. J., Smith, P. M., Seneca, S. H. and Lightowlers, R. N. (2004) Functional polypeptides can be synthesized from human mitochondrial transcripts lacking termination codons. Biochem. J. **377**, 725–731
19 Sambrook, J. and Russell, D. W. (2001) Molecular Cloning: A Laboratory Manual, 3rd edn., Cold Spring Harbor Laboratory Press, Cold Spring Harbor, NY
20 Schagger, H. and von Jagow, G. (1991) Blue native electrophoresis for isolation of membrane protein complexes in enzymatically active form. Anal. Biochem. **199**, 223–231
21 Schagger, H. and von Jagow, G. (1987) Tricine-sodium dodecyl sulfate-polyacrylamide gel electrophoresis for the separation of proteins in the range from 1 to 100 kDa. Anal. Biochem. **166**, 368–379
22 Houstek, J., Andersson, U., Tvrdik, P., Nedergaard, J. and Cannon, B. (1995) The expression of subunit c correlates with and thus may limit the biosynthesis of the mitochondrial F_0F_1-ATPase in brown adipose tissue. J. Biol. Chem. **270**, 7689–7694
23 Dubot, A., Godinot, C., Dumur, V., Sablonniere, B., Stojkovic, T., Cuisset, J. M., Vojtiskova, A., Pecina, P., Jesina, P. and Houstek, J. (2004) GUG is an efficient initiation codon to translate the human mitochondrial ATP6 gene. Biochem. Biophys. Res. Commun. **313**, 687–693
24 Moradi-Ameli, M. and Godinot, C. (1983) Characterization of monoclonal antibodies against mitochondrial F_1-ATPase. Proc. Natl. Acad. Sci. U.S.A. **80**, 6167–6171
25 Wharton, D. C. and Tzagoloff, A. (1967) Cytochrome oxidase from beef heart mitochondria. Methods Enzymol. **10**, 245–253
26 Rustin, P., Chretien, D., Bourgeron, T., Gerard, B., Rotig, A., Saudubray, J. M. and Munnich, A. (1994) Biochemical and molecular investigations in respiratory chain deficiencies. Clin. Chim. Acta **228**, 35–51
27 Fischer, J. C., Ruitenbeek, W., Trijbels, J. M. F., Veerkamp, J. H., Stadhouders, A. M., Sengers, R. C. A. and Janssen, A. J. M. (1985) Differential investigation of the capacity of succinate oxidation in human skeletal muscle. Clin. Chim. Acta **153**, 37–42
28 Fischer, J. C., Ruitenbeek, W., Trijbels, J. M. F., Veerkamp, J. H., Stadhouders, A. M., Sengers, R. C. A. and Janssen, A. J. M. (1986) Estimation of NADH oxidation in human skeletal muscle mitochondria. Clin. Chim. Acta **155**, 263–274

29 Chowdhury, S. K., Drahota, Z., Floryk, D., Calda, P. and Houstek, J. (2000) Activities of mitochondrial oxidative phosphorylation enzymes in cultured amniocytes. Clin. Chim. Acta **298**, 157–173
30 Baracca, A., Amler, E., Solaini, G., Parenti-Castelli, G., Lenaz, G. and Houstek, J. (1989) Temperature-induced states of isolated F_1-ATPase affect catalysis, enzyme conformation and high-affinity nucleotide binding sites. Biochim. Biophys. Acta **976**, 77–84
31 Pecina, P., Capkova, M., Chowdhury, S. K., Drahota, Z., Dubot, A., Vojtiskova, A., Hansikova, H., Houstkova, H., Zeman, J., Godinot, C. and Houstek, J. (2003) Functional alteration of cytochrome *c* oxidase by SURF1 mutations in Leigh syndrome. Biochim. Biophys. Acta **1639**, 53–63
32 Floryk, D. and Houstek, J. (1999) Tetramethyl rhodamine methyl ester (TMRM) is suitable for cytofluorometric measurements of mitochondrial membrane potential in cells treated with digitonin. Biosci. Rep. **19**, 27–34
33 Wanders, R. J. A., Ruiter, J. P. N., Wijburg, F. A., Zeman, J., Klement, P. and Houstek, J. (1996) Prenatal diagnosis of systemic disorders of the respiratory chain in cultured chorionic villus fibroblasts by study of ATP synthesis in digitonin-permeabilized cells. J. Inherit. Metab. Dis. **19**, 133–136
34 Dunabi, R., Boue-Grabot, M. and Mazat, J. P. (1998) Mitochondrial ATP synthesis in permeabilized cells: assessment of the ATP/O values *in situ*. Anal. Biochem. **263**, 169–175
35 Chomyn, A. (1996) *In vivo* labeling and analysis of human mitochondrial translation products. Methods Enzymol. **264**, 197–211
36 Plasek, J. and Sigler, K. (1996) Slow fluorescent indicators of membrane potential: a survey of different approaches to probe response analysis. J. Photochem. Photobiol. B **33**, 101–124
37 Hoffbuhr, K. C., Davidson, E., Filiano, B. A., Davidson, M., Kennaway, N. G. and King, M. P. (2000) A pathogenic 15-base pair deletion in mitochondrial DNA-encoded cytochrome *c* oxidase subunit III results in the absence of functional cytochrome *c* oxidase. J. Biol. Chem. **275**, 13994–14003
38 Carrozzo, R., Murray, J., Santorelli, F. M. and Capaldi, R. A. (2000) The T9176G mutation of human mtDNA gives a fully assembled but inactive ATP synthase when modeled in *Escherichia coli*. FEBS Lett. **486**, 297–299
39 Pansini, A., Guerrieri, F. and Papa, S. (1978) Control of proton conduction by the H^+-ATPase in the inner mitochondrial membrane. Eur. J. Biochem. **92**, 545–551
40 Hutcheon, M. L., Duncan, T. M., Ngai, H. and Cross, R. L. (2001) Energy-driven subunit rotation at the interface between subunit a and the c oligomer in the F_0 sector of *Escherichia coli* ATP synthase. Proc. Natl. Acad. Sci. U.S.A. **98**, 8519–8524
41 Buchet, K. and Godinot, C. (1998) Functional F_1-ATPase is essential in maintaining growth and membrane potential of human mitochondrial DNA-depleted rho degrees cells. J. Biol. Chem. **273**, 22983–22989
42 Shoubridge, E. A. (2001) Cytochrome *c* oxidase deficiency. Am. J. Med. Genet. **106**, 46–52
43 Rossignol, R., Faustin, B., Rocher, C., Malgat, M., Mazat, J. P. and Letellier, T. (2003) Mitochondrial threshold effects. Biochem. J. **370**, 751–762
44 Temperley, R. J., Seneca, S. H., Tonska, K., Bartnik, E., Bindoff, L. A., Lightowlers, R. N. and Chrzanowska-Lightowlers, Z. M. (2003) Investigation of a pathogenic mtDNA microdeletion reveals a translation-dependent deadenylation decay pathway in human mitochondria. Hum. Mol. Genet. **12**, 2341–2348
45 El Meziane, A., Lehtinen, S. K., Hance, N., Nijtmans, L. G., Dunbar, D., Holt, I. J. and Jacobs, H. T. (1998) A tRNA suppressor mutation in human mitochondria. Nat. Genet. **18**, 350–353
46 Hao, H., Morrison, L. E. and Moraes, C. T. (1999) Suppression of a mitochondrial tRNA gene mutation phenotype associated with changes in the nuclear background. Hum. Mol. Genet. **8**, 1117–1124
47 Ellis, T. P., Helfenbein, K. G., Tzagoloff, A. and Dieckmann, C. L. (2004) Aep3p stabilizes the mitochondrial bicistronic mRNA encoding subunits 6 and 8 of the H^+-translocating ATP synthase of *Saccharomyces cerevisiae*. J. Biol. Chem. **279**, 15728–15733
48 Mili, S. and Pinol-Roma, S. (2003) LRP130, a pentatricopeptide motif protein with a noncanonical RNA-binding domain, is bound *in vivo* to mitochondrial and nuclear RNAs. Mol. Cell. Biol. **23**, 4972–4982
49 Mootha, V. K., Lepage, P., Miller, K., Bunkenborg, J., Reich, M., Hjerrild, M., Delmonte, T., Villeneuve, A., Sladek, R., Xu, F. et al. (2003) Identification of a gene causing human cytochrome *c* oxidase deficiency by integrative genomics. Proc. Natl. Acad. Sci. U.S.A. **100**, 605–610

Received 12 March 2004/12 July 2004; accepted 21 July 2004
Published as BJ Immediate Publication 21 July 2004, DOI 10.1042/BJ20040407

Article 6

Available online at www.sciencedirect.com

SCIENCE DIRECT®

Biochimica et Biophysica Acta 1658 (2004) 115–121

BIOCHIMICA ET BIOPHYSICA ACTA
BBA

www.bba-direct.com

Review

Mitochondrial diseases and ATPase defects of nuclear origin

Josef Houštěk[a,*], Tomáš Mráček[a], Alena Vojtíšková[a], Jiří Zeman[b]

[a] *Institute of Physiology and Centre for Integrated Genomics, Academy of Sciences of the Czech Republic, Vídeňská 1083, CZ 142 20 Prague 4-Krc, Czech Republic*

[b] *Department of Pediatrics, 1st Faculty of Medicine, Charles University, Ke Karlovu 2, CZ 129 08, Prague, Czech Republic*

Received 11 March 2004; received in revised form 1 April 2004; accepted 20 April 2004
Available online 15 June 2004

Abstract

Dysfunctions of the F_1F_o-ATPase complex cause severe mitochondrial diseases affecting primarily the paediatric population. While in the maternally inherited ATPase defects due to mtDNA mutations in the *ATP6* gene the enzyme is structurally and functionally modified, in ATPase defects of nuclear origin mitochondria contain a decreased amount of otherwise normal enzyme. In this case biosynthesis of ATPase is down-regulated due to a block at the early stage of enzyme assembly – formation of the F_1 catalytic part. The pathogenetic mechanism implicates dysfunction of Atp12 or other F_1-specific assembly factors. For cellular energetics, however, the negative consequences may be quite similar irrespective of whether the ATPase dysfunction is of mitochondrial or nuclear origin.

Keywords: Mitochondrial disease; Cardiomyopathy; ATP synthase; Oxidative phosphorylation; Respiratory chain complex

1. Introduction

Last decade of bioenergetic research on mitochondrial diseases has uncovered an increasing number of human mitochondrial disorders that are caused by mutations in nuclear genes encoding the subunits of oxidative phosphorylation complexes (OXPHOS), or other proteins that are essential either for the biosynthesis of specific cofactors (such as heme) or assembly of heterooligomeric OXPHOS complexes from individual subunits (for review, see Ref. [1]). Up to now, numerous mutations in nuclear genes have been shown to cause a dysfunction of all mitochondrial respiratory chain complexes, NADH dehydrogenase (Complex I), succinate dehydrogenase (Complex II), bc_1 complex (Complex III), cytochrome *c* oxidase (Complex IV) and also F_1F_o-ATP synthase (ATPase, Complex V). Very often, these defects manifest rather early and affect paediatric population. Interestingly, the Complex I defects are mostly connected with mutations in genes encoding the subunits of the complex, while Complex IV and Complex III defects are caused by mutations in specific assembly proteins or biosynthetic factors. To the same category apparently belong the ATPase deficiencies of nuclear origin that are rather rare and biochemically manifest as a reduction of cellular content of ATPase complex that is otherwise structurally and functionally normal.

2. Selective defects of mitochondrial ATPase

Mitochondrial ATPase is the key enzyme of cellular energy conversion. ATPase uses the H^+ gradient generated by the respiratory chain as a driving force for the synthesis of ATP from ADP and phosphate. The mammalian ATPase complex is formed by 16 different subunits [2] and consists of the globular F_1 catalytic part connected by two stalks to the membrane-embedded F_o moiety, which translocates protons across the inner mitochondrial membrane. Two F_o subunits, subunit a (ATP6) and A6L (ATP8), are coded for by mitochondrial DNA (mtDNA) [3]; all other subunits are nuclearly encoded. Mitochondrial encephalomyopathies due to selective defects in mitochondrial ATPase are less frequent than the disorders of the respiratory chain complexes. They are mostly very severe and can be caused by

Abbreviations: OXPHOS, oxidative phosphorylation; ATPase, mitochondrial F_1F_o-ATP synthase; mtDNA, mitochondrial DNA

* Corresponding author. Tel.: +42-2-4106-2434; fax: +42-2-4106-2149.
E-mail address: houstek@biomed.cas.cz (J. Houštěk).

0005-2728/$ – see front matter © 2004 Elsevier B.V. All rights reserved.
doi:10.1016/j.bbabio.2004.04.012

mtDNA mutations as well as by mutations in nuclear genes.

3. *ATP6* mutations

All maternally inherited primary ATPase defects are associated with subunit a (see Ref. [4]), an essential component, together with multiple copies of the subunit c of the ATPase proton channel [5,6]. The *ATP6* gene is a hotspot of pathogenic mtDNA mutations affecting ATPase; no mutations have been found in the *ATP8* gene. *ATP6* mutations are mostly missense heteroplasmic mtDNA mutations affecting the protonophoric function of the subunit a. Higher prevalence show T8993G(C) mutations [7,8] which change Leu^{156} to Arg or Pro. At a lower mutation load they are manifested as a NARP syndrome (Neurogenic muscle weakness, Ataxia, Retinitis Pigmentosa), at heteroplasmy exceeding 90% they present as maternally inherited Leigh syndrome (severe and fatal encephalopathy). Less frequent are T9176G(C) mutations which change Leu^{217} [9,10] or a T8851G mutation [11] affecting Trp^{109}, both manifesting also as striatal necrosis syndromes (see Ref. [4]). Impairment of the ATPase H^+ channel by different *ATP6* mutations results often, but not always, in decreased ATP production, while the ATPase hydrolytic activity remains unchanged [12,13]. Mitochondria from T8993G cells are capable of ATP-dependent proton translocation [14] indicating that at least the vectorial proton transport by the enzyme from matrix to cytosol is unaffected. Increased lability of the ATPase complex, possibly due to altered assembly of subunit a, apparent as accumulation of incomplete ATPase assemblies, has been described in T8993G mutation [13,15]. Interestingly, these assembly intermediates could not be found in some other cases [16], which indicates that, similarly as in segregation of *ATP6* mutations [17], a different nuclear background and participation of putative regulatory factor(s) may be involved in their pathogenetic mechanism.

A completely different type of pathogenic mechanism is represented by homoplasmic mtDNA 2-bp microdeletion 9205delTA, so far found in two cases only [18,19]. This mutation removes the stop codon of the *ATP6* gene and affects the cleavage site between *ATP6* and *COXIII* transcripts. The biochemical and clinical presentations of these two cases are, however, strikingly different [20–22]. An involvement of some nuclear-encoded factor operating at the level of mitochondrial RNA processing is to be expected. Several proteins have been described in yeast (NCA2, NCA3, NAM1/MTF2, Aep3p) that are essential for proper processing of mitochondrial RNAs, namely of the *ATP8–ATP6* cotranscript (see Ref. [23]), but their mammalian orthologues were not found, possibly reflecting differences in the structure of mammalian mitochondrial RNAs that, in comparison with yeast, lack introns and 3- and 5-prime untranslated regions. Another group of factors involved in translation of mitochondrial RNAs is represented by proteins mediating mRNA–ribosome interactions. Search for mammalian orthologues in this group was more successful and an LRPPRC protein was identified using functional genomics approach [24]. It was shown that mutation in the *LRPPRC* gene causes the Leigh syndrome of French–Canadian type, which is a human mitochondrial COX deficiency [25]. Identification of additional mammalian factors specific for other mitochondrial transcripts can be foreseen.

4. ATPase defects of nuclear origin

ATPase defects due to a nuclear genome mutations where an alteration of mtDNA genes was excluded are characterised as selective decrease of ATPase content that is caused by diminished biosynthesis of the ATPase complex. An increasing number of cases diagnosed recently (Table 1) indicates that these defects may be more frequent than originally expected. ATPase deficiency of possible non-mitochondrial origin was first described in a child with 3-methylglutaconic aciduria and severe lactic acidosis [26]. An extremely low ATPase activity and low, tightly coupled, respiration rates were observed in muscle mitochondria, but no mutation was found in mtDNA genes encoding ATPase subunits. The nuclear origin of ATP synthase deficiency was demonstrated for the first time in 1999 [27] in a new type of fatal mitochondrial disorder. A child with severe lactic acidosis, cardiomyopathy and hepatomegaly died 2 days

Table 1
Patients with mitochondrial ATPase deficiency

Case	ATPase (%)	Onset/ survival	Biochemical data and phenotype	Reference
I	<10	neonate/15 months	LA, methylglutaconic aciduria, CM, developmental delay	[26]
IIa	<30	neonate/2 days	fatal LA, CM, hepatomegaly	[27]
IIb	<30	neonate/2 days	fatal LA, CM	
IIIa	<20	neonate/32 days	LA, CM, respiratory failure	[22]
IIIb	<30	neonate/3 years	LA, CM, short statute, failure to thrive, developmental delay	
IV	<30	neonate/8 years	LA, methylglutaconic aciduria, CM, developmental delay	[22]
V	<10	neonate/3 years	LA, CM, developmental delay	[28]
VI	<20	neonate/14 months	LA, methylglutaconic aciduria, dysmorphism, enlarged liver, marked brain atrophy	[29]
VII	<30	neonate/3 days	fatal LA, enlarged liver, small left ventricle, intracranial haemorrhage	[29]

LA—lactic acidosis, CM—cardiomyopathy.

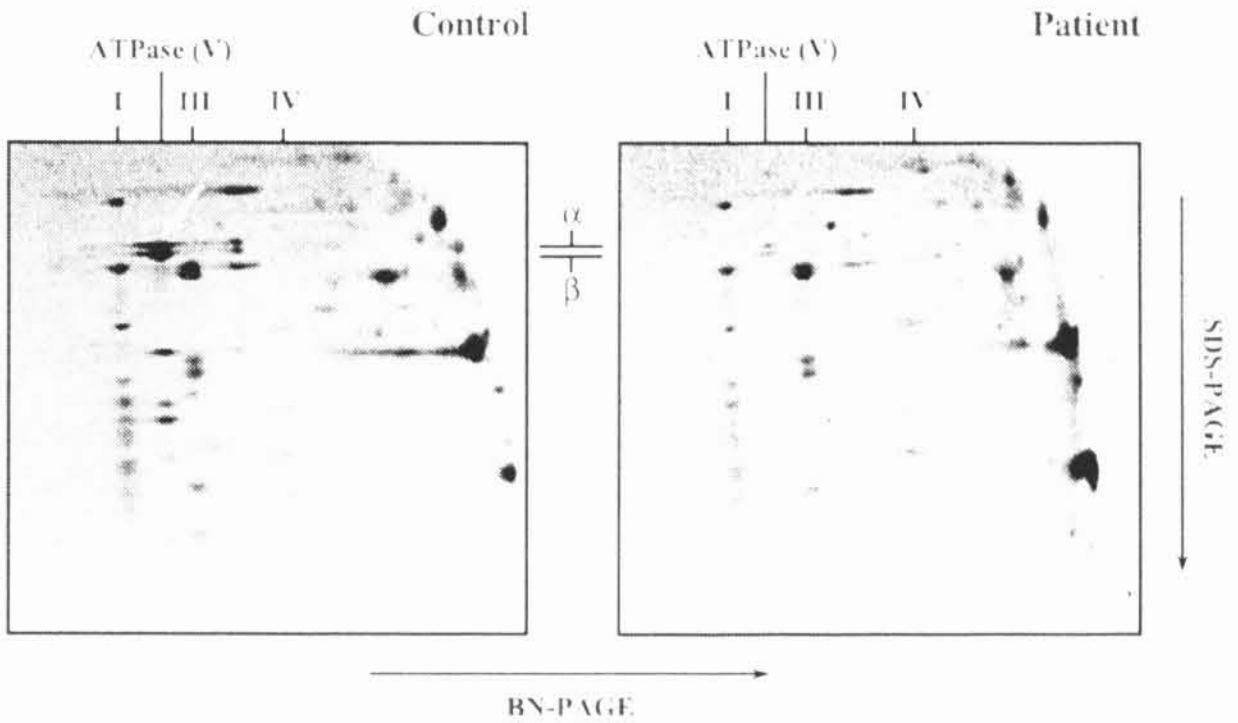

Fig. 1. OXPHOS complexes in a patient with ATPase deficiency. Blue-Native SDS two-dimensional electrophoresis was performed using laurylmaltoside-solubilised proteins from heart mitochondria from patient (IIa in Table 1) and control, the gel was stained with Coomassie blue. The position of ATPase complex and of respiratory chain complexes I, III and IV is indicated; white arrows point to α β F_1-ATPase subunits.

after birth. A generalised, 70–80% decrease in ATPase activity and ATP production was associated with corresponding selective decrease of the content of the ATPase complex, which had normal size and subunit composition (Fig. 1). Transmitochondrial cybrid cells made of patient's fibroblasts fully complemented the ATPase defect and confirmed the nuclear origin of impaired biogenesis of the enzyme complex [27]. Later on, two other similar cases of selective ATPase deficiency were found in the Czech Republic [22] and one in Austria [28]. Most recently, two patients with selective ATPase deficiency were described in Belgium [29]. In one of them, De Meirleir et al. located the pathogenic mutation in the *ATP12* gene for the first time (see further). As summarised in Table 1, most of the cases showed a reduction of ATPase content to <30% of the control, early onset of the disease, cardiomyopathy and survival of several days or weeks. Interestingly, methylglutaconic aciduria was found in several longer surviving patients. One of them showed a different phenotype of degenerative encephalopathy characterised by cortical and subcortical atrophy [29].

5. Altered biosynthesis of ATPase

The mechanism of ATPase biosynthesis is still not very well understood. The mammalian enzyme is expected to assemble stepwise (Fig. 2). Several transient assembly intermediates have been identified with initial formation of the F_1 catalytic part to which the nuclear encoded membrane sector subunits are added, followed by mtDNA-encoded subunits [30–32]. Native forms of ATPase can be easily revealed by Blue-Native electrophoresis [33] that became a very powerful approach to diagnostics of mitochondrial OXPHOS defects today. We have performed detailed studies on most of the diagnosed cases of selective ATPase deficiency and always found only a full-size ATPase complex to be present in cells and isolated mitochondria from the patient's tissues [27]. No accumulation of assembly intermediates analogous to subcomplexes observed in *ATP6* mutations or cells with doxycycline-inhibited translation of mitochondrial proteins [13,15,32] could be detected in fibroblasts with ATPase defects of nuclear origin. In [^{35}S]-methionine labelling experiments, decreased biosynthesis of the assembled ATPase has been found (Fig. 3). It contrasted with the increased biosynthesis of the β subunit of the F_1 catalytic part that had a very short half-life [27]. The cells also showed extramitochondrial accumulation of the β subunit, supporting the view that the biogenesis of ATPase is disturbed at an early stage when the F_1 catalytic part is formed.

6. F_1-ATPase assembly and affected nuclear factor(s)

The possible cause of insufficient ATPase biosynthesis can be a limited production or mutation of some of the

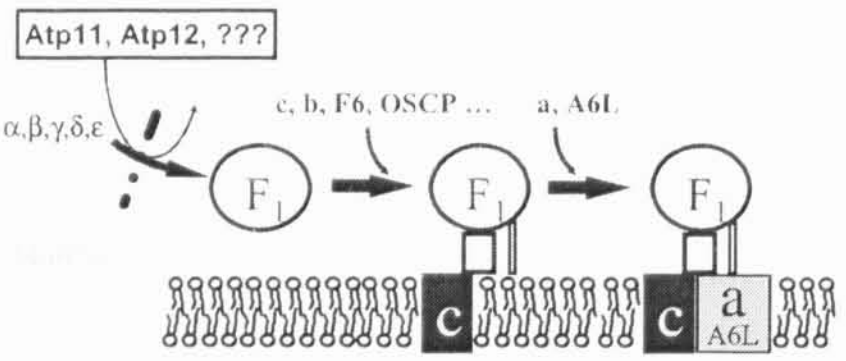

Fig. 2. ATPase assembly scheme.

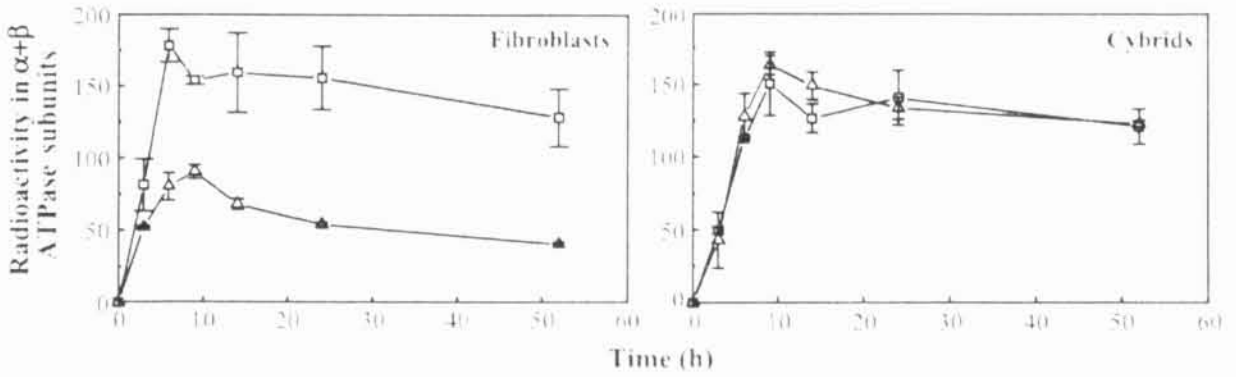

Fig. 3. Metabolic labelling of ATPase-deficient fibroblasts and derived transmitochondrial cybrids. Cells from patient (△) and control (□) were labelled for 3 h with [^{35}S]methionine, followed by 3–48-h chase with excess cold methionine. Aliquots of solubilised OXPHOS complexes were analysed by two-dimensional electrophoresis and radioactivity was determined by phosphorimaging (patient IIa in Table 1).

ATPase subunits. The cellular content of ATPase differs in mammalian tissues and it may vary also during ontogenetic development. Physiologically ATPase is down-regulated about 10-fold, relative to other OXPHOS complexes, in thermogenic brown fat where the electrochemical potential of proton gradient is dissipated in the form of heat by the uncoupling protein UCP1 [34]. Interestingly, the two-dimensional electrophoretic pattern of OXPHOS proteins in brown fat is almost identical with that found in patients with ATPase deficiency. In brown fat a selective transcriptional down-regulation of subunit *c* isogenes *P1* and *P2* and availability of the subunit c has been found as a limiting step for de novo synthesis of ATPase [35]. The transcriptional control of subunit c genes has been implicated in control of the cellular content of ATPase also in other mammalian tissues [36,37]. However, in ATPase-deficient patients expression of subunit c isogenes was normal or even increased [27] and the mRNA levels for other ATPase subunits did not show a significant decrease. As also sequencing of cDNAs of F_1 and F_0 subunits from patient cells was unable to detect any pathogenic mutation, the possible cause of the disease might be associated with a dysfunction of an ATPase-specific assembly factor.

Biosynthesis of eukaryotic ATPase is a highly ordered process, which involves several ATPase-specific assembly proteins. Studies in yeast identified five chaperone-type factors necessary for the assembly of the functional enzyme. Atp10p and Atp22p were found to mediate F_0 assembly [38,39] while Atp11p, Atp12p and Fmc1p are required for the F_1 part [40,41]. Fmc1p is essential at elevated growth temperatures but *FMC1* deletion could be rescued by overexpression of Atp12p [41]. Recently, human orthologues of Atp11p and Atp12p (Atpaf1p and Atpat2p according to new nomenclature) have also been identified. Like the yeast proteins, human Atp11p has chaperone-like activity toward the β subunit and human Atp12p interacts with the α subunit [42,43]. Expression of *ATP11* and *ATP12* in mammalian tissues is about two orders of magnitude lower than expression of genes for the corresponding F_1 subunits, in accordance with the chaperone function of these proteins. Interestingly, *ATP11* expression in mouse is nearly constant in all tissues, indicating that *ATP11* rather behaves like a maintenance gene. In contrast, *ATP12* expression differed up to 30-fold in different tissues and it was found to correlate well with mRNA levels of both F_1-α and F_1-β (BAT≫kidney, liver>-heart, brain>skeletal muscle), showing the highest mRNA level in the thermogenic, ATPase-poor brown adipose tissue [44].

The most recent molecular genetic studies by De Meirleir et al. [29] in two patients from Belgium with ATPase deficiency identified in one case the first mutation in *ATP12* (patient 6 in Table 1), which was homozygous TGG-AGG missense mutation in exon 3 changing Trp^{94} to Arg. No mutation in *ATP11* and *ATP12* was present in the second case. Similarly, we were unable to find any mutation in other cases that have been analysed (patients II–V in Table 1). Moreover, we were also unable to detect any decrease in *ATP11* and *ATP12* transcripts in these patients that would indicate their decreased content. Taken together, the available data suggest an involvement of another, yet unidentified ATPase assembly factor. This view might also be supported by the fact that the phenotype of the patient with *ATP12* mutation—marked brain atrophy, significantly differs from other patients presenting with cardiomyopathy (Table 1).

7. Biochemical changes in nuclear ATPase defects

Pronounced reduction of ATPase content in patient's fibroblasts strongly decreased the synthesis of ATP, ADP-stimulated respiration, and the discharge of mitochondrial membrane potential which showed even higher steady state values than the control cells [22,27,28]. However, even in cells with 90% decrease of ATPase content, a significant ATP production could be seen [28]. As apparent from inhibitor titration studies [45,46], individual OXPHOS enzymes of mitochondrial energy metabolism can be inhibited to a certain extent without noticeable reduction of the mitochondrial coupled respiration rate. These threshold effects are different for individual OXPHOS complexes and they also display tissue specificity. In the case of ATPase, some 10% of normal activity of the enzyme was found to be sufficient for 30–60% functionality of the whole respiratory chain, depending on the type of tissue. This would mean that, with respect of mitochondrial energy

provision, a significant decrease of ATPase capacity can be tolerated, at least under conditions when the energetic demands of the patient's organism are rather low.

For the pathogenetic mechanism of ATPase deficiency thus may be more relevant the mitochondrial ROS production related to the higher levels of $\Delta\Psi_m$, observed in patient's fibroblasts. An exponential increase of mitochondrial ROS production occurs at high levels of $\Delta\Psi_m$ above 140 mV [17,18]. On the contrary, decrease of $\Delta\Psi_m$ via stimulation of ATP synthase activity, a low ATP/ADP ratio, and substrate limitation or increased proton permeability due to external or internal uncoupling lower the amount of

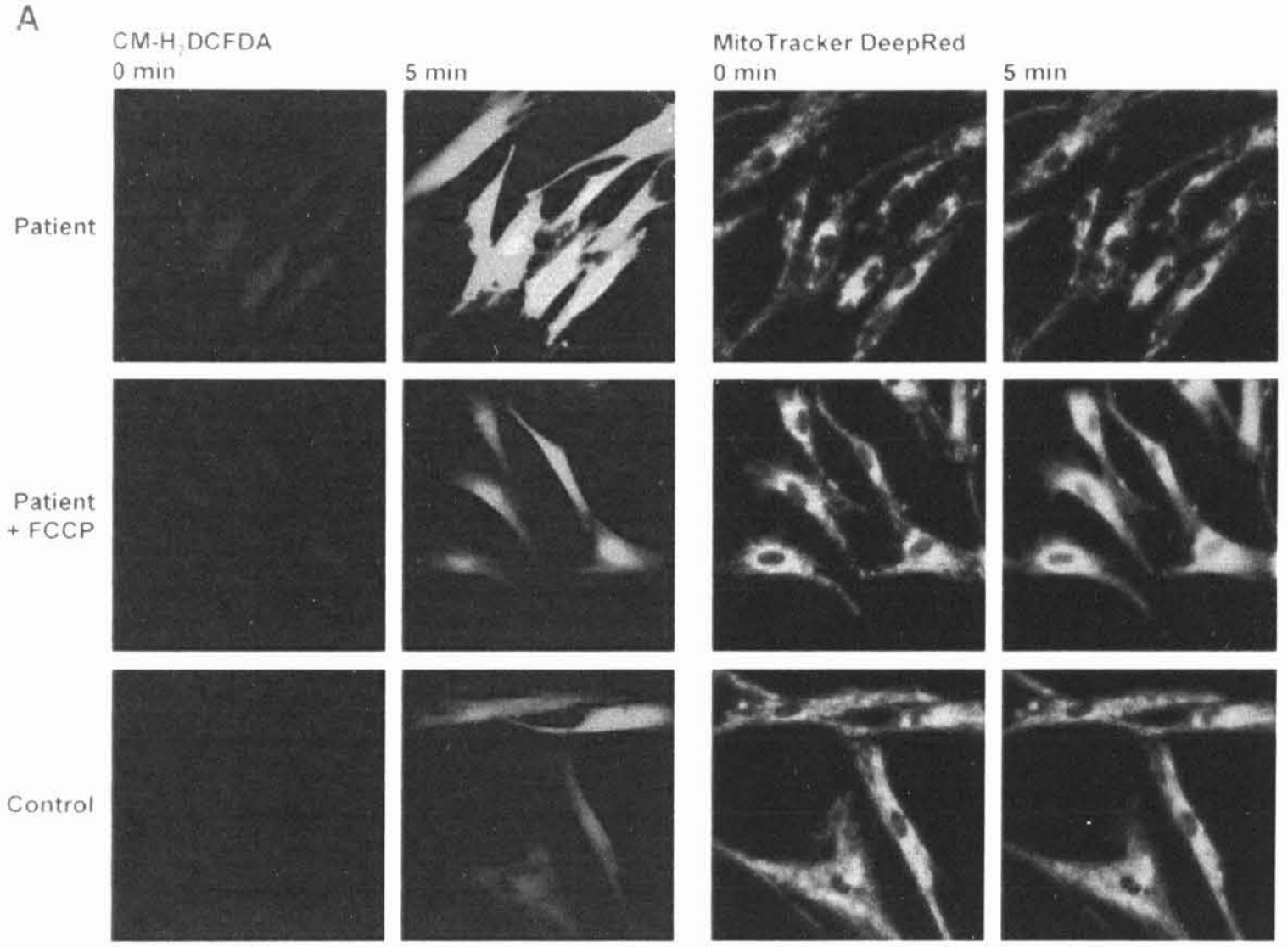

Fig. 4. ROS production analysed by confocal microscopy in ATPase-deficient cells. Intact fibroblasts (patient IV in Table 1) were labelled with 1 μM CM-H2DCFDA (5-(and-6)-chloromethyl-2′,7′-dichlorodihydrofluorescein diacetate) and 50 nM Mitotracker DeepRed and analysed on a Leica TCS SP2 microscope. (A) Increase in green fluorescence serves as a measure of ROS production in cell, as non-fluorescent CM-H2DCFDA is oxidized by ROS to fluorescent CM-DCFDA (fluorescent derivative). (B) Quantification of confocal images is shown. To compensate for mitochondrial content in patient and control cells, CM-DCFDA fluorescence was related to Mitotracker fluorescence.

ROS produced (see Ref. [49]). Our direct measurements in intact fibroblasts from patients with ATPase deficiency revealed pronounced activation of ROS production that was prevented by an uncoupler (Fig. 4). Interestingly, cells with *ATP6* mutations also show an altered discharge of $\Delta\Psi_m$ [22,50]. Therefore, it appears that the mitochondrial membrane potential is generally increased in both types of ATPase defects, irrespective of whether the inner mitochondrial membrane contains decreased amounts of normal ATPase complexes or normal content of altered ATPase complexes that are unable to operate as ATP synthase. In both situations, therefore, up-regulation of ROS production is to be expected to play a key role in the pathogenesis of the disease.

8. Conclusions

Involvement of nuclear genes in the pathogenesis of primary ATPase defects resulting in severe mitochondrial encephalo-cardiomyopathies may be rather complex. While selective ATPase deficiency is caused by a dysfunction of F_1-specific, nuclear-encoded assembly factor(s), other nuclear genes are likely to be involved in transmission and manifestation of mtDNA mutations in the *ATP6* gene that impair the function of the ATPase proton channel.

Acknowledgements

This work was supported by the Grant agency of the Ministry of Health of the Czech Republic (NR7790/3) and by institutional projects (AVOZ5011922, VZ 111100003).

References

[1] E.A. Shoubridge, Nuclear genetic defects of oxidative phosphorylation, Hum. Mol. Genet. 10 (2001) 2277–2284.
[2] J.E. Walker, I.R. Collinson, The role of the stalk in the coupling mechanism of F_1F_o-ATPases, FEBS Lett. 346 (1994) 39–43.
[3] S. Anderson, A.T. Bankier, B.G. Barrell, M.H.L. de Bruijn, A.R. Coulson, J. Drouin, I.C. Eperon, D.P. Nierlich, B.A. Roe, F. Sanger, P.H. Schreier, A.J.H. Smith, R. Staden, I.G. Young, Sequence and organization of the human mitochondrial genome, Nature 290 (1981) 457–465.
[4] E.A. Schon, S. Santra, F. Pallotti, M.E. Girvin, Pathogenesis of primary defects in mitochondrial ATP synthesis, Semin. Cell Dev. Biol. 12 (2001) 441–448.
[5] D. Stock, A.G. Leslie, J.E. Walker, Molecular architecture of the rotary motor in ATP synthase, Science 286 (1999) 1700–1705.
[6] M.L. Hutcheon, T.M. Duncan, H. Ngai, R.L. Cross, Energy-driven subunit rotation at the interface between subunit a and the c oligomer in the F(O) sector of *Escherichia coli* ATP synthase, Proc. Natl. Acad. Sci. U. S. A. 98 (2001) 8519–8524.
[7] I.J. Holt, A.E. Harding, R.K.H. Petty, J.A. Morgan-Hughes, A new mitochondrial disease associated with mitochondrial DNA heteroplasmy, Am. J. Hum. Genet. 46 (1990) 428–433.
[8] D.D. de Vries, B.G. van Engelen, F.J. Gabreels, W. Ruitenbeek, B.A. van Oost, A second missense mutation in the mitochondrial ATPase 6 gene in Leigh's syndrome, Ann. Neurol. 34 (1993) 410–412.
[9] D. Thyagarajan, S. Shanske, M. Vazquez Memije, D. De Vivo, S. DiMauro, A novel mitochondrial ATPase 6 point mutation in familial bilateral striatal necrosis, Ann. Neurol. 38 (1995) 468–472.
[10] R. Carrozzo, A. Tessa, M.F. Vazquez-Memije, F. Piemonte, C. Patrono, A. Malandrini, C. Dionisi-Vici, L. Vilarinho, M. Villanova, H. Schagger, A. Federico, E. Bertini, F.M. Santorelli, The T9176G mtDNA mutation severely affects ATP production and results in Leigh syndrome, Neurology 56 (2001) 687–690.
[11] L. De Meirleir, S. Seneca, W. Lissens, E. Schoentjes, B. Desprechins, Bilateral striatal necrosis with a novel point mutation in the mitochondrial ATPase 6 gene, Pediatr. Neurol. 13 (1995) 242–246.
[12] Y. Tatuch, B.H. Robinson, The mitochondrial DNA mutation at 8993 associated with NARP slows the rate of ATP synthesis in isolated lymphoblast mitochondria, Biochem. Biophys. Res. Commun. 192 (1993) 124–128.
[13] J. Houstek, P. Klement, J. Hermanska, H. Houstkova, H. Hansikova, C. van den Bogert, J. Zeman, Altered properties of mitochondrial ATP-synthase in patients with a T→G mutation in the ATPase 6 (subunit a) gene at position 8993 of mtDNA, Biochim. Biophys. Acta 1271 (1995) 349–357.
[14] A. Baracca, S. Barogi, V. Carelli, G. Lenaz, G. Solaini, Catalytic activities of mitochondrial ATP synthase in patients with mitochondrial DNA T8993G mutation in the ATPase 6 gene encoding subunit a, J. Biol. Chem. 275 (2000) 4177–4182.
[15] L.G. Nijtmans, N.S. Henderson, G. Attardi, I.J. Holt, Impaired ATP synthase assembly associated with a mutation in the human ATP synthase subunit 6 gene, J. Biol. Chem. 276 (2001) 6755–6762.
[16] J.J. Garcia, I. Ogilvie, B.H. Robinson, R.A. Capaldi, Structure, functioning, and assembly of the ATP synthase in cells from patients with the T8993G mitochondrial DNA mutation. Comparison with the enzyme in Rho(0) cells completely lacking mtDNA, J. Biol. Chem. 275 (2000) 11075–11081.
[17] L. Vergani, R. Rossi, C.H. Brierley, M. Hanna, I.J. Holt, Introduction of heteroplasmic mitochondrial DNA (mtDNA) from a patient with NARP into two human rho degrees cell lines is associated either with selection and maintenance of NARP mutant mtDNA or failure to maintain mtDNA, Hum. Mol. Genet. 8 (1999) 1751–1755.
[18] S. Seneca, M. Abramowicz, W. Lissens, M.F. Muller, E. Vamos, L. de Meirleir, A mitochondrial DNA microdeletion in a newborn girl with transient lactic acidosis, J. Inherit. Metab. Dis. 19 (1996) 115–118.
[19] D. Fornuskova, M. Tesarova, H. Hansikova, J. Zeman, New mtDNA mutation 9204delTA in a family with mitochondrial encephalopathy and ATPsynthase defect, Cas. Lek. Ces. 142 (2003) 313.
[20] R.J. Temperley, S.H. Seneca, K. Tonska, E. Bartnik, L.A. Bindoff, R.N. Lightowlers, Z.M. Chrzanowska-Lightowlers, Investigation of a pathogenic mtDNA microdeletion reveals a translation-dependent deadenylation decay pathway in human mitochondria, Hum. Mol. Genet. 12 (2003) 2341–2348.
[21] Z.M. Chrzanowska-Lightowlers, R.J. Temperley, P.M. Smith, S.H. Seneca, R.N. Lightowlers, Functional polypeptides can be synthesized from human mitochondrial transcripts lacking termination codons, Biochem. J. 377 (2004) 725–731.
[22] A. Vojtiskova, P. Jesina, M. Tesarova, M. Kalous, A. Dubot, C. Godinot, D. Fornuskova, V. Kaplanova, J. Zeman, J. Houstek, Mitochondrial membrane potential and ATP production in primary disorders of ATP synthase, Toxicol. Mech. Methods 14 (2004) 7–11.
[23] T.P. Ellis, K.G. Helfenbein, A. Tzagoloff, C.L. Dieckmann, Aep3p stabilizes the mitochondrial bicistronic mRNA encoding subunits 6 and 8 of the H^+-translocating ATP synthase of Saccharomyces cerevisiae, J. Biol. Chem. 279 (2004) 15728–15733.
[24] S. Mili, S. Pinol-Roma, LRP130, a pentatricopeptide motif protein with a noncanonical RNA-binding domain, is bound in vivo to mitochondrial and nuclear RNAs, Mol. Cell. Biol. 23 (2003) 4972–4982.
[25] V.K. Mootha, P. Lepage, K. Miller, J. Bunkenborg, M. Reich, M. Hjerrild, T. Delmonte, A. Villeneuve, R. Sladek, F. Xu, G.A.

Mitchell, C. Morin, M. Mann, T.J. Hudson, B. Robinson, J.D. Rioux, E.S. Lander, Identification of a gene causing human cytochrome *c* oxidase deficiency by integrative genomics, Proc. Natl. Acad. Sci. U. S. A. 100 (2003) 605–610.

[26] E. Holme, J. Greter, C.E. Jacobson, N.G. Larsson, S. Lindstedt, K.O. Nilsson, A. Oldfors, M. Tulinius, Mitochondrial ATP-synthase deficiency in a child with 3-methylglutaconic aciduria, J. Med. Genet. 32 (1992) 731–735.

[27] J. Houstek, P. Klement, D. Floryk, H. Antonicka, J. Hermanska, M. Kalous, H. Hansikova, H. Houstkova, S.K. Chowdhury, T. Rosipal, S. Kmoch, L. Stratilova, J. Zeman, A novel deficiency of mitochondrial ATPase of nuclear origin, Hum. Mol. Genet. 8 (1999) 1967–1974.

[28] J.A. Mayr, J. Paul, P. Pecina, P. Kurnik, H. Förster, U. Fötschl, W. Sperl, J. Houstek, Reduced respiratory control with ADP and changed pattern of respiratory chain enzymes due to selective deficiency of the mitochondrial ATP synthase, J. Med. Genet. 55 (2004) 1–7.

[29] L. De Meirleir, S. Seneca, W. Lissens, I. De Clercq, F. Eyskens, E. Gerlo, J. Smet, R. Van Coster, Respiratory chain complex V deficiency due to a mutation in the assembly gene ATP12, J. Med. Genet. 41 (2004) 120–124.

[30] P. Nagley, Eukaryote membrane genetics: the F_0 sector of mitochondrial ATP synthase, Trends Genet. 4 (1988) 46–52.

[31] R.G. Hadikusumo, S. Meltzer, W.M. Choo, M.J.B. Jean-Francois, A.W. Linnane, S. Marzuki, The definition of mitochondrial H^+ ATPase assembly defects in mit$^-$ mutants of *Saccharomyces cerevisiae* with a monoclonal antibody to the enzyme complex as an assembly probe, Biochim. Biophys. Acta 933 (1988) 212–222.

[32] L.G. Nijtmans, P. Klement, J. Houstek, C. van den Bogert, Assembly of mitochondrial ATP synthase in cultured human cells: implications for mitochondrial diseases, Biochim. Biophys. Acta 1272 (1995) 190–198.

[33] H. Schagger, G. von Jagow, Blue native electrophoresis for isolation of membrane protein complexes in enzymatically active form, Anal. Biochem. 199 (1991) 223–231.

[34] J. Houstek, J. Kopecky, M. Baudysova, D. Janikova, S. Pavelka, P. Klement, Differentiation of brown adipose tissue and biogenesis of thermogenic mitochondria in situ and in cell culture, Biochim. Biophys. Acta 1018 (1990) 243–247.

[35] J. Houstek, U. Andersson, P. Tvrdik, J. Nedergaard, B. Cannon, The expression of subunit c correlates with and thus may limit the biosynthesis of the mitochondrial F_0F_1-ATPase in brown adipose tissue, J. Biol. Chem. 270 (1995) 7689–7694.

[36] U. Andersson, J. Houstek, B. Cannon, ATP synthase subunit c expression: physiological regulation of the P1 and P2 genes, Biochem. J. 323 (1997) 379–385.

[37] H. Sangawa, T. Himeda, H. Shibata, T. Higuti, Gene expression of subunit c(P1), subunit c(P2), and oligomycin sensitivity-conferring protein may play a key role in biogenesis of H^+-ATP synthase in various rat tissues, J. Biol. Chem. 272 (1997) 6034–6037.

[38] S.H. Ackerman, A. Tzagoloff, ATP10, a yeast nuclear gene required for the assembly of the mitochondrial F_1–F_0 complex, J. Biol. Chem. 265 (1990) 9952–9959.

[39] K.G. Helfenbein, T.P. Ellis, C.L. Dieckmann, A. Tzagoloff, ATP22, a nuclear gene required for expression of the F_0 sector of mitochondrial ATPase in Saccharomyces cerevisiae, J. Biol. Chem. 278 (2003) 19751–19756.

[40] S.H. Ackerman, A. Tzagoloff, Identification of two nuclear genes (ATP11, ATP12) required for assembly of the yeast F_1-ATPase, Proc. Natl. Acad. Sci. U. S. A. 87 (1990) 4986–4990.

[41] L. Lefebvre-Legendre, J. Vaillier, H. Benabdelhak, J. Velours, P.P. Slonimski, J.P. di Rago, Identification of a nuclear gene (FMC1) required for the assembly/stability of yeast mitochondrial F(1)-ATPase in heat stress conditions, J. Biol. Chem. 276 (2001) 6789–6796.

[42] Z.G. Wang, P.S. White, S.H. Ackerman, Atp11p and Atp12p are assembly factors for the F(1)-ATPase in human mitochondria, J. Biol. Chem. 276 (2001) 30773–30778.

[43] A. Hinton, D.L. Gatti, S.H. Ackerman, The molecular chaperone, Atp12p, from Homo sapiens: in vitro studies with purified wild type and mutant (E240K) proteins, J. Biol. Chem. 279 (2004) 9016–9022.

[44] A. Pickova, J. Paul, V. Petruzzella, J. Houstek, Differential expression of ATPAF1 and ATPAF2 genes encoding F1-ATPase assembly proteins in mouse tissues, FEBS Lett. 551 (2003) 42–46.

[45] R. Rossignol, M. Malgat, J.P. Mazat, T. Letellier, Threshold effect and tissue specificity. Implication for mitochondrial cytopathies, J. Biol. Chem. 274 (1999) 33426–33432.

[46] R. Rossignol, B. Faustin, C. Rocher, M. Malgat, J.P. Mazat, T. Letellier, Mitochondrial threshold effects, Biochem. J. 370 (2003) 751–762.

[47] S.S. Liu, Cooperation of a "reactive oxygen cycle" with the Q cycle and the proton cycle in the respiratory chain-superoxide generating and cycling mechanisms in mitochondria, J. Bioenerg. Biomembranes 31 (1999) 367–376.

[48] S.S. Korshunov, V.P. Skulachev, A.A. Starkov, High protonic potential actuates a mechanism of production of reactive oxygen species in mitochondria, FEBS Lett. 416 (1997) 15–18.

[49] B. Kadenbach, Intrinsic and extrinsic uncoupling of oxidative phosphorylation, Biochim. Biophys. Acta 1604 (2003) 77–94.

[50] A. Dubot, C. Godinot, V. Dumur, B. Sablonniere, T. Stojkovic, J.M. Cuisset, A. Vojtiskova, P. Pecina, P. Jesina, J. Houstek, GUG is an efficient initiation codon to translate the human mitochondrial ATP6 gene, Biochem. Biophys. Res. Commun. 313 (2004) 687–693.

Article 7

Carcinogenesis vol.26 no.3 pp.531–539, 2005
doi:10.1093/carcin/bgi001

A new role for the von Hippel-Lindau tumor suppressor protein: stimulation of mitochondrial oxidative phosphorylation complex biogenesis

Eric Hervouet[1], Jocelyne Demont[1], Petr Pecina[2], Alena Vojtísková[2], Josef Houstek[2], Hélène Simonnet[1] and Catherine Godinot[1,3]

[1]Centre de Génétique Moléculaire et Cellulaire, UMR 5534, Centre National de la Recherche Scientifique—Université Claude Bernard de Lyon 1, F-69622 Villeurbanne, France and [2]Institute of Physiology and Centre for Integrated Genomics, Academy of Sciences of the Czech Republic, Vídeňská 1083, 142 20 Prague, Czech Republic
[3]To whom correspondence should be addressed
Email: godinot@univ-lyon1.fr

Although mitochondrial deficiency in cancer has been described by Warburg, many years ago, the mechanisms underlying this impairment remain essentially unknown. Many types of cancer cells are concerned and, in particular, clear cell renal carcinoma (CCRC). In this cancer, the tumor suppressor gene, *VHL* (von Hippel-Lindau factor) is invalidated. Previous studies have shown that the transfection of the *VHL* gene in *VHL*-deficient cells originating from CCRCs could suppress their ability to form tumors when they were injected into nude mice. However, various additional genetic alterations are observed in such cancer cells. In order to investigate whether *VHL* invalidation was related to the mitochondrial impairment, we have studied the effects of wild-type *VHL* transfection into *VHL*-deficient 786-0 or RCC10 cells on their oxidative phosphorylation (OXPHOS) subunit contents and functions. We show that the presence of wild-type VHL protein (pVHL) increased mitochondrial DNA and respiratory chain protein contents and permitted the cells to rely on their mitochondrial ATP production to grow in the absence of glucose. In parallel to mtDNA increase, the presence of pVHL up regulated the mitochondrial transcription factor A, as shown by western blot analysis. In conclusion, in CCRCs, pVHL deficiency is one of the factors responsible for down-regulation of the biogenesis of OXPHOS complexes.

Introduction

Clear cell renal carcinomas (CCRC) are the most common renal malignancy and represent >70% of kidney cancers. These cancers are characterized by bi-allelic inactivation of the von Hippel-Lindau (*VHL*) tumor suppressor gene, located at the level of the chromosome 3 short arm, at locus 3p25-26 (1–3). von Hippel-Lindau protein (pVHL) forms a complex with several proteins including elongins C and B, Cul2 and Rbx1 (also called Rox1 or Hrt1) (3). This complex displays E3 ubiquitin ligase activity that targets the alpha subunit of the heterodimeric transcription factor HIF (hypoxia-inducible factor) for ubiquitinylation, leading to its rapid proteasomal destruction (4). Three human HIFα proteins: HIF1α, HIF2α and HIF3α have been described. In the presence of oxygen, the HIFα chains are poly-hydroxylated on conserved prolyl and arginyl residues by oxygen-dependent prolyl (5–7) and arginyl hydroxylases (8). Once hydroxylated, the HIFα proteins bind to the pVHL complex to be ubiquitinylated (see review in ref. 9). Under low oxygen conditions (hypoxia, ischemia), hydroxylation is reduced and the stabilized HIFα chains accumulate in the nucleus where they form a complex with the constitutively expressed HIFβ. The latter complex can activate the transcription of >40 genes whose protein products play crucial roles in cellular adaptation to a low oxygen environment (10). It increases the synthesis of erythropoietin, of vascular endothelial growth factor, of glucose transporters and glycolytic enzymes in order to maintain ATP production despite the low efficiency of anaerobic metabolism compared with oxidative metabolism (11). It also shifts the balance between pro- and anti-apoptotic factors to promote their survival, favors cell proliferation (tumor growth factorα and TGFβ), stimulates synthesis of genes involved in iron regulation, in proteolysis (metalloproteinase) (12) or else in acid–base controlling metabolic pathways (carbonic anhydrase IX) (13). In cells lacking wild-type pVHL, these genes are constitutively expressed and contribute to tumor proliferation.

Recent studies in our laboratory (14) have shown that in CCRCs, the expression of most proteins involved in oxidative phosphorylation (OXPHOS) is strongly decreased while, in renal oncocytoma, OXPHOS complex proteins are all increased except those of complex I (15). Similarly, Cuezva *et al.* have shown that in CCRCs as well as in cancers from other tissues, a decreased bioenergetic function of mitochondria is associated with an increased glycolytic rate in accordance with the Warburg hypothesis (16). For example, the expression of the β subunit of the mitochondrial H^+-ATP synthase was found to be depressed in liver, kidney and colon carcinomas (17) or in lung, breast, esophagus or stomach cancers (18) while glycolytic markers were increased. This bioenergetic deficiency was the highest in patients with a poor prognosis. The glycolytic phenotype is well recognized in many cancer cells (19,20) but the mechanism by which mitochondrial deficiencies may be related to tumor development is poorly understood (21). It depends on the cancer type, as carcinogenesis in the liver involves a depletion of the whole cellular mitochondrial content whereas in kidney and colon carcinomas, OXPHOS subunits are more specifically reduced (17). As mentioned above, the up-regulation of glycolytic enzymes in renal carcinomas is due to the well-documented transcriptional activation of glycolytic enzymes by HIF in *VHL*-deficient cells after binding of HIF on hypoxia-responsive element sites

Abbreviations: CCRC, clear cell renal carcinoma; COX, cytochrome *c* oxidase; FCCP, carbonyl cyanide 4-trifluoromethoxyphenylhydrazone; HIF, hypoxia inducible factor; mtDNA, mitochondrial DNA; NRF_1 and NRF_2, nuclear respiratory factor 1 and 2; OXPHOS, oxidative phosphorylation; PGC1, peroxisome proliferator-activated receptor γ (PPAR-γ) coactivator 1; PRC, PGC1 regulated co-activator 1; pVHL, von Hippel-Lindau protein; TFAM, mitochondrial transcription factor A; TMRM, tetramethylrhodamine methyl ester; *VHL*, von Hippel-Lindau gene.

(HRE) present in the promoter of genes encoding such enzymes (20). However, it is not known whether, and how, HIF could also inhibit mitochondrial biogenesis. Besides, to our knowledge, HRE-like sites that might induce a silencing effect on the expression of OXPHOS genes have not been identified.

In addition to the *VHL* modifications, other genetic alterations (22–25), often associated with higher grades of tumors, have been observed in CCRCs. A multi-step process in which modifications of several chromosomes come into play to reach full malignancy characterizes these CCRCs. Although mitochondrial deficiency is not much more important in high than in low tumor grade CCRCs (14), it cannot be excluded that some of these additional genetic alterations might be responsible for the mitochondrial deficiency. In the present study, we have used CCRC cells initially devoid of active pVHL but transfected with ectopic wild-type *VHL* or with a void vector to test the specific influence of pVHL on the expression of proteins involved in OXPHOS. We show that the presence of pVHL, known to prevent the formation of tumors after injection in nude mice (26), stimulated the expression of OXPHOS proteins and restored the cell capacity to grow in the absence of glucose, that is under conditions in which mitochondria are the essential source of energy for the cell.

Materials and methods

Cell lines originating from CCRC patients

pVHL-deficient 786-0 cell clones transfected either with an empty vector (clone PRC3) or with wild-type *VHL* (clones WT8 and WT10) (26) were kindly provided by William Kaelin (Dana-Farber Institute, Boston, MA). pVHL-negative RCC10 cells and a clone stably transfected with wild-type *VHL* (clone 53) were generous gifts of Dr Karl H.Plate (Johann Wolfgang Goethe University, Frankfurt, Germany) (27). The CCRC cell lines are derived from human sporadic CCRCs and express inactive pVHL.

Cell culture

Cells were grown in RPMI 1640 medium with 10% fetal calf serum at 37°C in 5% CO_2 and routinely used at 70–80% confluence. For metabolic studies, the cell number was estimated by counting in the presence of 0.04% Trypan Blue and was followed for 2–6 days in culture medium containing either 2 g/l of D-glucose or 2 g/l of D-galactose. Nuclear morphology was assessed in re-suspended cells stained either with Hoechst and fixed with 3% formaldehyde or with acridine orange and ethidium bromide as described by Ghelli *et al.* (28).

Tissue samples

Tumors from CCRCs and their adjacent normal renal cortex were obtained from patients and their grades were characterized as described (14).

Mitochondrial enzyme activities

Activities of citrate synthase (29) and succinate cytochrome *c* reductase (30) were determined in cells spun down at 200 *g* for 5 min, frozen at −80°C, thawed and homogenized in NaCl, phosphate medium (1.54 mM KH_2PO_4, 0.15 M NaCl, 2.7 mM Na_2HPO_4, $7H_2O$, pH 7.4). ATPase activity was determined spectrophotometrically in an ATP regenerating system as described previously (31). About 5×10^6 frozen cells were permeabilized by incubation for 10 min in 1 ml ice-cold medium D (0.25 M sucrose, 20 mM Tris–HCl, pH 7.2, 40 mM KCl, 2 mM EGTA, 1 mg bovine serum albumin/ml) to which 0.01% digitonin and 10% Percoll™ were added; cells were spun down at 2200 *g* for 5 min, washed in 1 ml medium D and spun again at 6000 *g* for 5 min. The final pellet was homogenized in 80 µl of medium D. The mitochondrial ATPase activity was calculated as the difference between the rates measured before and after addition of 1 µg oligomycin and 2 µM aurovertin.

Polarographic measurements

Oxygen consumption of cells was measured at 30°C in K medium (80 mM KCl, 10 mM Tris–HCl pH 7.4, 3 mM $MgCl_2$, 1 mM EDTA, 5 mM KH_2PO_4) as described in (32) using a high resolution OROBOROS™ oxygraph.

Cytofluorometric analysis of mitochondrial membrane potential

About 5×10^6 cells were diluted to 1 mg protein/ml in K medium and then permeabilized with 0.1 mg digitonin/mg of protein for 15 min at room temperature in the presence of 20 nM TMRM. Analyses were performed as described before in (32).

Table I. PCR conditions used for mtDNA content analysis

cDNA	Forward primers reverse primers	Temperature (°C)	Size (bp)
SURF1	5′CCTTGCTCGGCCACTGTTCTTA3′ 5′ACAGCTCCTTGGAATGGTCAAAGGAC3′	60	82
Cytochrome *b*	5′GGCTTACTTCTCTTCCTTCTCTC3′ 5′TCCTAGTTTGTTAGGGACGG3′	60	117

Western blotting

Total proteins of frozen tissues or cells were extracted in lysis buffer: 10 mM Tris, 1 mM EDTA, pH 8, 1 mM PMSF, 2 µg/ml anti-proteases (Sigma-Aldrich™), 1 mM sodium vanadate, 1% deoxycholate. After protein quantification with the Bradford assay (from Bio Rad™), dithiothreitol (0.1 M) was added and the mix was incubated for 10 min on ice. Lysis was then achieved after adding 0.2% Triton X-100 and 1% SDS (final concentrations). Proteins (10–30 µg) were separated in a 12.5% acrylamide/bisacrylamide gel and transferred to a nitrocellulose BA83 membrane (Schleicher and Schuell™) that was pre-incubated with 5% skim milk in NaCl–phosphate buffer. The membrane was incubated for 2 h at room temperature with various primary antibodies (except anti-pVHL, that was incubated overnight at 4°C), washed four times with buffer A (NaCl–phosphate buffer containing 0.1% Tween 20), incubated for 1 h with horseradish peroxidase-conjugated anti-rabbit IgG (Bio-Rad™; 1/10 000) or anti-mouse IgG (Bio-Rad™; 1/3000) and washed with buffer A. Anti-13.4 kDa (1/3000), anti-core II (1/10 000), anti-iron sulfur protein, (anti-ISP) (1/25 000), antibodies were prepared as described by Legros *et al.* (33) against the corresponding proteins that belong to complex III (34). Anti-ATPase subunit 6 (1/500) was prepared as described by Dubot *et al.* (35). Anti-adenine nucleotide translocator, anti-Cox IV (1/2000) and anti-mitochondrial transcription factor A (TFAM) (1/1000) were generous gifts of Dr Brandolin (36), Dr Taanman (37) and Dr Rojo (38), respectively. Anti F_1-ATPase alpha subunit (1/20 000) was from Moradi-Améli and Godinot (39), and anti-pVHL (1/250) from Becton Dickinson™.

mtDNA quantification using real time PCR

Total DNA was extracted using the genomic DNA kit from Sigma-Aldrich™. To determine the mitochondrial to nuclear DNA ratio, the *SURF1* gene present as a single copy in each chromosome 9 allele of nuclear DNA and the *CYTB* gene present once in each of the multiple mtDNA copies were amplified using primers indicated in Table I. The PCR reaction was performed in a Roche Light Cycler apparatus, using the Faststart DNA master SYBR Green kit (Roche Manheim™, Germany). DNA (2 µl) was mixed with a buffer containing 5 mM $MgCl_2$, 0.2 mM dNTPs, 0.5 µM of forward and reverse primers, SYBR green I dye and 0.25 U Hot Start *Taq* DNA polymerase in a final volume of 20 µl. The reactions were performed as follows: initial denaturation at 95°C for 8 min, and 45 cycles at 95°C for 15 s, 60°C for 5 s and 72°C for 10 s. Each measurement was done four times and normalized in each experiment with serial dilutions of a control DNA sample.

Statistical analysis

Means from three or more independent experiments are given. Statistical comparison between different enzyme activities, mitochondrial DNA levels and TFAM content was performed by one way analysis of variance followed by Tukey's post hoc comparison for multiple data comparisons or by Student's paired *t*-test for paired data, as appropriate, using the Instat3™ software. Statistical significance was set at $^{*}P < 0.05$, $^{**}P < 0.01$ or $^{***}P < 0.005$.

Results

Stimulation of mitochondrial respiratory chain activities and OXPHOS capacity by transfection of wild-type VHL in VHL-deficient cells

The citrate synthase activity, often considered as proportional to the amount of mitochondria, has been measured in *VHL*-deficient cells or in cells transfected with wild-type *VHL*. Figure 1A shows that the presence of pVHL did not significantly modify the citrate synthase activity. The activity of complex II + III was determined by the succinate cytochrome *c*

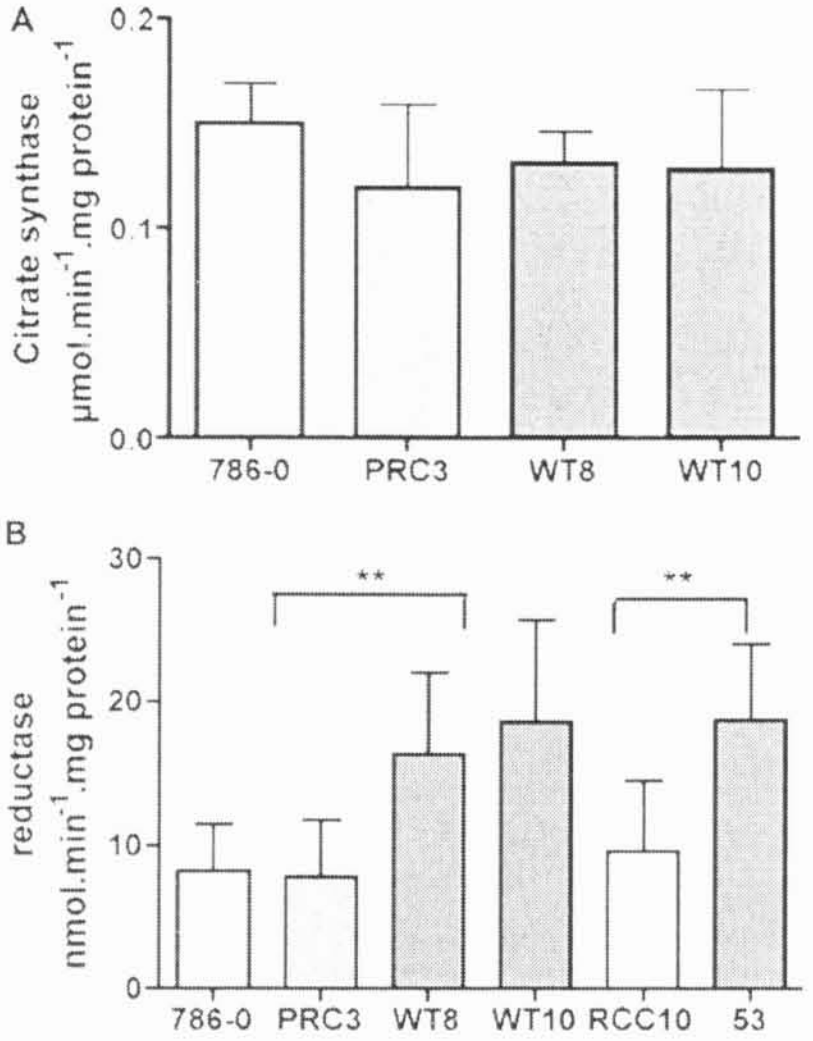

Fig. 1. Effect of wild-type *VHL* transfection into *VHL*-deficient CCRC cells on mitochondrial enzyme activities. Citrate synthase (**A**) and succinate–cytochrome *c* reductase (**B**) activities were measured in two different parental CCRC cell lines (786-0 and RCC10) and in the same cells transfected with wild-type *VHL* (WT8, WT10 and 53) or with an empty vector (PRC3). The data are given as mean + SD. Significant differences between *VHL*-deficient cells and cells transfected with *VHL* are marked with stars. $^{**}P < 0.01$ (three to six experiments).

reductase activity that could be suppressed by malonate or by antimycin A (Figure 1B). It was ~2-fold higher in *VHL*-transfected (WT8 and WT10) cells than in parental 786-0 cells or in PRC3 cells transfected with a void vector. Similar results were observed when RCC10-53 cells transfected with *VHL* were compared with *VHL*-deficient RCC10 parental cells.

To evaluate the overall OXPHOS capacity of 786-0 cells transfected or not with wild-type *VHL*, their rate of oxygen consumption was monitored after cell permeabilization with 0.1 mg digitonin/mg of protein in the presence of substrates and inhibitors of OXPHOS (Figure 2). Although in each experiment, there was a tendency for up-regulation in the rates of pyruvate + malate and succinate oxidation [average increase of 38% in the presence of ADP and of 11% in the presence of carbonyl cyanide 4-trifluoromethoxyphenylhydrazone (FCCP)], and of cyanide-sensitive oxidation of ascorbate + *N,N,N′,N′*-tetramethyl-*p*-phenylenediamine (TMPD), reflecting the cytochrome *c* oxidase (COX) activity, the differences were not statistically significant because relatively large variations in oxygen consumption rates were observed from one experiment to the other.

The ATPase activity, sensitive to oligomycin that inhibits only the whole F_0–F_1 complex, and to aurovertin known to inhibit as well F_0–F_1 complex as free F_1 or F_1 not fully assembled with all other F_0 subunits was similar in 786-0 cells devoid of *VHL* or transfected with *VHL*. This activity was of 0.166 ± 0.019 µmol of ATP hydrolyzed per minute and

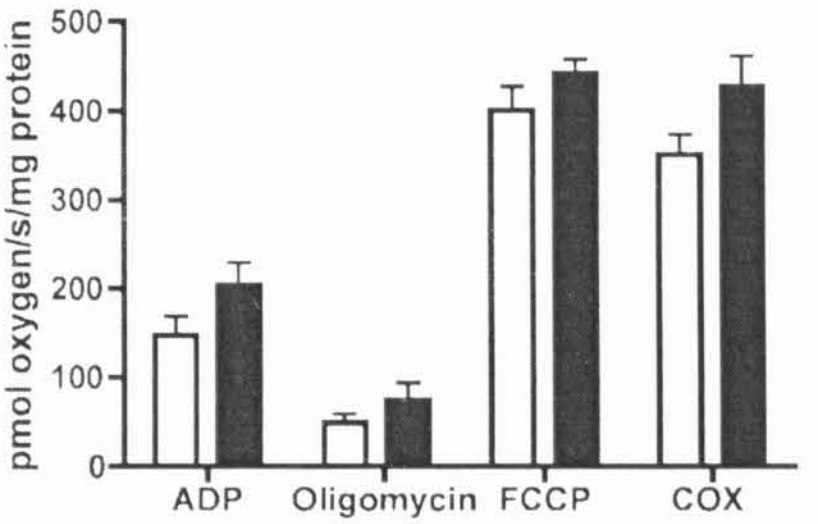

Fig. 2. Increase in oxygen consumption capacity in 786-0 cells transfected with VHL. Cells were permeabilized with digitonin (0.1 mg/mg protein) and oxygen consumption (pmol/s/mg protein) was monitored after successive additions of substrates and inhibitors of the mitochondrial respiratory chain (10 mM pyruvate + 3 mM malate, 1 mM ADP, 10 mM succinate, 10 µM oligomycin, 1 µM FCCP, 1 µM antimycin A, 5 mM ascorbate, 300 µM TMPD, 500 µM KCN). The graph shows mean values + SD from four experiments of pyruvate + malate + succinate oxidation stimulated by ADP (state 3 ADP) or FCCP (state 3u FCCP) and KCN-sensitive ascorbate + TMPD oxidation (COX) or inhibited by oligomycin in parental 786-0 cells (white boxes) and WT 8 transfected with wild-type VHL cells (black boxes).

per milligram of protein in *VHL*-deficient 786-0 cells (mean of nine assays ±SEM) and of 0.165 ± 0.009 (15 assays) for cells transfected with *VHL* (WT-8). The percentage of ATPase activity that was sensitive to aurovertin but insensitive to oligomycin did not appear to be modified by the presence of pVHL.

Lack of effect of VHL transfection on the mitochondrial membrane potential of VHL-deficient cells

VHL-deficient 786-0 cells (PRC3 or 786-0 parental) and cells transfected with *VHL* (WT8, WT10) were permeabilized and treated with different concentrations of digitonin (0–0.5 mg/mg of protein) to optimize the cell permeabilization conditions, as tested with propidium iodide fluorescence and TMRM staining with FACS. A complete permeabilization was obtained with 0.1 mg digitonin/mg of protein that gave a maximal TMRM signal (not shown). Simultaneously to the measurement of TMRM fluorescence, MitoTracker Green (Molecular Probes™) fluorescence was determined. The latter fluorescence is considered as proportional to the amount of mitochondria, independently of the membrane potential. In this way, the membrane potential could be normalized to the amount of mitochondria in each cell line. The normalized intensities of TMRM fluorescence were not significantly different in *VHL*-deficient 786-0 cells and in cells expressing wild-type pVHL. In all cases, the high TMRM fluorescence observed in state 4 was collapsed after FCCP addition and was decreased after ADP addition (the ADP decrease was prevented by oligomycin, aurovertin or atractyloside, data not shown) similarly for all types of cells. This indicated that the mitochondria present in *VHL*-deficient cells were able to maintain a membrane potential similar to that of cells expressing wild-type pVHL.

Increase in OXPHOS protein contents by transfection of VHL in VHL-deficient cells

Total proteins were extracted from *VHL*-deficient (786-0 parental, PRC3) and *VHL*-transfected cells (WT8, WT10)

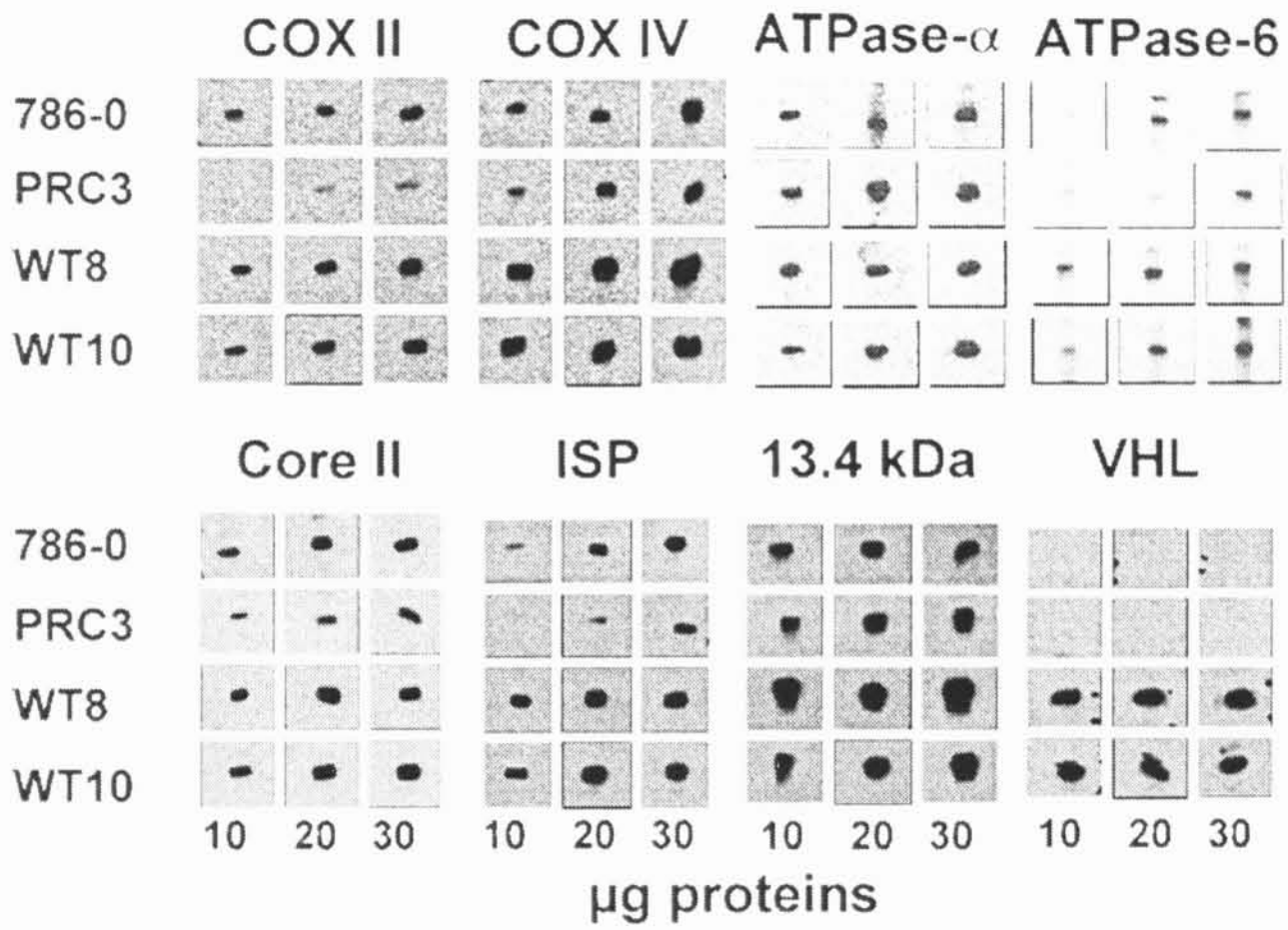

Fig. 3. Increase in OXPHOS protein contents in 786-0 cells transfected with *VHL*. Western blot analysis of OXPHOS subunits and of pVHL in 786-0 parental, 786-0-PRC3, 786-0-WT8 and 786-0-WT10 cells. Increasing amounts (10–30 µg) of proteins were used to estimate the proportionality between antibody signal and protein amounts. Antibodies directed against complex IV subunits: Cox II (mtDNA-encoded) and Cox IV (nuclear origin), against complex III subunits: core II, ISP and 13 kDa, which are all nuclear-encoded, against complex V: ATPase F_1 alpha subunit (nuclear origin), ATPase-6 (mtDNA-encoded) and pVHL, were used.

and western blot analysis was performed using antibodies specific for pVHL and for OXPHOS complex subunits. Increasing protein amounts (10–30 µg) were used in each experiment to estimate the proportionality between the signal and the amount of protein for each tested antibody. After transfer, the membranes were stained with Ponceau Red to verify that similar protein amounts were present for each cell type. In Figure 3, the signal observed with the anti-pVHL antibody confirmed that pVHL was only present in *VHL*-transfected cells. Staining obtained with antibodies against complex III subunits (core II, 13.4 kDa and iron sulfur protein), complex IV subunits (COX II subunit encoded by mitochondrial DNA and COX IV subunit encoded by nuclear DNA) and complex V (F_0-ATPase 6 subunit of mitochondrial origin) was much stronger in cells transfected with *VHL* than in *VHL*-deficient cells. This was particularly striking when antibodies against the 13.4 kDa complex III subunit or against the cytochrome *c* oxidase subunit IV were used. The anti-ATPase α subunit was the only exception to this rule: no significant difference between cells expressing pVHL and cells deficient in pVHL could be observed with this antibody.

It was checked that respiratory chain subunit contents that were lower in 786-0 cells than in *VHL*-transfected cells, were also depleted in tumor samples as compared with their normal adjacent renal tissue and that therefore, this depletion was not limited to the 786-0 tumor cell line. Total proteins of CCRC tumor samples and of normal adjacent tissues were extracted and western blot analysis was performed with antibodies directed against different subunits of respiratory chain complexes, and against pVHL. In agreement with the above results, a strong decrease in OXPHOS complex contents of CCRC tumor samples was observed (Figure 4). Subunits of

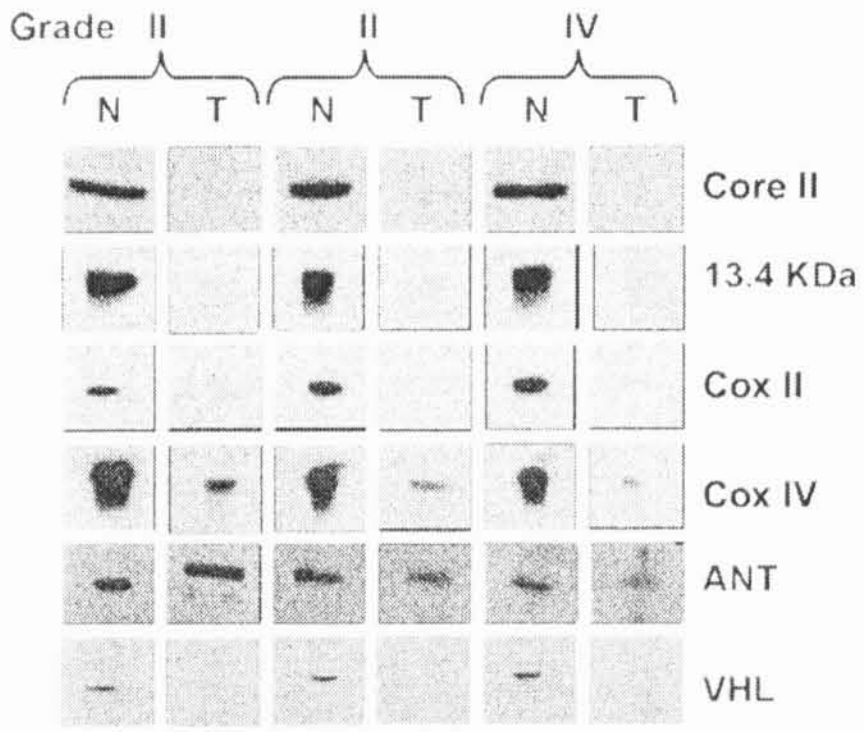

Fig. 4. Decreased amounts of OXPHOS proteins in CCRC tumor samples as compared with normal adjacent kidney. Western blot analysis was performed as in Figure 3, using 20 µg of proteins from tumor tissues (T) or from their normal adjacent counterpart (N) from the same kidney. Cancer grades II or IV were determined according to the Fuhrman's classification (40). Antibodies against respiratory chain complex subunits are named as described in the legend to Figure 3. ANT represents the adenine nucleotide translocator.

ubiquinol-cytochrome *c* reductase (core II and 13.4 kDa subunits) and of cytochrome *c* oxidase (subunit II and subunit IV) were barely detectable in tumors as compared with normal adjacent tissues. In addition, all three CCRC samples tested

in this experiment were deficient for pVHL but contained similar amounts of adenine nucleotide translocator. It should be noted that the differences in the amounts of OXPHOS proteins between normal and tumor tissues were more pronounced than those observed between 786-0 cells expressing pVHL versus null (compare Figures 3 and 4). However, the protein amount detected by western blot should not be considered as a precise quantification because the signal intensity is only proportional to the amount of proteins in a restricted range and the respiratory chain subunit amounts remaining in the tumor are probably below the respective antibody detection limits.

Increase in mtDNA level by VHL transfection in VHL-deficient cells

In CCRCs, the decrease in OXPHOS activities is concomitant to a decrease in mtDNA content (14). We therefore determined the effect of *VHL* transfection on the amount of mtDNA to know whether an increase in mtDNA could be correlated to OXPHOS stimulation by pVHL observed above by oxypolarography, by enzymatic analysis or by western blot. Total DNA was extracted from 786-0 parental cells or cells transfected with an empty vector (PRC3) or with a vector expressing wild-type pVHL (WT8 and WT10) in order to quantify mtDNA by real time PCR. Nuclear or mitochondrial DNA was amplified in the presence of primers designed for *SURF1* or *CYTB* genes, respectively (Figure 5). The ratio between mitochondrial DNA and nuclear DNA levels appeared about two times higher in cells transfected with *VHL* (WT8 or WT10) than in *VHL*-deficient cells (786-0 parental cells or PRC3 cells). Similar data were obtained when comparing *VHL*-deficient RCC10 cells to the RCC10-53 cells transfected with *VHL*.

Capacity of VHL-deficient cells to rely on ATP provided by OXPHOS for their growth

Studies made by Steinberg *et al.* (41) have clearly shown that glycolysis is activated in CCRCs. The question was raised to know whether the OXPHOS activity remaining in *VHL*-deficient 786-0 cells was efficient enough to sustain cell growth and survival. In previous studies using cells exhibiting partial OXPHOS deficiency, growth impairment has been reported when the cells were incubated in a medium containing galactose in place of glucose (28,42,43). Galactose is not efficiently utilized by mammalian cells as a glycolytic substrate and these cells are forced to rely almost exclusively on OXPHOS for ATP production (43). *VHL*-deficient (786-0 parental) and *VHL*-transfected (WT8) cells seeded at 1.5×10^3 cells/dish (40 mm) were cultured in DMEM supplemented with SVF (10%) and either D-glucose or D-galactose (1–5 g/l). Preliminary experiments showed that optimal growth rate was observed when the sugar concentration was at least 2 g/l. Figure 6A compares the growth curves of *VHL*-deficient 786-0 cells or 786-0 cells transfected with wild-type *VHL* in media containing pyruvate and either glucose or galactose. Both *VHL*-deficient cells and cells transfected with *VHL* exhibited an exponential growth in the presence of glucose for 4–6 days until cells were confluent. However, in glucose-containing medium, the *VHL*-deficient cells grew at a slower rate (initial doubling time of 28 h) than the cells transfected with *VHL* (initial doubling time of 19 h). In contrast, in glucose-depleted galactose-containing medium, the *VHL*-deficient 786-0 cells failed to divide. The cells expressing pVHL

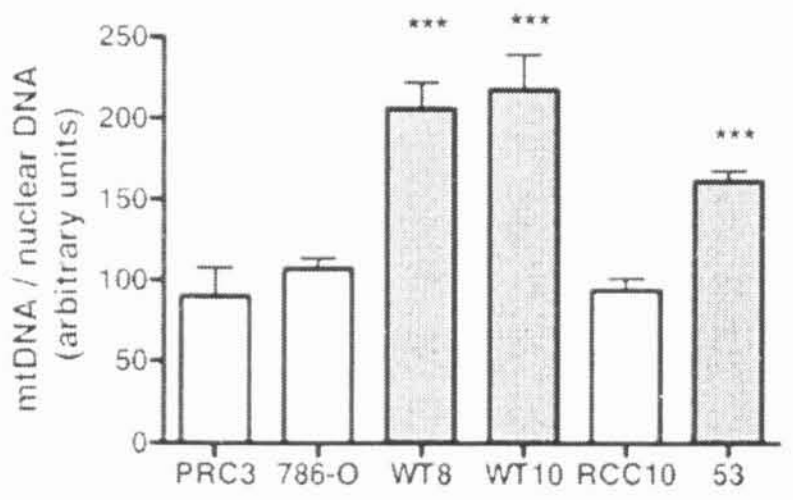

Fig. 5. Increase in mtDNA/nuclear DNA in 786-0 cells transfected with wild-type *VHL*. The ratios mtDNA/nuclear DNA were estimated using real time PCR. The amount of a mitochondrial gene (cytochrome *b*), which is present at multiple copies per cell and that of a nuclear gene (*SURF1*) present at only two copies per cell, were measured. The data are given as a mean of five independent determinations ± SD. Significant differences between *VHL*-deficient cells and cells transfected with *VHL* are marked with stars (***$P < 0.005$).

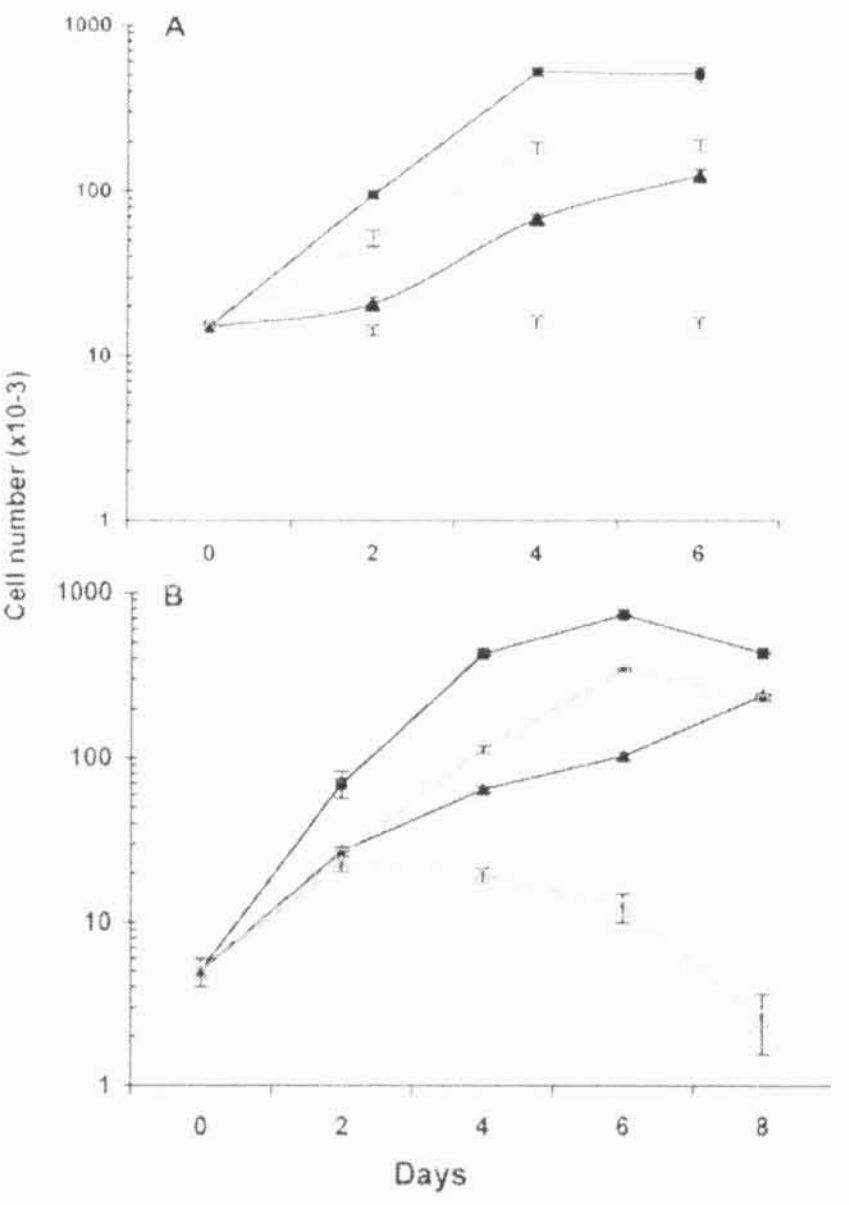

Fig. 6. Growth curve of *VHL*-deficient 786-0 cells or 786-0 cells transfected with *VHL* in medium containing either glucose (square symbols) or galactose (triangles). (**A**) Culture medium with 4.5 mM sodium pyruvate; *VHL*-deficient 786-0 parental cells (gray dashed lines) or *VHL*-transfected WT8 cells (black lines) were seeded at 1.5×10^3 cells/40-mm diameter dish and cultured in DMEM supplemented with 11 mM glucose (black lines) or galactose (dashed lines). (**B**) id in culture medium without pyruvate. Each point is the mean of three to nine determinations ± SEM.

(WT10) grew at a reduced rate in glucose-depleted galactose medium, when compared with that observed in glucose medium (initial doubling time of 32 h in galactose instead of 19 h in glucose). *VHL*-deficient PRC3 cells transfected with a void vector behave similarly as the *VHL*-deficient 786-0 cells and the *VHL*-transfected WT8 clone could be maintained in the presence of galactose in a similar manner as that of the WT10 clone (not shown). When pyruvate was removed from the culture medium (Figure 6B), the *VHL*-deficient cells progressively died in glucose-depleted galactose-containing medium. After 6 days, almost all the *VHL*-deficient cells grown in the absence of pyruvate in glucose-depleted galactose-containing medium were floating. In contrast, cells transfected with *VHL* could grow in the presence as well as in the absence of added pyruvate.

Effect of pVHL expression on the level of mitochondrial transcription factor A involved in mtDNA maintenance and synthesis

The above data showed that, although the membrane potential was maintained in the absence of pVHL, a decrease in OXPHOS capacity sufficient to prevent the cells from growing in the absence of glucose was observed. This was related to a diminution in the contents of several OXPHOS complex proteins. The lowered level of mtDNA could explain the decreased amount of OXPHOS subunits. Yet, it remains to understand how pVHL could regulate mtDNA synthesis, which is known to be under the control of nuclear genes (44–47). As expected from the mtDNA increase (Figure 5), the protein expression of TFAM was higher in cells containing pVHL than in cells devoid of pVHL (Figure 7). Interestingly, the TFAM protein amount was also decreased in *VHL*-deficient tumor samples when compared with normal adjacent tissues.

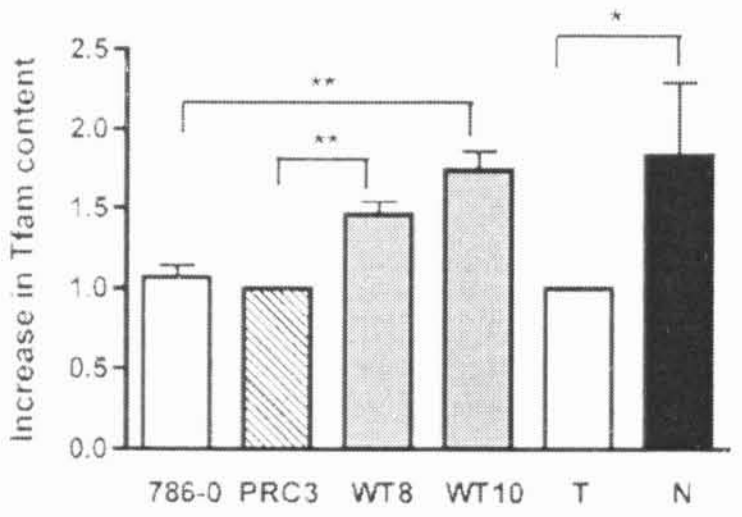

Fig. 7. Influence of pVHL on TFAM protein expression. The TFAM protein amount present in cell lines expressing pVHL (WT8 and WT10), *VHL*-deficient (786-0) or transfected with an empty vector (PRC3) and in tumors (T) or in their adjacent normal kidney (N) was analyzed by western blot, as described in Figure 3, using 10 or 20 μg protein loads in the gel electrophoresis and anti-TFAM antibody. The signal obtained on the western blot film was scanned and quantified with the Image Quant software™. The ratio between the signal intensity observed in the studied cells to that observed in the absence of pVHL (PRC3 cells) was calculated in each experiment. The given value represents the mean of six determinations ± SD. For the tumors, the ratio between normal adjacent kidney and tumor was calculated and the given value is the mean ratio obtained for four different tumors ± SD. $^{*}P < 0.05$; $^{**}P < 0.01$. No pVHL could be detected in these four tumors.

Discussion

The data presented in this report demonstrate that transfection of *VHL* in *VHL*-deficient cells increased mitochondrial OXPHOS protein or DNA contents and their functions. Indeed, *VHL* transfection increased the expression of respiratory chain complexes, stimulated succinate-cytochrome *c* reductase and cytochrome *c* oxidase activities, improved the rate of substrate oxidation and restored their ability to grow in the absence of glucose that is at the only expense of ATP provided by mitochondria. Therefore, the absence of *VHL* gene expression was at least one of the components involved in mitochondrial impairment in *VHL*-deficient cells.

On the opposite, *VHL*-transfection in *VHL*-deficient cells modified neither their mitochondrial membrane potential nor their oligomycin- and aurovertin-sensitive ATPase activity. It means that the mitochondria present in *VHL*-deficient cells can maintain their membrane potential even though their respiratory chain content was lower than that of cells transfected with *VHL*. Previous studies had shown that the mitochondrial membrane potential can be maintained in ρ^- cells devoid of mtDNA and hence unable to synthesize ATP, provided that the F_1-ATPase and the adenine nucleotide translocator remained active (31,48). The *VHL*-deficient cells contained similar ATPase activity and amounts of F_1-ATPase subunit as cells transfected with *VHL* (Figure 3). F_1-ATPase was also found in all tested tumor samples as an at least partly assembled F_0–F_1 complex, although its activity could be decreased in some cases (14). Adenine nucleotide translocator was also present in CCRC tumor samples (this work and ref. 49) as well as in renal cancer cell lines (49). The maintenance of this mitochondrial membrane potential is essential for cell survival. Indeed it is necessary in mitochondria for the import of proteins involved in the citric acid cycle and amino acid, fatty acid or nucleic acid metabolism. On the contrary, mitochondrial synthesis of ATP may be suppressed without inducing cell death provided that glycolysis could yield enough ATP to the cytoplasm. It is therefore not surprising that these cancer cells could maintain their mitochondrial membrane potential. The ATPase activity was decreased in most high-grade CCRC tumor biopsies, and the proportion between free F_1 and assembled F_0–F_1 complex was somewhat variable in previously analyzed tumor biopsies (14). Transfection with *VHL* did not modify the amount of F_1 but increased that of subunit 6, as mentioned above. The lower amount of ATPase subunit 6 in *VHL*-deficient cells than in cells transfected with *VHL* implies that the whole amount of complex V was lower in *VHL*-deficient cells. If free F_1 compensated for the lack of complex V this could maintain the ATPase activity and hence the membrane potential (31). But free F_1 or complex V devoid of subunit 6 should be aurovertin-sensitive and not oligomycin-sensitive. The fact that pVHL did not change the relative sensitivity to aurovertin and to oligomycin suggested that *VHL* transfection did not significantly change the proportion of active ATP synthase made of intact oligomycin-sensitive F_0–F_1 complex to that of active ATPase containing F_1 or incomplete F_0–F_1 complex. Previous studies on CCRC biopsies have shown that, unexpectedly, the presence of free F_1 was associated to low aurovertin-sensitive ATPase activity (14), which suggests that either the F_1-ATPase activity was partly inhibited in these tumors or that the aurovertin-sensitivity was decreased. Moreover, taking into account the fact that dissociation of F_1-sector from F_0 leads to loss of ATP synthase

activity but to an increase of ATPase activity up to a factor of 10 (50), the measured ATPase activity may not be directly related to the F_1 or F_0–F_1 amounts and identical rates of ATP hydrolysis in *VHL*-deficient or *VHL*-transfected cells may be fortuitous. Further studies will be necessary to understand the mechanisms regulating F_0–F_1 assembly and activity in these tumor cells. Anyhow, these data suggest that pVHL differentially regulates the biogenesis and/or assembly of F_0–F_1 and that of respiratory chain complexes.

The differences in the respiratory chain activities and subunit contents observed between *VHL*-deficient cells and cells transfected with wild-type *VHL* were not as high as those observed between tumor samples and adjacent renal cortex: the respiratory chain subunit contents were approximately two times higher in *VHL* containing cells than in *VHL*-deficient cells (Figure 3) and 5–10-fold higher in renal cortex than in tumor tissue (Figure 4). The succinate-cytochrome *c* reductase activity measured in normal kidney homogenates were on the average five times higher than that of adjacent tumors (14) and two to three times higher in cells transfected with *VHL* than in parental tumor cells or in cells transfected with a void vector (Figure 1B). The cytochrome *c* oxidase activity was also much more reduced when tumors were compared with normal tissue (14) than when *VHL*-deficient cells were compared with cells transfected with *VHL* (Figure 2). It should be noticed that the specific activities of these complexes calculated per milligram of protein were comparable in *VHL*-deficient cultured cells and in patient tumor biopsies. One reason to explain the difference between the high renal cortex activities and the comparatively low activity of cells expressing pVHL could be that, *in vivo*, the normal proximal renal tubule from which these tumors are originated is irrigated by an abundant oxygen flow and must express a high OXPHOS activity to sustain the energy-demanding pumping activity of the kidney that is not needed in cells cultured *ex vivo* (51). It has been demonstrated clearly, at least in the heart and muscle, that an increased energy demand stimulates mitochondrial biogenesis (52). Another hypothesis explaining a more pronounced decrease in OXPHOS functioning observed between tumor and adjacent tissue than between *VHL*-deficient and *VHL*-transfected cells might be related to the additional modifications of genes that would cooperate with *VHL* to up-regulate mitochondrial biogenesis. Indeed, in spite of the large incidence of pVHL inactivation in CCRCs, many other chromosomal alterations have been observed in these cancers (reviews in refs 24,25). In the three tumors analyzed in this study, the western blot analysis of tumor tissues revealed a very low content of core II and 13 kDa complex III subunits as well as COX II and COX IV subunits. In a previous paper (14), an average of ~20% residual enzyme activity was observed in such tumors. As mentioned above, the difference between residual complex activities in the tumors (14) and apparent residual amounts of subunits belonging to these complexes (Figure 4) might be due to the restricted range of proportionality between the amount of proteins and the antibody detection limits.

The mitochondrial biogenesis down-regulation induced by the lack of pVHL mainly concerns the OXPHOS complexes and not all mitochondrial activities. Indeed, there was no significant difference in citrate synthase activity between cultured cells containing or devoid of pVHL (Figure 1) although this activity was lowered by a factor of about two in tumor CCRC biopsies as compared to normal adjacent renal cortex (14). Therefore, while the absence of pVHL is correlated with a decrease in the biogenesis of OXPHOS complexes both in cultured cells and in tumors, a *VHL*-independent mechanism down-regulating citrate synthase activity is responsible for the low citrate synthase activity observed in tumors. Among OXPHOS subunits that have been tested in this study, those encoded by mtDNA, COX II and ATPase 6 were both decreased. Similarly, subunits encoded by nuclear genes were also decreased in the case of complex III and complex IV. On the contrary, the F_1-ATPase α subunit expression was not modified. The assembly of this subunit to form the F_1 complex or an incomplete F_0–F_1 sub-complex in mammalian cells does not require the presence of the subunit 6 of mitochondrial origin as F_1 can be assembled in ρ^0 cells (31,53). On the contrary, a lack of mitochondrially encoded subunits prevents complex IV or complex III from being stably assembled (54,55). Limiting amounts of mitochondrially encoded subunits can therefore explain the decreased activities of these two complexes.

mtDNA content was decreased by a factor of about two when comparing both renal carcinoma to normal kidney or *VHL*-deficient cells to cells transfected with *VHL*. Therefore, the *VHL*-induced OXPHOS complex down-regulation is probably due to this mtDNA decrease, which suggests that *VHL* was somehow involved in the regulation of mtDNA replication and transcription. The mitochondrial transcription factor A, TFAM was also increased by *VHL* transfection in parallel to the mtDNA increase. This could be related either to an increased stability of the TFAM protein or to an up-regulation of its synthesis. TFAM is a nuclear-encoded mitochondrial transcription factor, which is imported into the mitochondria, binds to light and heavy strand promoter of mtDNA and is known to be essential for the maintenance and repair of mtDNA (45). TFAM co-localizes with mtDNA in nucleoprotein complexes (38). The stability of TFAM is tightly associated to the presence of mtDNA within the cell since cells permanently (56) or transiently (57) depleted of mtDNA (ρ^0 cells) are characterized by the absence of detectable levels of TFAM protein. However, the *TFAM* transcript is expressed at normal levels in the ρ^0 cells (56). Chronic electrical stimulation increases muscle mitochondrial biogenesis (58) through an increase of *TFAM* and of mitochondrial *COX III* mRNA expression (59). Similarly, elevated *TFAM* mRNA expression was matched by a parallel increase in mitochondrial *COX I* and *COX II* mRNAs in rat hepatoma cells (60). However, reported studies made either by Serial Analysis of Gene Expression (SAGE) in 786-0 cells transfected or not with *VHL* (61,62) or by microarray analysis of CRCC biopsies compared with their normal adjacent tissue (63–65) did not put forward prominent changes in the expression of genes encoding OXPHOS complex subunits in mitochondrial DNA or that of nuclear genes encoding factors known to regulate mitochondrial biogenesis such as *TFAM*, *NRF1*, *NRF2*, *PGC1* or *PRC* (see review, ref. 66). Preliminary experiments using a semi-quantitative RT–PCR analysis initiated in our laboratory did not either suggest important modifications in the expression of these genes. Peroxisome proliferator-activated receptor γ (PPAR-γ) coactivator 1 (PGC1) or PGC1 regulated co-activator 1 (PRC) are considered to orchestrate mitochondrial biogenesis. PGC1 can up-regulate nuclear genes that are required for mitochondrial biogenesis in part through a direct interaction with NRF1 (nuclear respiratory factor 1). PRC that is cell-cycle regulated in cultured cells under conditions where PGC1 is not expressed interacts with NRF1 and its target genes, similarly to PGC1. Since other less well characterized signaling

pathways may also interfere with mitochondrial biogenesis (66), a more extensive study of expression of genes encoding mitochondrial proteins will still be necessary to ascertain whether transcription regulation is involved or not in mitochondrial biogenesis down-regulation of cancers. However, our working hypothesis rather favors mechanisms involving regulation at the level of translation or of protein stability. For example, TFAM is stabilized by its interaction with mtDNA as its transcript level is not changed in ρ° cells while the protein is very low (see above).

The data presented in this work show that *VHL*-transfection of *VHL*-deficient CCRC cells rendered the cells able to survive and grow in the absence of glucose. Indeed, replacing glucose by galactose in the culture medium almost completely prevented cell growth, which means that the rate of ATP synthesis provided by the partially deficient mitochondria was not sufficient to sustain growth of pVHL-deficient cells. It has been shown that when glucose is replaced by galactose in OXPHOS-partially deficient cells such as cells from patients (Leber Hereditary Optic Neuropathy), cell death occurs by apoptosis (30). In 786-0 cells, no sign of apoptosis could be put forward (data not shown). Gajewski *et al.* (67), have shown that, in wild-type cells, normal ATP levels were maintained in all cell compartments when the cells were grown in the absence of glucose and presence of pyruvate, which is metabolized in the mitochondria. On the contrary, when cells exhibiting an OXPHOS dysfunction were grown in the absence of glucose and presence of pyruvate, ATP levels were reduced in the mitochondria and to a greater extent, in the nucleus. In our experiments, in the absence of pVHL, a similar depletion of nuclear ATP could occur and therefore, cell division would be stopped by limitation of the high-energy compounds necessary to replicate nuclear DNA. Although HeLa cell growth in galactose induced an increase in mitochondrial oxidative capacity when the treatment was applied for 3 weeks (68), the OXPHOS contents of *VHL*-deficient cells was probably too low for the cells to overcome the mitochondrial deficiency.

In conclusion, it has been demonstrated for the first time, that the *VHL* tumor suppressor product up-regulates mitochondrial OXPHOS complex biogenesis and function. Further studies will be needed to understand the mechanisms of this regulation, at the level of gene transcription, of post-transcriptional modifications or of protein turnover.

Acknowledgements

Dr M.Esteban is gratefully acknowledged for providing us cells and for valuable discussions. We also thank Dr Brandolin for adenine nucleotide translocator antibody, Dr Taanman for anti-Cox II antibody and Dr R.Bouvier of the Service of Anatomy and Cytopathology (Hospital Edouard Herriot, Lyon, France) for characterization of tumor biopsy samples. Dr A.Lombes and Dr M.Rojo are gratefully acknowledged for their gift of TFAM antibody and for stimulating discussions. This work was supported by the LRCC ('Ligue Regionale Contre le Cancer'), by the CNRS, by the INSERM (VIE0208), by the MŽCR (NR7790-3) and by the GAČR (303/03/0749). We also thank EGIDE for granting subsidies for travels between France and Czech Republic.

References

1. Seizinger,B.R., Rouleau,G.A., Ozelius,L.J. *et al.* (1988) Von Hippel-Lindau disease maps to the region of chromosome 3 associated with renal cell carcinoma. *Nature*, **332**, 268–269.
2. Kaelin,W.G., Iliopoulos,O., Lonergan,K.M. and Ohh,M. (1998) Functions of the von Hippel-Lindau tumour suppressor protein. *J. Intern. Med.*, **243**, 535–539.
3. Kaelin,W.G. (2002) Molecular basis of the *VHL* hereditary cancer syndrome. *Nature Rev. Cancer*, **2**, 673–682.
4. Maxwell,P.H., Wiesener,M.S., Chang,G.W., Clifford,S.C., Vaux,E.C., Cockman,M.E., Wykoff,C.C., Pugh,C.W., Maher,E.R. and Ratcliff,P.J. (1999) The tumour suppressor protein VHL targets hypoxia-inducible factors for oxygen-dependent proteolysis. *Nature*, **399**, 271–275.
5. Epstein,A.C., Gleadle,J.M., McNeill,L.A. *et al.* (2001) *C. elegans* EGL-9 and mammalian homologs define a family of dioxygenases that regulate HIF by prolyl hydroxylation. *Cell*, **107**, 43–54.
6. Jaakkola,P., Mole,D.R., Tian,Y.M. *et al.* (2001) Targeting of HIF-alpha to the von Hippel-Lindau ubiquitylation complex by O2-regulated prolyl hydroxylation. *Science*, **292**, 468–472.
7. Bruick,R.K. and McKnight,S.L. (2001) A conserved family of prolyl-4-hydroxylases that modify HIF. *Science*, **294**, 1337–1340.
8. Lando,D., Peet,D.J., Gorman,J.J., Whelan,D.A., Whitelaw,M.L. and Bruick,R.K. (2002) FIH-1 is an asparaginyl hydroxylase enzyme that regulates the transcriptional activity of hypoxia-inducible factor. *Genes Dev.*, **16**, 1466–1471.
9. Safran,M. and Kaelin,W.G.Jr (2003) Molecular basis of the *VHL* hereditary cancer syndrome. *J. Clin. Invest.*, **111**, 779–783.
10. Semenza,G.L. (2004) Hydroxylation of HIF-1: oxygen sensing at the molecular level. *Physiology*, **19**, 176–182.
11. Semenza,G.L. (2000) HIF-1: using two hands to flip the angiogenic switch. *Cancer Metastasis Rev.*, **19**, 59–65.
12. Krishnamachary,B., Berg-Dixon,S., Kelly,B. *et al.* (2003) Regulation of colon carcinoma cell invasion by hypoxia-inducible factor 1. *Cancer Res.*, **63**, 1138–1143.
13. Wykoff,C.C., Beasley,N.J., Watson,P.H. *et al.* (2000) Expression of the hypoxia-inducible and tumor-associated carbonic anhydrases in ductal carcinoma *in situ* of the breast. *Cancer Res.*, **60**, 7075–7083.
14. Simonnet,H., Alazard,N., Pfeiffer,K., Gallou,C., Beroud,C., Demont,J., Bouvier,R., Schagger,H. and Godinot,C. (2002) Low mitochondrial respiratory chain content correlates with tumor aggressiveness in renal cell carcinoma. *Carcinogenesis*, **23**, 759–768.
15. Simonnet,H., Demont,J., Pfeiffer,K., Guenaneche,L., Bouvier,R., Brandt,U., Schagger,H. and Godinot,C. (2003) Mitochondrial complex I is deficient in renal oncocytomas. *Carcinogenesis*, **24**, 1461–1466.
16. Warburg,O. (1956) On respiratory impairment in cancer cells. *Science*, **123**, 309–314.
17. Cuezva,J.M., Krajewska,M., de Heredia,M.L., Krajewski,S., Santamaria,G., Kim,H., Zapata,J.M., Marusawa,H., Chamorro,M. and Reed,J.C. (2002) The bioenergetic signature of cancer: a marker of tumor progression. *Cancer Res.*, **62**, 6674–6681.
18. Isidoro,A., Martinez,M., Fernandez,P.L., Ortega,A.D., Santamaria,G., Chamorro,M., Reed,J.C. and Cuezva,J.M. (2004) Alteration of the bioenergetic phenotype of mitochondria is a hallmark of breast, gastric, lung and oesophageal cancer. *Biochem. J.*, **378**, 17–20.
19. Pedersen,P.L. (1978) Tumor mitochondria and the bioenergetics of cancer cells. *Prog. Exp. Tumor Res.*, **22**, 190–274.
20. Dang,C.V. and Semenza,G.L. (1999) Oncogenic alterations of metabolism. *Trends Biochem. Sci.*, **24**, 68–72.
21. Eng,C., Kiuru,M., Fernandez,M.J. and Aaltonen,L.A. (2003) A role for mitochondrial enzymes in inherited neoplasia and beyond. *Nature Rev. Cancer*, **3**, 193–202.
22. Velickovic,M., Delahunt,B., Storkel,S. and Grebem,S.K. (2001) VHL and FHIT locus loss of heterozygosity is common in all renal cancer morphotypes but differs in pattern and prognostic significance. *Cancer Res.*, **61**, 4815–4819.
23. Dreijerink,K., Braga,E., Kuzmin,I. *et al.* (2001) The candidate tumor suppressor gene, RASSF1A, from human chromosome 3p21.3 is involved in kidney tumorigenesis. *Proc. Natl Acad. Sci. USA*, **98**, 7504–7509.
24. Martinez,A., Fullwood,P., Kondo,K., Kishida,T., Yao,M., Maher,E.R. and Latif,F. (2000) Role of chromosome 3p12-p21 tumour suppressor genes in clear cell renal cell carcinoma: analysis of VHL dependent and VHL independent pathways of tumorigenesis. *Mol. Pathol.*, **53**, 137–144.
25. Meloni-Ehrig,A.M. (2002) Renal cancer: cytogenetic and molecular genetic aspects. *Am. J. Med. Genet.*, **115**, 164–172.
26. Iliopoulos,O., Kibel,A., Gray,S. and Kaelin,W.G.Jr (1995) Tumour suppression by the human von Hippel-Lindau gene product. *Nature Med.*, **1**, 822–826.
27. Krieg,M., Haas,R., Brauch,H., Acker,T., Flamme,I. and Plate,K.H. (2000) Up-regulation of hypoxia-inducible factors HIF-1alpha and HIF-2alpha under normoxic conditions in renal carcinoma cells by von Hippel-Lindau tumor suppressor gene loss of function. *Oncogene*, **19**, 5435–5443.
28. Ghelli,A., Zanna,C., Porcelli,A.M., Schapira,A.H., Martinuzzi,A., Carelli,V. and Rugolo,M. (2003) Leber's hereditary optic neuropathy

(LHON) pathogenic mutations induce mitochondrial-dependent apoptotic death in transmitochondrial cells incubated with galactose medium. *J. Biol. Chem.*, **278**, 4145–4150.
29. Srere,P.A. (1969) Citrate synthase. *Methods Enzymol.*, **13**, 3–26.
30. Bouzidi,M.F., Carrier,H. and Godinot,C. (1996) Antimycin resistance and ubiquinol cytochrome c reductase instability associated with a human cytochrome b mutation. *Biochim. Biophys. Acta*, **1317**, 199–209.
31. Buchet,K. and Godinot,C. (1998) Functional F1-ATPase essential in maintaining growth and membrane potential of human mitochondrial DNA-depleted rho° cells. *J. Biol. Chem.*, **273**, 22983–22989.
32. Pecina,P., Capkova,M., Chowdhury,S.K. *et al.* (2003) Functional alteration of cytochrome c oxidase by SURF1 mutations in Leigh syndrome *Biochim. Biophys. Acta*, **1639**, 53–63.
33. Legros,F., Chatzoglou,E., Frachon,P., Ogier De Baulny,H., Laforet,P., Jardel,C., Godinot,C. and Lombes, A. (2001) Functional characterization of novel mutations in the human cytochrome b gene *Eur. J. Hum. Genet.*, **9**, 510–518.
34. Yu,C. A., Zhang,L., Deng,K.P., Tian,H., Xia,D., Kim,H., Deisenhofer,J. and Yu,L. (1999) Structure and reaction mechanisms of multifunctional mitochondrial cytochrome bc1 complex. *Biofactors*, **9**, 103–109.
35. Dubot,A., Godinot,C., Dumur,V., Sablonniere,B., Stojkovic,T., Cuisset,J.M., Vojtiskova,A., Pecina,P., Jesina,P. and Houstek,J. (2004) GUG is an efficient initiation codon to translate the human mitochondrial ATP6 gene. *Biochem. Biophys. Res. Commun.*, **313**, 687–693.
36. Brandolin,G., Boulay,F., Dalbon,P. and Vignais,P.V. (1989) Orientation of the N-terminal region of the membrane-bound ADP/ATP carrier protein explored by antipeptide antibodies and an arginine-specific endoprotease. Evidence that the accessibility of the N-terminal residues depends on the conformational state of the carrier. *Biochemistry*, **28**, 1093–1100.
37. Taanman,J.W., Burton,M.D., Marusich,M.F., Kennaway,N.G. and Capaldi,R.A. (1996) Subunit specific monoclonal antibodies show different steady-state levels of various cytochrome-c oxidase subunits in chronic progressive external ophthalmoplegia. *Biochim. Biophys. Acta*, **1315**, 199–207.
38. Legros,F., Malka,F., Frachon,P., Lombes,A. and Rojo,M. (2004) Organization and dynamics of human mitochondrial DNA. *J. Cell. Sci.*, **117**, 2653–2662.
39. Moradi-Ameli,M. and Godinot,C. (1983) Characterization of monoclonal antibodies against mitochondrial F1-ATPase. *Proc. Natl Acad. Sci. USA*, **80**, 6167–6171.
40. Moline,V., Cochand-Prioley,B., Staroz,F., Vieillefond,A., et les members du GETUR (1998) Classification des tumeurs primitives du rein de l'adulte. *Ann. Pathol.*, **18**, 29–47.
41. Steinberg,P., Storkel,S., Oesch,F. and Thoenes,W. (1992) Carbohydrate metabolism in human renal clear cell carcinomas *Lab. Invest.*, **67**, 506–511.
42. Robinson,B.H., Petrova-Benedict,R., Buncic,J.R. and Wallace,D.C. (1992) Nonviability of cells with oxidative defects in galactose medium: a screening test for affected patient fibroblasts. *Biochem. Med. Metab. Biol.*, **48**, 122–126.
43. Chu,E.H., Sun,N.C. and Chang,C.C. (1972) Induction of auxotrophic mutations by treatment of Chinese hamster cells with 5-bromodeoxyuridine and black light. *Proc. Natl Acad. Sci. USA*, **69**, 3459–3463.
44. Scarpulla,R.C. (2002) Transcriptional activators and coactivators in the nuclear control of mitochondrial function in mammalian cells. *Gene*, **286**, 81–89.
45. Ekstrand,M.I., Falkenberg,M., Rantanen,A., Park,C.B., Gaspari,M., Hultenby,K., Rustin,P., Gustafsson,C.M. and Larsson,N.G. (2004) Mitochondrial transcription factor A regulates mtDNA copy number in mammals. *Hum. Mol. Genet.*, **13**, 935–944.
46. Wu,Z., Puigserver,P., Andersson,U. *et al.* (1999) Mechanisms controlling mitochondrial biogenesis and respiration through the thermogenic coactivator PGC-1. *Cell*, **98**, 115–124.
47. Andersson,U. and Scarpulla,R.C. (2001) Pgc-1-related coactivator, a novel, serum-inducible coactivator of nuclear respiratory factor 1-dependent transcription in mammalian cells. *Mol. Cell. Biol.*, **21**, 3738–3749.
48. Appleby,R.D., Porteous,W.K., Hughes,G., James,A.M., Shannon,D., Wei,Y.H. and Murphy,M.P. (1999) Quantitation and origin of the mitochondrial membrane potential in human cells lacking mitochondrial DNA. *Eur. J. Biochem.*, **262**, 108–116.
49. Faure Vigny,H., Heddi,A., Giraud,S., Chautard,D. and Stepien,G. (1996) Expression of oxidative phosphorylation genes in renal tumors and tumoral cell lines. *Mol. Carcinogen.*, **16**, 165–172.
50. Penefsky,H.S. (1974) Mitochondrial and chloroplast ATPases. In Boyer,P.D. (ed.) *The Enzymes*, Academic Press, New York, pp. 375–395.
51. Bolon,C., Gauthier,C. and Simonnet,H. (1997) Glycolysis inhibition by palmitate in renal cells cultured in a two chamber system. *Am. J. Physiol.*, **273**, C1732–1738.
52. Moyes,C.D. and Hood,D.A. (2003) Origins and consequences of mitochondrial variation in vertebrate muscle. *Annu. Rev. Physiol.*, **65**, 177–201.
53. Garcia,J.J., Ogilvie,I., Robinson,B.H. and Capaldi,R.A. (2000) Structure, functioning, and assembly of the ATP synthase in cells from patients with the T8993G mitochondrial DNA mutation. Comparison with the enzyme in Rho(0) cells completely lacking mtDNA. *J. Biol. Chem.*, **275**, 11075–11081.
54. Taanman,J.W. and Williams,S.L. (2001) Assembly of cytochrome c oxidase: what can we learn from patients with cytochrome c oxidase deficiency? *Biochem. Soc. Trans.*, **29**, 446–451.
55. Grivell,L.A. (1989) Nucleo-mitochondrial interactions in yeast mitochondrial biogenesis. *Eur. J. Biochem.*, **182**, 477–493.
56. Larsson,N.G., Oldfors,A., Holme,E. and Clayton,D.A. (1994) Low levels of mitochondrial transcription factor A in mitochondrial DNA depletion. *Biochem. Biophys. Res. Commun.*, **200**, 1374–1381.
57. Davis,A.F., Ropp,P.A., Clayton,D.A. and Copeland,W.C. (1996) Mitochondrial DNA polymerase gamma is expressed and translated in the absence of mitochondrial DNA maintenance and replication. *Nucleic Acids Res.*, **24**, 2753–2759.
58. Carroll,S., Nicotera,P. and Pette,D. (1999) Calcium transients in single fibers of low-frequency stimulated fast-twitch muscle of rat. *Am. J. Physiol.*, **277**, C1122–1129.
59. Gordon,J.W., Rungi,A.A., Inagaki,H. and Hood,D.A. (2001) Effects of contractile activity on mitochondrial transcription factor A expression in skeletal muscle. *J. Appl. Physiol.*, **90**, 389–396.
60. Dong,X., Goshal,K., Majumder,S., Yadav,S.P. and Jacob,S.T. (2002) Mitochondrial transcription factor A and its downstream targets are up-regulated in a rat hepatoma. *J. Biol. Chem.*, **277**, 43309–43318.
61. Caldwell,M.C., Hough,C., Furer,S., Linehan,W.M., Morin,P.J. and Gorospe,M. (2002) Serial analysis of gene expression in renal carcinoma cells reveals VHL-dependent sensitivity to TNFalpha cytotoxicity. *Oncogene*, **21**, 929–936.
62. Jiang,Y., Zhang,W., Kondo,K., Klco,J.M., St Martin,T.B., Dufault,M.R., Madden,S.L., Kaelin,W.G. Jr and Nacht,M. (2003) Gene expression profiling in a renal cell carcinoma cell line: dissecting VHL and hypoxia-dependent pathways. *Mol. Cancer Res.*, **1**, 453–462.
63. Galban,S., Fan,J., Martindale,J.L., Cheadle,C., Hoffman,B., Woods,M.P., Temeles,G., Brieger,J., Decker,J. and Gorospe,M. (2003) von Hippel-Lindau protein-mediated repression of tumor necrosis factor alpha translation revealed through use of cDNA arrays. *Mol. Cell. Biol.*, **23**, 2316–2328.
64. Wykoff,C.C., Sotiriou,C., Cockman,M.E., Ratcliffe,P.J., Maxwell,P., Liu,E. and Harris,A.L. (2004) Gene array of VHL mutation and hypoxia shows novel hypoxia-induced genes and that cyclin D1 is a VHL target gene. *Br. J. Cancer*, **90**, 1235–1244.
65. Amatschek,S., Koenig,U., Auer,H. *et al.* (2004) Tissue-wide expression profiling using cDNA subtraction and microarrays to identify tumor-specific genes. *Cancer Res.*, **64**, 844–856.
66. Kelly,D.P. and Scarpulla,R.C. (2004) Transcriptional regulatory circuits controlling mitochondrial biogenesis and function. *Genes Dev.*, **18**, 357–368.
67. Gajewski,C.D., Yang,L., Schon,E.A. and Manfredi,G. (2003) New insights into the bioenergetics of mitochondrial disorders using intracellular ATP reporters. *Mol. Biol. Cell.*, **14**, 3628–3635.
68. Rossignol,R., Gilkerson,R., Aggeler,R., Yamagata,K., Remington,S.J. and Capaldi,R.A. (2004) Energy substrate modulates mitochondrial structure and oxidative capacity in cancer cells. *Cancer Res.*, **64**, 985–993.

Received July 8, 2004; revised November 5, 2004; accepted December 2, 2004